THESE

présentée pour obtenir le grade de

DOCTEUR DE L'UNIVERSITE LOUIS PASTEUR
DE STRASBOURG

Discipline : sciences chimiques

Multi-rotaxanes bidimensionnels

Entrelacs d'anneaux et de fils moléculaires autour de métaux pentacoordinés

Benoît CHAMPIN

Soutenue publiquement le 17 novembre 2006 devant la commission d'examen :

Prof. Jean-Marc PLANEIX (Strasbourg, France)	Président
Prof. Edwin CONSTABLE (Bâle, Suisse)	Rapporteur externe
Prof. Frédéric FAGES (Marseille, France)	Rapporteur externe
Dr. Jean-Pierre SAUVAGE (Strasbourg, France)	Directeur de thèse

THESIS

submitted to The University Louis Pasteur of Strasbourg
in fulfilment of the requirements for the degree of

DOCTOR of PHILOSOPHY

Discipline: chemical sciences

2-dimensional multi-rotaxanes

Molecular rings and threads woven around pentacoordinated metal centres

Benoît CHAMPIN

Defended in public on November 17th, 2006 in front of the following jury:

Prof. Jean-Marc PLANEIX (Strasbourg, France)	President
Prof. Edwin CONSTABLE (Basel, Switzerland)	External referee
Prof. Frédéric FAGES (Marseille, France)	External referee
Dr. Jean-Pierre SAUVAGE (Strasbourg, France)	Supervisor

Imagination is more important than knowledge,
for knowledge is limited to all we know and understand,
while imagination embraces the entire world,
and all there will ever be to know and understand.

A. Einstein

Remerciements

Ce travail a été réalisé sous la direction de Monsieur Jean-Pierre Sauvage, Directeur de recherche au CNRS. Je tiens ici à lui présenter mes plus sincères remerciements pour m'avoir permis de réaliser mon travail de thèse dans son laboratoire. Il m'a donné l'opportunité de découvrir tous les aspects de la vie de chercheur dans des conditions privilégiées, tant par les moyens matériels à disposition dans l'équipe que par les rencontres fréquentes avec les professeurs invités, et les responsabilités confiées aux doctorants. Son implication dans la formation des étudiants, son enthousiasme à toute épreuve et sa curiosité scientifique ont été une constante source de motivation. Les discussions dans son bureau, mais aussi en salle café ou devant la paillasse sont là pour témoigner de son engagement auprès des « jeunes » du laboratoire, et pour cela je l'en remercie. Je tiens aussi à le remercier d'avoir accepté et respecté mon engagement dans diverses activités pédagogiques qui m'ont parfois maintenu loin de la paillasse !

Je tiens à remercier Monsieur Jean-Marc Planeix, Professeur à l'Université Louis Pasteur de Strasbourg, Monsieur Edwin Constable, Professeur à l'Université de Bâle, et Monsieur Frédéric Fages, Professeur à l'Université de la Méditerranée de Marseille, d'avoir accepté de juger ce travail et pour la discussion scientifique enrichissante que nous avons pu avoir durant la soutenance.

Que la Région Alsace et le CNRS soient remerciés ici d'avoir financé mon travail de recherche au travers de la Bourse de Docteur Ingénieur (BDI) dont j'ai bénéficié pendant 3 ans.

Je remercie Valérie Sartor, Chargé de recherche au CNRS, de m'avoir accompagné sur le chemin de ce travail pendant mes deux premières années de thèse. Nos discussions et fous rires dans son bureau m'ont manqué après son départ. Le téléphone nous a heureusement permis de garder le contact, scientifique et amical.

Je ne peux m'empêcher d'avoir une pensée pour Jean-Marc Kern, Professeur à l'Université de Strasbourg, qui m'a mis le pied à l'étrier de l'enseignement en préparation à l'agrégation de chimie, et qui est parti bien trop tôt.

L'ambiance d'un laboratoire est un facteur crucial pour la réussite d'une thèse, on s'en rend compte souvent trop tard, mais dans mon cas, j'ai eu la chance de passer des années inoubliables parmi vous. Je remercie donc les anciens – Etienne, Benoist, Pierre, Damien, Sylvestre, Masatoshi, Jack, Bryce, Elisabetta – qui ont su m'accueillir parmi leur troupe, notamment durant les fameuses « pauses clopes » dans la cage d'escalier, et ce malgré mon statut de non-fumeur ! Mais aussi Ulla, Oliver et Pirmin qui bien que germanophones sont des gens vraiment très bien. Je pense surtout à ceux qui sont encore là aujourd'hui – Stéphanie, Valérie, Jean-Paul, Angélique, Julien, Fabien, Julie, Jacques, Maryline, Tessy, Yann, Jonathan, David, Safaa – qui m'apportent tous les jours le plein de bonne humeur ! Spéciale dédicace à Krëscht : j'étais venu à Strasbourg pour faire une thèse ; j'y ai trouvé un ami, un vrai.

Il y a également tous les chimistes hors-labo : Hélène et Clémence qui m'ont accueilli en DEA et avec qui j'ai tant partagé (piscine, soirées, ragots, cours d'agreg !), Marie et Gégé toujours souriantes et serviables, Annabelle qui reste en contact même depuis Lausanne, la coloc' des filles d'Heidelberg – Nadia, Natha et Carole – qui sont toujours un rayon de soleil et de bonne humeur quand on se revoit, et tous ceux que j'oublie encore…

Je remercie Patrice Staub, Louise et Geneviève pour nos discussions non-scientifiques, pour leur gentillesse. Et merci d'avoir apporté un peu d'Alsace dans ce laboratoire très cosmopolite ! (ah les bredele et le vin chaud…)

Je tiens à remercier ma famille et mes parents pour leur amour et leur soutien au cours de ces longues années d'études. Ce n'a pas toujours été facile d'ouvrir la voie, mais vous avez toujours cru en moi, même dans les périodes difficiles. Je suis fier d'être allé avec et grâce à vous au bout de ce chemin.

Enfin, Olivier, tu sais ce que les vagues disent au sable…

Abstract

This work belongs to the field of chemical topology. Two synthetic approaches are described here in order to obtain a rotaxane tetramer using 5-coordinate metal centres. The first one aims at interweaving four identical ditopic ligands, and the other one is based on the threading of two molecular rods through two bis-macrocycles.
Two chapters of this manuscript are dedicated to the first strategy. We imagined the synthesis of a ligand bearing a phenanthroline unit (bidentate) on the string and a terpyridine unit (terdentate) at the junction with the macrocycle, so that the chelate coordination axes would be perpendicular to one another. This should therefore favour the formation of the tetramer species.
First, the synthesis in 8 steps of an acyclic analogue is reported, and this product was fully characterized. Coordination chemistry of this ligand to zinc(II) afforded the dimer species as the sole product of the reaction, as shown by DOSY NMR. Coordination of the ligand to a metal center having more demanding stereoelectronic requirements such as copper(II) yielded a mixture of the dimer and trimer species. These results tend to prove that entropy is a prevailing factor in the complexation process.
The synthesis in 15 steps of the desired ditopic macrocyclic ligand is then reported. This product was fully characterized, and its coordination to zinc(II) metal centre afforded a rotaxane dimer, as proven by DOSY NMR. When using copper(II) as a template, a mixture of a rotaxane dimer and trimer could be obtained.
In the last chapter, we paid attention to the second synthetic route to a rotaxane tetramer. Hence, the synthesis of a new bis-macrocyclic ligand built around two terpyridine units attached back-to-back is reported. This product was obtained *via* a classical homocoupling strategy, and also *via* a much more efficient heterocoupling pathway using the Suzuki protocole. This product, made in 13 steps from 1,10-phenanthroline, was fully characterized and preliminary studies were made in order to thread two bis-bipyridine based molecular rods through two bis-macrocycles.

Keywords

Organic synthesis, synthesis of complexes, chemical topology, rotaxane, macrocycle, phénanthroline, terpyridine, Suzuki coupling, boronic esters, zinc(II), cuivre(II), DOSY, bis-macrocycle

Disciplines

Organic chemistry and coordination chemistry

Laboratory

Laboratoire de Chimie Organo-Minérale
LC3 – UMR 7177 CNRS/ULP
Institut de Chimie, Université Louis Pasteur
4 rue Blaise Pascal, BP 1032
67070 Strasbourg Cedex

Résumé

Ce travail de thèse s'inscrit dans le domaine de la topologie chimique. Afin de synthétiser un tétramère de rotaxane autour de métaux pentacoordinés, nous décrivons ici deux approches différentes, l'une basée sur l'entrelac de quatre ligands ditopiques identiques, et l'autre basée sur l'enfilage de deux bis-anneaux sur deux rails moléculaires.
Deux chapitres de ce manuscrit sont consacrés à la première stratégie. Pour cela, la synthèse d'un ligand possédant un groupement phénanthroline (bidentate) sur l'axe et un groupement terpyridine (tridentate) dans l'anneau a été imaginée afin que les axes de coordination des deux chélates soient orthogonaux l'un par rapport à l'autre, cette condition devant favoriser l'obtention d'un assemblage à quatre motifs.
Dans un premier temps, la synthèse d'un analogue acyclique est décrite. Le produit est obtenu après 8 étapes de synthèse et complètement caractérisé. La chimie de coordination de ce ligand a tout d'abord été étudiée avec le zinc(II), et nous avons pu prouver, notamment par DOSY, la formation d'un dimère comme seul produit de réaction. La réaction du ligand avec un métal ayant des exigences stéréoelectroniques plus grandes, tel que le cuivre(II), a conduit à la formation d'un mélange de dimère et de trimère. Ces résultats prouvent que l'entropie demeure un facteur essentiel dans le processus de complexation.
Dans un deuxième temps, nous décrivons la synthèse en 15 étapes du ligand ditopique macrocyclique désiré. Ce produit a été complètement caractérisé et l'étude de sa coordination au zinc(II) a prouvé la formation unique d'un dimère de rotaxane, caractérisé notamment par DOSY. L'utilisation de cuivre(II) a conduit à la formation d'un mélange de dimère et de trimère de rotaxane.
Dans le dernier chapitre, nous nous sommes intéressés à une deuxième approche de synthèse d'un tétramère de rotaxane. Pour cela, nous décrivons la synthèse d'un nouveau ligand bis-macrocyclique autour de deux terpyridines connectées dos-à-dos. Ce produit a été obtenu par une voie classique d'homocouplage, ainsi que par un hétérocouplage de type Suzuki beaucoup plus efficace. Ce produit, issu d'une synthèse en 13 étapes à partir de la 1,10-phénanthroline, a été complètement caractérisé et a fait l'objet d'études préliminaires d'enfilage sur un rail moléculaire de type bis-bipyridine.

Mots-clefs

Synthèse organique, synthèse de complexes, topologie chimique, rotaxane, macrocycle, phénanthroline, terpyridine, couplage de Suzuki, esters boroniques, zinc(II), cuivre(II), DOSY, bis-macrocycle

Disciplines

Chimie organique et chimie de coordination

Laboratoire

Laboratoire de Chimie Organo-Minérale
LC3 – UMR 7177 CNRS/ULP
Institut de Chimie, Université Louis Pasteur
4 rue Blaise Pascal, BP 1032
67070 Strasbourg Cedex

Contents

List of Figures

Nomenclature

δ	-	chemical shift
bipy	-	2,2'-bispyridine
CN	-	coordination number
CPK	-	Corey-Pauling-Koltun (models)
CV	-	cyclovoltammetry
D	-	diffusion coefficient
DMF	-	*N*,*N*-dimethylformamide
DMSO	-	*N*,*N*-dimethylsulfoxide
DOSY	-	diffusion-ordered spectroscopy
EPR	-	Electron Paramagnetic Resonance (spectroscopy)
ES-MS	-	ElectroSpray Mass Spectroscopy
EI-MS	-	Electron Impact Mass Spectroscopy
FAB-MS	-	Fast Atom Bombing Mass Spectroscopy
HR ES-MS	-	High Resolution ES-MS
J	-	coupling constant
MALDI	-	Matrix Assisted Laser Desorption Ionization
m/z	-	mass-to-charge ratio
NBS	-	*N*-bromosuccinimide
NCS	-	*N*-chlorosuccinimide
NMR	-	Nuclear Magnetic Resonance (spectroscopy)
Ms	-	Mesyl-
PG	-	Protective Group
ppm	-	parts per million
phen	-	1,10-phenanthroline
RCM	-	Ring Closing Metathesis (reaction)
Rf	-	Retention factor
terpy	-	2,2' : 6',2"-terpyridine
THF	-	TetraHydroFuran
THP	-	TetraHydroPyran
TLC	-	Thin Layer Chromatography

Chapter 1
General Introduction

The purpose of this Ph.D. thesis is to synthesize 2-dimensional multi-rotaxanes by threading molecular rods through molecular rings using pentacoordinated metal centres as templates. The complexity of such kind of architectures can be used to design molecular machines and devices. Therefore this work deals with topological chemistry, the use of metal centre as template and molecular machines. The aim of this general introduction is to give a non-exhaustive overview of these three fields, in order to better understand the birth of the project and its purpose.

1.1 Chemical topology

When one looks in the dictionary, so called “hard sciences” such as mathematics, computer science, chemistry or physics, are said to rely either on experimental, quantifiable data or the scientific method, and focus on accuracy and objectivity. But when you compare chemistry to all of these fields, you realize that chemistry has its specific features. It has, first of all, relationships with all other sciences; it is a central science and is very important for all the others. You cannot develop computers without chemistry because you have to make the materials. You cannot develop pharmaceuticals without chemistry because you have to make the molecules. You cannot go into space without chemistry because you need, again, the materials, and so on. The other aspect, which is probably even more important, is that

chemistry can act on matter. As said Pr. Jean-Marie Lehn after getting the Nobel Prize in 1987, "*with chemistry, it's sort of a feeling of power, it's Prometheus bringing to mankind the fire stolen from heaven. The fire transforms things, and chemistry is really the fire that transforms matter*". You are able to act on substances, to understand those which already exist, and you have the possibility to make things which did not exist. As chemists, we do not only have the opportunity to observe, study and recreate existing species or phenomena, but we also have the tools to create as many new molecules, structures, shapes and functionalities as we want, and imagination is our only limit. In that sense, chemistry has definitely something in common with art, which is you act and you create something.

Yet, Nature has often been a great source of inspiration, and before starting to synthesize brand new molecules, chemists have spent decades trying to understand the basic mechanisms of chemistry, and to use them to easily build small molecules having the desired functions. Nevertheless, chemists got rapidly interested not only in the function of a molecule, but also in its shape and geometry. One of the big challenges of the past years was thus to create nice and complex 2-dimensional structures, such as ring-shaped compounds. This field of research was all the more interesting that there is an obvious connection between the structure and the function of a molecule. This field of research naturally extended to 3-dimensional complex structures, among which we can cite cage-molecules such as cryptands,[1-3] carcerands,[4, 5] cryptophanes,[6, 7] or the elegant and now very classical family of ball-shaped fullerenes[8, 9] and especially the Buckminsterfullerene C_{60} (Figure 1.1).

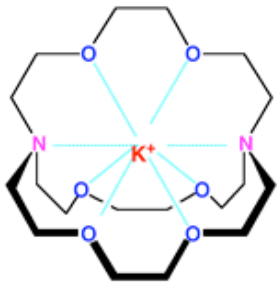

Complexation of
[2.2.2]-cryptand with K^+

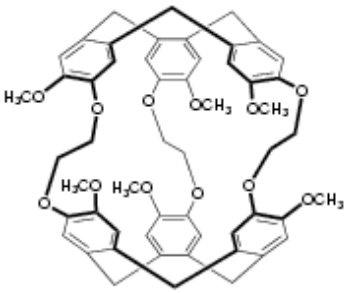

Cryptophane-A

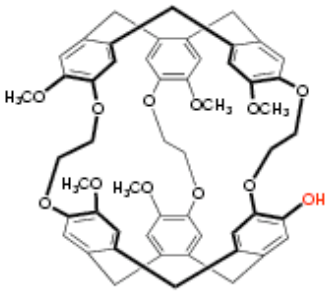

Cryptophanol-A

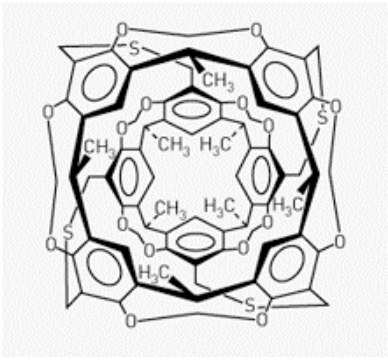

Carcerand

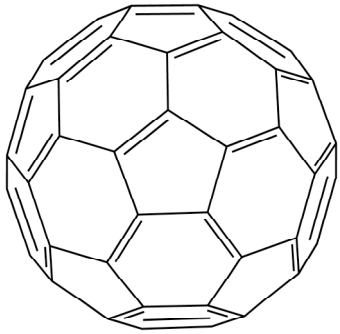

Fullerene C_{60}

Figure 1.1: Examples of ball-shaped molecules

Yet, as complicated as the structure of the molecule may be, most of synthetic or natural organic compounds have a "trivial topology". What does it mean? Is topology connected to geometry?

1.1.1 Topological concepts[10-16]

When teaching chemistry, molecules generally are presented at first as being rigid objects. Stereochemical representations are shown where tetrahedral, octahedral, and other rigid structures for molecules are carefully drawn. Molecular models are also generally rigid. What are the consequences if one begins to consider molecules as being totally flexible, allowing any degree of stretching, bending or flattening, but no breaking of bonds? This is a fundamental concept involved in chemical topology.

Topologically, two objects are identical if one can be deformed into the other in a continuous fashion as long as nothing is broken or no holes are punched through during the process. Therefore a flat piece of clay with a hole in it is topologically equivalent to a coffee cup (Figure 1.2) because, clearly, the clay can be molded into the coffee cup without any breaking. In fact, topologically, the piece of clay and the coffee cup are the same as a torus.

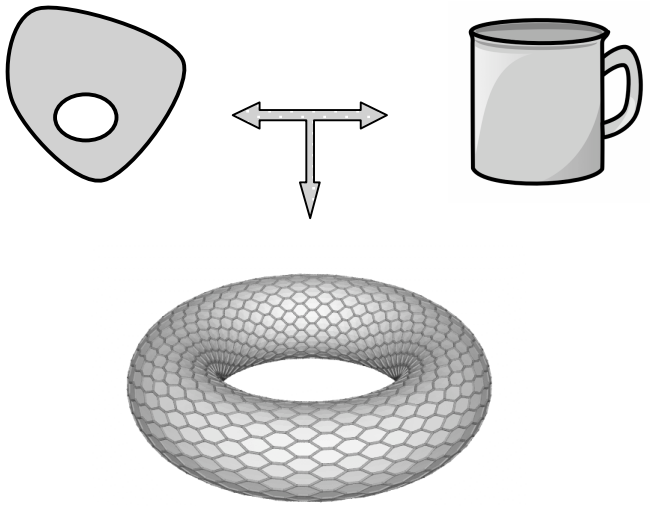

Figure 1.2: Coffee cup topology

The same concept can be used in describing molecules. Topologically, a molecule is simply a collection of vertices – atoms – connected to each other by edges – bonds –, with no regard to angles or length.[17] There is a characteristic in common to the drawings of a molecule on a sheet of paper: they are representations of a three-dimensional object in a two-dimensional plane. In effect, the molecule is projected onto a flat surface. Topologically, one is allowed to try to flatten out any molecule. However, it is possible to imagine a situation where, in the flattening out process, two or more bonds will remain crossing over each other, and no distortion will uncross them.

Figure 1.3: Representations of bicyclo[2.2.2]octane

The example of bicyclo[2.2.2]octane given in Figure 1.3, where it is drawn with crossing bonds, is obviously one where the two bonds shown crossing is not a structural requirement of the molecule. Topologically, you merely have to pull the crossing bond out of the way. In topological terms, any such structure that can be flattened in a way so that it has no crossing bonds is said to be "topologically trivial" and to have a planar graph.[18] The opposite situation is called a non-planar graph, where the crossing bonds preclude the possibility of flattening out the molecule, which is said to be "topologically not trivial".

As mentioned earlier, it is quite surprising to realize that there are not too many examples of molecules with non-planar graphs. Even molecules that are structurally quite complex, such as Buckminsterfullerene (Figure 1.4), have planar graph; i.e., topologically it is not a structural requirement that bonds must cross. This molecule is essentially a sphere with holes in it, and this sphere can be flattened out with no crossing bonds, as shown in Figure 1.4 (a Schlegl diagram).

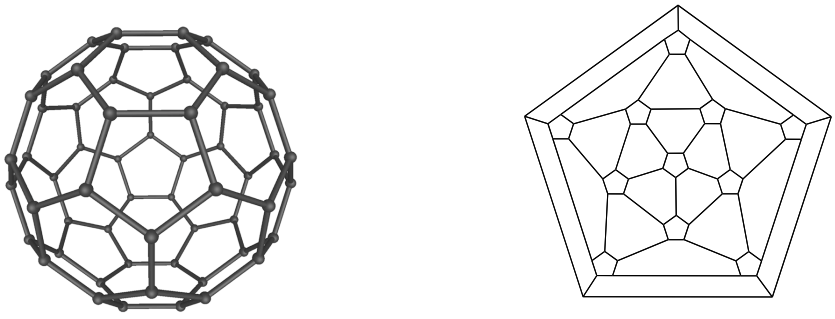

Figure 1.4: Three-dimensional perspective and planar graph of Buckminsterfullerene

The concept of crossing and non-crossing can be illustrated by representations called Kuratowski diagrams. Two examples will be given. One is called the $K_{3,3}$ diagram where three points are connected to each of three other points. This is shown in Figure 1.5, where the left illustration shows an obvious way to connect the points, leading to many crossings, and the right illustration shows the connections with the minimal, and unavoidable, number of crossings, i.e., one. Another is the K_5 graph, five points, each one connected to the other four (Figure 1.5), also with one required crossing. Any molecule that has a connectivity of either $K_{3,3}$ or K_5 will be a molecule with a non-planar graph.

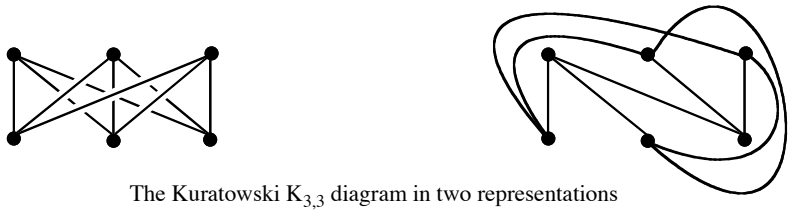

The Kuratowski $K_{3,3}$ diagram in two representations

The Kuratowski K_5 diagram in two representations

Figure 1.5: Kuratowski $K_{3,3}$ and K_5 diagrams

1.1.2 Molecules of topological interest

1.1.2.1 K_5 and $K_{3,3}$ examples

Actual examples of these topologically interesting molecules were quite a rarity until recently, thanks to many groups, including ours, who decided few years ago to investigate this new field of fundamental research and to try and create molecules having non-planar graphs. Considering first the K_5 situation, one of the most elegant examples is a polyquinane reported in 1998[19] (Figure 1.6). The five interconnected atoms are indicated.

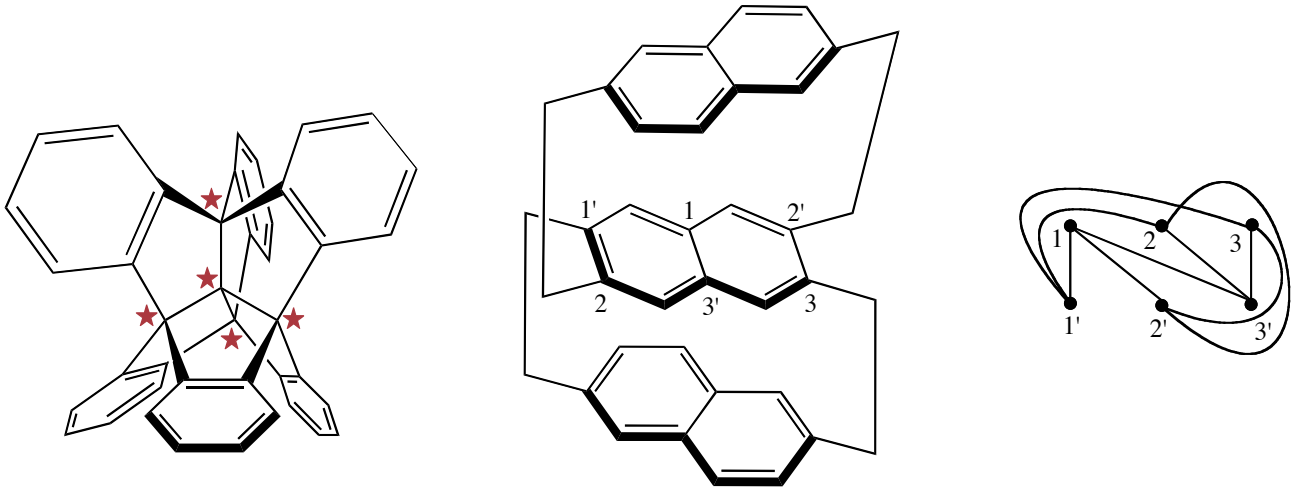

Figure 1.6: On the left, a polyquinane K_5 molecule; in the middle, a triple-decker naphthalene cyclophane $K_{3,3}$ molecule; on the right, the Kuratowski $K_{3,3}$ diagram

There are now also several examples of $K_{3,3}$ molecules. For example, in 1983, a triple decker naphthalene cyclophane was synthesized[20] (Figure 1.6). However, probably the most intriguing example of this type of molecule was reported in 1982. It is interesting not only from the point of view of its $K_{3,3}$ topology, but from the fact that it is a truly flexible molecule. This is the Möbius ladder,[21] shown in Figure 1.7, with its Kuratowski diagram. The molecule is related to the Möbius strip that is topologically curious because it can be made from a two-sided strip of paper, but when the strip is given a half-twist and the two ends joined, a ring of only one side is obtained.

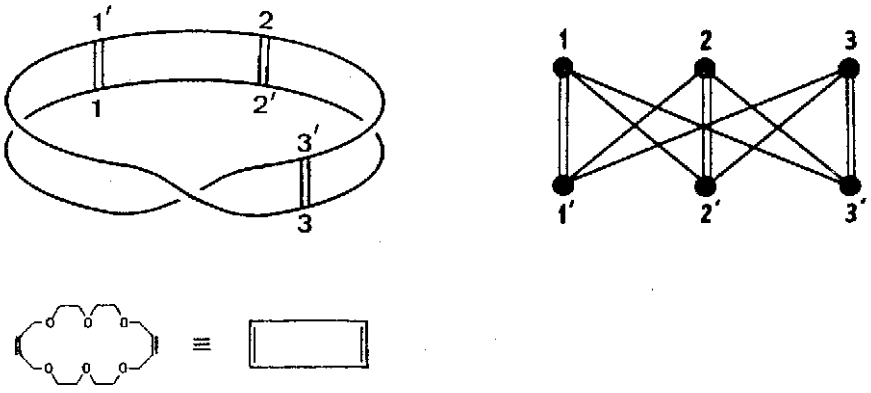

Figure 1.7: The Möbius ladder with its Kuratowski diagram

1.1.2.2 Knots, catenanes and rotaxanes

Topological chemistry appeared during the 60's. Frisch and Wasserman were the first who introduced the concept of topological isomerism, before Walba developed it on a more theoretical point of view.[10-16]

a) Catenanes

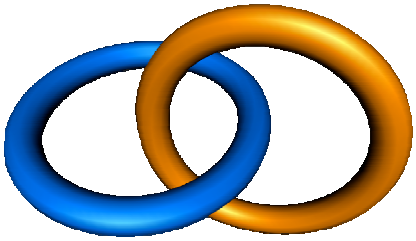

Figure 1.8: Representation of a catenane, two interlocked rings

Experimental topological chemistry, i.e. synthesis of "non trivial" molecules, first tried to reach the easiest object: a [2]-catenane, which consists in two interlocked rings with a physical link between the rings, but no chemical bonds between the links (Figure 1.8). It has a non-planar graph since you have two remaining crossings when drawing the molecule on a two-dimensional surface.

First attempts to synthesize such a molecule simply relied on randomness, trying to thread statistically a molecular filament into a macrocycle.[22-24] But the yields were very poor, and chemists decided to direct their synthesis by pre-organizing the precursors into space. Purely organic catenanes were first synthesized by Schill and Lüttringhaus,[25-27] in a very elegant manner, but due to the high number of steps, the overall yield was quite poor (Figure 1.9).

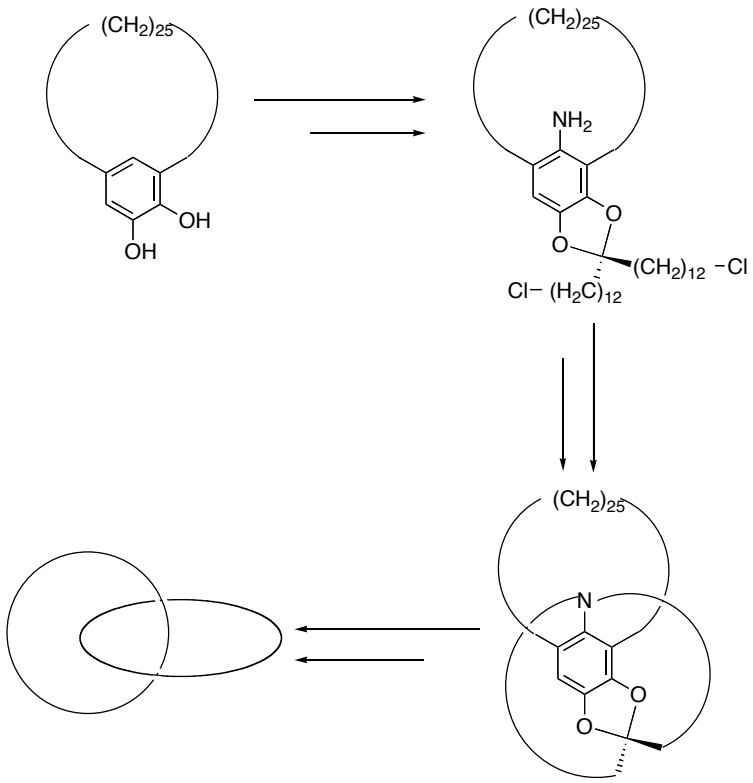

Figure 1.9: Directed synthesis of catenanes by Schill *et al.*

Almost twenty years later, Christiane Dietrich-Buchecker and Jean-Pierre Sauvage proposed to use a transition metal centre as a template to form the desired [2]-catenane.[28-30] The tetrahedral geometry around the copper(I) complex organized the two phenanthroline units in such a way that further cyclization and demetallation gave rise to both rings of the catenane.

Other very efficient synthetic paths have then been successfully investigated: we can cite the group of Fraser Stoddart, who discovered in 1989 that catenanes can be made using pi-donor pi-acceptor interactions,[31] and the groups of Fritz Vögtle[32] and Chris Hunter[33] who imagined in 1992 a strategy using a non ionic template effect, based on hydrogen bonds and pi-pi interactions (Figure 1.10).

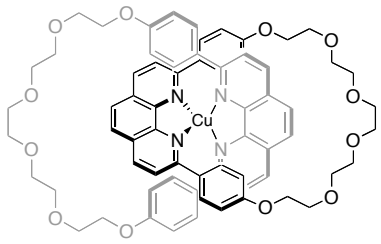

Sauvage, Dietrich-Buchecker, 1983

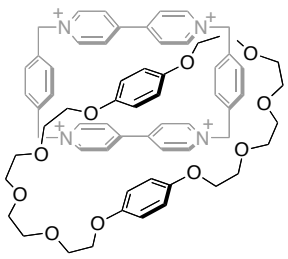

Stoddart, 1989

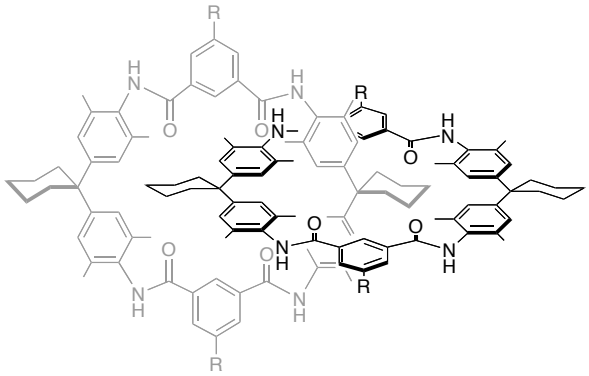

R= OMe Vögtle, 1992
R= H Hunter, 1992

Figure 1.10: Three archetypes of covalent catenanes

b) Rotaxanes

One calls [2]-rotaxane a ring threaded around an axle, the ends of which are terminated by two bulky groups larger than the ring.[15] These "stoppers" prevent the ring from de-threading in case the link between the axle and the ring is broken (Figure 1.11).

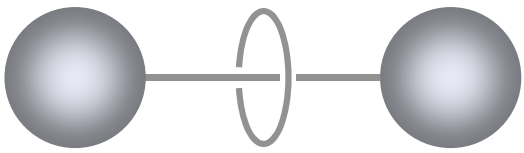

Figure 1.11: Representation of a [2]-rotaxane

Strictly speaking, the topology of a [2]-rotaxane is trivial: any kind of deformation being possible in the "topology world", one can enlarge the ring and make it pass over the bulky

stoppers. Yet, by its effects in the real and physical world, the stoppered thread can be compared to an infinitely large ring with its two ends being at infinity. The geometry of a [2]-rotaxane is thus comparable to the one of a [2]-catenane.

Similarly to the quest of the [2]-catenane, various routes have been taken to achieve the synthesis of a [2]-rotaxane by pre-organizing the building blocks thanks to different kinds of interactions: coordination on metals,[34] hydrophobic effects,[34, 35] hydrogen-bond formation,[36-38] charge-transfer interactions,[38-40] or covalent bond formation.[12, 41]

c) Knots

Among the most fascinating objects displaying non-trivial topological properties, interlaced designs and knots occupy a special position. The simplest non-trivial knot is the trefoil knot,[1] a closed ring with a minimum of three crossing points. This leads us to the interesting concept of topological isomerism, which is better understandable on an example. The three objects *a*, *b* and *c* of Figure 1.12 are topological stereoisomers – although they might consist of exactly the same atoms, and chemical bonds connecting these atoms, they cannot be interconverted by any type of continuous deformation in three-dimensional space. In addition, compounds *a* and *b* are topological enantiomers because the mirror image of any presentation of *b* is identical to a given presentation of *a*.

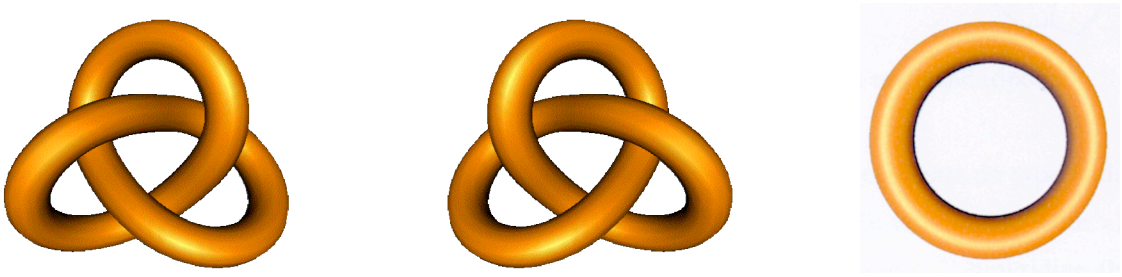

a *b* *c*

Figure 1.12: Schematic representations of: (a) and (b) the two topological enantiomers of the trefoil knot, (c) a ring

[1] Mathematically, a simple ring is also a knot

Several attempts were made to synthesize a trefoil knot, but the randomness of the Möbius strip approach[10, 42] or the numerous difficult steps of a directed synthesis were highly limiting factors. Finally, Christiane Dietrich-Buchecker and Jean-Pierre Sauvage used the same methodology as for the catenane synthesis: pre-organization of two threads bearing two phen nuclei around copper(I) centres formed a double helix which is the ideal precursor to the trefoil knot. Subsequent cyclization and demetallation yielded the desired product, with a very poor yield (3%).[43] Several improvements were made afterwards,[44] especially in the cyclization step, using a ring closing metathesis (RCM) reaction catalyzed by the Grubbs catalyst[45] (74% yield).

If the synthesis of amazingly complex natural products is still an extremely active area of research with formidable challenges,[46-48] one can see throughout these examples that unnatural compounds also represent exciting objectives for many reasons. Beyond aim related to applications, the making of a novel molecular system can represent an exciting challenge in itself, not only because of the possibility of discovering the new properties of a so far unknown compound, but also for its attractive shape, topology, *etc*. In other words, the synthesis itself of the compound to be made and the hypothetical properties of the target molecules are two distinct incitements. The synthesis of catenanes, rotaxanes and knots combines both sets of motivation but it also adds an aesthetic dimension to the chemical problem. Indeed the search for aesthetically attractive molecules has been a goal since the very origin of chemistry.

1.1.3 Topology in Nature

If in the beginning, such molecules were mainly perceived as synthetic challenges, they were soon connected to nature and reality with the discovery in the early 60's of catenated and knotted DNA[49-51] (Figure 1.13).

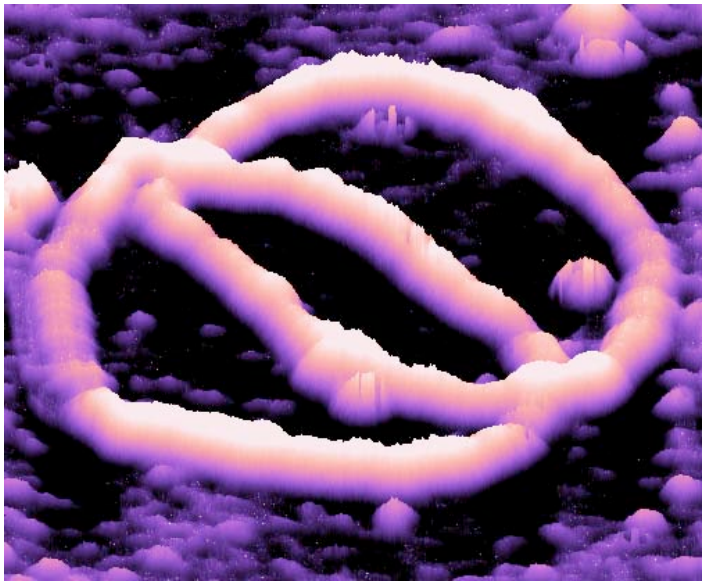

Figure 1.13: Image of a DNA catenane produced by RecQ helicase and DNA topoisomerase III, in the presence of SSB protein. Atomic force microscopy was used to visualize the DNA, which had been coated with RecA protein to enhance resolution and thereby facilitate tracing of the path followed by the duplex DNA strands

Another very striking example has been published more recently,[52] showing that complex catenated structures exist in Nature: the crystal structure of the double-stranded DNA bacteriophage HK97 mature empty capsid was determined. This membrane is made of 12 pentameric and 60 hexameric rings of covalently joined subunits that loop through each other, creating protein chainmail: topologically linked protein catenanes arranged with isocaedral symmetry (Figure 1.14). Catenanes provide here a stabilization mechanism for the very thin HK97 capsid.

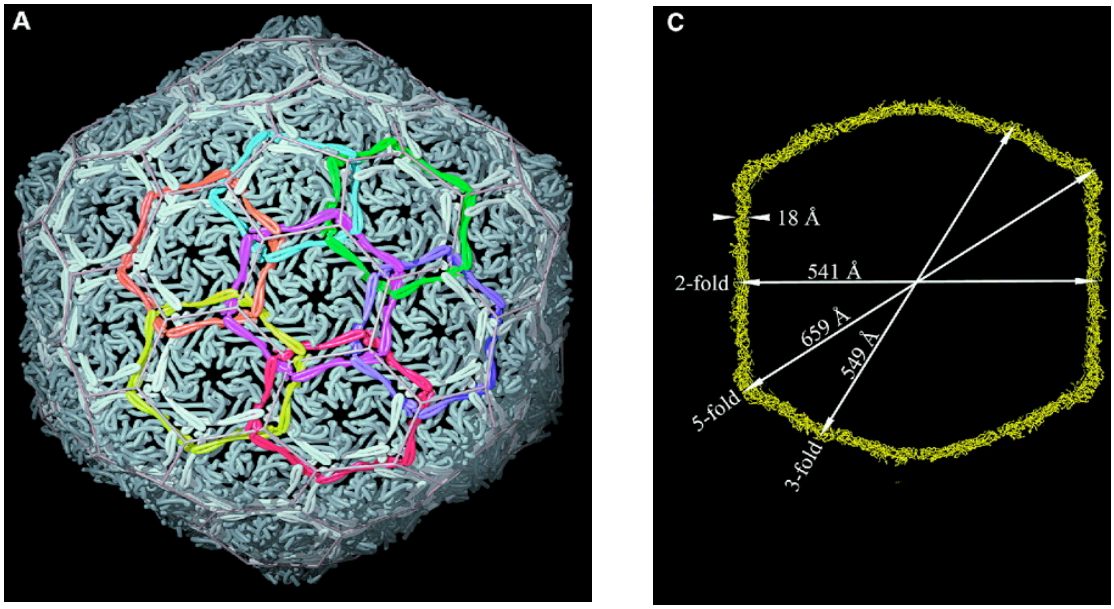

Figure 1.14: (A) Capsid chainmail: the subunits that are cross-linked into rings are coloured identically, highlighting the catenated circle topology. (C) Cross section through the unusually thin empty capsid

Thus, unexpectedly, chemical topology, actively supported by rigorous mathematical theories, glided furtively from pure curiosity towards much more concrete and tangible domains. After numerous answers were brought to the synthetic challenge itself, there arose ever more insistently the quest for functions and properties of such special compounds. Already, even if still far from real applications, one can imagine, based on interlocked, threaded or knotted multi-component molecules, new organic materials, specific polymers, molecular devices or machines able to process and transfer energy, electrons or information.

Among all the strategies that have been briefly exposed to create molecules having non trivial topology, the use of a metal centre has been extensively made especially in our group. Besides those topologically interesting architectures, the template effect of metal centres has been used by many groups to direct the self-assembly of magnificient complex structures.

1.2 Complex molecular architectures built around metal centres

First, one have to clarify two concepts, which are quite close, and that one might easily confuse: template effect and self-assembly.

The template effect,[53, 54] using metal centers, ionic or non ionic interactions, enables to *pre-organize* the ligands with respect to one another, and then one or several final steps yield the desired three-dimensional structure. In the case of the formation of catenanes or knots described above, metal centres are used as templates, i.e. metal centres are kinds of nuts pre-organizing the three-dimensional structure of the molecule, which is then cyclized. But once the desired geometry or topology is achieved, metal centers are usually removed, yielding for example the free catenane from the copper-complexed catenate. Metal centers are thus not part of the final molecule.

In the case of self-assembly, the use of metal centres is completely different. When Stoddart, Hunter, Vögtle or Sauvage are building catenanes using template effect, the strategy is quite predictable and based on pre-organization. In the example published by Fujita *et al*. in 1994, there is no pre-organization.[34] The catenane is in equilibrium with many other species thanks to the lability of the Pd-N bond. Other external factors such as concentration or polarity of the solvent are responsible for the formation (or not) of the catenane. In that case, metal centres are really part of the final structure.

In this section, a non-exhaustive and arbitrary presentation of molecular architectures built around metal centres will be made, using either the template effect or self-assembly processes.

1.2.1 Double helical compounds

As shown earlier, the strategy which first yielded the trefoil knot relied on the synthesis of two bis-chelating molecular threads that can be interlaced on two transition metal centres, leading to a double helix. After cyclization and demetallation, the knot could be obtained. An important prerequisite for the success of this approach was thus the formation of a helical dinuclear complex. Although the preparation of double helices from various transition metals and bis-chelate ligands is very likely to have occurred long ago, it is only during the late 70's that the first such system was recognized and characterized.[55] Moreover, scientific interest of these arrangements was not obvious at all. One of the earliest dinuclear helical complexes was identified by Fuhrhop and co-workers in 1976.[55] His pioneer zinc complex is represented in Figure 1.15.

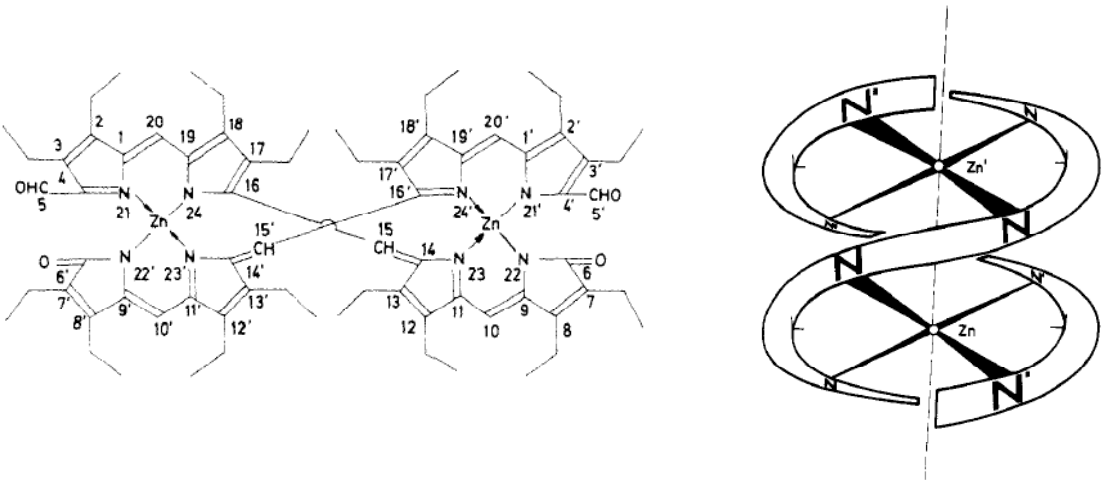

Figure 1.15: Bis-helical dimer (structure and schematic drawing) by Fuhrhop *et al*.

During the 80's, several laboratories prepared and investigated double-stranded helical complexes, systems containing either pyrrolic ligand[56, 57] and derivatives[58-60] (with Zn^{2+}, Ag^{+}, Cu^{+}) or oligomers of 2-2'-bipyridine.[61, 62] "Helicates" [61-65] may consist of up to five copper(I) centres and these systems are reminiscent of the DNA double helix.

1.2.2 Molecular Borromean rings

An object of particular interest in knot theory is known as the Borromean rings, whose realization in a wholly synthetic molecular form has been reported two years ago by Stoddart and co-workers.[66] It is comprised of three interlocked rings such that scission of any one ring leads to the other two falling apart (Figures 1.16A and 1.16B). This magnificent structure was obtained by a strict self-assembly protocol, that brings the components of the three rings together in one step under comprehensive template-directed control (Figure 1.16D).

The 18 components were assembled by formation of 12 imine and 30 dative bonds, associated with the coordination of the three interlocked macrocycles to total of six zinc(II) ions (the silver sphere shown in Figure 1.16C). This all-in-one strategy combines the virtues of reversibility, proofreading, and the error checking associated with supramolecular and dynamic covalent chemistry, with the geometrical precision afforded by coordination chemistry. The flexibility and reversibility in the coordination sphere were met by using kinetically labile zinc(II) ions, that template the formation of the Borromean rings with maximal site occupancy being honored.

The final dodecacation (Figure 1.16C) was fully characterized by NMR spectroscopy, ESI-mass spectrometry and X-ray crystallography (Figure 1.17).

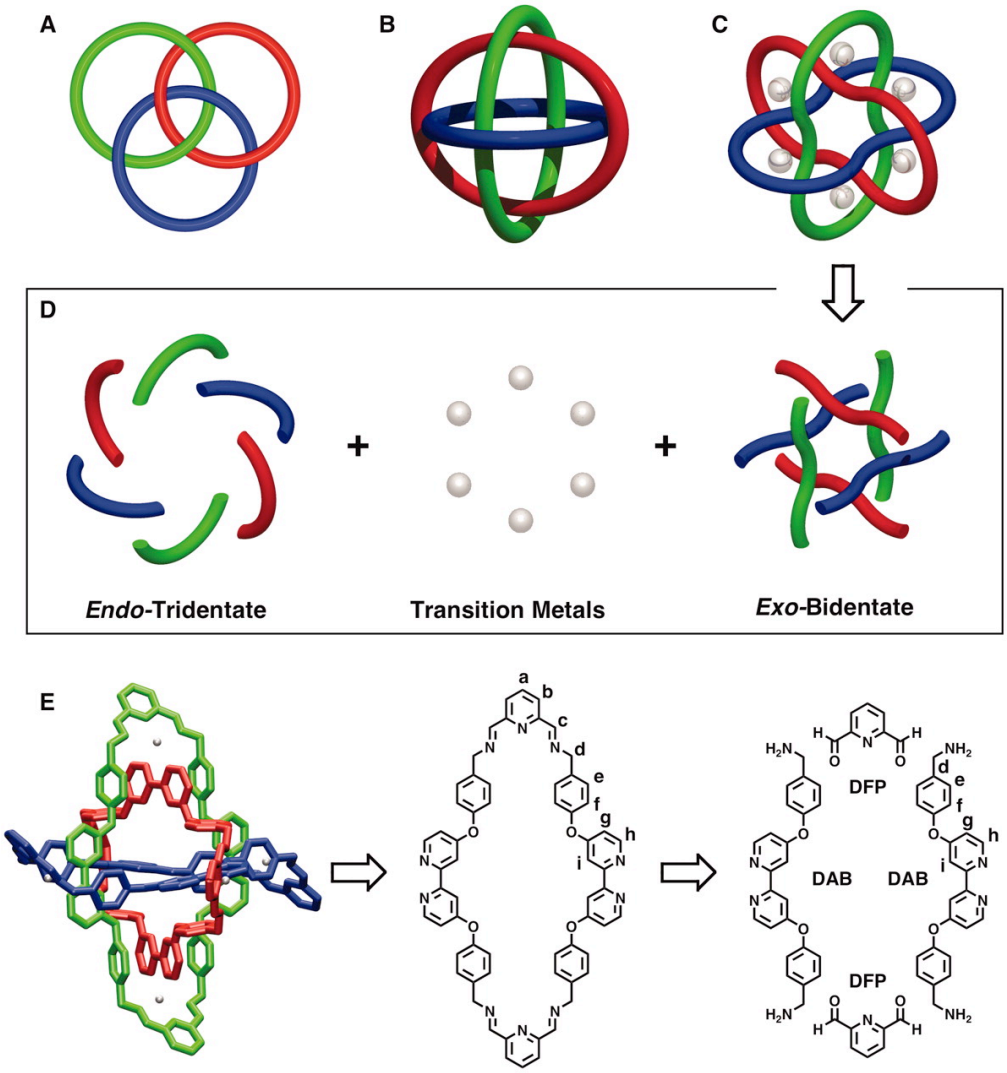

Figure 1.16: The Borromean rings can be depicted in many ways: (A) a planar Venn representation, (B) a more informative orthogonal arrangement; (D) Retrosynthetic disconnection of the Borromean rings; (E) Retrosynthesis

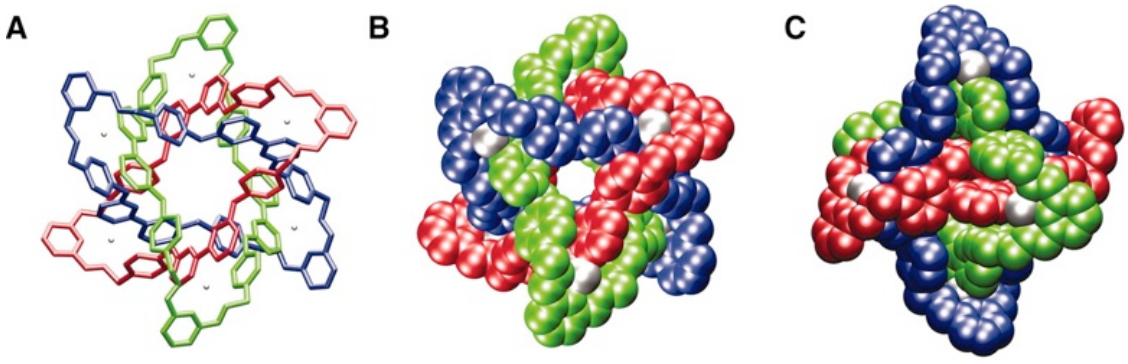

Figure 1.17: Different structural representations of the dodecacation in the solid state: (A) tubular representation; (B) and (C) space-filling representations of A

1.2.3 New self-assembled structural motifs built around metal centres[67]

Multisite ligands containing two or several aromatic polyimines and their complexes have been extensively used to construct elegant multinuclear architectures such as helical complexes mentioned above,[61, 68] but also grids,[69] racks[70] and ladders[71] (Figure 1.18). A characteristic common to all of these motifs is the formation of coordination bonds at alternating right angles to each other.

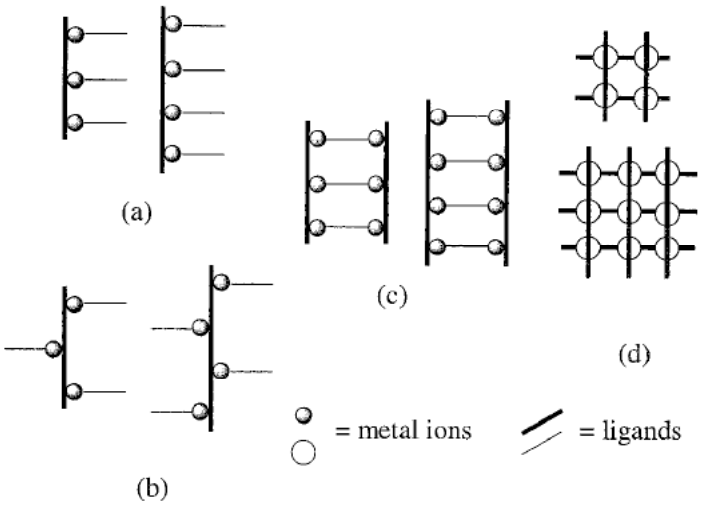

Figure 1.18: Schematic illustrations of (a) *syn*-rack, (b) *trans*-rack, (c) ladder, and (d) grid architectures

A variety of coordination complexes displaying grid (G) secondary structural motifs have been reported. These include [2 x 2]G (Figure 1.19)[72], [2 x 3]G[73] and [3 x 3]G.[69, 74] The ligands used to build these motifs are characteristically planar and contain rigidly linear spacers between their binding sites.

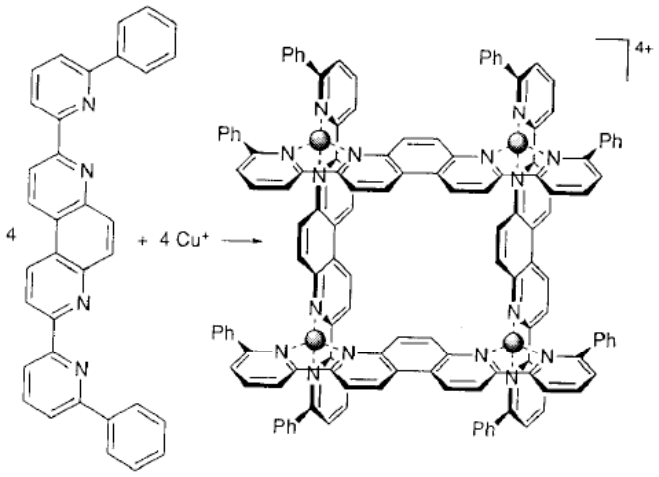

Figure 1.19: A self-assembled inorganic [2 x 2]G. The shade circles represent Cu(II) ions

Ladders and racks resemble grids in that multiple coordinations occur down the length of a linear polydentate ligand. However they differ in that a second, mono- or bidentate ligand is always necessary. This ligand must have binding sites at either one (rack) or at both ends (ladder).

All known ladders (L) have been formed as secondary structural motifs by thermodynamic self-assembly. Several [2 x 2]L and [2 x 3]L have been reported.[71] These include the complexes illustrated in Figure 1.20.

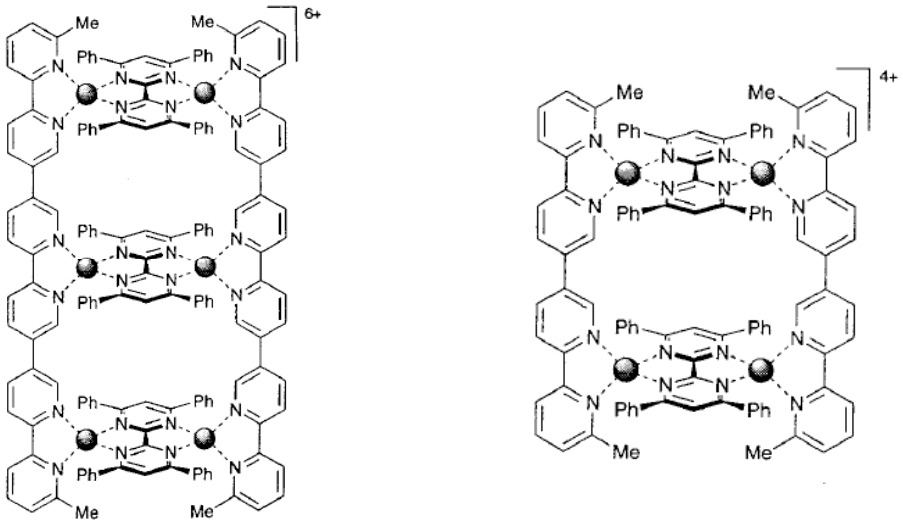

Figure 1.20: Self-assembled tetra- and hexanuclear ladders.
The shade circles depict Cu(I) ions

Since racks (R) have only one linear polytopic ligand present, they may display structural isomers if the linkers in that ligand permit rotational freedom. The *syn* isomer (Figure 1.21) involves an eclipsed conformation of metal ions and "rung" ligands down one side of the central ligand. The *trans* isomer contains the metal ions and "rung" ligands alternatively coordinated on opposite sides of the central ligand. Several compounds having [2]R[75] and [3]R[70] rack secondary structure have been reported (Figure 1.21)[70] and all were obtained by thermodynamic self-assembly.

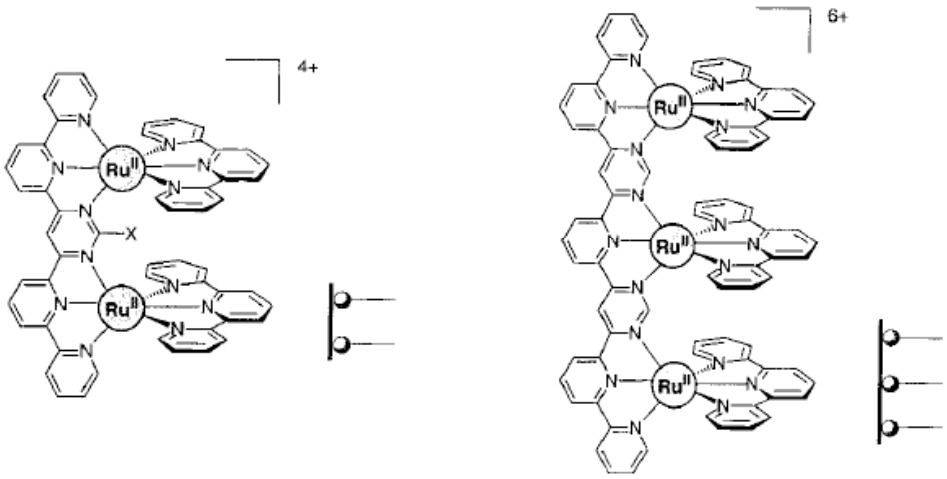

Figure 1.21: Self-assembled bi- and trinuclear racks

1.2.4 Coordination assemblies from a Pd(II)-cornered complex[76]

Over the last 15 years, major efforts in Fujita's lab have been dedicated to metal-directed self-assembly of discrete two- and three-dimensional structures. The $[enPd(II)]^{2+}$ unit (en = ethylenediamine) has emerged as a versatile building block in these processes. In particular, the 90° coordination angle of the metal has been judiciously used in the design of new discrete structures.

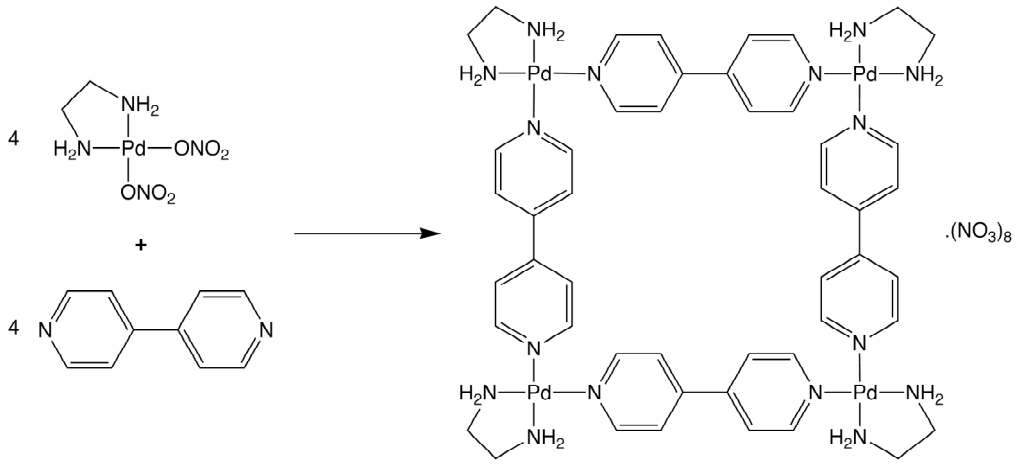

Figure 1.22: Self-assembly of a square complex by Fujita *et al.*

In 1990, this group demonstrated the spontaneous formation of a square metal complex with four palladium centres, one at each corner of the square.[77, 78] As mentioned in section 1.2 about the strategy used by this group to make a [2]-catenane, there is no pre-organization in this protocol: the desired molecule is in equilibrium with other species (oligomers…etc) thanks to the lability of the Pd-N bond. Other external parameters are responsible for the formation of the molecular square, and one can truly understand the whole process once the product is formed. In that case, many attempts were made, using different metal centres (Ni, Co, Fe, Mn…), end-cap groups (diamines, diphosphines, dithiols…), and linear bridging ligands (4,4'-bipyridines, dicyanides, diacetylenes…). While in most cases uncharacterizable mixtures or insoluble polymeric materials were formed, the best solution was obtained when [enPd(NO_3)$_2$] and 4,4'-bipyridine were combined in aqueous-alcohol solution (Figure 1.22).

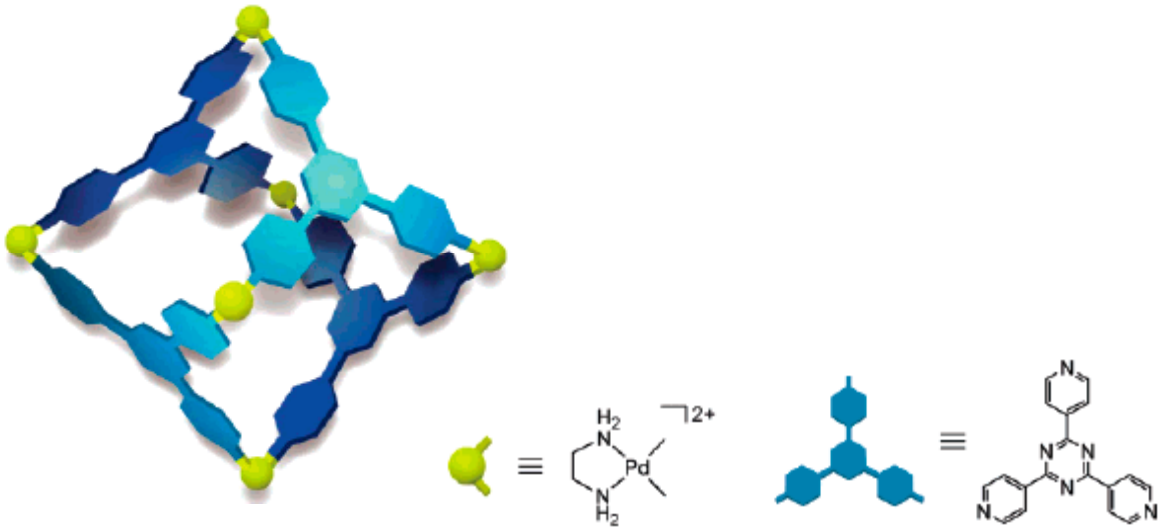

Figure 1.23: Schematic representation of M_6L_4 cage

Using the same strategy and the $[enPd(II)]^{2+}$ unit, but varying the chemical nature of the bridging ligand, a whole family of architectures such as cages, bowls, boxes, tubes, catenanes and spheres was achieved by this group in the last few years[76] (Figure 1.24).

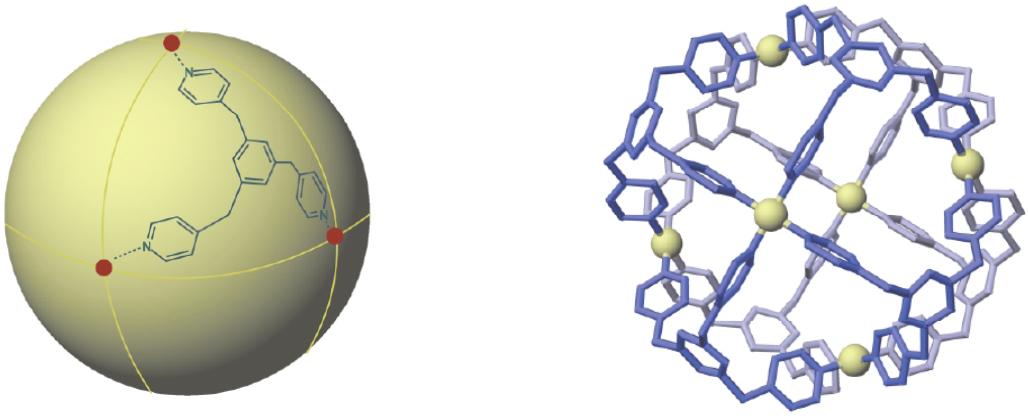

Figure 1.24: Cartoon representation of a molecular sphere, conceptualized from eight tripodal tridentate ligands, and six metal ions that can provide a square planar coordination environment. Crystal structure of $[M_6L_8]^{12+}$

Construction of beautiful interlocked structures and magnificent architectures around metal centres is thus a wonderful tour de force, and many synthetic answers have been brought to this challenge. The beauty of these achievements is indisputable. Moreover, based on these very special molecules, molecular devices or machines able to process and transfer energy, electrons or information have been designed and optimized.

1.3 Transition metal complexes as molecular machines prototypes

In the course of the last 15 years, a new field has experienced a spectacular development: the elaboration of dynamic molecular systems for which large amplitude motions can be induced and controlled from the outside.[79, 80] In this research area, the molecules, often referred to as "molecular machines", display two or several distinct geometries which can be interconverted into one another in a reversible way by various processes.

The rapid growth of this field can be linked to the discovery and a better understanding of numerous dynamic biological systems (motor proteins) whose controlled motions correspond to important biological functions. Such biological motors have been studied in great detail[81] and, for several of them, it has even been possible to visualize the movement while they are in action.[82, 83] Classical examples are ATP synthase, a rotary motor, the actin-myosin complex of the striated muscle, acting as a linear motor, or the kinesins, essential motor proteins able to "walk" on the microtubules and to transport important molecular components of the cell over large distances.

In this section, we will mostly focus on transition metal-containing molecular machines but purely organic systems are equally important. The contributions of Balzani, Stoddart, Leigh, Harada and others and their coworkers, using catenanes or rotaxanes, represent real

breakthroughs.[84-90] Similarly, the non interlocking systems proposed by Feringa, Kelly and others are particularly novel and can also be regarded as pioneering contributions.[91-97] The photochemical isomerisation of C=C double bonds is a useful process which has been utilized to set molecular fragments in motion within a given molecule.[98, 99]

The use of transition metal complexes is particularly attractive since metal centres are often electroactive, allowing to induce rearrangements *via* a metal-localized redox signal, thus circumventing any potential difficulty associated to the generation of organic radicals. In addition, the structure of some transition metal complexes can be profoundly modified by modifying the pH of the medium or by generating a dissociative excited state, thus allowing to set some parts of the compounds in motion using a chemical signal or a photonic impulse.

It should be noted that the coverage in this chapter is by no means exhaustive. We have rather selected a few representative examples in the recent literature but our choice is, of course, arbitrary and reflects our scientific interests.

1.3.1 Electrochemically controlled molecular motions

1.3.1.1 Transition metal-complexed catenanes and rotaxanes

a) A copper-complexed [2]catenane in motion with three distinct geometries

Multistage systems seem to be uncommon, although they are particularly challenging and promising in relation to nano-devices aimed at important electronic functions and, in particular, information storage.[100-103] Among the few examples which have been reported in recent years, three-stage catenanes are particularly significant since they lead to unidirectional rotary motors.[93] In the mid-90s, our group has described a particular Cu-complexed [2]-catenane which represents an example of such a multistage compound.[104] The molecule displays three distinct geometries, each stage corresponding to a different coordination number of the central complex (CN = 4, 5, or 6). The principle of the three stage

electrocontrollable catenane is represented in Figure 1.25.

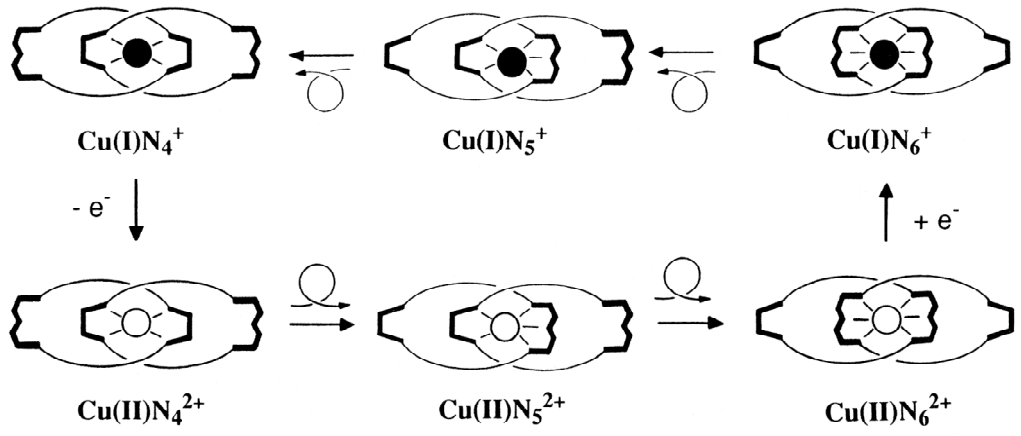

Figure 1.25: A three-configuration Cu(I) catenate whose general molecular shape can be dramatically modified by oxidizing the central metal (Cu(I) to Cu(II)) or reducing it back to the monovalent state. Each ring of the [2]-catenate incorporates two different coordinating units: the bidentate dpp unit (dpp = 2,9-diphenyl-1,10-phenanthroline) is symbolized by a U whereas the terpy fragment (2,2':6',2''-terpyridine) is indicated by a stylized W. Starting from the tetracoordinate monovalent Cu complex ($Cu(I)N_4^+$; top left) and oxidizing it to the divalent state ($Cu(II)N_4^{2+}$), a thermodynamically unstable species is obtained which should first rearrange to the pentacoordinate complex $Cu(II)N_5^{2+}$ by gliding of one ring (left) within the other and, finally, to the hexacoordinate stage $Cu(II)N_6^{2+}$ by rotation of the second cycle (right) within the first one. $Cu(II)N_6^{2+}$ is expected to be the thermodynamically stable divalent complex. The double ring-gliding motion following oxidation of $Cu(I)N_4^+$ can be inverted by reducing $Cu(II)N_6^{2+}$ to the monovalent state ($Cu(I)N_6^+$; top right), as represented on the top line of the Figure

Similarly to the very first and simpler catenane made in our group for which a large amplitude motion can deliberately be triggered by an external signal,[105] the gliding of the rings in the present system relies on the important differences of stereochemical requirements for coordination of Cu(I) and Cu(II). For the monovalent state the stability sequence is CN = 4 > CN = 5 > CN = 6. On the contrary, divalent Cu is known to form stable hexacoordinate complexes, with pentacoordinate systems being less stable and tetrahedral Cu(II) species being even more strongly disfavoured.

The synthesis of the key catenate $[Cu(I)N_4]^+PF_6^-$ (Figure 1.26a) derives from the usual three-dimensional template strategy.[106, 107]

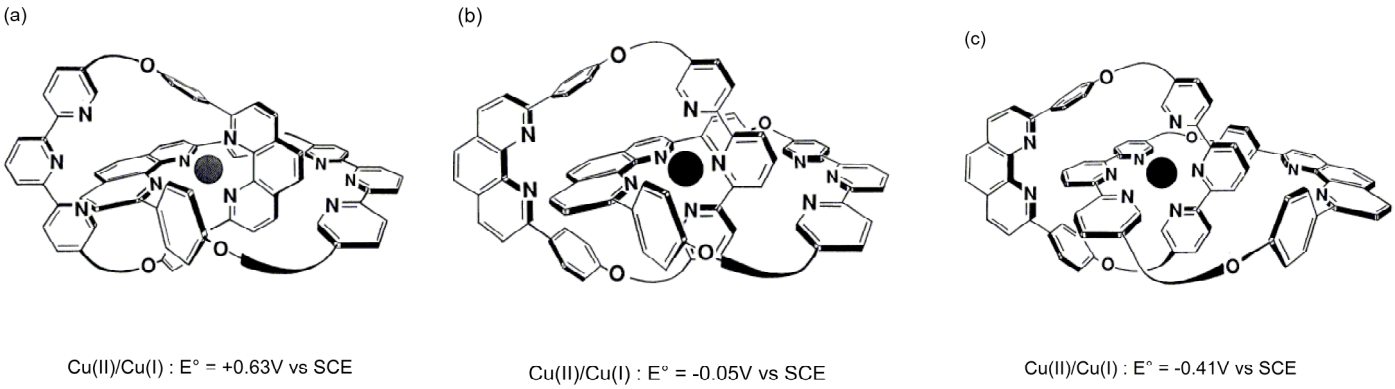

Figure 1.26: The three forms of the copper-complexed catenane, each species being either a monovalent or a divalent complex. (a) 4-coordinate complex (b) 5-coordinate complex (c) 6-coordinate complex

The cycle depicted in Figure 1.25 was completed. The changeover process for the monovalent species is faster than the rearrangement of the Cu(II) complexes, as previously observed for the previously reported simpler catenate.[105] In fact, the rate is comparable to the CV time scale and three Cu species are detected when a CV of a MeCN solution of $[Cu(II)N_6]^{2+}(BF_4^-)_2$ is performed. The waves at +0.63 V and -0.41 V correspond, respectively, to the tetra- and hexacoordinate complexes mentioned above. By analogy with the value found for the previously reported copper-complexed catenane,[105] the wave at -0.05 V is assigned to the pentacoordinate couple (Figure 1.26b).

b) Intramolecular motion within a heterodinuclear bismacrocycle transition-metal complex

Wozniak and coworkers described recently the first heterodinuclear bismacrocyclic transition-metal complex (Figure 1.27) that exhibits potential-driven intramolecular motion of the interlocked crown-ether unit.[108, 109] Although the system contains transition metals, the main interaction between the various subunits, which also allowed the construction of the catenane, is an acceptor-donor interaction of the charge transfer type.

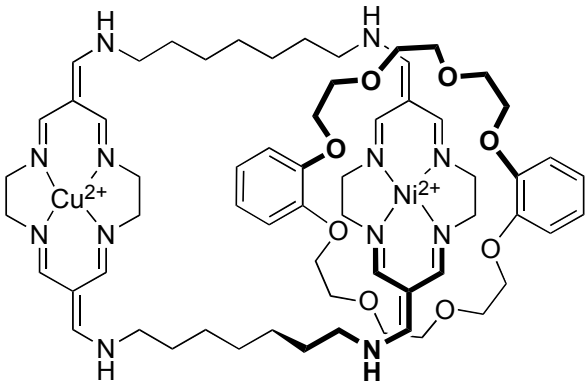

Figure 1.27: Heterodinuclear [2]catenane by Wozniak *et al.*

The reported heterodinuclear catenane should allow a controlled translocation of the crown-ether unit back and forth between two different metal centres in response to an external stimulus, specifically a potential applied to the electrode (Figure 1.28).

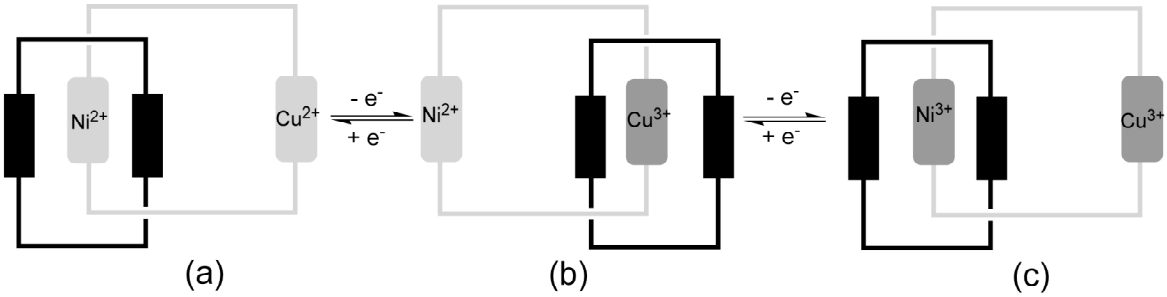

Figure 1.28: Schematic representation of electrochemically controlled molecular motion

The present system can be set in motion using two consecutive redox signals. The main feature of the machine-like catenane is that the preferred conformation will be such that the most electro-deficient transition metal macrocyclic complex will lie in between the two aromatic donor fragments of the crown ether.

The bis-macrocyclic ring is positively charged because of the presence of Ni(II) and Cu(II). The crown ether and the bis-azamacrocyclic ring form a sandwich-like structure in such a way

that one of the crown ether aromatic rings is located between the two metal-coordinated macrocyclic rings. The second aromatic ring is located almost parallel to the previous one outside the two linked macrocycles.

As nickel(II) is a better acceptor than copper(II), the situation at the beginning of the process is the one depicted in Figure 1.28a. Then, upon oxidation of the molecule, the copper(II) centre turns into copper(III) since oxidation of the nickel(II) centre is more difficult. But Cu(III) being of course a better acceptor than Ni(II), the crown ether relocates from the nickel(II) centre to the copper(III) centre (Figure 1.28b). By increasing the potential, the nickel(II) centre is finally oxidized, and the new nickel(III) centre is, as expected, a stronger acceptor than the copper(III) centre. Hence, the crown ether ring moves for the second time, yielding the third situation (Figure 8c).

c) A fast-moving electrochemically driven machine based on a pirouetting copper-complexed rotaxane[110]

The rate of the motion in artificial molecular machines and motors is obviously an important factor. Depending on the nature of the movement, it can range from microseconds, as in the case of organic rotaxanes acting as light-driven molecular shuttles,[111] to seconds, minutes or even hours in other systems involving threading-unthreading reactions[112, 113] or metal-centred redox processes based on the Cu(II)/Cu(I) couple.[105]

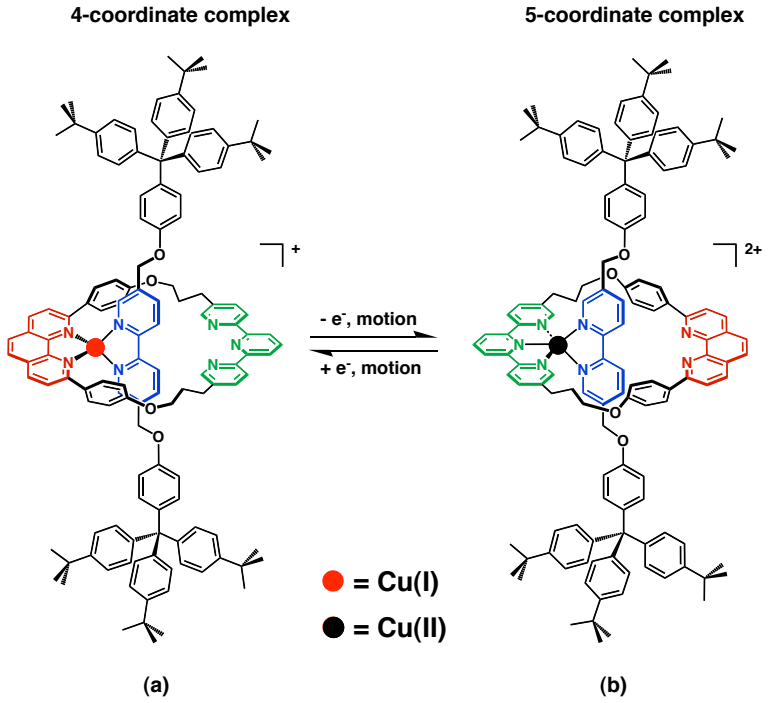

Figure 1.29: Electrochemically induced pirouetting of the ring in a rotaxane; the bidentate chelate and the tridentate fragment are alternatively coordinated to the copper centre

In order to increase the rate of motions, a new rotaxane in which the metal centre is as accessible as possible was prepared, the ligand set around the copper centre being thus sterically little hindering compared to previous related systems. Ligand exchange within the coordination sphere of the metal is thus facilitated as much as possible. The two forms of the new bistable rotaxane are depicted in Figure 1.29. The molecular axis contains a "thin" 2,2'-bipyridine motif, which is less bulky than a 1,10-phenanthroline fragment and thus is expected to spin more readily within the cavity of the ring. In addition, the bipy chelate does not bear substituents in α-position to the nitrogen atoms. The 4-coordinate species rearranges to the 5-coordinate species after oxidation and vice versa. The electrochemically driven motions were studied by cyclic voltammetry (CV).

A lower limit for the rate constant k of the rearrangement of the 5-coordinate species can be estimated as over 500 s^{-1} (or $\tau < 2$ ms, with $\tau = k^{-1}$). The rearrangement rate for the 4-coordinate Cu(II) complex is smaller ($k = 5\ s^{-1}$) than for the monovalent complex. It is

nevertheless several orders of magnitude larger than in related catenanes or rotaxanes with more encumbering ligands.

This example shows that subtle structural factors can have a very significant influence on the general behaviour (rate of the movement, in particular) of copper(II/I)-based molecular machines. Further modifications will certainly lead to new systems with even shorter response times.

1.3.1.2 Other related non-interlocking systems

The first example of redox-driven translocation of a metal centre was based on the couple Fe(III)/Fe(II) and took place in ditopic ligands containing a trishydroxamate compartment,[114, 115] suitable for the Fe(III) cation and three bipyridine functions which show a very high affinity towards Fe(II). The translocation was driven through auxiliary redox reactions: reduction of Fe(III) with ascorbic acid and oxidation of Fe(II) with peroxydisulfate. The translocation could be followed both visually and spectrophotometrically (Figure 1.30).

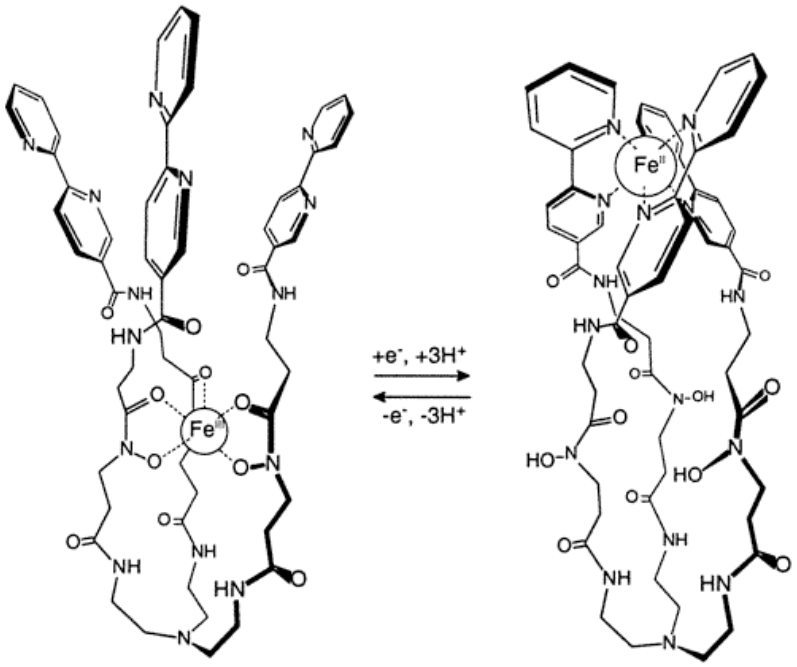

Figure 1.30: Redox-driven translocation of an iron centre within a ditopic system containing a hard and a soft compartment

A ditopic ligand was designed in which one compartment displays a selective affinity towards the oxidized metal centre $M^{(n+1)+}$ whereas the other compartment shows a higher affinity towards the reduced cation M^{n+}. On the basis of the assumption that the oxidized cation is hard and the reduced one is soft, the ditopic system should contain a hard compartment (A) and a soft compartment (B) (Figure 1.31). Thus, the hard cation stays in the hard compartment. When the metal centre is reduced to its soft version M^{n+}, it moves to the soft compartment B. Therefore the metal centre can be translocated at will between A and B in a repeatable way upon reduction and oxidation of the metal centre in an electrochemical way.

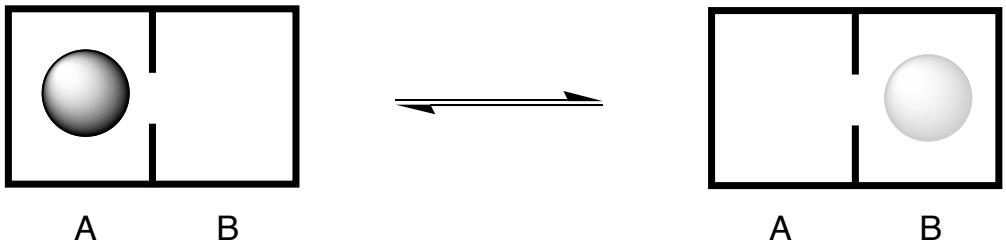

Figure 1.31: Schematic representation of the principle of translocation process

Another example which fits the same mechanistic scheme is provided by the octadentate ligand depicted in Figure 1.32.[116] The system operates through the Cu(II)/Cu(I) couple. It contains the hard compartment A consisting of four amine groups and the soft compartment B with two 2,2'-bipyridine functions.

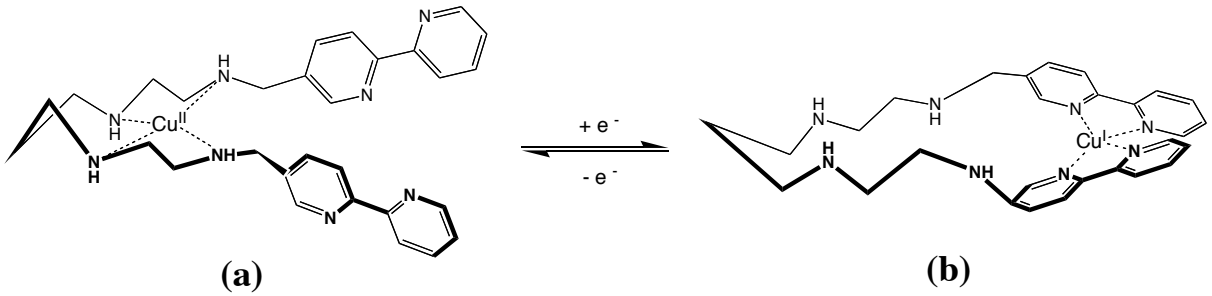

Figure 1.32: Redox-driven translocation of a copper centre based on the Cu^{II}/Cu^{I} change

The translocation process is fast and reversible and can be followed both visually and spectrophotometrically. An MeCN solution containing equimolar amounts of the ligand and Cu(II) is blue-violet (d-d absorption band; λ_{max} = 548 nm, ε = 120 $M^{-1}.cm^{-1}$), which indicates that the oxidized cation resides in the tetramine compartment (Figure 1.32a). On addition of a reducing agent (ascorbic acid), the solution takes the brick-red colour typically observed with the $[Cu^{I}(bpy)_2]^+$ chromophore (MLCT transition, λ_{max} = 430 nm, ε = 1450 $M^{-1}.cm^{-1}$), indicating that the Cu(II)/Cu(I) reduction process has taken place and that the metal centre has translocated fast to the soft $(bpy)_2$ compartment (Figure 1.32b). On addition of an oxidizing reagent, the solution takes again its original blue-violet colour, indicating that the metal centre (now Cu(II)) has again moved back to the tetramine compartment.

1.3.2 Light-driven molecular machines

1.3.2.1 Photoinduced decoordination and thermal recoordination of a ring in a ruthenium(II)-containing [2]catenane[117]

Our group has recently described multicomponent ruthenium(II) complexes in which one part of the molecule can be set in motion photochemically.[118, 119] Among the light-driven molecular machine prototypes which have been described in the course of the last few years, a very distinct family of dynamic molecular systems takes advantage of the dissociative character of ligand-field states in $Ru(diimine)_3^{2+}$ complexes.[120-125] In these compounds, one part of the system is set in motion by photochemically expelling a given chelate, the reverse motion being performed simply by heating the product of the photochemical reaction so as to regenerate the original state. In these systems, the light-driven motions are based on the formation of dissociative excited states. Complexes of the $[Ru(diimine)_3]^{2+}$ family are particularly well adapted to this approach. If distortion of the coordination octahedron is sufficient to significantly decrease the ligand field, which can be realized by using one or

several sterically hindering ligands, the strongly dissociative ligand-field state (^{3}d-d* state) can be efficiently populated from the metal-to-ligand charge transfer (^{3}MLCT) state to result in expulsion of a given ligand. The principle of the whole process is represented in Figure 1.33.

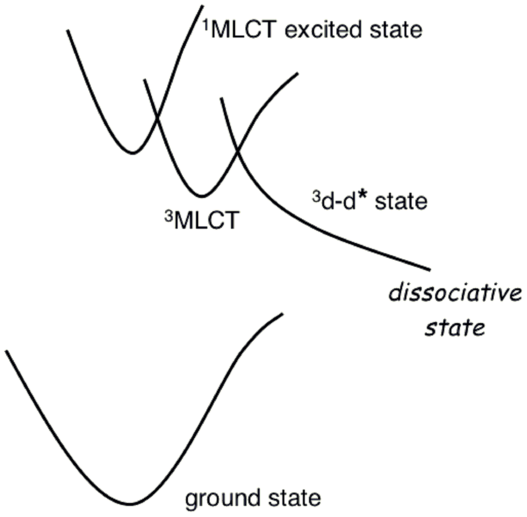

Figure 1.33: The ligand-field state ^{3}d-d* can be populated from the ^{3}MLCT state, provided the energy difference between these two states is not too large: formation of this dissociative state leads to dissociation of a ligand

It is thus essential that the ruthenium(II) complexes which are to be used as building blocks of the future machines contain sterically hindering chelates so as to force the coordination sphere of the metal to be distorted from the perfect octahedral geometry.

The [2]catenanes (a) and (c) (Figure 1.34) were synthesized[126] by using an octahedral ruthenium(II) centre as template. Compound (a) consists of a 50-membered ring which incorporates two phen units and a 42-membered ring which contains the bipy chelate. Compound (c) contains the same bipy-incorporating ring as (a), but the other ring is a 63-membered ring. Clearly, from CPK model considerations, (c) is more adapted than (a) to molecular motions in which both constitutive rings would move with respect to one another

since the situation is relatively tight for the latter catenane. The light-induced motion and the thermal back reaction carried out with (c) or (a) are represented in Figure 1.34. They are both quantitative, as shown by UV/Vis measurements and by ^{1}H NMR spectroscopy.

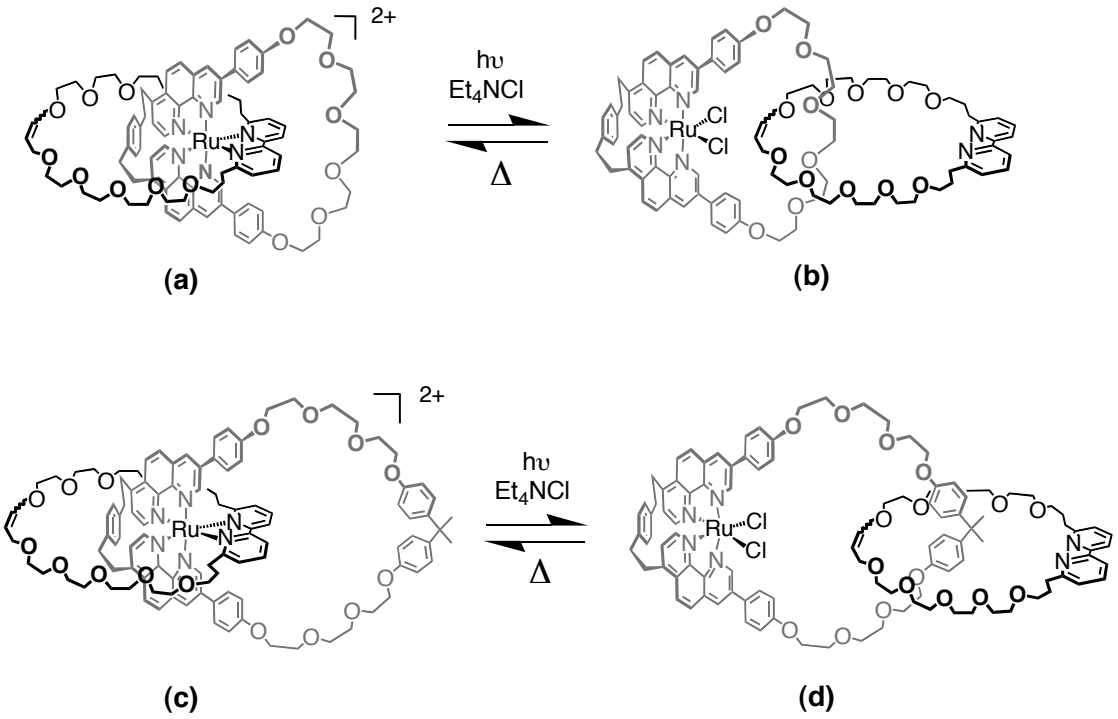

Figure 1.34: Catenanes **(a)** or **(c)** undergo a complete rearrangement by visible light irradiation: the bipy-containing ring is efficiently decoordinated in the presence of Cl^-. By heating the photo-products **(b)** or **(d)**, the starting complexes **(a)** or **(c)** are quantitatively regenerated

It is hoped that, in the future, an additional tuneable interaction between the two rings of the present catenanes, (b) or (d) will allow better control over the geometry of the whole system. In parallel, two-colour machines will be elaborated, for which both motions will be driven by photonic signals operating at different wavelengths.

1.3.2.2 A photochemically driven molecular-level abacus

Recently, Credi *et al* reported[127, 128] the design, synthesis and machine-like performance of a [2]rotaxane, in which the ring component can be induced by light excitation to move, that is switch between two different recognition sites or "stations" of the dumbbell-shaped component (Figure 1.36). Such a molecule exhibits an abacus-like geometry and, since it

behaves according to binary logic, it could, in principle, be used for information processing[129-133] at the molecular level.

The design principles at the basis of the light-driven molecular machines developed by this group[134] have been employed to obtain the rotaxane depicted in Figure 1.35,[127] specifically designed to achieve photoinduced ring shuttling.

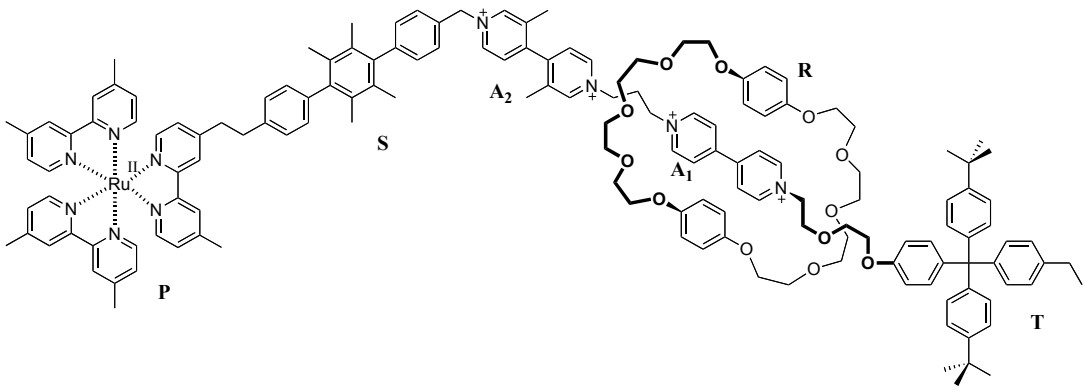

Figure 1.35: Chemical structure of the rotaxane by Credi *et al.*

This compound is made of a π-electron-donating macrocycle as the ring **R**, and a dumbbell-shaped component which contains (i) a $[Ru(bpy)_3]^{2+}$-type complex (**P**) as one of its stopper, (ii) a 4,4'-bipyridinium unit ($\mathbf{A_1}$) and a 3,3'-dimethyl-4,4'-bipyridinium unit ($\mathbf{A_2}$) as electron-accepting stations, (iii) a *p*-terphenyl-type ring system as a rigid spacer (**S**), and (iv) a tetraarylmethane group as the second stopper (**T**). The stable translational isomer of the rotaxane is the one in which the **R** component encircles the $\mathbf{A_1}$ unit, in keeping with the fact that this station is a better electron-acceptor than the other one.

Two working schemes have been devised for the photoinduced switching of **R** between stations $\mathbf{A_1}$ and $\mathbf{A_2}$ – (i) a mechanism based fully on processes which only involves the rotaxane components, that is an intramolecular mechanism, and (ii) a mechanism which requires the help of external reactants, that is a sacrificial mechanism (Figure 1.36).

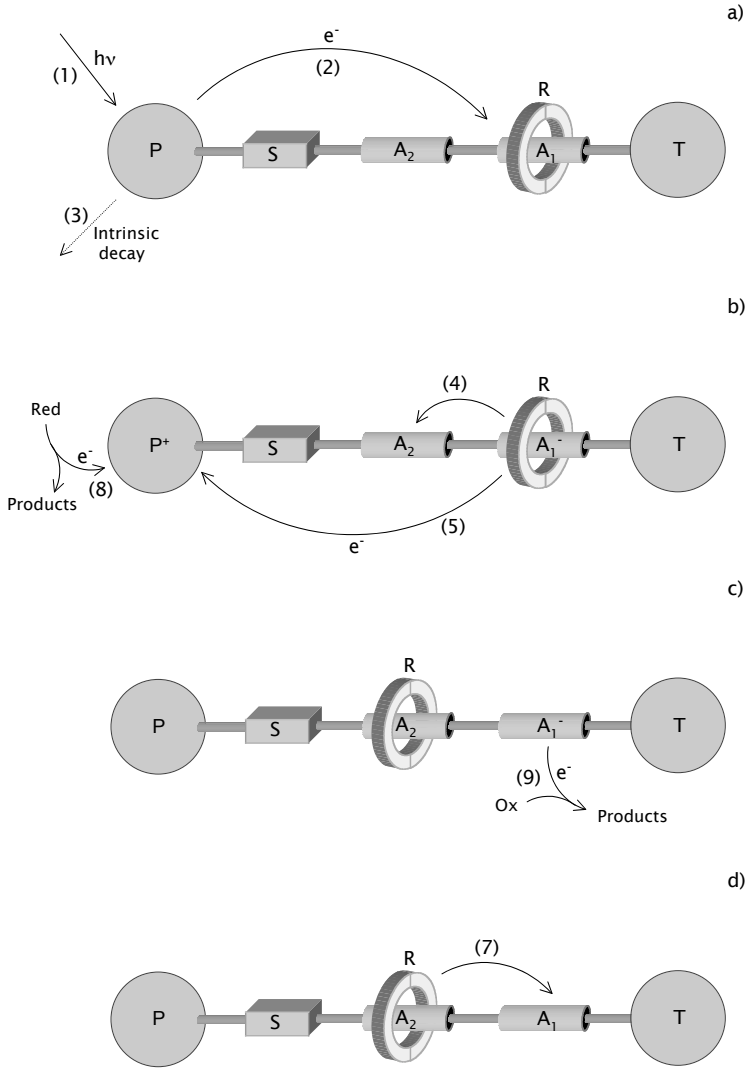

Figure 1.36: Working scheme employing a sacrificial mechanism for the light-driven switching of the ring R between the two stations A_1 and A_2. The dashed lines indicate processes that compete with those needed to make the machine work: steps (3) and (5)

The results obtained[127] have shown that the photochemically driven switching can be performed successfully by the sacrificial mechanism, which is based on the following operations :

a) *Destabilization of the stable translational isomer*: light excitation of the photoactive unit **P** (step 1) is followed by the transfer of an electron from the excited state to the $\mathbf{A_1}$ station, which is encircled by the ring **R** (step 2), with the consequent "deactivation" of this station; such a photoinduced electron-transfer process has to compete with the intrinsic decay of **P*** (step 3).

b) *Ring displacement after scavenging of the oxidized photoactive unit*: if the solution contains a suitable reductant Red (triethanolamine (TEOA), which is a very good scavenger of oxidized Ru-polypyridine complexes), a fast reduction of Red with $\mathbf{P}^{+}$ (step 8) competes successfully with the back electron transfer reaction (step 5). In such a case, the displacement of the ring to $\mathbf{A_2}$ (step 4), even if it is slow, can take place because the originally occupied station remains in its reduced state $\mathbf{A_1}^{-}$.

c) *Electronic reset*: after an appropriate time, restoration of the electron-acceptor power of the $\mathbf{A_1}$ station can be obtained by oxidizing $\mathbf{A_1}^{-}$ with a suitable oxidant Ox (dioxygen in that case) (step 9).

d) *Nuclear reset*: as a consequence of the electronic reset, back movement of the ring from $\mathbf{A_2}$ to $\mathbf{A_1}$ takes place (step 7).

Such mechanical motions with a "power stroke" and a "recovery stroke", which are reminiscent of the workings of a simple piston, have also been reported in other systems not containing transition metal.[111]

1.3.3 Molecular motions triggered by a chemical signal

1.3.3.1 Molecular machines based on metal ion translocation

Molecular machines could enter the field of molecular recognition by acting as receptors with a useful implemented function: to recognize and bind a substrate only when the proper external stimulus is applied. The molecular machine of Fabbrizzi, Pallavicini *et al*[135] behaves as such a receptor which merges the advantages of the lock-and-key principle (selectivity) with those of its adaptive behaviour that is activation in the presence of substrates. Moreover a drastic colour change associated with movement and recognition events turns this system into a very efficient colorimetric sensor.

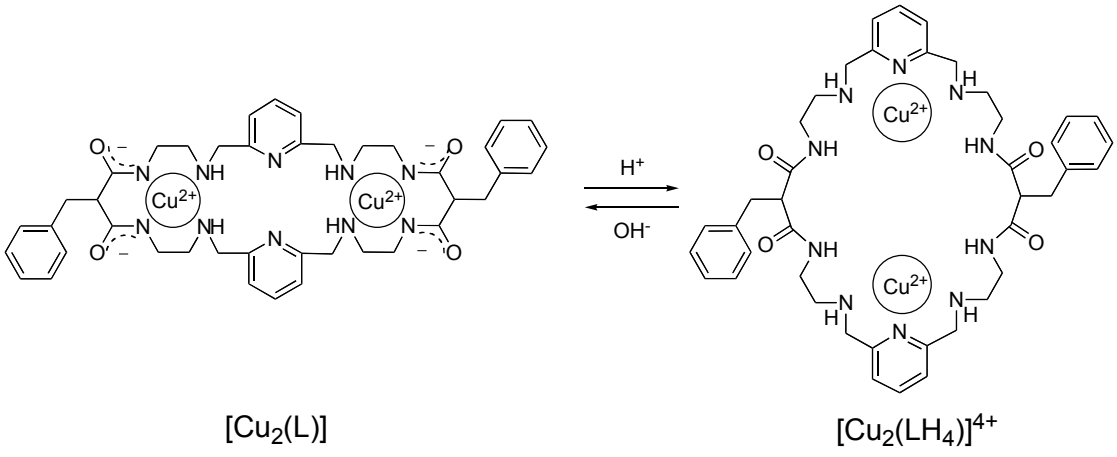

Figure 1.37: pH-dependent intramolecular translocation of the Cu^{2+} ions

Macrocycle LH_4 contains two couples of polydentate compartments capable of binding copper(II) ions and comprises two diamide-diamine tetradentate and two pyridine-diamine (PDA) tridentate binding sets which share the four secondary amino groups.[136] Two distinct colours and types of bands are observed as a function of pH.

At low pH (3-6) the amide groups are protonated, thus they are non-coordinating and the two copper(II) ions are coordinated by the two available separated tridentate PDA units. This form is complex $[Cu_2(LH_4)]^{4+}$, in which each copper(II) is tricoordinated by the ligand (λ_{max}= 660 nm, deep blue), with the other coordination positions occupied by water.[137]

On raising the pH (6-9) two water molecules are deprotonated to give the blue species $[Cu_2(LH_4)(OH)_2]^{2+}$ and $[Cu_2(LH_4)(OH)]^{3+}$. But if the pH is raised above 10.5 the four amide protons are released and each copper(II) moves inside one of the two deprotonated diamide-diamine moieties to give the neutral complex $[Cu_2(L)]$ (Figure 1.37).[138] This is reflected by a purple-pink solution.

This system was modified into a molecular receptor recognizing specifically the substrate imidazole.

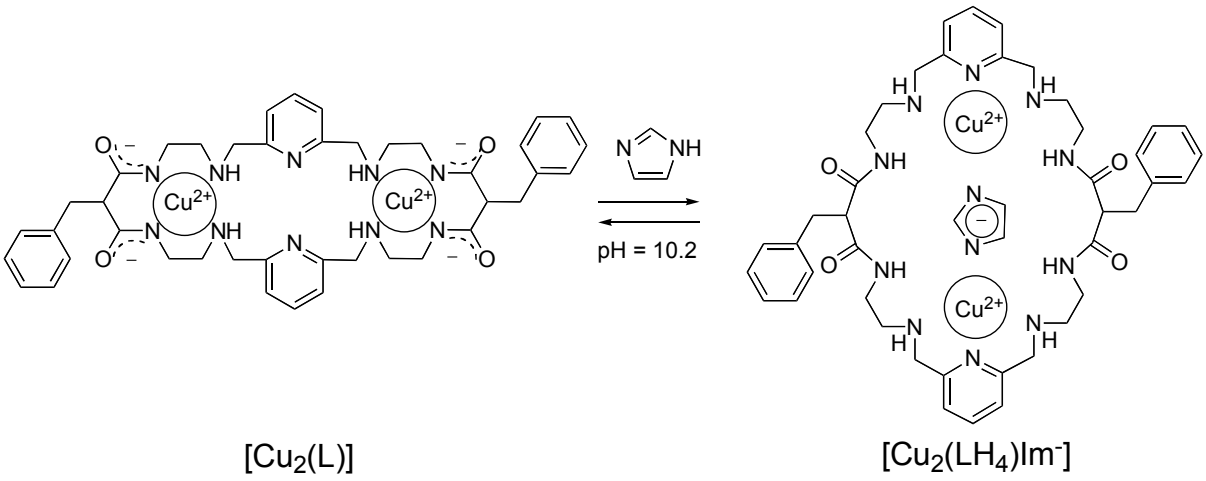

Figure 1.38: The imidazole-induced translocation equilibrium at pH = 10.2

The lock-and-key principle could be achieved in this system with imidazole. In a sharp pH range (10.0 < pH < 10.4) and in the absence of imidazole, the $[Cu_2(L)]$ species is predominant in its closed form (95%) whereas in the presence of imidazole, it represents 10% of the mixture and the $[Cu_2(LH_4)(Im^-)]$ species is around 90% (Figure 1.38). The species contains a bridging imidazolate anion which forms thanks to the particularly stable [Cu(II)-Im^--Cu(II)] disposition.[139] Therefore, in this system, it is the substrate itself which makes the cations translocate and causes the system to open, thus allowing binding to take place. This recognition is associated with an obvious colour change thus providing a signal for selective inclusion.

1.3.3.2 Contraction/stretching process of a muscle-like rotaxane dimer[140, 141]

Linear machines and motors are essential in many biological processes such as, in particular, contraction and stretching of the skeletal muscles. In relation to “artificial muscles”, one-dimensional molecular assemblies able to undergo stretching and contraction motions represent thus an exciting target.

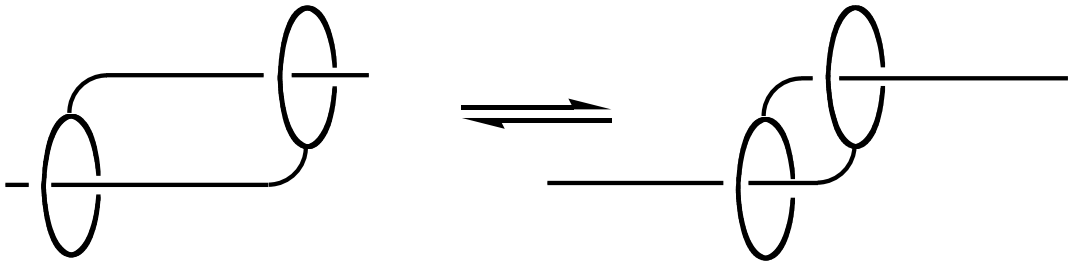

Figure 1.39: Gliding of the filaments in a rotaxane dimer: interconversion of the stretched geometry and the contracted conformation

A multicomponent system able to contract or stretch under the action of an external chemical signal was designed and made in our group a few years ago. The system is based on a symmetrical doubly threaded topology as represented in Figure 1.39. The motion is easy to visualize: both "strings" (mimicking the myosin-containing thick filament and the actin thin filament of the striated muscle) move along one another but stay together thanks to the rotaxane nature of the system.

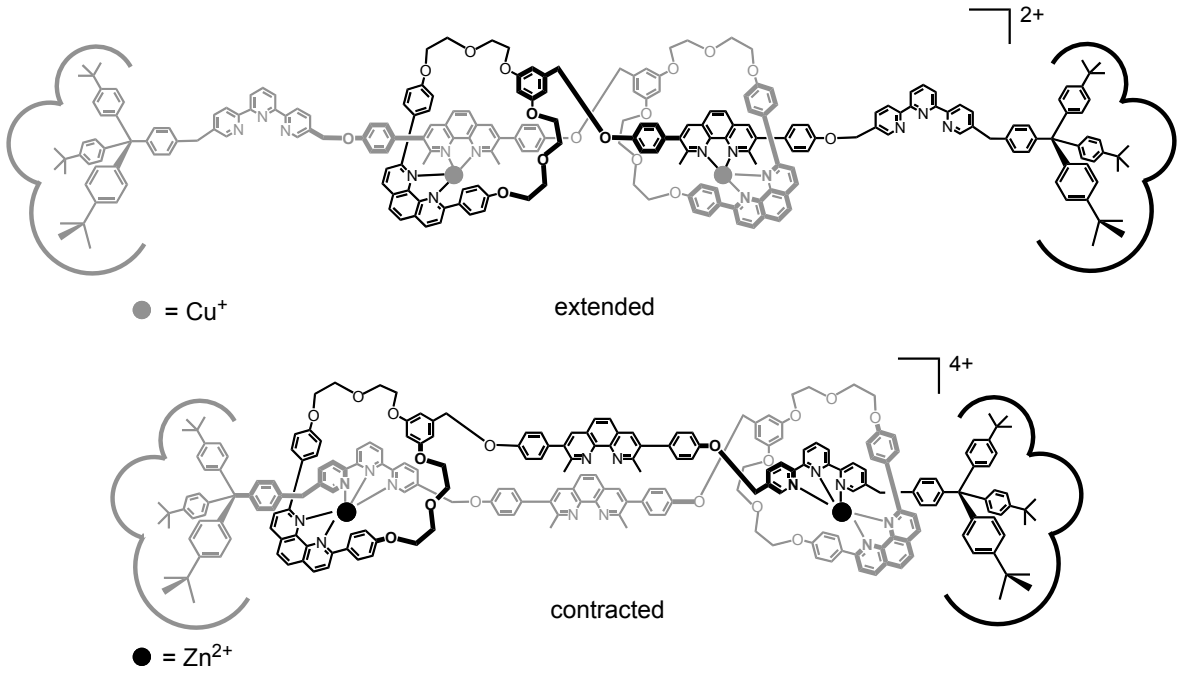

Figure 1.40: The two states of the muscle-like molecule

The copper-complexed rotaxane dimer was synthesized (more than 20 steps from commercially available compounds). As shown in Figure 1.40, each "filament" contains both a bidentate chelate (coordinated to copper(I) in the extended situation) and a tridentate chelate of the terpy type, which is free in the copper(I) complex. The rotaxane dimer was set in motion by exchanging the complexed metal centres. The free ligand, obtained in quantitative yield by reacting the 4-coordinate copper(I) complex (stretched geometry) with an excess of KCN, was subsequently remetalated with $Zn(NO_3)_2$ affording quantitatively the 5-coordinate Zn^{2+} complex in the contracted situation (Figure 1.40). The reverse motion, leading back to the extended situation, could be easily induced upon addition of excess $Cu(CH_3CN)_4^+$. From CPK model estimations, the length of the organic backbone changes from 85 to 65 Å between both situations.

1.4 Design of the Ph.D. project

1.4.1 From the molecular muscle prototype and beyond

As mentioned in section 1.3, topologically interesting molecules are not only synthetic challenges. Beautiful complex structures exist in Nature. When you look at the crystal structure of the capsid of the bacteriophage virus HK97 presented in section 1.3,[52] you realize that the scaffolding of interlocked cyclic proteins make the thin membrane resistant to physical, mechanical and chemical attacks. It is thus a great challenge for chemists to try and make such complicated architectures and see whether they would present interesting properties. Few years ago, our group imagined to build a rotaxane tetramer (Figure 1.41) which can be seen as an orientated molecular square. Once polymerized, such kind of a structure bearing interlocked molecular rings and threads would lead to a thin and resistant two-dimensional membrane, reminiscent of the one of the capsid of virus HK97.

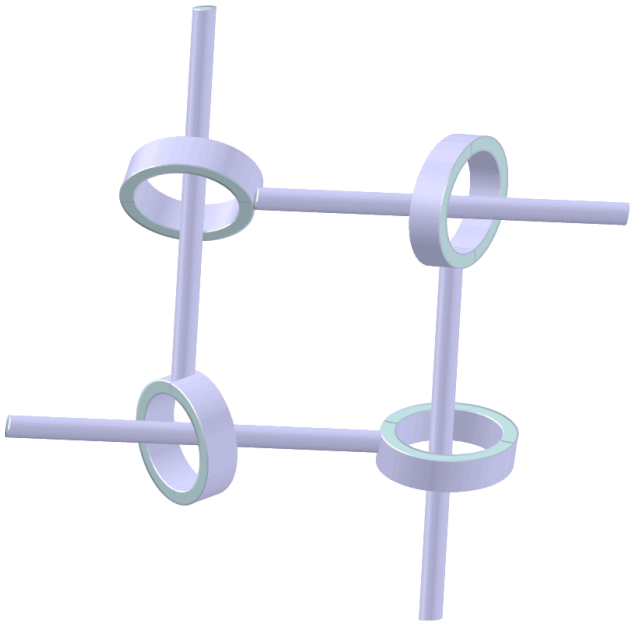

Figure 1.41: Schematic representation of a rotaxane tetramer

The ligand used in the molecular muscle prototype would be the perfect candidate to perform such an assembly into a tetrameric array. But when you look at the crystal structure (Figure 1.42) of the copper complex of the precursor of the molecular muscle, which is a rotaxane dimer, you clearly see that each ligand is bent and nothing can prevent the structure from deforming and yielding the smallest molecule possible. The design of the ligand had to be optimized.

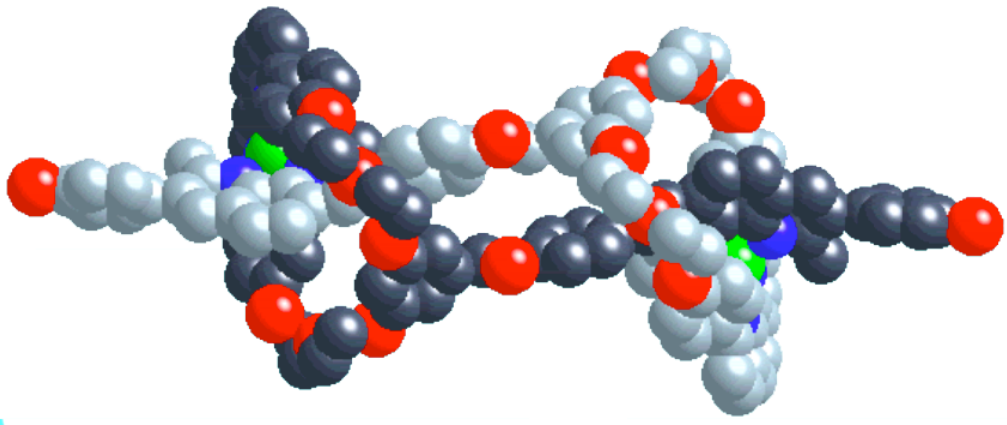

Figure 1.42: Crystal structure of the molecular muscle precursor

1.4.2 Chelates with orthogonal coordination axes

In order to obtain a tetramer of rotaxane, we thus decided to rigidify the ligand, especially the connection between the thread and the ring. When the phen unit was put at the opposite of this connection in the muscle project, we decided in our case to put the chelate in the ring at the exact junction of the thread and the macrocycle. This connection is thus expected not to be flexible anymore. The chelate on the thread is kept identical to the muscle project. The designed ligand is thus bearing two chelates units having their coordination axes orthogonal to each other, which should provide a square upon addition of a metal centre as template (Figure 1.43).

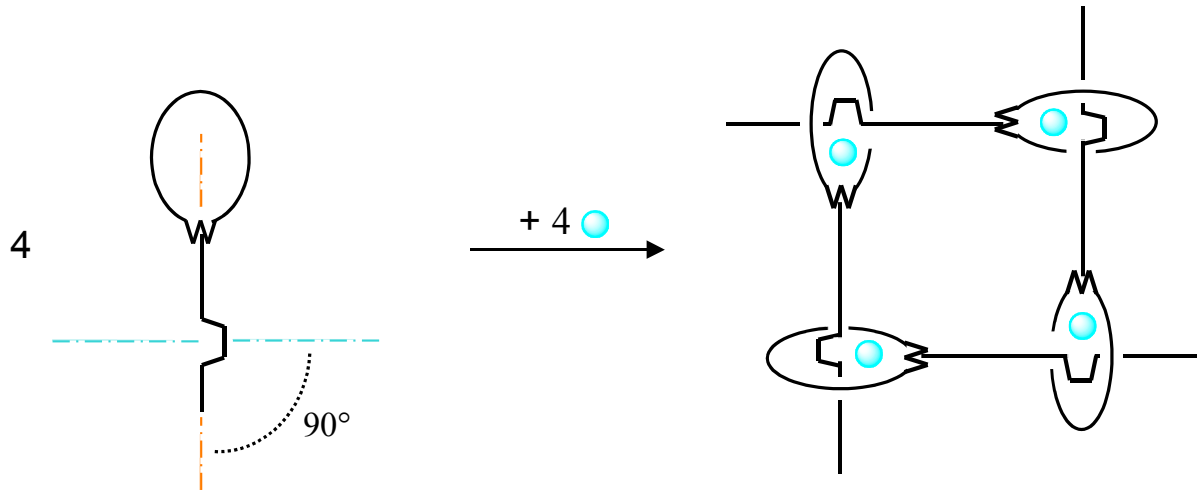

Figure 1.43: Design of a ligand with chelate coordination axes orthogonal to one another

The last degree of freedom is the choice of the chelate units. Our group has extensively used and studied 2,2':6',2"-terpyridine (*terpy*) and 1,10-phenanthroline (*phen*) units in the past as building blocks for the construction of molecular machines, new topologies or molecular models to study electron transfer. Hence, two different and complementary projects were imagined: (1) synthesis of a homochelate ligand, bearing one phen unit in the macrocycle and an other one in the thread, and assembly around a 4-coordinate metal centre, (2) synthesis of a

heterochelate ligand, bearing a terpy unit in the macrocycle and a phen nucleus in the thread, and assembly around a 5-cordinate metal centre (Figure 1.44). Tomas Kraus, a postdoctoral fellow in the laboratory, carried out the first project[142] and I investigated the second project.

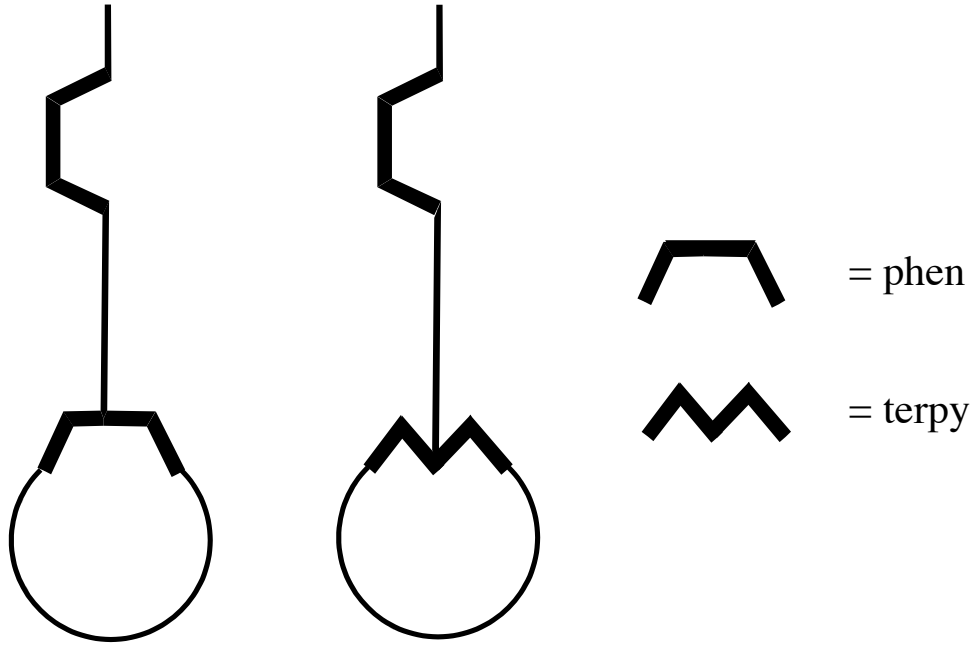

Figure 1.44: Two complementary projects

1.4.3 The work of Tomas Kraus[142]

In order to obtain the desired ligand, the phen nucleus at the junction of the thread and the macrocycle had to be functionalized both in positions 2 and 9, and in the back. But this latter functionalization was not straightforward as the phen nucleus, compare to the terpy one, does not have a natural axial symmetry in the back. In order to achieve such a symmetry, Tomas imagined to synthesize a macrocyclic precursor containing two carbonyl functions respectively in 5 and 6 positions, and this dione could be transformed into a 5-membered ring, either oxazole or imidazole depending on the conditions used. The final ligand was thus achieved in 13 steps from 1,10-phenanthroline (Figure 1.45).

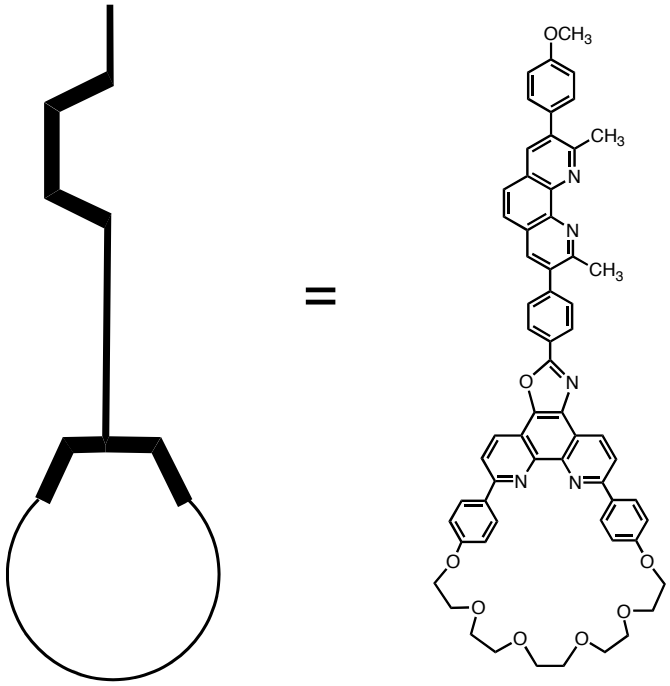

Figure 1.45: Representation and chemical structure of the ditopic homochelate ligand synthesized by Tomas Kraus

Upon addition of Cu(I) salt to a solution of the homochelate ligand in acetonitrile, the mixture turned brown-red, indicating the formation of a copper(I) complex bearing phen units as ancillary ligands. But the nuclearity of the complex could not be guessed at this stage. ES-MS clearly demonstrated that, depending on the concentration used, two distinct species could be observed: at concentration 10^{-5} M, only one significant peak at 1059.29 D was observed, with isotope spacing corresponding to a triply charged species $[\mathbf{L}+Cu]_3^{3+}$. At the highest concentration measured, 10^{-2} M, a major peak at 1059.32 D was observed, with isotope spacing corresponding to the species $[\mathbf{L}+Cu]_4^{4+}$, and a peak at 1461.15 D corresponding to $[(\mathbf{L}+Cu)_4PF_6]^{3+}$ was also observed. ^{1}H NMR studies of the methoxyl group chemical shift confirmed those results (Figure 1.46): at high concentration ($5x10^{-3}$M), the tetramer is the major compound (trimer/tetramer ratio = 27:73), and upon dilution to 10^{-3} and then $5x10^{-5}$, the

trimer becomes predominant (58:42). But the process is really slow since it takes days for the system to evolve from the former to the latter situation.

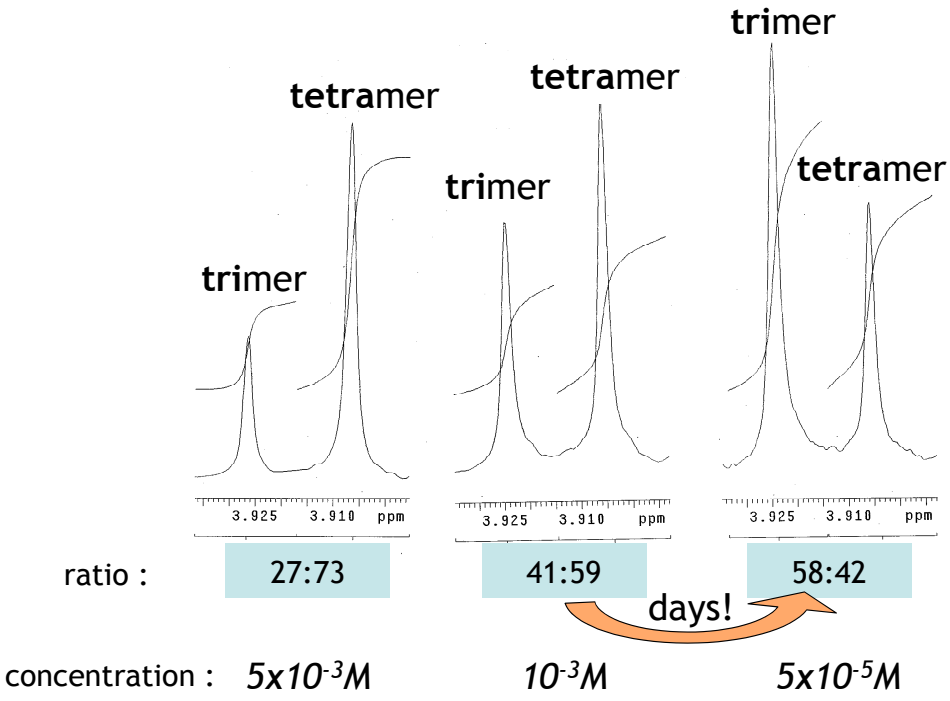

Figure 1.46: ^{1}H NMR studies proving the dependence of the trimer/tetramer ratio on concentration

These results clearly show that the tetramer is in equilibrium with the trimer, that no other species are formed, and that playing on the concentration can shift the equilibrium. Entropic factors seem to be critical in that case. Indeed, for entropic reasons, the smallest assembly is expected to be formed preferentially. On the other hand, the strainless tetrahedral geometry of the 4-copper(I) complex should be favored in terms of enthalpy. Thus, the delicate balance of the two factors determines the ratio of the two species, which can be tuned by changing the solution concentration (Figure 1.47).

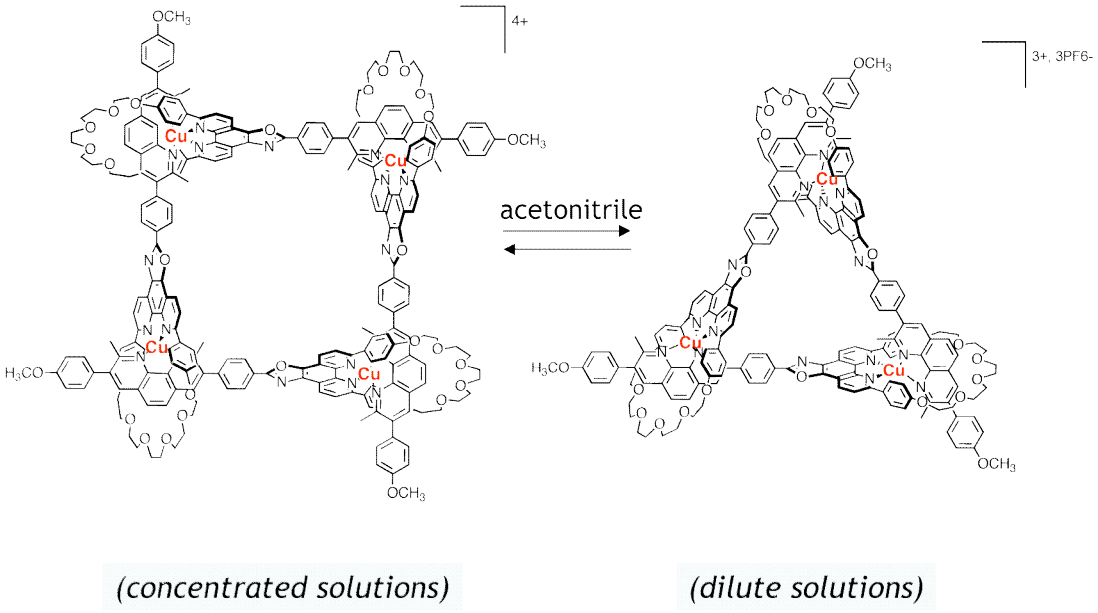

Figure 1.47: Equilibrium trimer/tetramer tuned by concentration

The same kind of related observations have been made by Fujita and co-workers when trying to assemble 4,4'-bipyridine units and Pd(II) centres into a square: triangles have often been observed as by-products, and the result presented in section 2.4 is the only case in which triangles were not observed.

1.4.4 General overview of the Ph.D. thesis

In the first two chapters of this manuscript, we will present the results obtained in the heterochelate ligand project in order to build two-dimensional multirotaxanes (tetramer, trimer or dimer). Considering the high level of complexity in the design and synthesis of the target ligand, the project splits into two complementary sub-projects. In Chapter 2, we will discuss the design and synthesis of an acyclic precursor of the heterochelate ligand. We will see that obtaining a macrocyclic terpyridine functionalized in the back is not an easy task, and we will thus present in Chapter 2 the synthesis of 4'-(4-bromophenyl)-5,5"-dimethyl-

2,2':6',2"-terpyridine, precursor of the acyclic derivative of the target ligand, which was then obtained by coupling the terpy moiety with a dissymmetric phenanthroline under classical Suzuki conditions. Coordination chemistry of this acyclic ligand with 5-coordinate metal centres, namely Zn(II) and Cu(II), will be presented.

In Chapter 3, we will present the synthesis of the target macrocyclic heterochelate ligand. Several strategies have been investigated to functionalize the terpy nucleus in the 5 and 5" positions in order to obtain a precursor of a macrocyclic compound. Lithiation of the methyl positions appeared to be the best pathway, and the macrocycle bearing a terpy functionalized in the back was then obtained very efficiently. Suzuki coupling with the phen moiety then yielded the desired compound. Coordination chemistry of this highly rigid macrocyclic ligand with 5-coordinate metal centres was then investigated, and comparison with the results obtained with the acyclic compound will be presented.

In Chapter 4, we will present the synthesis of a brand new bis-macrocyclic compound bearing a terpy nucleus in each ring, that could be obtained on the way leading to the heterochelate macrocyclic compound. Two strategies yielding this compound will be presented, one much more efficient than the classical other one. The first attempts to thread two molecular rails through two of these bis-macrocycles, and thus to make another kind of tetramer of rotaxane, will be discussed.

Chapter 2
Acyclic heterochelate project: a highly rigid ditopic conjugate with orthogonal coordination axes

2.1 Design of the ligand: orthogonal coordination axes

The synthesis of a rotaxane tetramer is a real challenge. The choice of the building blocks and their connections is thus crucial. One can imagine to obtain a square-like structure by various pathways. The specificity of our group over the past few years has been to use metal centres as templates to build complex architectures, and especially topologically interesting structures.[15, 143-145]

Considering the results obtained in the synthesis of the molecular muscle prototype, the need to rigidify the chemical structure of the ligand was obvious. We thus kept the idea of building a ditopic ligand, but it had to be highly rigid in order to prevent the molecule from bending and thus yielding the dimer.

When the work of Tomas Kraus was dealing with synthesizing a ditopic ligand bearing two phen units,[142] ours was to achieve a heterochelate ditopic ligand bearing both a phen and a terpy unit. The terpy unit being a terdentate ligand and the phen unit a bidentate one, assembly of these chelates would occur upon addition of a 5-coordinate metal. Tomas Kraus used the classical coordination chemistry of phen units on copper(I) which has been extensively used and studied in the laboratory.

As mentioned in chapter 1, considering the difficulty of synthesizing the target ditopic ligand bearing a macrocycle, we first investigated the synthesis of its acyclic derivative and the assembly of such a ligand with copper(II) and zinc(II).

As far as we know, two-site ligands whose chelate coordination axes are orthogonal to one another are not common. Such compounds should favour the formation of multinuclear complexes with well defined geometries and nuclearities.[76, 146, 147] Once incorporated in macrocyclic systems, they will also allow the synthesis of multi-rotaxanes, as will be detailed in chapter 3. The coordination principle is given in Figure 2.1.

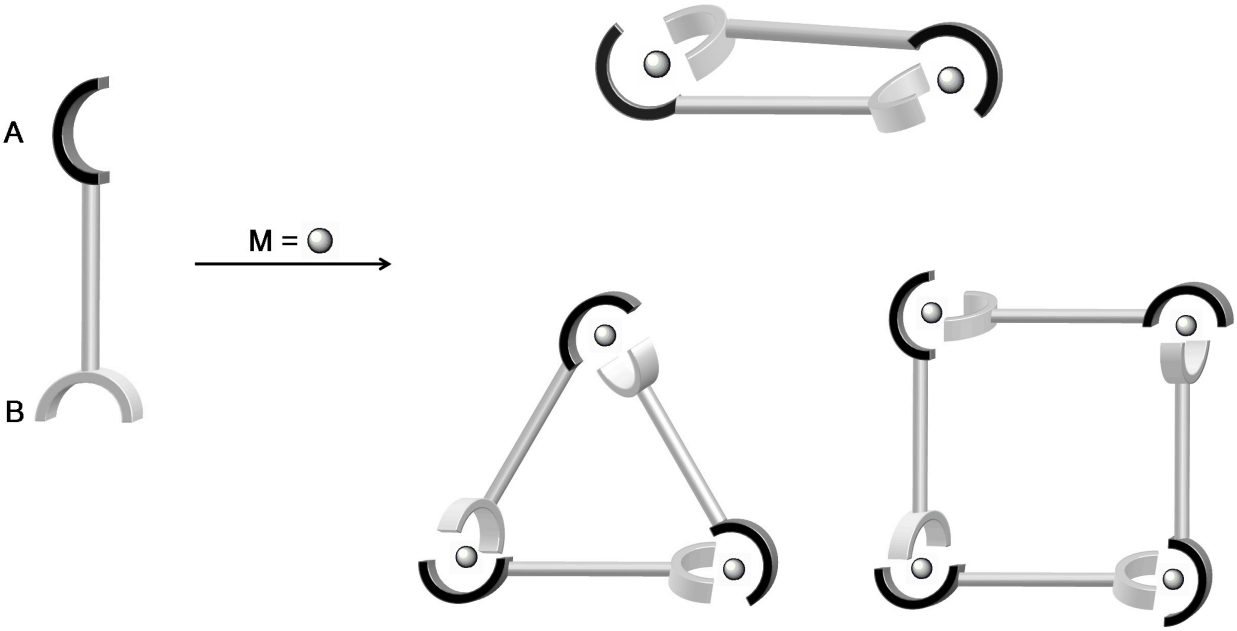

Figure 2.1: Formation of M(A)(B) complexes should lead to oriented cyclic structures. Depending on the coordination sphere geometry of the transition metal used, various rings and nuclearities could be obtained. (A = bidentate; B = terdentate)†

If the complexed metal M has a strong preference for 5-coordinate situations, M(A)(B) complexes should be strongly favoured versus symmetrical complexes of the $M(A)_2$ or $M(B)_2$ type.

† Recently, the synthesis of various metallamacrocycles has been reported using terpy-based ligands, by Constable *et al.*[148]

The present chapter is dealing with the synthesis and the properties of such a 2-site ligand, containing a terpy unit attached to a phen nucleus (Figure 2.2).‡ The rigid linker used (1,4-phenylene) has been chosen as short and rigid as possible, and connects the two chelates via appropriate positions (4' position of terpy and 3 position of phen) so as for the coordination axes to be perpendicular to one another. The geometry of terpy is indeed very appropriated to an axial functionalization in the back (via 4' position), whereas such kind of symmetry was not easy to introduce in the project of Tomas Kraus. The terpy nucleus is functionalized at 5 and 5" positions with methyl groups in order to prepare the further introduction of a macrocycle. The phen unit bears an anisyl group which will act as a ^{1}H NMR probe during the synthesis.

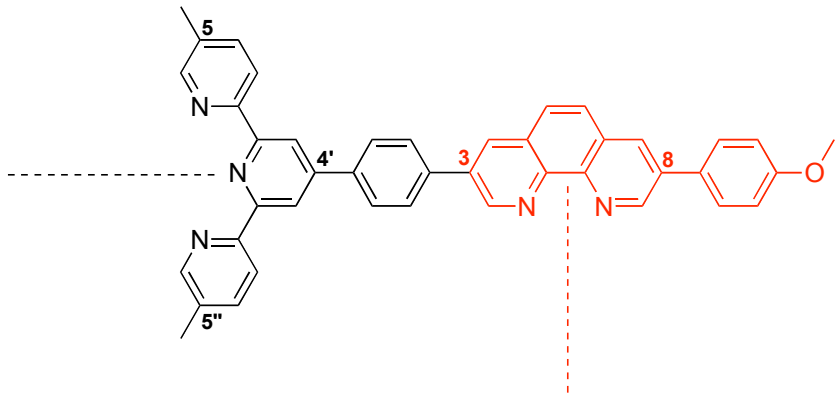

Figure 2.2: Chemical structure of the target molecule, whose chelate coordination axes are orthogonal to one another

‡ It should be noted that recently, the synthesis of a ligand incorporating directly bonded phen and terpy nuclei has been reported by Gaviña *et al.*[149] In that case, the phen unit is connected to the 5 position of the terpy.

2.2 Synthesis of the acyclic phen-terpy conjugate

2.2.1 Retrosynthetic scheme

The strategy to obtain the desired molecule is quite straightforward: each chelate is introduced in a fragment, and both of them will be coupled with one another under Suzuki classical conditions (Figure 2.3). The spacer between both chelates was decided to be incorporated in the terpy fragment using the Kröhnke synthesis. As far as the phen fragment is concerned, dissymmetry had to be introduced so as to have an anisyl unit on one side, and a precursor to the Suzuki coupling on the other side. The synthesis of the terpy and phen moieties will be presented in the next paragraph.

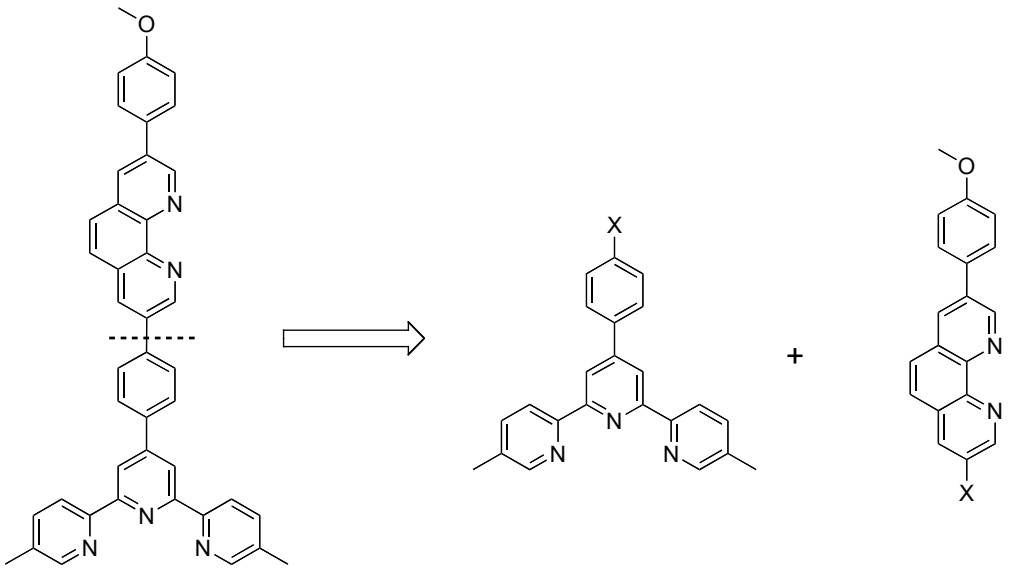

Figure 2.3: Retrosynthetic scheme

2.2.2 Synthesis of the terpy moiety

The Kröhnke synthetic pathway relies on the coupling of an azachalcone with a pyridinium iodide, and in our case, both of these building blocks are obtained from the same compound: 2-acetyl-5-methylpyridine **1**. As the terpy moiety is a central building block both in this project and in the macrocyclic ligand project, each step of this synthesis was optimized in order to obtain the highest yields possible and the largest amount of compound **4**.

2.2.2.1 Synthesis of 2-acetyl-5-methylpyridine 1

Compound **1** had previously been made by reacting Grignard reagent with the nitrile derivative.[150] We developed a new efficient route inspired by the procedure described by Holm.[151] In a first step, 2-bromo-5-methylpyridine was transformed into its lithiated derivative by addition of n-butyllithium in diethylether at –78°C under argon. 1.1 equivalents of N,N-dimethylacetamide were then cautiously added to the solution mixture. Further hydrolysis, extraction and purification by column chromatography afforded **1** in 52% yield (Figure 2.4).

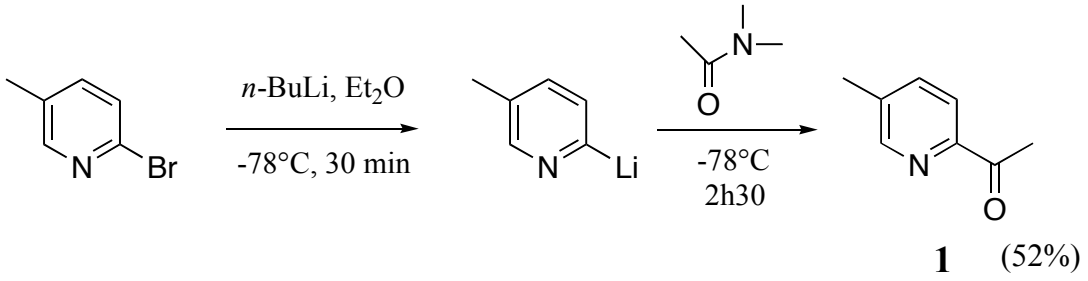

Figure 2.4: Synthesis of compound **1**

2.2.2.2 Synthesis of 4-bromo-2'-azachalcone 2

Compound **2** was obtained thanks to a classical Claisen-Schmidt condensation between an aldehyde having no α-hydrogens (4-bromobenzaldehyde) and the ketone **1** (Figure 2.5). The crossed-coupling reaction was carried out in methanol in the presence of a strong base (NaOH, 1M). The β-hydroxy ketone was thus formed, but the conditions used were sufficient to cause dehydration. The α,β-unsaturated ketone, referred here as azachalcone by the presence of the pyridyl nucleus, was thus produced in a good yield (86% after recrystallization).[152, 153] The reaction conditions employed in the present experiment favoured the formation of the desired compound because this material was not soluble in the aqueous-alcohol solvent and precipitated out from the solution as it formed, thus driving the reaction to completion.

Compound **2** had never been synthesized before, so it has been fully characterized by ^{1}H and ^{13}C NMR, and EI-MS.

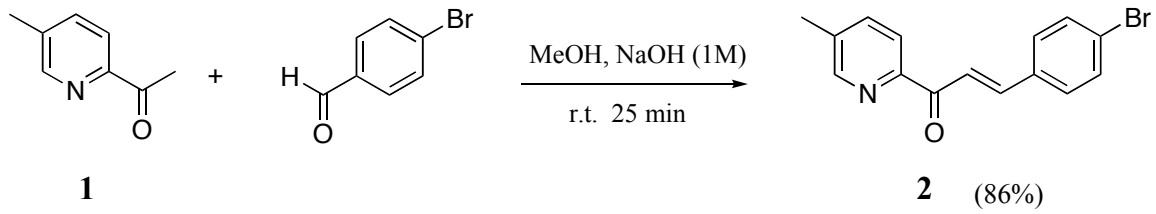

Figure 2.5: Synthesis of compound **2**

2.2.2.3 Synthesis of 1-(5-methyl-2-pyridylacetyl)pyridinium iodide 3

Compound **3** was obtained by reaction under argon between **1** and 1.1 equivalents of iodine in freshly distilled pyridine, which played here both the role of solvent and reagent.[154] The first step of this reaction must have been the iodination of the methylated ketone **1**, which then underwent nucleophilic substitution of pyridine, hence yielding **3** as final product, which

precipitated out of the solution mixture. After recrystallization in pure methanol, the product was obtained with a good yield (74%) as sparkling green needles (Figure 2.6). It should be noted that the amount of pyridine is critical in this procedure: the lesser the better, certainly for obvious solubility reasons. The yield of this step was thus improved from 23% to 74%.

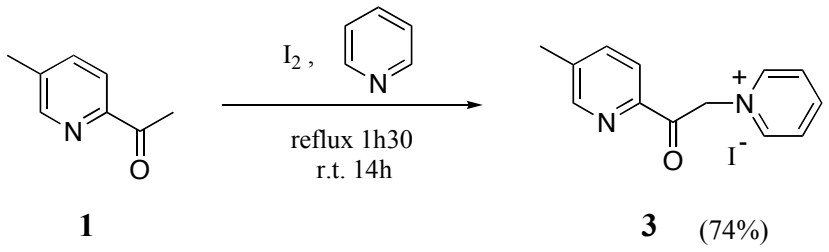

1 **3** (74%)

Figure 2.6: Synthesis of compound **3**

2.2.2.4 Synthesis of 4'-(4-bromophenyl)-5,5"-dimethyl-2,2':6',2"-terpyridine 4

Terpyridine **4** was obtained following the Kröhnke procedure, between azachalcone **2** and pyridinium iodide **3** in acetic acid (Figure 2.7). A Michaël addition afforded in a first step a diketone intermediate, which was not isolated. After playing the role of a base in the first step, ammonium acetate enabled the central ring of the terpyridine to close and thus afforded the final compound **4** in 60% yield after column chromatography. This new compound has been fully characterized by ^{1}H and ^{13}C NMR, HMQC and HMBC 2D ^{1}H-^{13}C experiments, EI-MS and elementary analysis.

It should be noted that we managed to synthesize compound **4** via an alternative route, replacing acetic acid by methanol. In that case, terpy **4** spontaneously precipitated out of the solution mixture, and no further purification was needed. The overall yield was the same than in the first route.

This optimized synthetic pathway afforded more than 8 grams of terpyridine **4**.

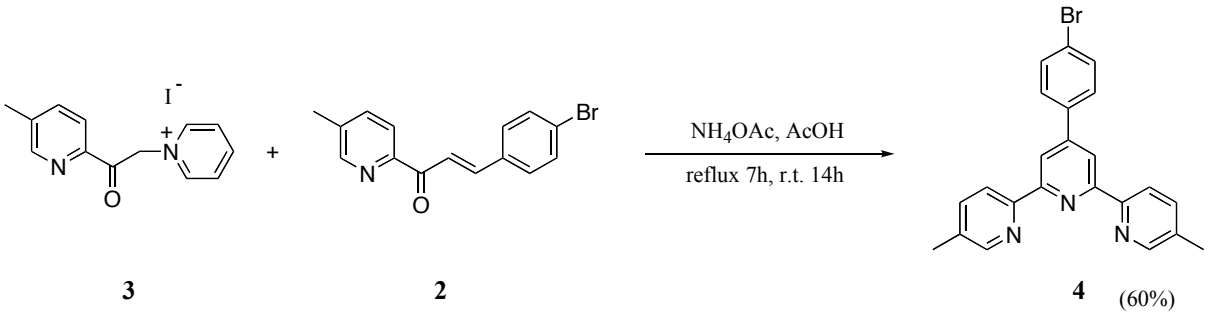

3 **2** **4** (60%)

Figure 2.7: Synthesis of compound **4**

2.2.3 Synthesis of the phen building block

In order to incorporate the phen nucleus in a thread having an axial symmetry, a phen substituted in 3 and 8 position was necessary. Synthesis of the dissymmetrical phen unit could be achieved in 2 steps from 1,10-phenanthroline. In a first step (Figure 2.8), a mixture of bromine and 1,10-phenanthroline in presence of S_2Cl_2 and pyridine in refluxing 1-chlorobutane afforded 3,8-dibromophenanthroline **5** in 30% yield after column chromatography.[155, 156]

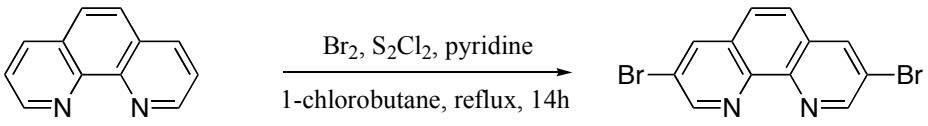

5 (30%)

Figure 2.8: Synthesis of compound **5**

The second step is the one in which dissymmetry is introduced. In order to incorporate only one anisyle group, a statistical Suzuki coupling reaction[156, 157] was performed under classical conditions, using 0.9 equivalent of p-anisylboronic acid, Na_2CO_3 as a base and $Pd(PPh_3)_4$ as a catalyst (Figure 2.9). The mono-coupled product **6** was isolated in 46% yield.

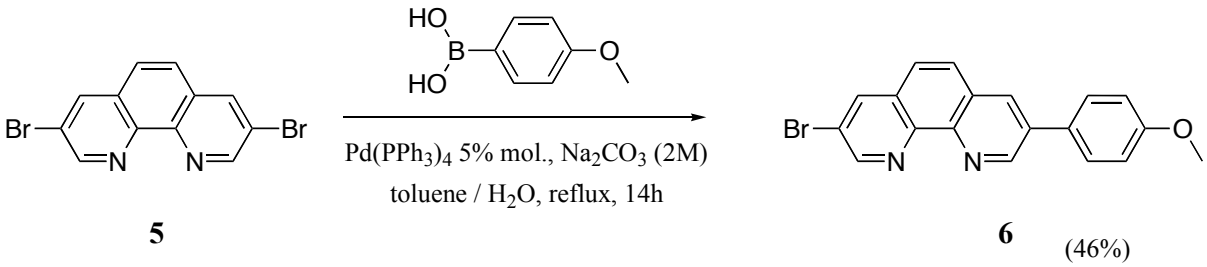

5 **6** (46%)

Figure 2.9: Synthesis of compound **6**

2.2.4 Connection of phen and terpy nuclei

In order to make a Suzuki coupling between the two chelating fragments, one of them should bear a boronic acid (or ester) function. However both fragments are bearing an aryl bromide function. One of the two fragments should thus be turned into its boronic derivative. It appeared that introducing a boronic function directly on the 3 position of the phen was impossible. The only possibility would have been to introduce another phenylene spacer bearing the boronic functionnality. But once coupled with the terpy fragment, this double-phenylene bridge might have been too long for preventing the bending of the ligand. In spite of the "price" of the terpy moiety **4**, we thus decided to modify the functionality at the back of the terpy by changing the bromine atom for a boronic ester function in presence of bis(neopentyl glycolato)diboron according to the well described procedure[158] (Figure 2.10). Remarkably, compound **7** was thus obtained in quantitative yield from **4**, and was fully characterized.

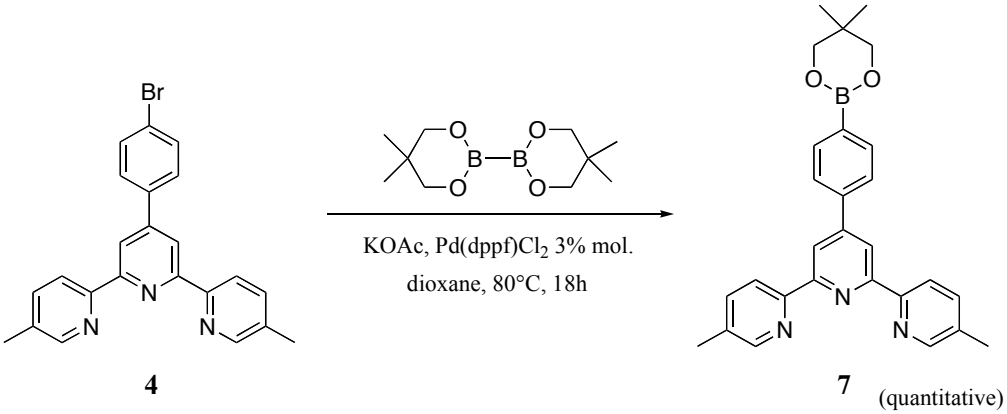

Figure 2.10: Synthesis of compound **7**

A last Suzuki coupling reaction between **6** and **7** under classical conditions yielded the phen-terpy conjugate **8** (24%), containing 7 conjugated 6-membered aromatic rings and 42 delocalized π electrons (Figure 2.11). This low yield is certainly due to the use of a batch of catalyst, which appeared later to be old and not as efficient as expected.

Nevertheless, compound **8** has been fully characterized by ^{1}H and ^{13}C NMR, HMQC and HMBC 2D ^{1}H-^{13}C experiments, HR ES-MS and DOSY (diffusion-ordered spectroscopy).

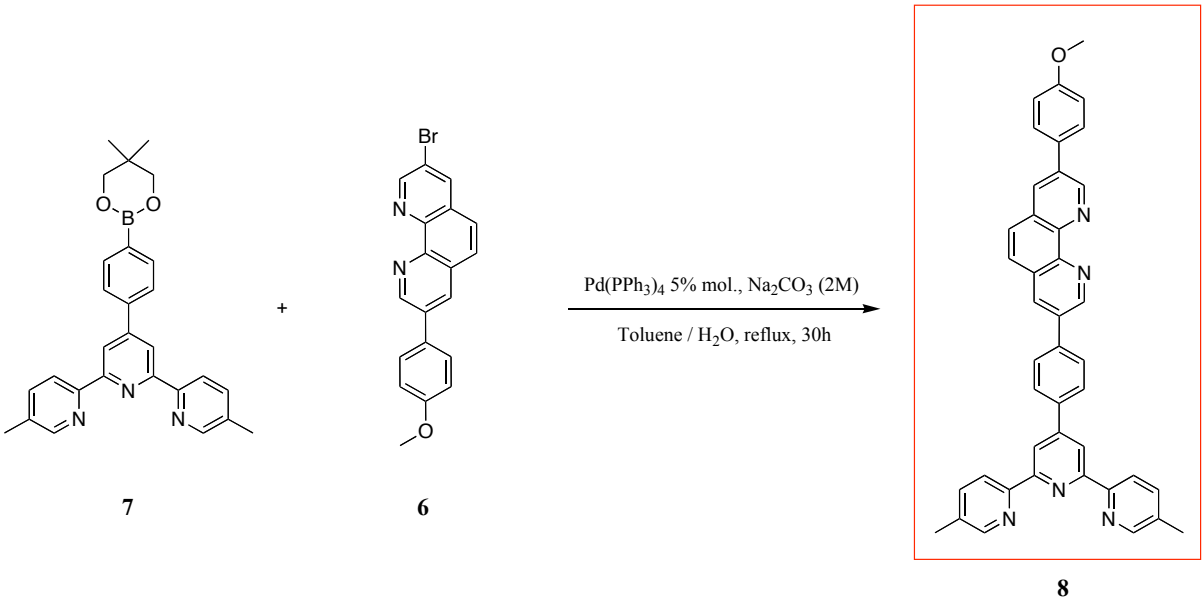

Figure 2.11: Synthesis of compound **8**

2.3 Coordination studies of the phen-terpy conjugate

2.3.1 Zinc(II) complex

2.3.1.1 Synthesis

Zn^{2+} forms stable 5-coordinate complexes and it is most of the time sufficiently labile to allow formation of coordination compounds under thermodynamic control. This metal was thus selected for complexation studies with ligand **8**. It should be noticed that non-distorted trigonal bipyramid geometries, with their two A and B chelates orthogonal to one another, are expected to favour formation of 4-metal centre assemblies similar to that represented in Figure 2.1. By contrast, other 5-coordinate geometries such as, for example, square pyramid or distorted trigonal pyramid, should afford smaller rings such as 3-metal assemblies or even dinuclear species.

For entropic reasons, the reaction between Zn^{2+} and **8** is expected to lead to the smallest possible complex[≠]. Nevertheless the size of the species obtained has to be compatible with the coordination constraints imposed by the metal and the ligand. If distortion of Zn^{2+} coordination sphere and/or of the ligand backbone costs less than the entropic price needed to build the large ideal 4-metal species, lower nuclearities will be formed. This is the case in the present system.

To our surprise, the dimer was the sole complex formed, without formation of tetramer nor even trimer complexes. The reaction is represented in Figure 2.12 as well as a molecular model of the complex.

[≠] *Translational* entropy would favour formation of the highest number of small assemblies, when *conformational* entropy would favour the formation of polymers

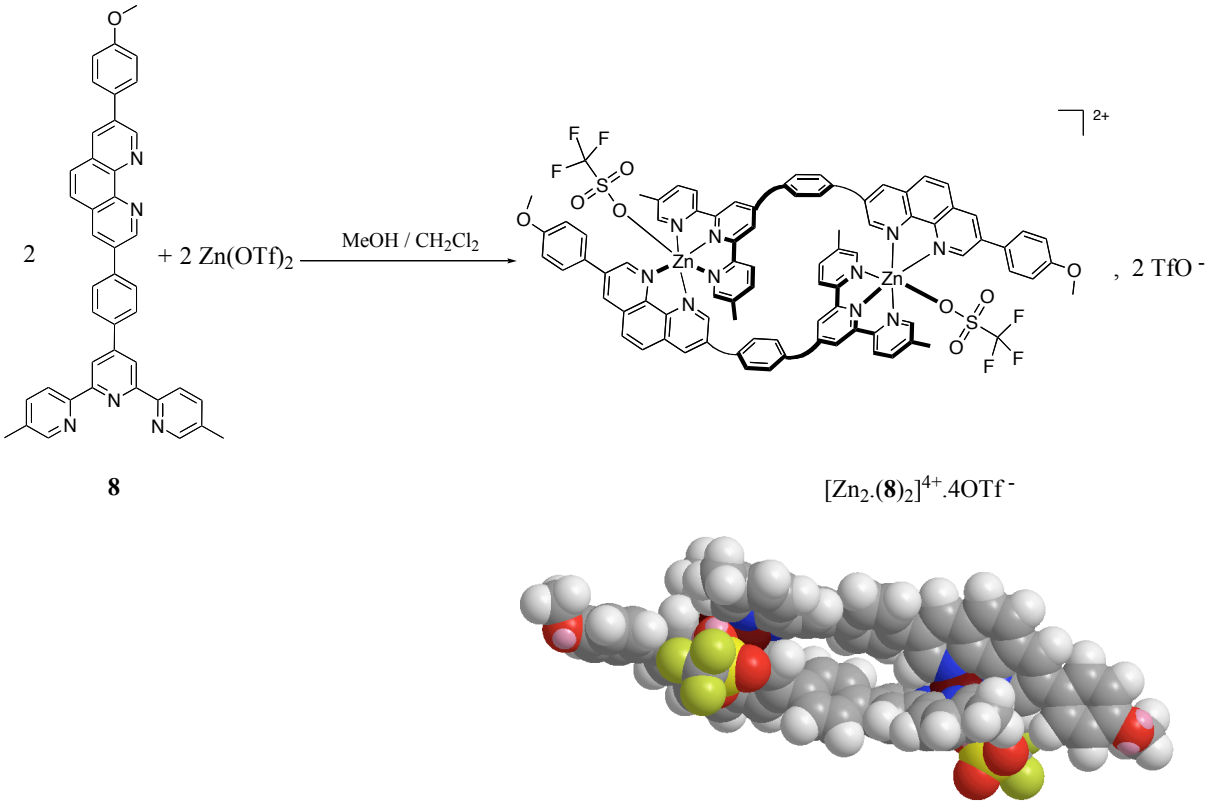

Figure 2.12: Reaction between **8** and Zn^{2+} leading to the dimer complex, and its molecular model (Chem 3D software; energy minimized using MM2 software)

The coordination reaction of Zn^{2+} to **8** was carried out by mixing equimolar amounts of respectively **8** in CH_2Cl_2 and $Zn(OTf)_2$ in MeOH. The resulting orange coloured solution was allowed to stir for 28 hours. The solvent was then evaporated. The crude mixture was taken in methanol, filtered, and the filtrate evaporated to dryness. The dimer complex $[Zn_2.(\mathbf{8})_2]^{4+}.4OTf^-$ was obtained in good yield (78%) as a yellow solid. It is only sparingly soluble in common organic solvents.

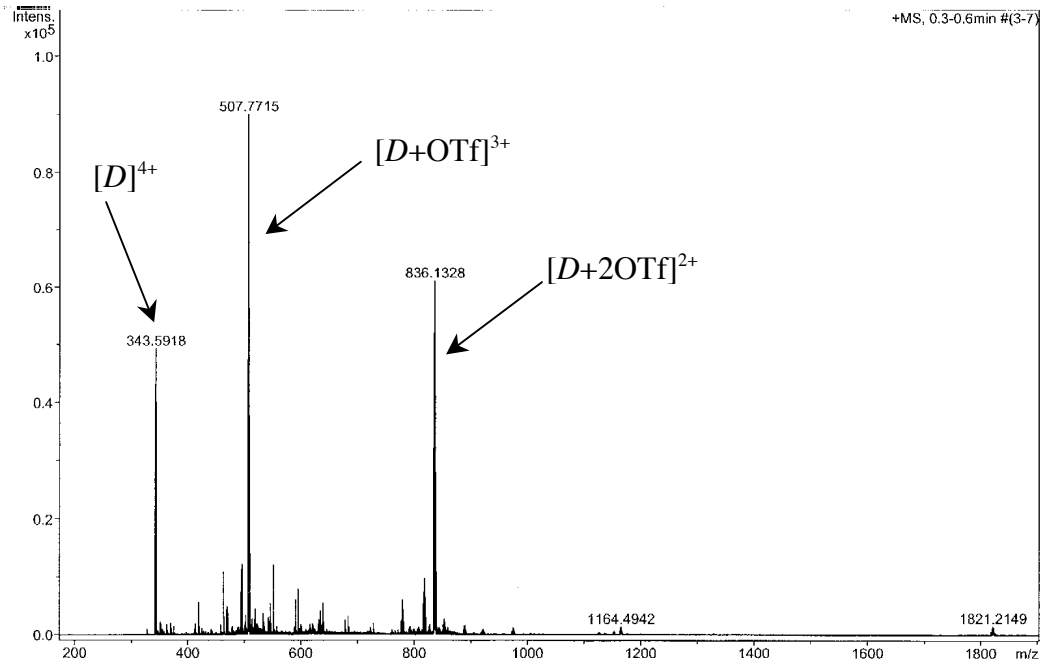

Figure 2.13: HR ES-MS of the zinc(II) dimer complex

2.3.1.2 ES-MS studies

At this stage, it is difficult to know if, in solution, the Zn^{2+} centres are really 5-coordinate or if the counterion (CF_3-SO_3^- = OTf^-) participates in the Zn^{2+} complexation. The X-ray structure of a recently published hexanuclear complex with Borromean rings as organic backbone[66] showed that 6-coordinate Zn^{2+} complexes with $Zn(N)_5(OTf^-)$ coordination spheres are stable. The dimer complex with two 6-coordinate Zn^{2+} centres is moreover certainly less strained in terms of organic ligand distortion than the putative analogous complex in which the Zn^{2+} centres would be 5-coordinate. The chemical structure of $[Zn_2.(\mathbf{8})_2]^{4+}$ (*D*) was proven by electrospray ionization mass spectroscopy (ES-MS) and ^{1}H NMR spectroscopies. HR ES-MS analysis of the yellow solid (Figure 2.13) revealed three major peaks at mass-to-charge (*m*/*z*) ratios of 342.6, 506.4, and 834.6, corresponding to $[D]^{4+}$, $[D+OTf]^{3+}$, and $[D+2OTf]^{2+}$,

respectively (Figure 2.14), a situation that is consistent with the proposed dimer compound $[Zn_2.(\mathbf{1})_2].4OTf$.

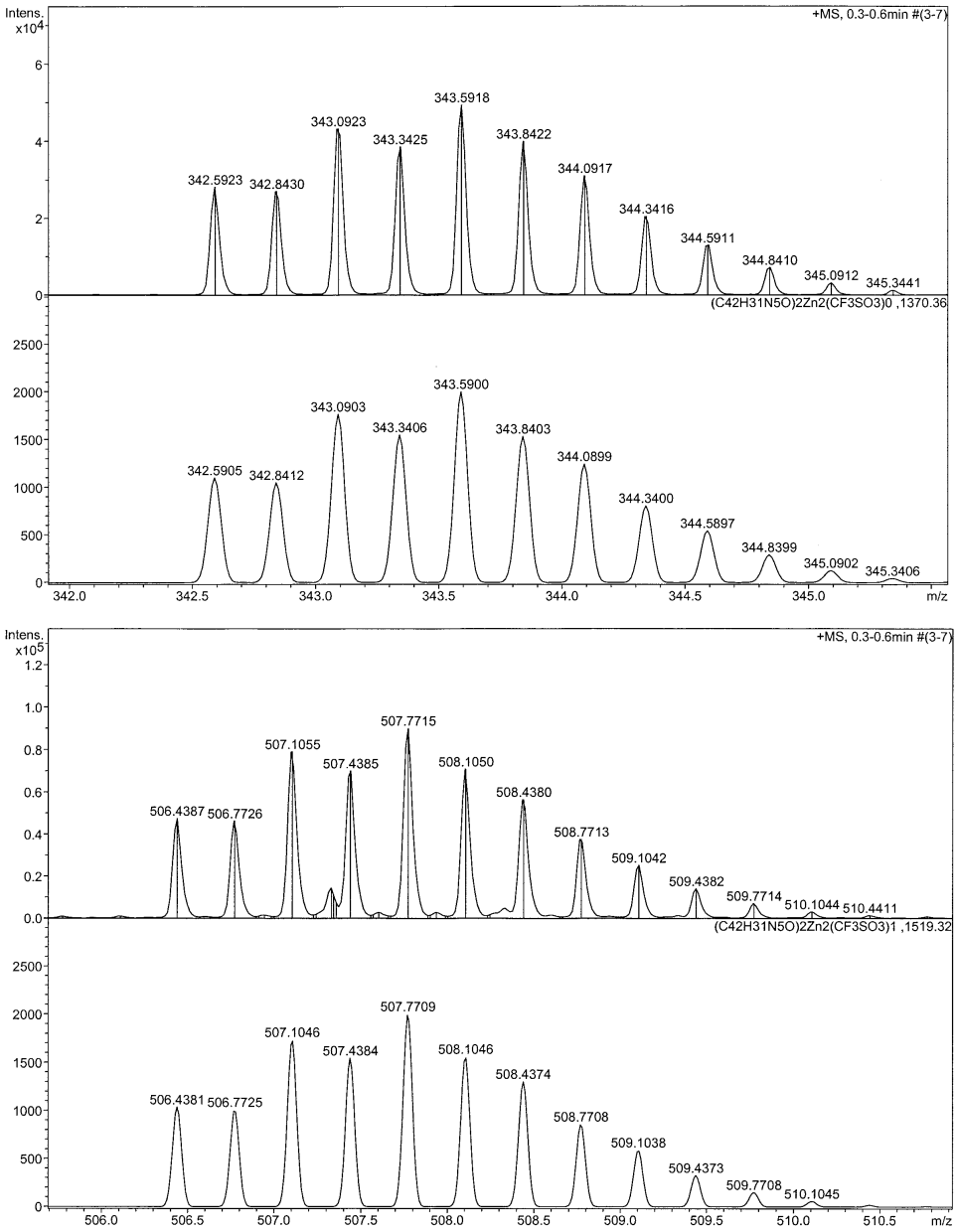

Figure 2.14: Expanded isotopic distribution patterns for $[M]^{4+}$ and $[M+OTf]^{3+}$, which correlate well with the calculated distributions

2.3.1.3 NMR studies

DOSY experiment carried out on a solution of the yellow solid in MeOD (Figure 2.16) revealed unambiguously the presence of a single species, characterized by its diffusion coefficient (D = 470 $\mu m^2/s$; monomer **8** in CD_2Cl_2: D = 1000 $\mu m^2/s$) and its hydrodynamic radius (r_H = 8.5 Å; monomer **8**: r_H = 5.3 Å). Computational simulation of the hydrodynamic radius of an ellipsoid object which matches the experimental value of the radius enabled us to predict the size of the product in solution: a = 14 Å and b = c = 6 Å. The object is thus a prolate ellipsoid (Figure 2.15), which is consistent with the proposed dimer compound $[Zn_2.(\mathbf{8})_2]$.4OTf. The ratio a/b being approximately around 2, it would nevertheless be impossible to exclude the possibility of having an oblate ellipsoid (a = b = 14 Å and c = 6 Å), which would be more consistent with the geometry of the tetramer species. But considering both the results of ES-MS and DOSY experiments, we can tell that the sole product formed during the complexation process is the dimer species $[Zn_2.(\mathbf{8})_2]$.4OTf.

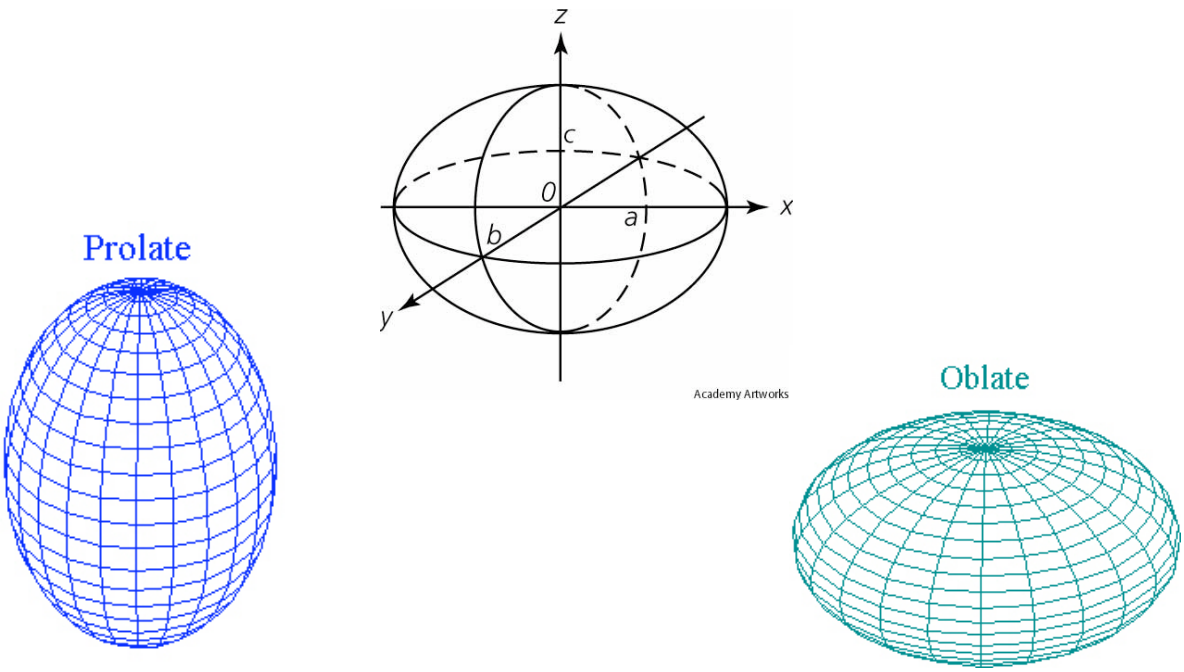

Figure 2.15: Ellipsoid parameters *a*, *b* and *c*; prolate and oblate ellipsoids

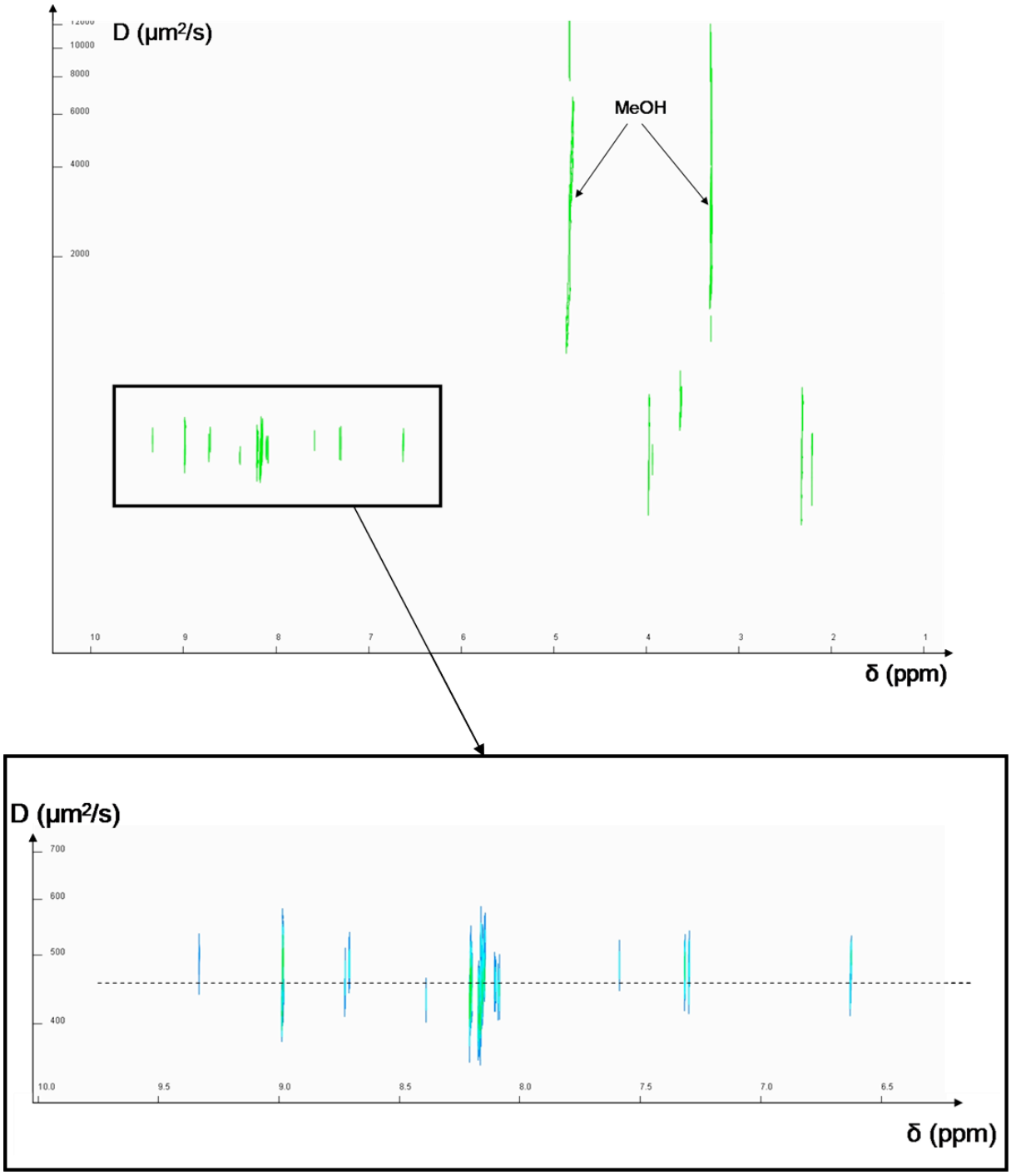

Figure 2.16: DOSY experiment on the dimer complex in MeOD, and zoom on the aromatic region of the spectrum. Apart from the MeOH broad signals, a single product is present

Moreover, ^{1}H NMR clearly shows what was expected for a dimer species: the geometry around the zinc centre is so distorted that the p_2 proton of the phen part of one monomer

points right in the shielding cone of the central ring of the terpy fragment of the other monomer, and consequently the p_2 proton signal is strongly shifted upfield ($\Delta\delta$ = 2.82 ppm).

2.3.1.4 Conclusion

In conclusion, a new phen-terpy conjugate **8** has been synthesized which contains two chelates whose coordination axes are perpendicular to one another. Whereas the expected structure for the Zn^{2+} complex formed with ligand **8** was that of a tetramer ($[Zn_4.(\mathbf{8})_4]^{8+}$), a dimer was the sole product observed. The present example tends to indicate that entropy is a prevailing factor in the complexation process: the reaction leads to the smallest possible complex in spite of probable distortion of the Zn^{2+} coordination sphere and constraints within the organic ligand **8**. Obviously, the use of other transition metal centres than Zn^{2+} with more demanding stereoelectronic requirements, making distortion more difficult, should favour formation of trimers or tetramers. This will be the object of the next paragraph.

2.3.2 Copper(II) complexes

2.3.2.1 Choice of copper(II) as a new template and synthesis of the complexes

The achievement of such complicated structures around metal centres is in our case carried out under thermodynamic control, thanks to labile coordination bonds between the ligands and the metal centre. Indeed the system has to have the possibility to create and break bonds at will, so that it can self-repair its own mistakes, and eventually converge to the most stable product, this one being hopefully the desired one.

The choice of the metal centre is therefore of prime importance. It has to be labile enough in order to enable equilibration and self-repair at the molecular level so as to reach the

thermodynamically most stable situation. At the same time, it must have more demanding stereoelectronic requirements than Zn(II), whose coordination sphere was completely distorted in the previous example and did not impose the desired geometry.

Among the first row transition metal ions, copper displays unusual features related to the geometrical properties of its complexes: the stereoelectronic requirements of copper(I) and copper(II) are markedly different. This characteristic has provided the driving force for setting molecular systems in motion, as seen in chapter 1. Whereas a coordination number (CN) of 4, usually with a roughly tetrahedral arrangement of ligands, corresponds to stable monovalent systems, copper(II) requires a higher coordination number. The most commonly encountered copper(II) complexes have a CN of 5 (square pyramidal or trigonal bipyramidal geometries) or 6 (octahedral arrangement, with Jahn-Teller distortion).

In spite of its paramagnetic character, which would prevent us from using NMR spectroscopy to identify species formed, copper(II) was thus a nice candidate for our studies, especially considering its more demanding stereoelectronic requirements.

The choice of the counterion was again crucial: it should be as less coordinative as possible in order to avoid its coordination to the copper centre, which should remain 5-coordinate. Among the different copper(II) salts available, we decided to use tetrafluoroborate copper(II).

The coordination experiment was carried out by mixing equimolar amounts of ligand **8** in CH_2Cl_2 and $Cu(BF_4)_2$ in CH_3CN respectively (Figure 2.20). The solution turned instantaneously olive green, which is characteristic of Cu(II) complexes bearing phen and/or terpy units in their coordination sphere. The solution was let stir for 19 hours at room temperature, and by addition of diethyl ether a green solid precipitated out. It was then filtered, washed, dissolved again in an acetone/acetonitrile/methylene chloride mixture, and recovered as a solid by addition of diethyl ether in a good yield (89%).

2.3.2.2 ES-MS studies

As proton NMR was not possible on this paramagnetic complex, we first investigated the composition of the mixture by ES-MS (Figures 2.17 to 2.19). It clearly showed the presence of two species corresponding to the dimer and the trimer. The respective amount of each compound could not be evaluated since intensity of peaks in the ES-spectrogram is connected to the amount of product by a response factor, which is specific to each species.

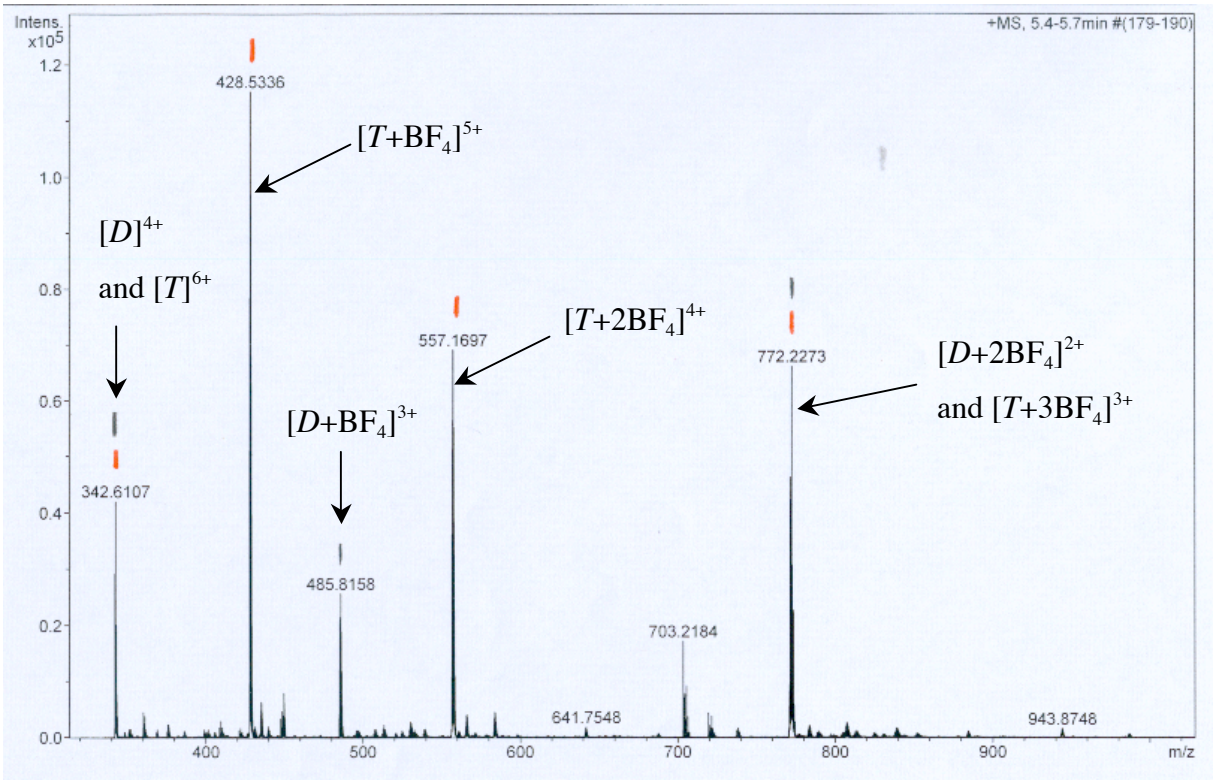

Figure 2.17: HR ES-MS of the mixture of copper(II) dimer and trimer complexes $[Cu_2(\mathbf{8})_2]^{4+}$ and $[Cu_3(\mathbf{8})_3]^{6+}$ (*D* and *T* respectively)

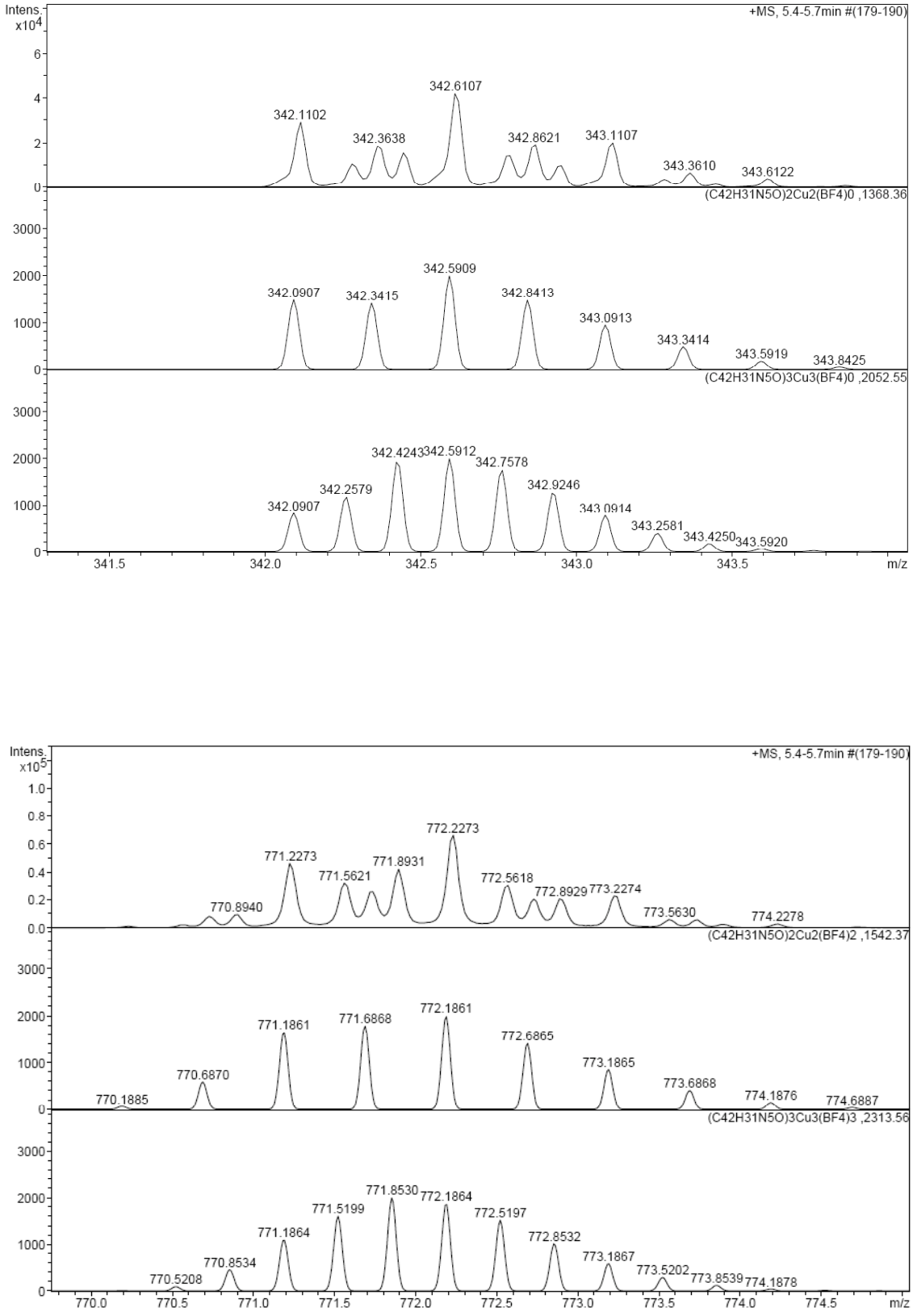

Figure 2.18: m/z ratio experimental regions (1st line) at 342.6 and 772.2 are superpositions of the calculated isotopic patterns of the dimer (2nd line) and the trimer complexes (3rd line)

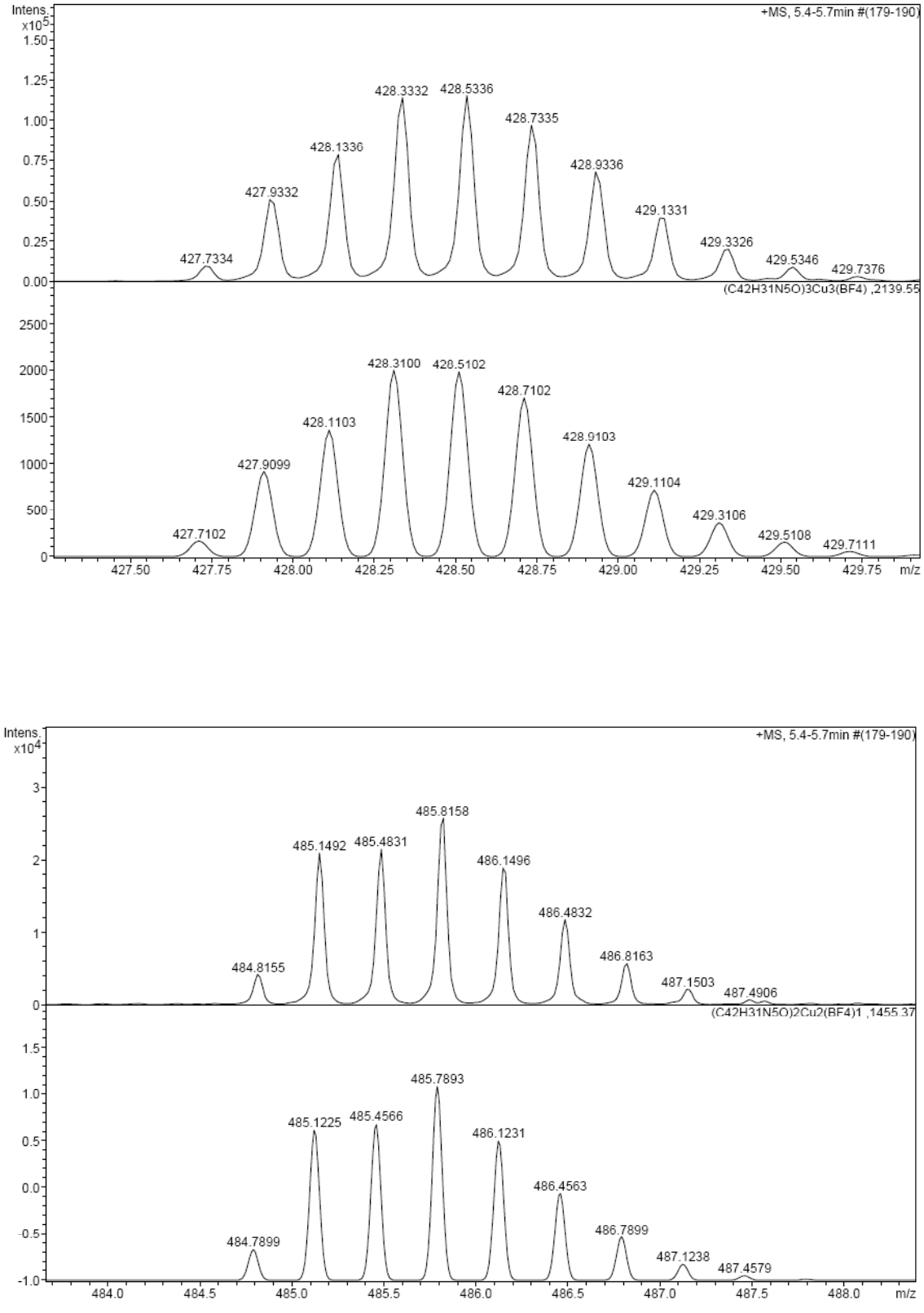

Figure 2.19: Expanded isotopic distribution patterns for $[T+BF_4]^{5+}$ and $[D+BF_4]^{3+}$, which correlate well with the calculated distributions

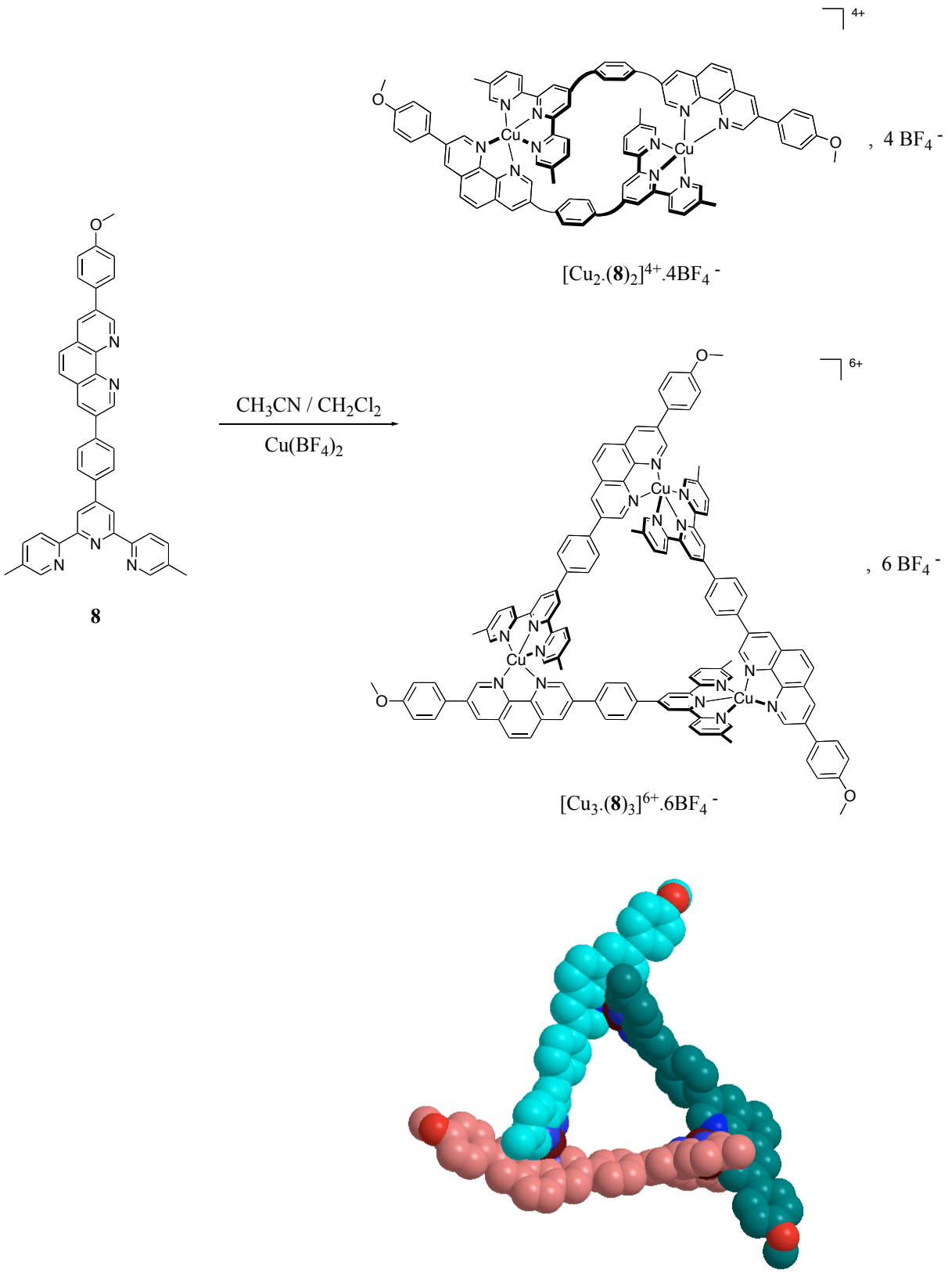

Figure 2.20: Formation of the dimer and trimer species, and molecular model of the trimer species (Chem 3D software), whose energy was minimized using MM2 software

The major peaks at mass-to-charge (*m/z*) ratios of 342.6, 428.5, 557.2 and 772.2 correspond to the trimer species $[Cu_3.(\mathbf{8})_3]^{6+}$ (*T*), with respectively no BF_4^- as counterion $[T]^{6+}$, one counterion $[T+BF_4]^{5+}$, two counterions $[T+2BF_4]^{4+}$, and three counterions $[T+3BF_4]^{3+}$. The other peaks at 342.6, 485.8 and 772.2 correspond to the dimer species $[Cu_2.(\mathbf{8})_2]^{4+}$ (*D*), with respectively no BF_4^- as counterion $[D]^{4+}$, one counterion $[D+BF_4]^{3+}$, and two counterions $[D+2BF_4]^{2+}$. The m/z ratio regions at 342.6 and 772.2 are thus superpositions of the isotopic patterns of both the dimer and the trimer species, as shown in Figure 2.18.

2.3.2.3 EPR studies

The EPR spectrum of the frozen solution obtained at 100K is also consistent with a mixture of two species (Figure 2.21). Indeed, the EPR spectrum looks like a superposition of 2 axial type spectra, each one characterized by two *g* values, $g_\perp$ and $g_{//}$. The local environment of copper centres is thus not anisotropic since the existence of two *g* values proves that copper complexes in solution have an axial symmetry (either trigonal bipyramid or square-based pyramid for 5-coordinate species, or octahedron for 6-coordinate species). Moreover, the parallel hyperfine tensor values $A_{//}$ are quite close to each other ($A_{//}^1$ = 15.4 mT and $A_{//}^2$ = 14.5 mT), meaning that both species have the same kind of chemical environment, which is consistent with the dimer and trimer species observed in the mass-spectrum. The fact that $g_{//}$ values are close but different ($g_{//}^1$ = 2.25; $g_{//}^2$ = 2.32) suggests that geometrical environments around copper centres are quite different. This is consistent with a rather distorted dimer species and a less constrained trimer species.

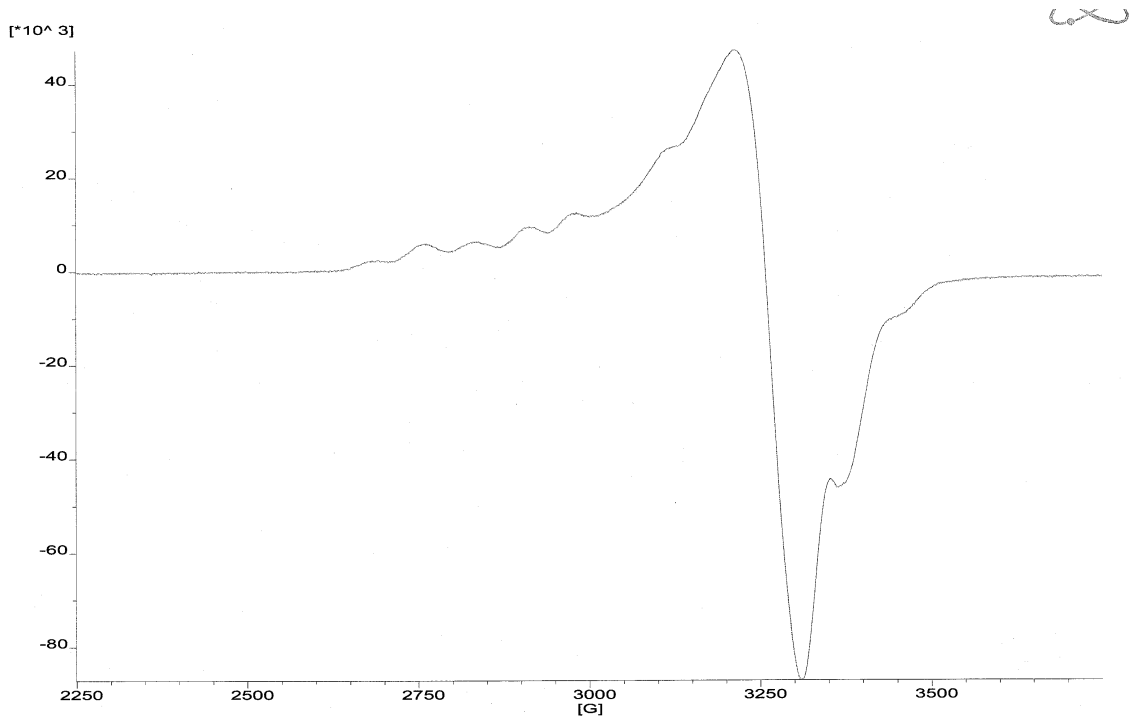

Figure 2.21: EPR spectrum of the mixture of the copper(II) complexes

It should be noted that the sole result of the EPR study can not be conclusive since one can find many different theoretical spectra that would fit the experimental curve. But considering the ES-MS analysis of the solution that proved unambiguously the formation of both the dimer and the trimer species, the EPR results corroborate these conclusions.

Moreover, cyclic voltammetry of a DCM/MeCN (80/20) solution of the olive green solid showed two reversible reduction waves at respectively + 0.15 V and – 0.05 V (vs SCE). These values are reminiscent of the ones obtained for 5-coordinate copper species.

2.3.2.4 Conclusion

Having changed the nature of the metal centre caused a noteworthy modification of the assembly process and yielded once again the dimer, but also, for the first time with this ligand, the trimer species. As expected, the copper metal centre managed to impose a more controlled geometry in its inner coordination sphere, thus disfavouring the formation of the dimer and enabling the trimer to exist. Yet the dimer still exists, which tends to prove that the battle between entropy and enthalpy that was exposed for the zinc(II) coordination chemistry is still taking place. Even if one has changed the balance and made the formation of the trimer possible, entropy is still an important factor which imposes the formation of the smallest assembly.

2.4 Conclusion

In this chapter, we described the synthesis of a new highly rigid ditopic ligand whose chelate coordination axes are perpendicular to one another. The synthesis has been optimized and several Suzuki C-C coupling reactions afforded the desired product which was fully characterized. It should be noted that all the molecules whose synthesis is reported here are new, except the phen derivatives **5** and **6**, and molecule **1** which has been synthesized previously according to an alternative route.

Coordination chemistry of such a ditopic ligand with zinc(II) afforded in good yield a dimeric structure as the sole product formed. Contrary to what was expected from the ideal geometries of the ligand and of the zinc(II) coordination sphere, neither the trimer nor the tetramer species could be observed. Formation of the dimer has been proven by ES-MS, ^{1}H NMR and diffusion-ordered spectroscopies.

By changing the nature of the metal ion into copper(II), which has more demanding stereoelectronic requirements, we managed to obtain in a good yield a mixture of a trimer and a dimer structure, as shown by ES-MS, EPR and CV. The exact ratio of trimer/dimer could not be determined.

It thus appears that translational entropy is a very important factor in such complexation process, leading to the smallest possible structure, in spite of the enthalpic cost of probable distortion of the zinc(II) coordination sphere and constraints within the ligand. Such kind of behaviour could be moderated by introducing a metal with more stereoelectronic requirements, making distortion more difficult.

These results are quite promising and should enable us to prepare multi-rotaxanes by adapting this methodology to a cyclic derivative of ligand **8** described in the present chapter. The next chapter will thus present the synthesis of the final macrocyclic heterochelate ligand, and its coordination with respectively zinc(II) and copper(II).

Chapter 3
Multi-rotaxanes based on a macrocyclic ditopic ligand with orthogonal coordination axes

The previous chapter detailed the synthesis a rigid ditopic ligand having its chelate coordination axes perpendicular to one another. Such kind of ligand, when put in reaction with preferentially 5-coordinate metal ions such as zinc(II) and copper(II), afforded very nice assemblies made of two or three ligands linked around a metal centre. Unfortunately, we did not manage to observe the formation of the expected tetramer structure, in spite of the perpendicular preorganization of the chelates.

Nonetheless, such beautiful structures are very close to the ideal topologies that we were looking for. The last step, which would lead to multi-rotaxanes, is to incorporate a macrocyclic unit in the ligand, in order to obtain a structure where molecular rings and threads are wrapped around metal centres (Figure 3.1).

Therefore, the present chapter is dealing with the design and synthesis principles of such kind of macrocyclic ditopic ligand. The complexation experiments of this ligand with zinc(II) and copper(II) will be presented, and the effect of the presence of the ring on the assembly process and on the nuclearities of the complexes formed will be explored.

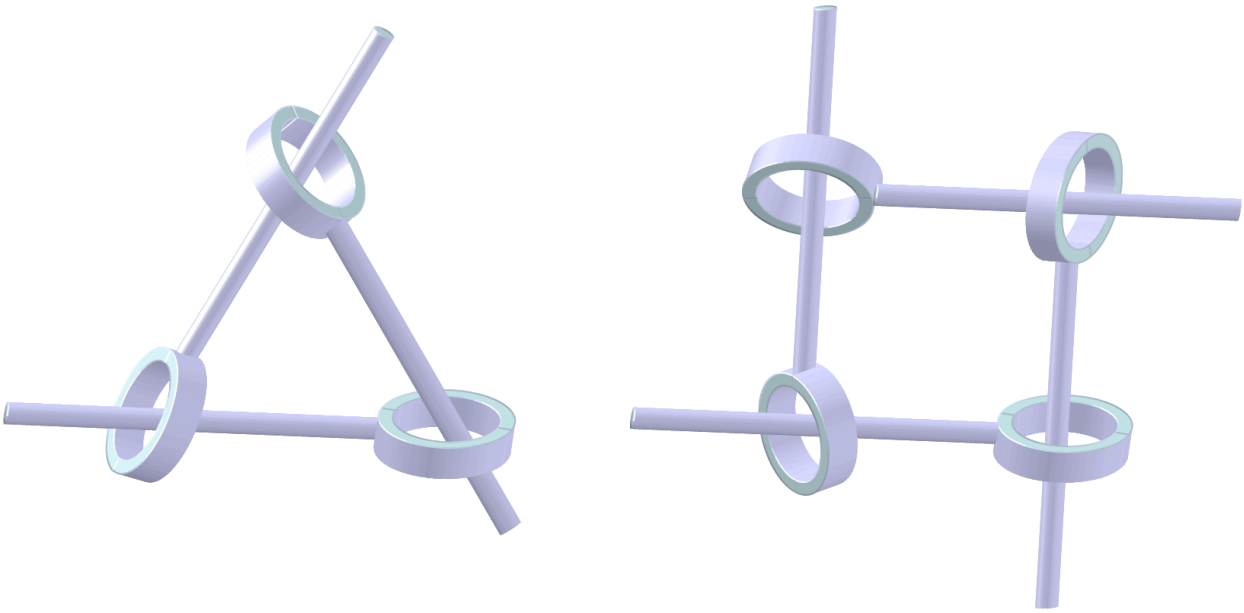

Figure 3.1: 2-dimensional multi-rotaxanes; examples of trimer and tetramer structures

3.1 Design and synthesis principles

In order to synthesize multi-rotaxanes, the design of ligand **8** had to be improved and a macrocycle had to be incorporated so that molecular threads and rings could intertwine with one another. The size of the ring had to be chosen carefully: it had to be wide enough so that the phen unit of another molecule could enter it, and at the same time not too wide in order to prevent the macrocycle from flipping around the axle.

We decided to use our terpy building block, molecule **4**, as reactant to obtain the macrocycle, and then keep the Suzuki coupling reaction as the last step of the synthesis of the target molecule.

3.1.1 Functionalization of the methyl positions

3.1.1.1 Benzylic bromination

Several strategies were investigated in order to functionalize ligand **4** and incorporate a macrocycle on methyl positions 5 and 5'' of the terpy nucleus. Indeed, we had chosen to put methyl groups in 5 and 5'' positions of terpy **4** because we wanted to adapt what Maria Consuelo Jimenez-Molero *et al*. had done with a similar but simpler terpy.[159] In their case, the chelate was not functionalized in the back. The strategy they used was a benzylic bromination using N-bromosuccinimide (NBS) in benzene under irradiation[160] (Figure 3.2). The reaction could be monitored by TLC and the resulting mixture of products bearing one, two or three bromine atoms could be purified by selective crystallization. The desired product, having only one bromine atom per methyl group, was the only one which crystallized and was recovered with a good yield (48 %).

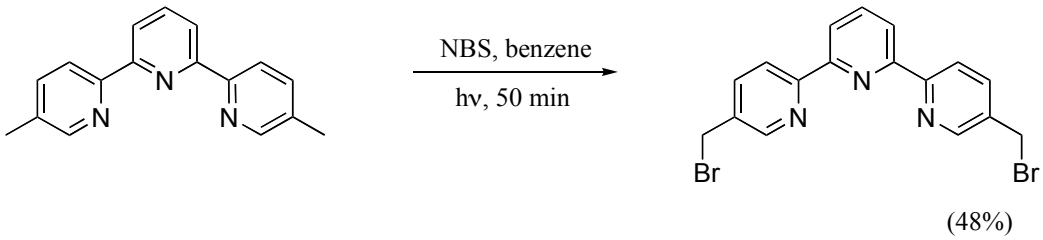

Figure 3.2: Benzylic bromination of 5,5''-dimethylterpyridine

Hence we tried the same reaction with terpy **4**, using NBS in benzene under argon (Figure 3.3). We irradiated the reaction mixture by fractions of 5 minutes and the reaction was monitored by TLC. We did the reaction numerous times, using different qualities and quantities of NBS, varying the time of irradiation, but each time, after 2 to 4 hours of irradiation, a mixture of products was obtained, containing one, two or three bromine atoms

on the benzylic positions (compounds **9**, **10** and **11** respectively). We thus decided to try a selective crystallization, but each time, the whole mixture precipitated out and no selectivity was observed. Classical separation by column chromatography was unsuccessful either, due to the very close R_f of the brominated products.

As this strategy did not work, we decided to investigate another reaction path to functionalize the methyl groups.

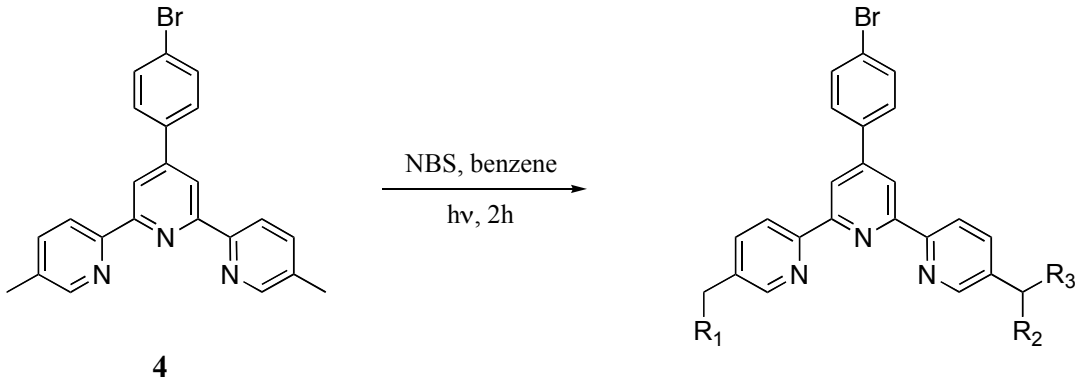

4

9 : R_1 = H ; R_2 = H ; R_3 = Br

10 : R_1 = Br ; R_2 = H ; R_3 = Br

11 : R_1 = Br ; R_2 = Br ; R_3 = Br

Figure 3.3: Benzylic bromination of terpyridine **4**

3.1.1.2 Perhalogenation of the methyl groups

As we did not manage to separate the different brominated compounds obtained *via* the benzylic bromination, we decided to explore a new synthetic pathway and to fully halogenate the methyl positions. Indeed, once fully halogenated, the product could then be transformed into its methyl ester derivative, then reduced into the benzylic alcohol and finally transformed into the benzylic brominated derivative, precursor of the macrocycle (Figure 3.4).

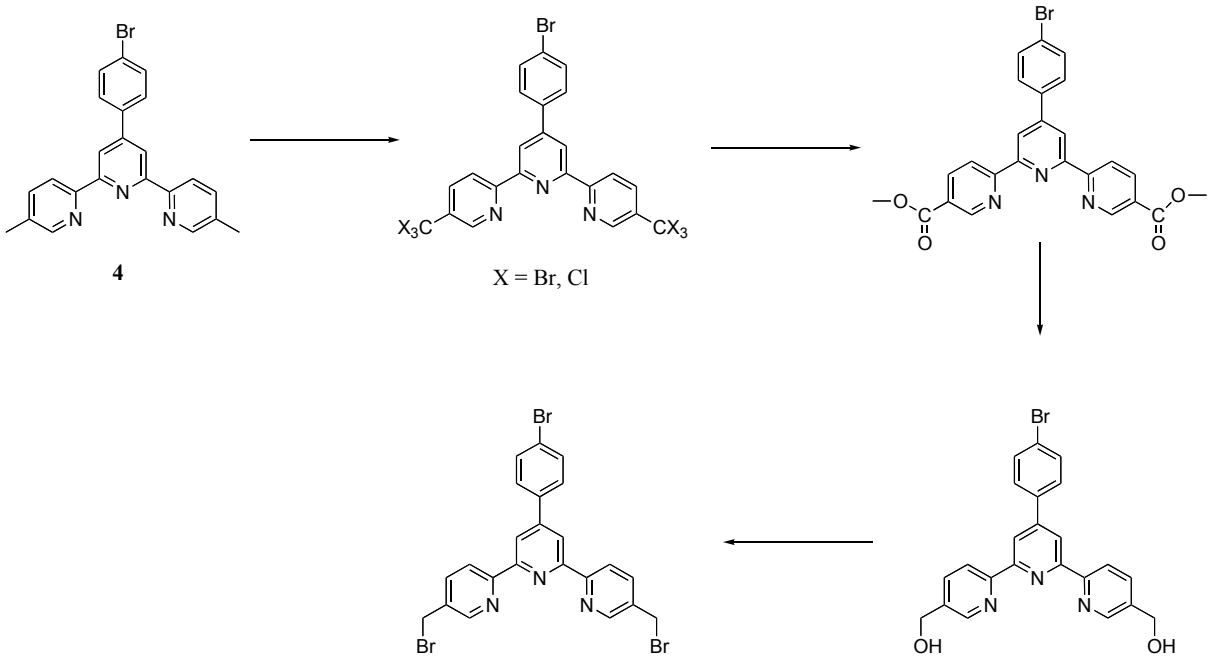

Figure 3.4: Alternative synthetic strategy leading to 5,5''-dibromomethyl-4'-(4-bromophenyl)terpyridine

A very similar pathway has already been published on a bipyridine derivative,[161-165] and the first step was a perchlorination of the methyl positions. We decided to adapt this methodology to our case, even if the methyl groups of **4** are in β position to the nitrogen atoms whereas they are in α position in the bipyridine. We will see shortly the influence of that difference on the reactivity of the molecule.

Two different procedures could be found in the literature yielding full chlorination of benzylic positions: use of N-chlorosuccinimide (NCS) in presence of a peroxyde in refluxing CCl_4,[161] or no radical initiators but light irradiation.[163] We have tried both of them, and both failed.

When terpy **4** was put to react with NCS in presence of benzyl peroxyde in refluxing CCl_4, no reaction was observed, even after 6 hours of reflux, and the starting material was recovered (Figure 3.5).

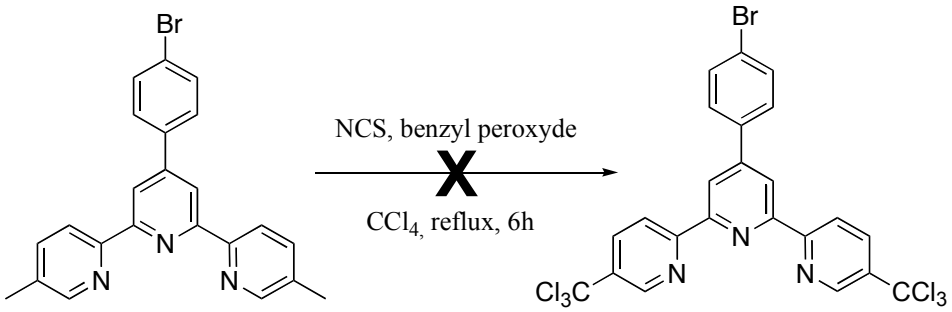

4

Figure 3.5: Perchlorination attempt on terpyridine **4**

Hence we tried the reaction without radical initiators, but under irradiation (250 W lamp). We even scanned all the parameters of the reaction, by varying the quantity and the quality of NCS, distilling or not CCl_4, carrying the reaction under argon or not, and varying the times of irradiation. Compared to the reaction conditions with benzyl peroxyde, the good point of these new conditions was that chlorination of the starting material was observed, and formation of new compounds during irradiation was monitored by TLC. But even under the best conditions (freshly recrystallized NCS, freshly distilled CCl_4, under argon) and after one day of irradiation, what was obtained was a statistic distribution of chlorinated products. Analysis by mass spectroscopy clearly showed that the reaction was not complete, and that the major peaks were related to compounds bearing respectively two and four chlorine atoms.

It was thus impossible to apply this strategy to our molecule, all the more that all these test reactions had been carried out on very few amounts of compounds, and scaling up these amounts with the same source of light would implicate longer irradiation times!

It should also be noted that the same kind of strategy has been investigated with bromination instead of chlorination. Terpy **4** was put in freshly distilled benzene in presence of freshly recrystallized NBS, under argon, and the solution mixture was irradiated (250 W lamp) for more than 30 hours, until no evolution on TLC was observed. ES-MS analysis also showed a statistic distribution of brominated products, centered on peaks related to compounds bearing respectively 2 and 3 bromine atoms (Figure 3.6).

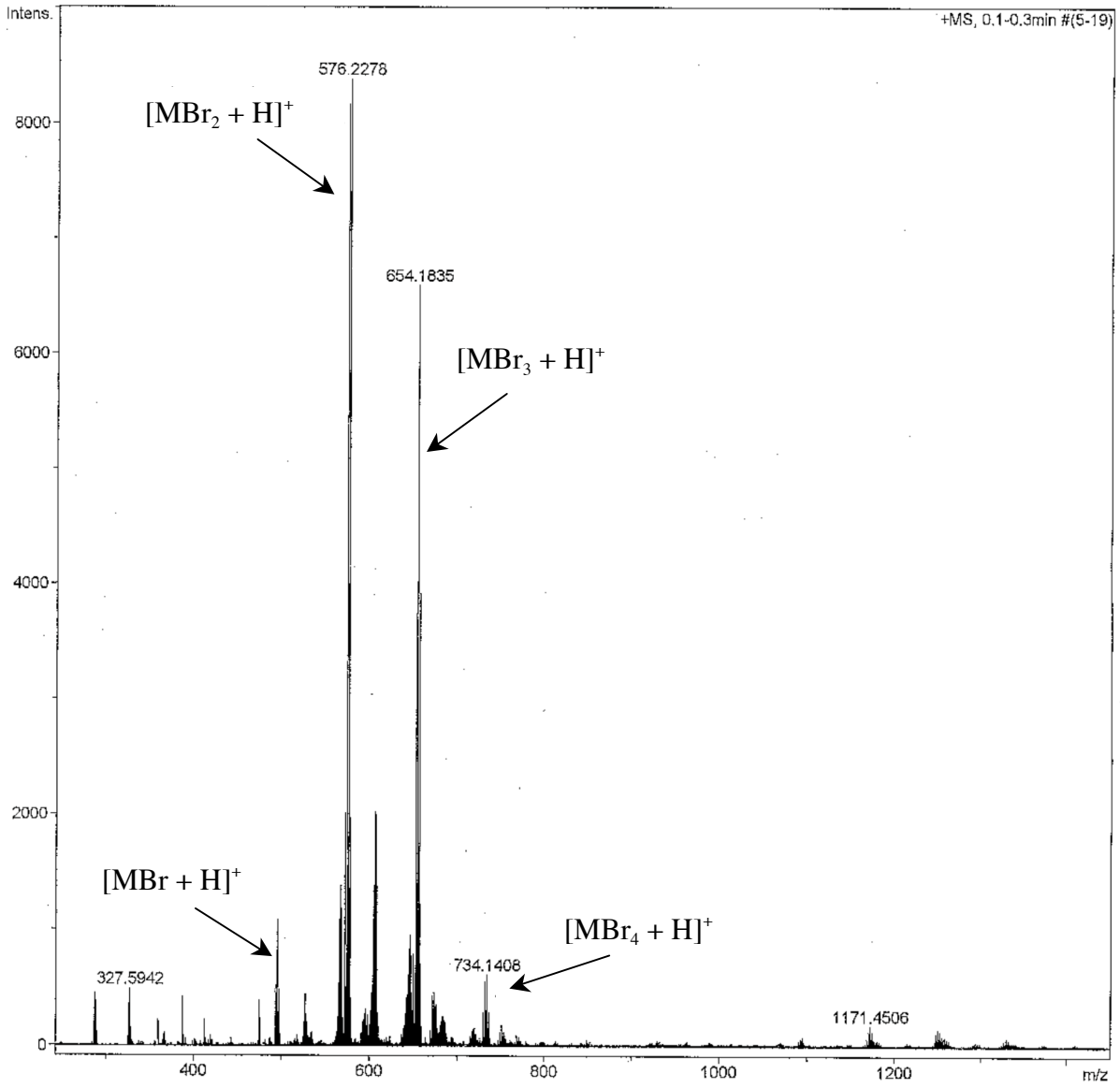

Figure 3.6: ES-MS distribution of brominated compounds

Finally, it should be reminded that when one looks at the net charge on each atom of a pyridine ring, it is well known that the carbon in meta position is less electrodeficient than the carbon in ortho, as the net charge of the former is roughly equal to zero (- 0.004), whereas the net charge of the latter position is positive (+ 0.075). One can thus argue that this electronic atomic charge difference might be responsible for the difference of reactivity observed on a bipyridine nucleus and on our terpy with respect to benzylic chlorination (and bromination).

3.1.2 Macrocyclisation of terpy 4

3.1.2.1 Synthetic strategy

Years ago, before an efficient way of preparing macrocycle precursors by brominating the methyl positions of a terpy was found, people in the laboratory used to employ a less efficient but still working strategy: alkylation using LDA.[166, 167]

As halogenation did not work in our case, we thus explored the alkylation pathway. The idea was to deprotonate the methyl groups with LDA, form a highly reactive di-anion,[166, 167] have it reacted with the proper ethylene glycol chain, and thus yield a terpy with two pending arms. The macrocycle would then be obtained by using a clipping agent, such as bisphenol A, which has been extensively used in the past few years in our group (Figure 3.7).

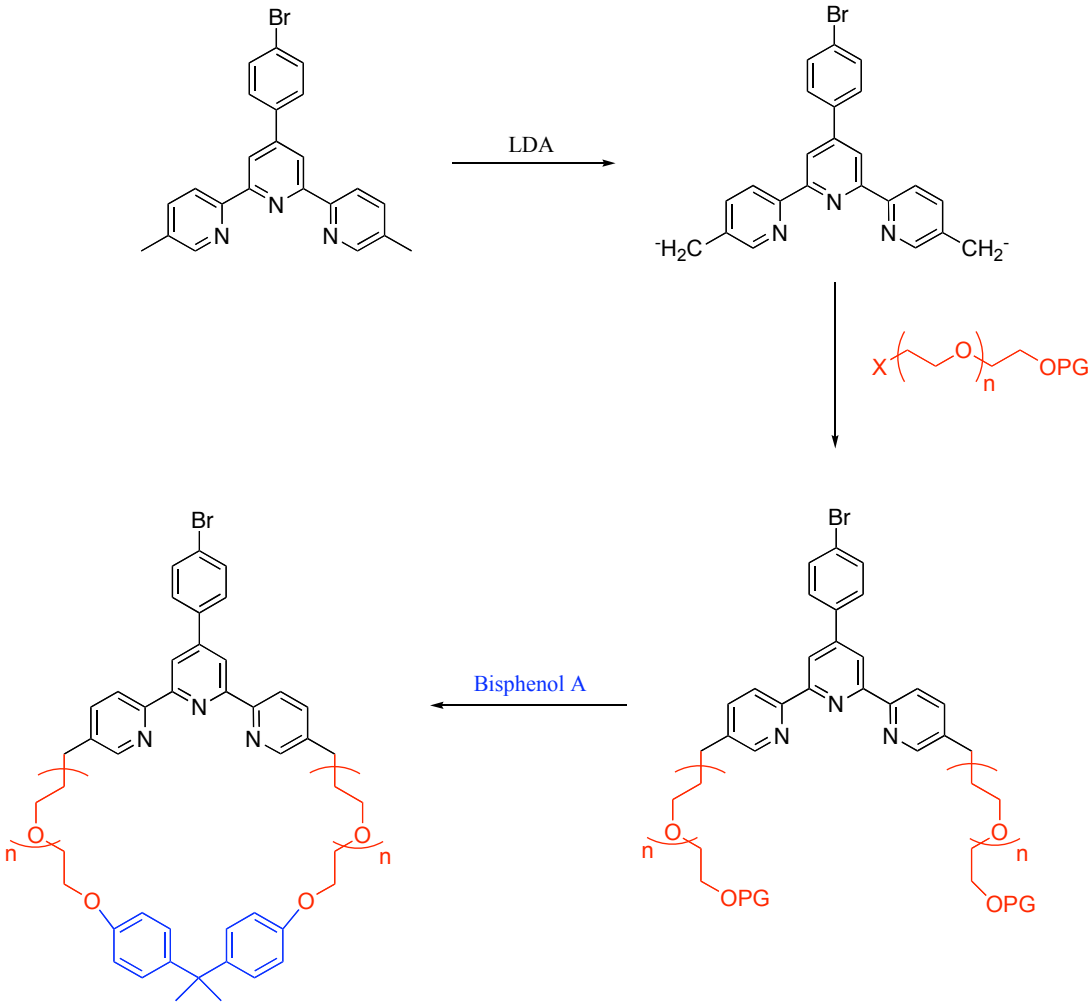

Figure 3.7: Synthetic strategy towards terpyridine **4** in a macrocycle

3.1.2.2 Design of the macrocycle: choice and synthesis of the "arms"

The choice of the arms and especially their length is crucial in order to form a macrocycle with the appropriate size. The classical "arms" which have been used in the lab are polyethylene glycol derivatives, since they are easy to synthesize, protect and deprotect. They are also quite flexible, which is very important during the threading step. In our case, after examining the CPK models carefully, we decided to use a derivative of diethylene glycol, where one alcohol function is protected by a THP protective group on one side, and the other extremity is activated by an iodine atom. After clipping the macrocycle with bisphenol A, the

ring will contain 34 atoms in its interior. The macrocycle was thus called MT_{34} where M stands for macrocycle and T for terpyridine.

Chain **12** was synthesized in two steps from chlorodiethylene glycol (Figure 3.8). The first step is a classical protection of the alcohol function into its THP derivative via an acetalization reaction.[168] The alcohol was dissolved in dichloromethane, and freshly distillated DHP was added dropwise into the alcoholic solution vigorously stirred at 0°C. Few drops of HCl were then added as a catalyst, and the reaction mixture was allowed to warm to 40°C for about an hour. Acetals are stable in a basic medium and are therefore easily isolated after destruction of the catalyst with a strong inorganic base (K_2CO_3). This reaction was quantitative (99%) and the yellowish oil recovered after work up was used without further purification.

The next step was the introduction of the iodine atom. The reaction was carried out by mixing **12** and NaI in refluxing acetone overnight.[169] Product **13** was isolated in very good yield (83%).

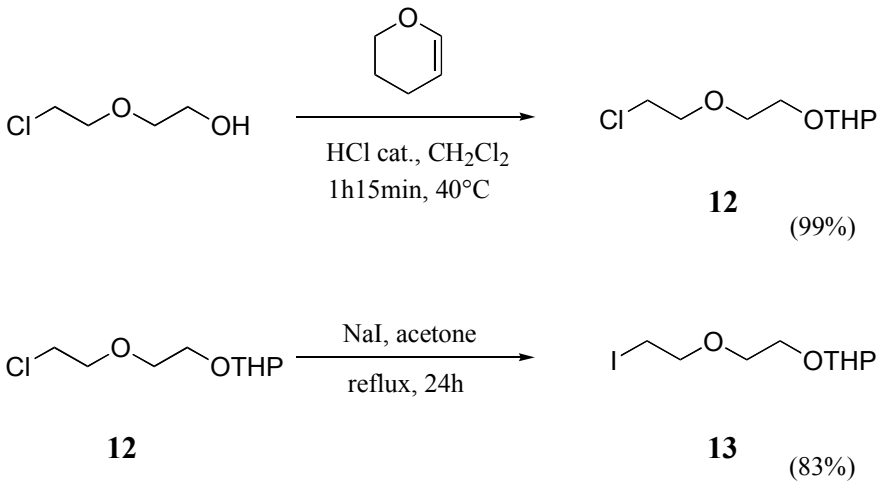

Figure 3.8: Synthesis of compounds **12** and **13**

It should be noted that identification of these products, which have very close functionalities, has been possible using ^{13}C NMR. Especially, the signal related to the carbon bearing the halide was strongly upfield shifted when passing from the chlorine to the iodine atom. The purity of the product could thus unambiguously be checked by NMR spectroscopy to within about 95%, which was good enough for the next reaction.

These two steps were very easy to deal with and very efficient, so it was possible to synthesize several tens of grams of the final chain **13**.

3.1.2.3 Alkylation reaction

The alkylation reaction is quite difficult to handle and one should be very careful and very neat in the manipulation of highly reactive species. We first prepared a fresh solution of LDA by adding n-BuLi onto a diisopropylamine solution at -78°C. The LDA solution was then transferred to a solution of terpy in distilled THF at -78°C *via* the canula transfer technique.

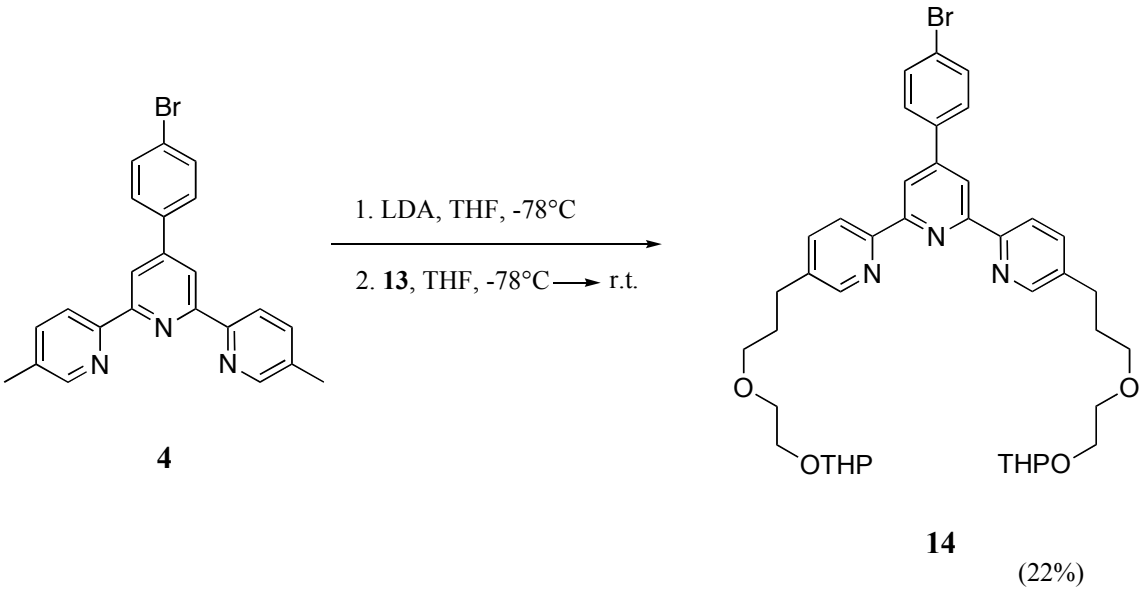

4

14

(22%)

Figure 3.9: Synthesis of compound **14**

The reaction turned rapidly deep green, which was consistent with the formation of a highly conjugated di-anion. In the meantime, a solution of the diethylene glycol derivative **13** in freshly distilled THF was cooled down to –78°C and transferred into the main flask containing the di-anion using once again the canula transfer technique. The reaction was let stir for several hours and was allowed to warm gently to room temperature (Figure 3.9). At the end of the day, the reaction mixture turned clear orange, indicating that there was no more active species in solution. The crude mixture was then purified by a long column chromatography which could separate the desired product **14** (22%) from its monoalkylated derivative (20%) and from the starting material (29%).

It should be noted that recovering almost 30% of the starting material is not such a bad thing in that reaction, since such amount of compound could be recycled and engaged in another alkylation reaction.

Still, the yield of this step is quite poor, especially compared to the 55% yield obtained on a simpler dimethylterpyridine.[105, 170] This makes this step the weakest link of the whole synthetic chain, but this reaction was the only one which enabled us to functionalize the terpy nucleus and to go on towards the final macrocycle.

Considering the low yield of this step, this reaction was carried out several times until few grams of product **14** were obtained.

3.1.2.4 Towards the macrocycle precursor

Once precursor **14** of the macrocycle was obtained, the rest of the synthetic route was quite straightforward and inspired by previous work carried out in the laboratory by Jean-François Nierengarten:[171] deprotection,[172] mesylation[173] and bromination[171] (Figure 3.10).

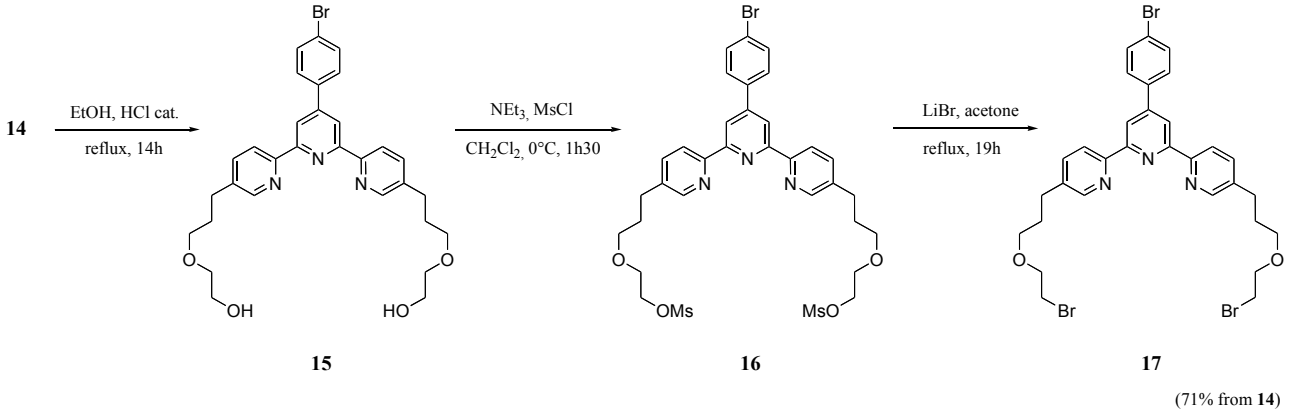

Figure 3.10: Synthetic route from **14** to **17**

THP groups were first removed under classical acidic conditions (refluxing EtOH, HCl cat.), yielding the dialcohol **15**. The hydroxyl functions were then activated in presence of mesylchloride and triethylamine in dichloromethane at 0°C, and compound **16** was used without further purification for the next step: bromination using LiBr in refluxing acetone. The final product, **17**, was purified by column chromatography and isolated with an overall yield of 71% from **14**, over three steps.

A terpyridine unit, functionalized in its 4' back position, and bearing in 5 and 5'' positions two pending arms ended by an alkyl bromide was thus synthesized and was the perfect candidate for further macrocycle formation.

3.1.2.5 High-dilution step: macrocyclisation

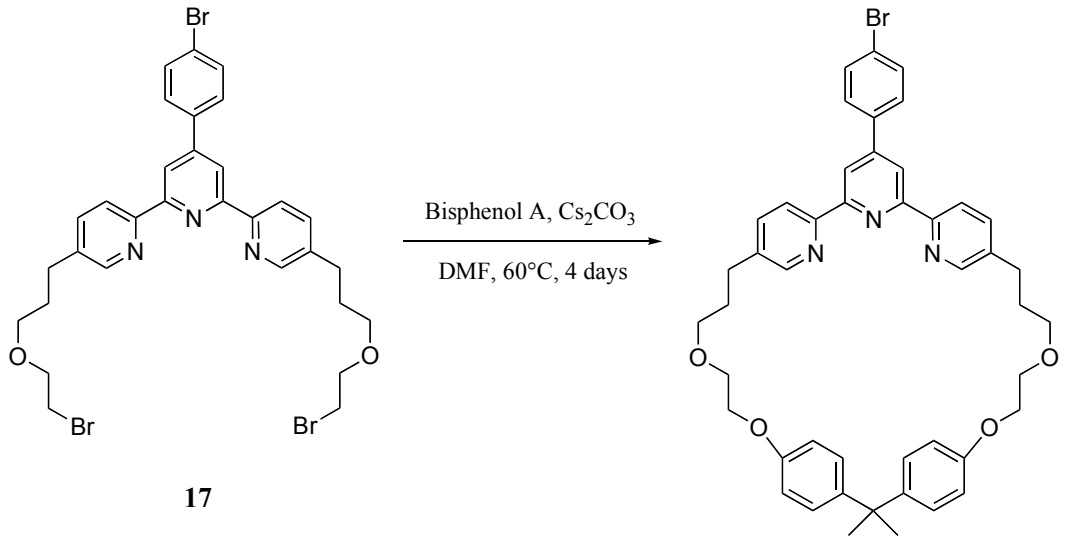

17

18 (MT_{34}) (57%)

Figure 3.11: Synthesis of compound **18**: high-dilution step

A classical Williamson reaction between a diphenol (bisphenol A) and the alkyl bromides on each arm of terpy **17** was imagined to close the ring (Figure 3.11). In order to avoid intermolecular coupling reactions, which would lead to oligomers formation, we had to use high-dilution conditions and apparatus. The terpyridine precursor **17** and bisphenol A were dissolved in dry DMF and transferred into a syringe adapted on a syringe pump. In the meantime, a suspension of cesium carbonate in dry DMF under argon was heated up to 60°C in a special high dilution round bottom flask. The total amount of DMF and the rate of addition were calculated so that concentration of products in solution was never over 10^{-5} $mol.L^{-1}$. After a bit less than 4 days of addition, the solvent was removed, and the crude mixture was washed and purified on column chromatography, affording the desired macrocyclic product **18** MT_{34} with 57% yield. This new product has been fully characterized by ES-MS, NMR spectroscopy (COSY, ROESY, HMQC, HMBC) and elemental analysis.

3.1.3 Synthesis of the final ditopic macrocyclic conjugate

The same strategy as in the acyclic project was used to obtain a ditopic ligand bearing two chelates units whose coordination axes are perpendicular to one another. We can even say that it was a good test to first try the Suzuki coupling reaction on the acyclic terpyridine rather than directly on MT_{34} which is far more difficult to obtain.

It should nonetheless be noted that at this stage of the synthesis, there are two different possibilities to couple MT_{34} and a dissymmetric phen unit: 1) we can use the exact same strategy as in the acyclic project and transform MT_{34} into its boronic ester derivative, which is then coupled with phen **6**, or 2) considering the value of MT_{34} on a synthetic point of view, one can imagine to put the boronic ester function on the phen fragment. But as explained in Chapter 2, introducing a boronic ester function on the phen unit would imply introducing a new phenylene bridge, when we want the connection between the two chelates to be as short as possible so that the final structure is highly rigid.

Therefore, the same conditions as in chapter 2 were used to couple MT_{34} and the dissymmetric phen unit **6** (Figure 3.12). The bromine atom at the back of the macrocycle was thus changed for a boronic ester function in presence of bis(neopentyl glycolato)diboron in freshly distilled dioxane. Compound **19** was thus obtained in quantitative yield (NMR purity) from MT_{34} and used without further purification for the next step. It was nevertheless fully characterized by ES-MS and NMR spectroscopies.

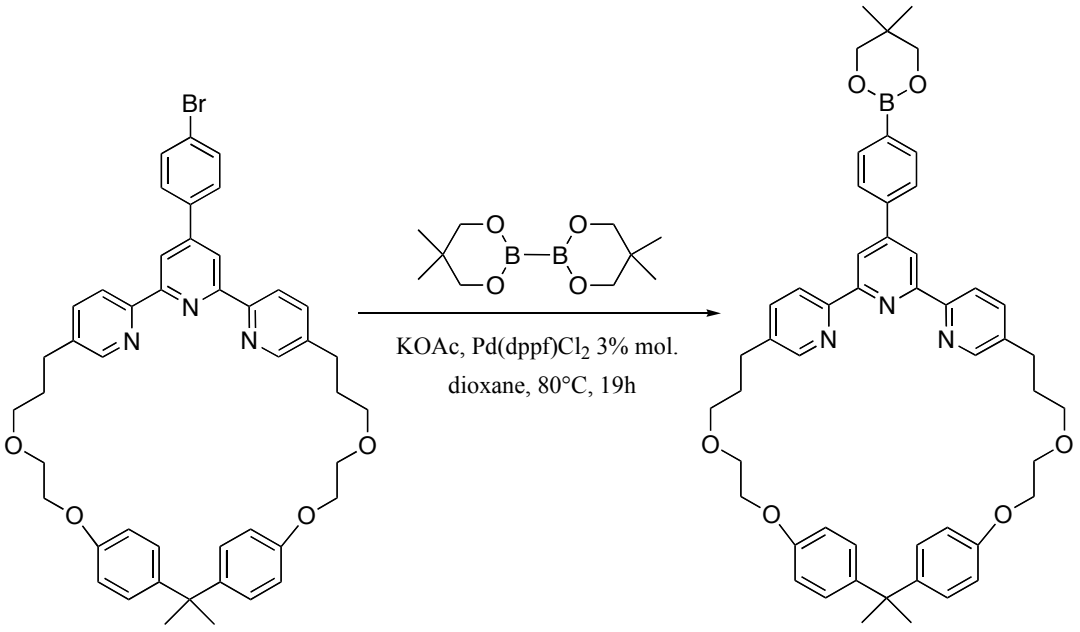

18 (MT_{34}) **19**

Figure 3.12: Synthesis of compound **19**

The next step is the Suzuki C-C coupling reaction, and has been carried out under classical conditions, using $Pd(PPh_3)_4$ as a catalyst, and Na_2CO_3 as a base, in a mixture of toluene and water (Figure 3.13). Compound **6** was introduced in slight deficit so that the reaction could be monitored by TLC. Disappearance of the spot related to **6** after 46 hours of reflux indicated when the reaction was over. The crude mixture was purified by column chromatography over alumina, and we could isolate 15 mg (40% over the two steps) of the final compound **20**, which has been fully characterized by ES-MS and NMR spectroscopy (COSY, HMQC, HMBC).

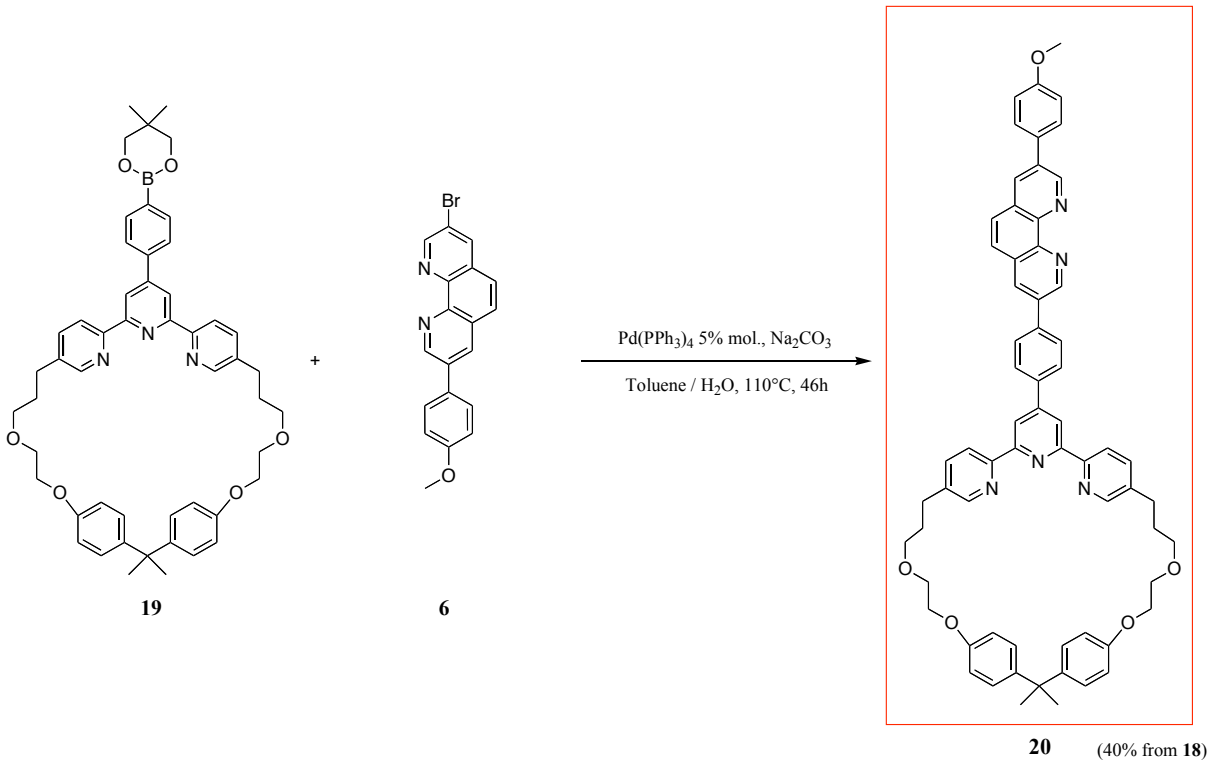

Figure 3.13: Synthesis of compound **20**

3.1.4 Conclusion

A new macrocyclic ditopic ligand bearing a terpy nucleus in the ring and a phen nucleus on the thread has been synthesized in 13 steps from its two commercially available precursors, 1,10-phenanthroline and 2-bromo-5-methylpyridine. This highly rigid ligand is the macrocyclic analogue of ligand **8** presented in Chapter 2. Therefore **20** also contains two chelates whose coordination axes are perpendicular to one another. Contrary to what was expected, the synthesis of a macrocycle incorporating a terpy functionalized both in 5,5'' positions and in the back was not straightforward, in spite of the obvious axial symmetry provided by the 4' back position. Nonetheless, the synthesis of **20** could be achieved *via*

alkylation of the methylene positions with LDA, and subsequent Suzuki C-C coupling reactions.

It was then very stimulating to investigate the coordination properties of this new ligand, and to compare them with the results obtained with the acyclic ligand **8**. We were especially eager to discover whether the presence of a ring would change the nuclearities and the distribution of the complexes formed and if rotaxane trimers or even tetramers could be expected. That is the object of the next section.

3.2 Coordination studies: multi-rotaxanes synthesis

We decided to explore the exact same coordination studies with ligand **20** as with ligand **8** so that we could draw comparison between the two and measure the influence of the ring in the formation of the complexes. We thus investigated coordination studies with zinc(II) and copper(II).

3.2.1 Zinc(II) complex

3.2.1.1 Synthesis

The coordination studies of the acyclic derivative **8** with zinc(II) indicated unambiguously the formation of the dimer as the sole product, which proved that entropy was the prevailing factor in the coordination process. Despite the enthalpic cost of the deformation of the organic backbone of the ligand and the constrains imposed on the coordination sphere of the metal ions, the smallest possible complex was obtained.

It was thus interesting to discover whether the presence of the ring would have an influence on the nuclearities of the complexes obtained. If the supplementary distortion of the macrocyclic backbone would imply a too high enthalpic cost to pay, larger assemblies could be expected. But if formation of the smallest possible complex is still the best energetic compromise, rotaxane dimer should be obtained. This is exactly what happened, without formation of trimer or tetramer species. The reaction is represented in Figure 3.14, as well as a molecular model (Chem 3D software) of the complex, whose structure was obtained by minimizing its energy using a MM2 software.

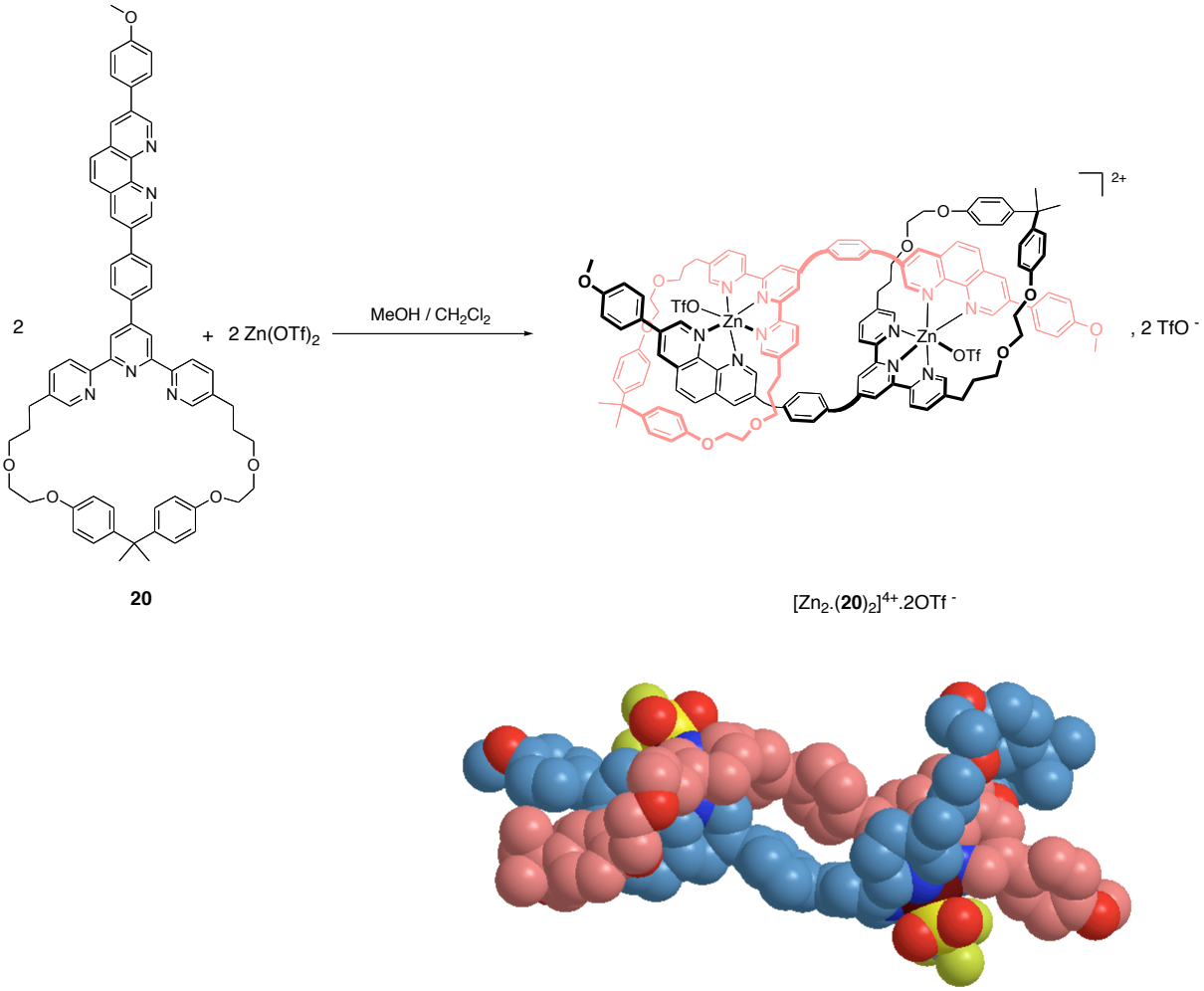

Figure 3.14: Reaction between **20** and Zn^{2+} leading to the rotaxane dimer, and its molecular model (Chem 3D software; energy minimized using MM2 software)

The coordination reaction of Zn^{2+} to **20** was carried out by mixing equimolar amounts of respectively **20** in CH_2Cl_2 and $Zn(OTf)_2$ in MeOH. The resulting orange coloured solution was allowed to stir for 24 hours, the solvent was then evaporated, the crude mixture was taken in a mixture of dichloromethane and methanol, filtered, and the filtrate evaporated to dryness. The dimer complex $[Zn_2.(\mathbf{20})_2]^{4+}.4OTf^-$ was obtained in good yield (76%) as a yellow solid. It is only sparingly soluble in common organic solvents.

3.2.1.2 ES-MS studies

At this stage, as in the acyclic case, it is difficult to know if, in solution, the Zn^{2+} centres are really 5-coordinate or if the counterion participates in the Zn^{2+} complexation. The dimer complex with two 6-coordinate Zn^{2+} centres is certainly less strained in terms of organic ligand distortion than the putative analogous complex in which the Zn^{2+} centres would be 5-coordinate. The chemical structure of $[Zn_2.(\mathbf{20})_2]^{4+}$ (*M*) was proven by electrospray ionization mass spectroscopy (ES-MS) and ^1H NMR spectroscopies. ES-MS analysis of the yellow solid revealed three major peaks at mass-to-charge (*m*/*z*) ratios of 526.7, 751.9, and 1202.3, corresponding to $[M]^{4+}$, $[M+OTf]^{3+}$, and $[M+2OTf]^{2+}$, respectively. This situation is consistent with the proposed dimer compound $[Zn_2.(\mathbf{20})_2].4OTf$ (Figure 3.15).

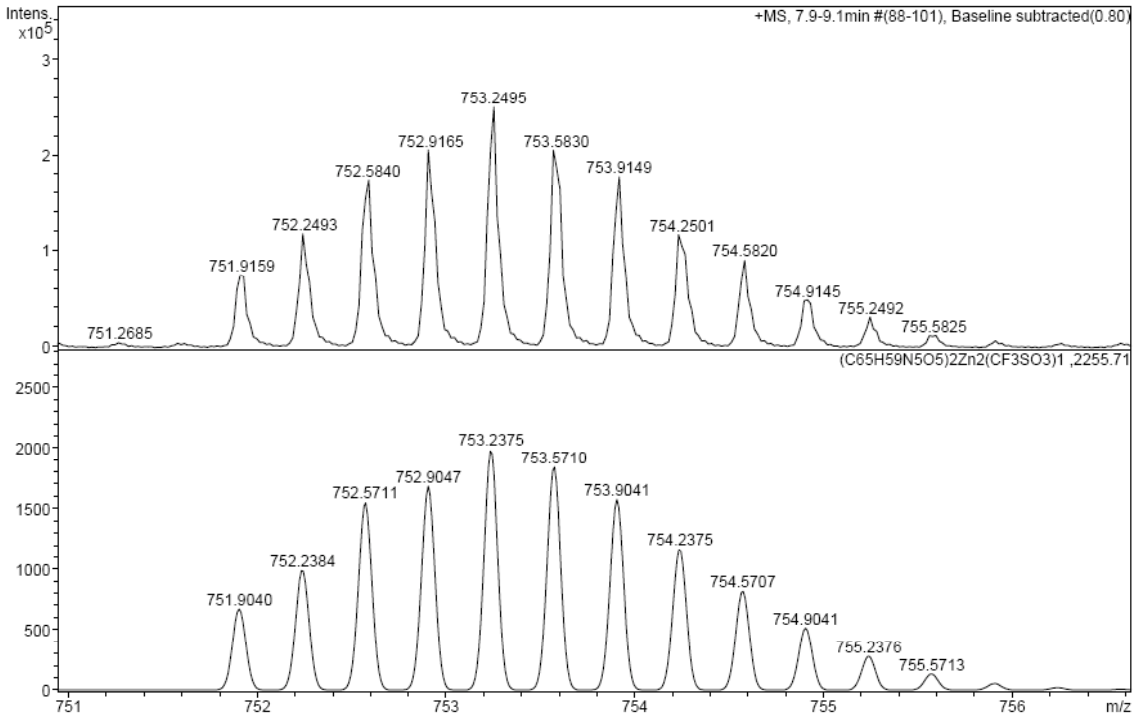

Figure 3.15: Isotopic distribution pattern at m/z = 753.2
(top: experimental; bottom: calculated)

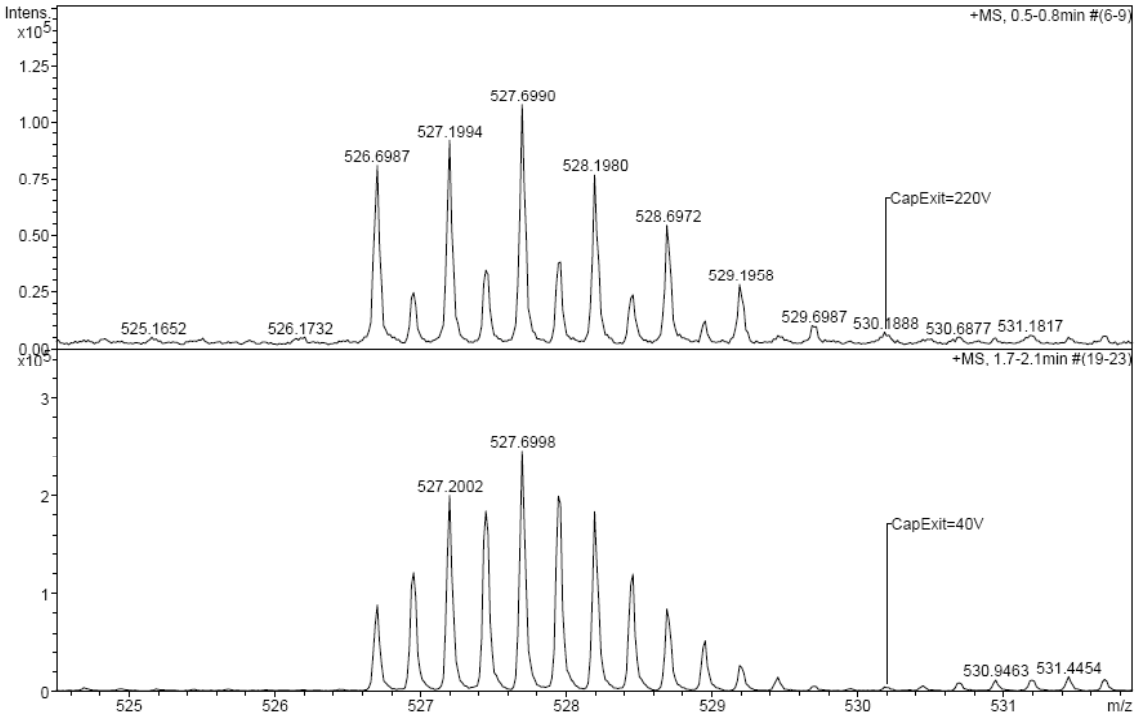

Figure 3.16: Influence of the capillary exit tension on the isotopic distribution pattern at m/z = 527.7. When CapExit = 220V, an isotopic distribution relative to the monomer appeared

It should be noted that the rotaxane dimer formed is quite sensitive. If the capillary exit voltage is higher than 60V, an isotopic distribution relative to the monomer appeared in the peak at 527.7 (see Figure 3.16), and it is even impossible to observe the sole distribution of the dimer in the peak centered at 1202.3.

3.2.1.3 NMR studies

Contrary to the acyclic system, the ^{1}H NMR study was quite difficult and not as clean. The product was indeed barely soluble in common organic solvent and, in deuterated dichloromethane, where the best results have been obtained, the 1D spectrum was not clean and difficult to understand. There were too many peaks and all of them emerged from three broad and flat bands in the aromatic, anisyl and methyl regions. At this point, it was difficult to understand if what we observed was polymers, oligomers, or dynamic phenomena and slow conformational equilibria.

Indeed, in a previous work in the lab,[174] the NMR study of a rotaxane built around a ruthenium centre showed that the macrocycle, bearing also a bisphenol A fragment, could flip around the axle. The movement, slowed by the sterical hindrance due to the bisphenol A moiety, could therefore be characterized unambiguously *via* variable temperature (VT) NMR studies. We thus built the CPK model of the dimer of rotaxane whose existence had been proven by ES-MS. And we discovered that it was difficult but possible for the ring of one monomer to flip around the thread of the other one. This slow movement could explain the large band observed on the 1D ^{1}H NMR spectrum.

Hence, we investigated the influence of the following parameters on the appearance of the spectrum: concentration and temperature.

We studied samples whose concentrations varied from 10^{-3} to 10^{-5} mol.L^{-1}. At high concentration, there was no change in the spectrum, and especially no peaks related to species of higher nuclearities appeared. Entropy is definitely the prevailing factor in the formation of the complexes. At low concentrations, the ratio (fine peaks)/(large band) increased and at the lowest concentration, we could observe peaks related to the monomer. These observations are consistent with the fact that when diluting, thermodynamics favours species of lower nuclearities. Moreover, the stability constant of zinc(II) complexes are not very high. It is thus normal that upon dilution, the complexation equilibria are shifted towards the regeneration of the monomer.

In order to better understand the putative conformational equilibria at stake, we carried out VT NMR experiments. When decreasing the temperature in CD_2Cl_2, sharp peaks broadened, but no coalescence was observed: molecular movements were slowed down and the molecular structures were frozen in a variety of conformations leading to a broadening of the peaks.
When increasing the temperature in $C_2D_2Cl_4$ up to 100°C, all the peaks sharpened, but the whole spectrum became very complicated and signals related to the monomer clearly appeared.

In conclusion, these first NMR studies were not very conclusive. Nonetheless, conformational equilibria may be in part responsible for the broad signals observed. We thus decided to run DOSY experiment in order to identify the exact number of species in solution. (Figure 3.17)

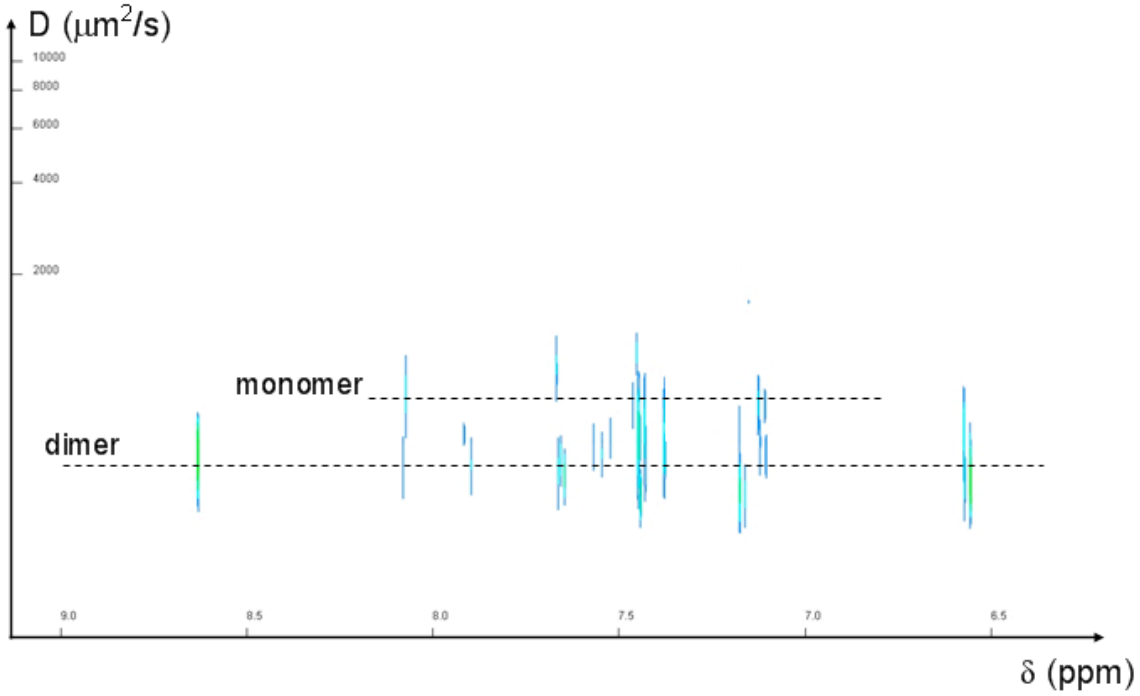

Figure 3.17: DOSY experiment in CD_2Cl_2 at medium concentration. Zoom on the aromatic region of the spectrum. Both the monomer and the rotaxane dimer are present

At medium concentrations (10^{-4} mol.L^{-1}) in CD_2Cl_2, a main species was observed, characterized by its diffusion coefficient (D = 510 μm²/s) and its hydrodynamic radius (r_H = 10.4 Å). Computational simulation of the hydrodynamic radius of an ellipsoid object which matches with the experimental value of the radius enabled us to predict the size of the product in solution: a = 15 Å and b = c = 8 Å. The object is thus a prolate ellipsoid, which is consistent with the proposed dimer of rotaxane [Zn_2.(**20**)$_2$].4OTf.

We could also see traces of monomer (D = 1000 μm²/s). This indicates that the stœchiometry of the reaction may not have been strictly respected, which is possible considering the small amounts of product we worked with. At higher concentrations, we could see the dimer species, the monomer and also oligomers (low D). Due to the very low amount of product **20** (15 mg) which had to be engaged in various complexation reactions, and due to time constraints, we could not synthesize a larger amount of **20**, nor make the zinc complexes one more time.

Nonetheless, the rotaxane dimer was unambiguously identified by ES-MS, and as part of the NMR mixture *via* its diffusion coefficient very similar to the one obtained for its acyclic derivative. This is normal since the general shapes of these two molecules are very similar and are modeled by the same ellipsoid. ROESY experiment also clearly showed correlation between protons of the phen and the bisphenol A moieties, proving that both monomers are interwoven.

3.2.1.4 Conclusion

Very similarly to what was observed with the acyclic heterochelate ligand **8**, coordination of its macrocyclic derivative **20** with zinc(II) yielded a dimer of rotaxane which has been characterized by ES-MS and DOSY NMR. For reasons that we could not fully understand, the 1D NMR spectrum was very complicated. Due to time constraints and lack of starting material **20**, we could not perform these investigations further on. Nevertheless, we were very glad to observe formation of the dimer of rotaxane, even if no trace of complexes of higher nuclearities could be observed. It should then be pointed out that the macrocycle seemed to have no influence on the complexes formation, and that once again translational entropy was the prevailing factor.

3.2.2 Copper(II) complexes

In order to compare the behaviour of the acyclic and macrocyclic ligands **8** and **20** towards complexation in the exact same conditions, we then investigated the complexation of **20** with copper(II). It was indeed very interesting to know if the copper(II) centres would have the

same influence on the nuclearities obtained with the macrocyclic ligand **20** as with the acyclic derivative **8**, and see whether rotaxane trimers or even tetramers could be obtained.

The coordination experiment was carried out under identical conditions, by mixing equimolar amounts of respectively ligand **20** in CH_2Cl_2 and $Cu(BF_4)_2$ in CH_3CN (Figure 3.18). The solution turned instantaneously olive green. The solution was let stir for 16 hours at room temperature, and by addition of diethyl ether a green solid precipitated out, which was then filtered, washed, dissolved again in an acetone/acetonitrile/methylene chloride mixture, and recovered as a solid by addition of diethyl ether in a good yield (92%).

As proton NMR was not possible on this paramagnetic complex, we investigated the composition of the mixture by ES-MS (Figure 3.19), which clearly showed the presence of two species corresponding to the dimer and the trimer of rotaxane. The major peaks at mass-to-charge (*m*/*z*) ratios of 526.2 and 730.6 correspond to the dimer species $[Cu_2.(\mathbf{20})_2]^{4+}$ (*D*), with respectively no BF_4^- as counterion $[D]^{4+}$ and one counterion $[D+BF_4]^{3+}$. The other peaks at 526.2 and 648.8 correspond to the trimer species $[Cu_3.(\mathbf{20})_3]^{6+}$ (*T*), with respectively no BF_4^- as counterion $[T]^{6+}$ and one counterion $[T+BF_4]^{5+}$ (Figure 3.19). It should be noted that once again, the ratio dimer/trimer could not be evaluated with to this method. Due to the small amount of copper complexes formed, it was not possible to run other conclusive characterizations such as cyclic voltammetry, or EPR spectrum. In order to do so, another batch of ligand **20** had to be prepared, but time constraints made it impossible.

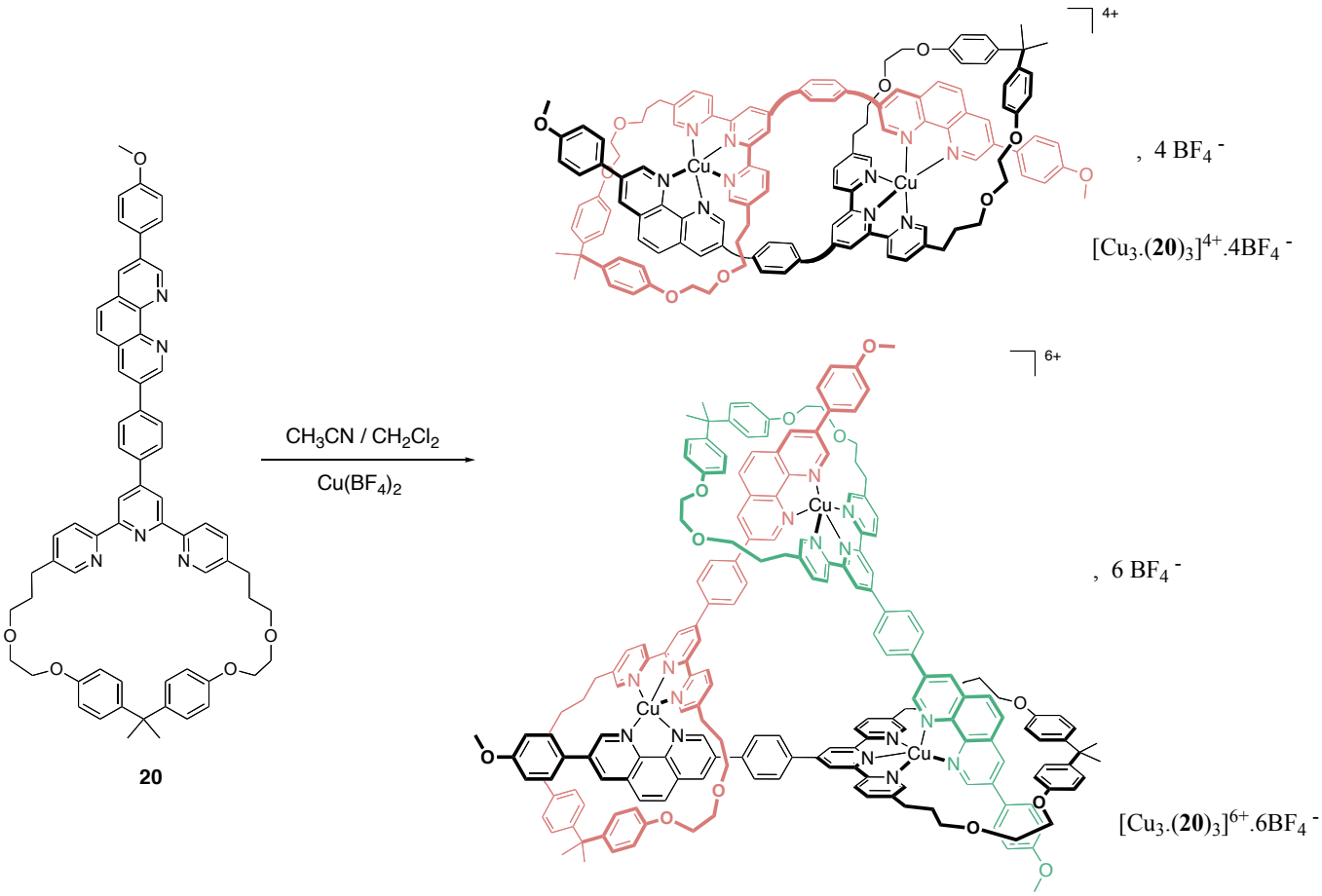

Figure 3.18: Formation of the rotaxane dimer and trimer using copper(II) as a template

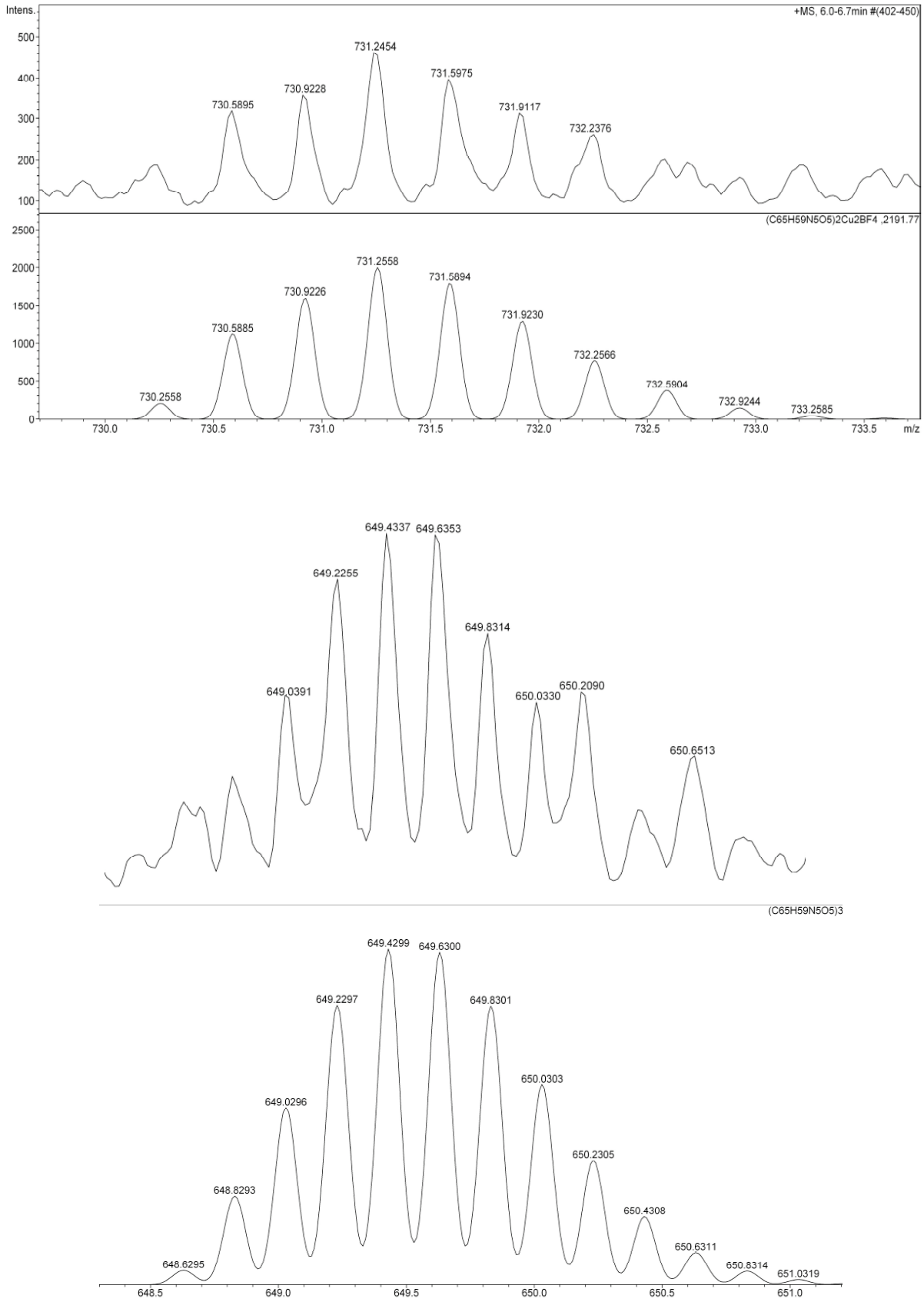

Figure 3.19: Isotopic distribution patterns for $[D+BF_4]^{3+}$ and $[T+BF_4]^{5+}$ at m/z = 731.2 and 649.4 respectively. For each compound, the experimental spectrogram (top), correlate with the calculated pattern (bottom)

It is obvious that once again, changing the nature of the metal ion caused a modification of the assembly process and yielded a mixture of the rotaxane dimer and trimer. As in the acyclic project, the copper metal centre imposed a more drastic geometry in its inner coordination sphere, thus disfavouring the formation of the dimer and enabling the trimer to exist. Yet the dimer still exists, which tends to prove that the battle between entropy and enthalpy that was mentionned for the zinc(II) coordination chemistry is still taking place. Even if one has changed the balance and made the formation of the trimer possible, entropy is still an important factor which imposes the formation of the smallest assembly.

Moreover, it was expected that the macrocycle backbone may have an influence on the nature of the complexes formed due to steric hindrance. Considering the results obtained, it does not look so. There is indeed no trace of tetramer of rotaxane, which was initially our target molecule. In spite of the rigidity and the preorganization of ligand **20**, entropy tends to favour the formation of the smallest assemblies.

3.3 Conclusion

In this chapter, we described the synthesis of a new macrocyclic ditopic ligand whose chelate coordination axes are perpendicular to one another. The synthesis has been optimized and several Suzuki C-C coupling reactions afforded the desired product, which was fully characterized. It should be noted that all the molecules whose synthesis is reported here are new.

Coordination chemistry of such a macrocyclic ditopic ligand with zinc(II) afforded in good yield a rotaxane dimer as the sole product formed, and not a trimer or a tetramer, contrary to

what was expected from the ideal geometries of the ligand and of the zinc(II) coordination sphere. This has been proven by ES-MS, ^{1}H NMR and diffusion-ordered spectroscopies.

By changing the nature of the metal ion into copper(II), which has more demanding stereoelectronic requirements, we managed to obtain in a good yield a mixture of a rotaxane trimer and dimer, as shown by ES-MS. The exact ratio of trimer/dimer could not be determined.

As in the acyclic system, it thus appeared that translational entropy is a very important factor in such complexation processes, leading to the smallest possible structure, in spite of the enthalpic cost of probable distortion of the zinc(II) coordination sphere and constraints within the ligand. Such kind of behaviour was moderated by introducing a metal with more stereoelectronic requirements, making distortion more difficult.

Even if the desired tetramer of rotaxane could not be obtained, those results are nonetheless very promising in terms of potential applications as molecular machines. Indeed, the dimer of rotaxane presented here is the ideal precursor to a new molecular muscle. In the future, one can also imagine to functionalize the trimer of rotaxane in the same way so as to obtain an "expandable" triangular structure which would be a new 2-dimensional molecular device.

After trying to prepare a rotaxane tetramer by intertwining four identical ditopic ligand, we imagined a strategy which would yield another kind of rotaxane tetramer: a bis-[3]-rotaxane. This will be presented in the next chapter.

Chapter 4
A terpy-based bis-macrocycle: towards a [4]pseudo-rotaxane

4.1 An alternative strategy towards a square-like stucture

4.1.1 Strategy principle

The two previous chapters described the synthesis of highly rigid ditopic ligands whose geometry had been designed so that the chelate coordination axes would be perpendicular to one another. Complexes of various nuclearities were expected depending on the metal centers used. In particular when the ligand was bearing a macrocycle in its organic backbone, a rotaxane tetramer was expected to be formed.

In spite of the well preorganized structure of the ligands bearing or not a macrocycle, the tetramer structure was never observed, but we managed to clearly identify the formation of both a rotaxane dimer and trimer.

The approach we used in order to prepare a rotaxane tetramer was thus to assemble four identical ditopic ligands around metal centres. Because of entropy, such kind of attractive architectures could not be observed and distortion of the organic backbones yielded lower nuclearities. But another approach yielding a square-like structure was imagined, based on the assembly of two rod-like compounds with two bis-macrocycles. (Figure 4.1)

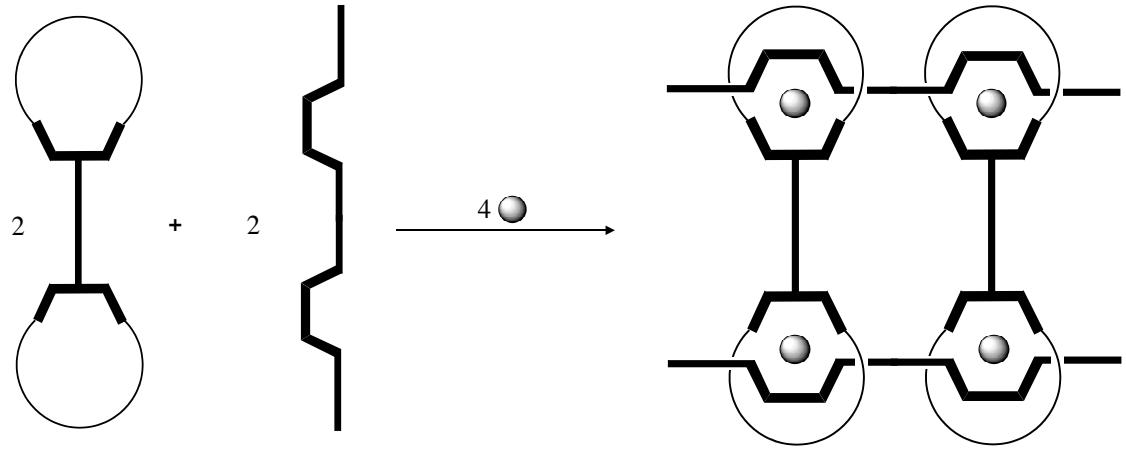

Figure 4.1: Strategy principle towards a cyclic pseudo[4]rotaxane

4.1.2 A cyclic pseudo[4]rotaxane using the Cu(I) as a template

Such kind of strategy has already been applied in a research project developed in our group whose aim is to build sophisticated two-dimensional molecular machines. The precursor of this large molecular device has been published recently.[175] By taking advantage of the template effect of Cu(I), two bis-macrocycles and two linear threads could be assembled to form a 2D interlocking network, as shown in Figure 4.2. Purely organic systems displaying the same topological properties have recently been reported by Aricó *et al.*[176]

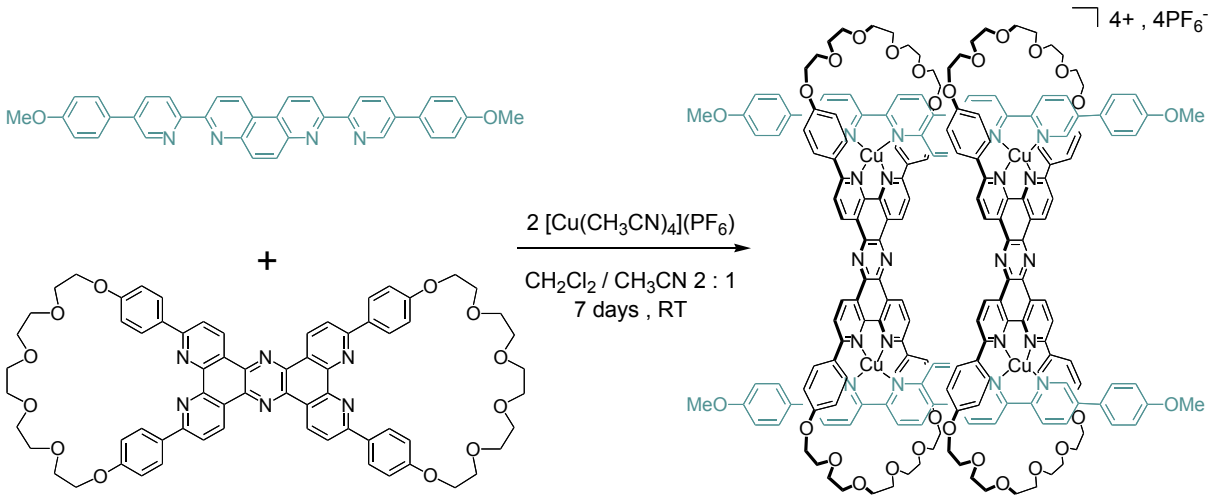

Figure 4.2: Synthesis of a cyclic pseudo[4]rotaxane around copper(I) metal centres

One of the key factors to the success of the present threading reaction, leading to the pseudo[4]rotaxane, is the rigidity of the organic fragments used. In fact, these ligands cannot easily lead to other discrete complexes than the desired 4-metal system. Two phenanthrolines attached back-to-back and included in a bis-macrocycle were previously published by our group,[177] whereas the bis-bidentate thread built around a 4,7-phenanthroline nucleus was a new compound.[175] The backbone of the central 4,7-phenanthroline unit forces the two bipyridine chelates in the same direction and provides the system with the required rigidity.

In conclusion, the gathering and threading effect of copper(I) turned out to be, once again, particularly efficient. It allowed assembly of a pseudo-rotaxane tetramer quantitatively from 4 organic fragments. We will use the same strategy in order to synthesize a rotaxane tetramer using a terpy-based bis-macrocycle and zinc(II) as a template.

4.2 Synthesis of a terpy-based bis-macrocycle

In chapter 2, we described the synthesis of compound **18**, a macrocycle having 34 atoms in its interior and including a terpy functionalized in the back by a bromophenylene fragment. This compound would be the ideal candidate as a precursor to a bis-macrocycle including two terpy attached back-to-back. Two synthetic pathways yielding the bis-macrocycle will be presented here.

4.2.1 Homocoupling strategy

Considering the presence of an aryl bromide at the back of compound **18**, the obvious strategy to make a bis-macrocycle was to use a classical homocoupling reaction using a nickel(II) catalyst.[178-180] Moreover, this strategy had already been used successfully in our group to synthesize bis-terpy attached back-to-back and then to study electron or energy transfer between metal centres coordinated to the terpy units.[181-183] But it was the first time that such kind of homocoupling reaction was adapted to a terpy included in a macrocycle (Figure 4.3).

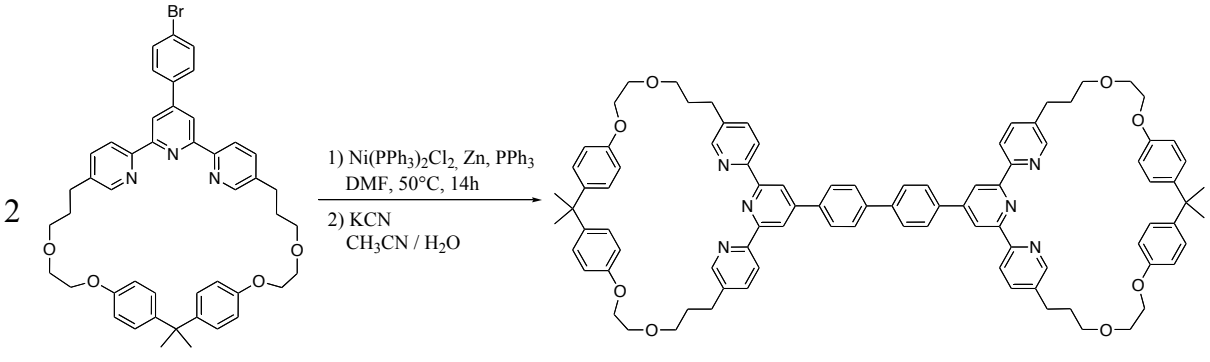

18 **21** (20%)

Figure 4.3: Synthesis of the terpy-based bis-macrocycle **21** *via* the homocoupling strategy

The method uses the *in situ* generated reactive reagent $Ni[PPh_3]_4$, from air-stable easily available bis[triphenylphosphine]nickel dichloride, by reduction with zinc dust in the presence of triphenylphosphine. Once the reaction turned dark red, indicating the formation of the Ni(0) reactive species, **18** was added and the reaction was stirred at 50°C under argon and monitored by TLC. After 14 hours, the starting material was consumed. The solvent was then evaporated. In order to remove the nickel centre coordinated to the terpy nucleus, the crude mixture was taken in water and acetonitrile, and KCN was added. The mixture was refluxed for 90 minutes. The organic layer was decanted and column chromatography afforded **21** as a white solid (20%). This new product was fully characterized by ES-MS and NMR spectroscopies.

Despite several attempts and varying the parameters (amount of catalyst, time of reaction, smoother work-up conditions), the yield could not be increased. Such a poor yield was not acceptable, and represented a real waste of compound **18**, yet so "expensive" to make.
We thus decided to adapt the Suzuki coupling protocol to the synthesis of this bis-macrocycle.

4.2.2 Suzuki coupling strategy

Considering the good results obtained on the Suzuki coupling reactions used to make the sophisticated macrocyclic ditopic ligand **20** presented in chapter 3, we decided to employ the same strategy and to couple **18** with its boronic ester analogue **19** (Figure 4.4).

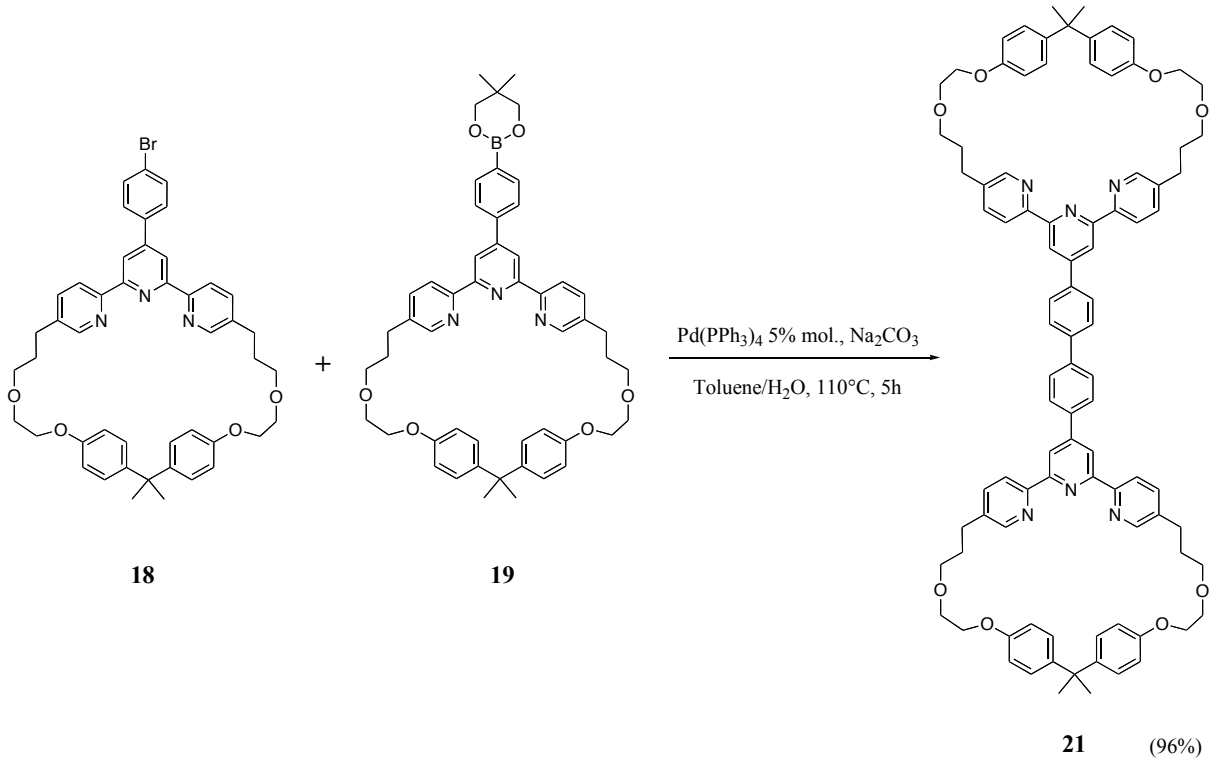

Figure 4.4: Synthesis of **21** *via* the Suzuki coupling protocole

Compound **19** was freshly prepared according to the same procedure as the one described in chapter 3. The C-C coupling reaction has then been carried out under the classical Suzuki conditions, using $Pd(PPh_3)_4$ as a catalyst, Na_2CO_3 as a base, in a mixture of toluene, water and ethanol (6:2:1). Compound **18** was introduced in slight deficit, assuming that the boronic ester was obtained in 80% yield. The reaction was monitored by TLC. After 5 hours, the spot related to **18** disappeared, indicating the end of the reaction. The crude mixture was purified by column chromatography over alumina, and 14.5 mg (96%) of compound **21** could be isolated (77% over the two steps).

The overall yield of synthesis of compound **21** was thus critically affected by the change of strategy, and in spite of its two steps, the Suzuki pathway was definitely more efficient than the classical homocoupling with nickel catalyst.

At this time, our concern was to try and assemble this bis-macrocycle with the same molecular thread as in the copper(I) cyclic [4]rotaxane.[175] But in our case, one should use a 5-coordinate metal centre, so that the terpy moiety of the bis-macrocycle would assemble with the bipy moiety of the thread. This will be discussed in the next section.

4.3 Towards a 5-coordinate metal center based [4]pseudo-rotaxane

Due to the small amount of bis-macrocycle **21**, the threading reaction could be attempted only once. The following is thus preliminary results, and many investigations are currently in progress.

In order to assemble the bis-macrocyle **21** bearing two tridentate chelates (terpyridines) with the same molecular thread as the one used in the copper(I) system which bears two bidentate chelates (bipyridines), one should use a preferentially 5-coordinate metal center. As in the assemblies presented in the previous chapters, we chose Zn(II) which enables more characterizations of the products formed thanks to ES-MS and ^{1}H NMR.

Contrary to the system built around copper(I) in which both building blocks were barely soluble in common organic solvents, the bis-macrocycle **21** we used in our system was perfectly soluble in dichloromethane. The bis-bipy thread was thus added as a solid to a solution of **21** in dichloromethane. One equivalent of $Zn(OTf)_2$ in methanol was then added to the colourless suspension, which turned instantaneously bright yellow (Figure 4.5). After one day, the solution was still bright yellow and a suspension was still present, indicating that the

complexation process was not complete. This is in accordance with the fact that only one equivalent of the metal center over the two necessary for the formation of the desired assembly had been added. The second equivalent was thus added and the suspension disappeared immediately, while the colour of the solution did not change. After two more days, the solution remained yellow and perfectly clear. This indicates that coordination of the ligands to the zinc(II) metal centres makes them perfectly soluble, exactly as observed in the copper(I) system.

Considering the rigidity of the organic fragments used, these ligands cannot easily lead to other discrete complexes than the desired 4-metal system. Hence, regarding both the solubilization of the ligands and their structural rigidity, we assumed at this stage that the [4]pseudo-rotaxane had been formed in solution.

Evaporation of the solvents afforded a yellow solid. Due to solubility problems, we could not prepare a clear solution of this solid in any deuterated solvent. The ^{1}H NMR spectrum of such a suspension was as expected very complicated and did not give any proof of formation of the desired product.

Both MALDI-MS and ES-MS indicated that no threaded species were present. The only species that could be observed were the ligands coordinated respectively to two zinc metal centres, the rest of the coordination sphere being occupied by triflates or chlorine atoms.

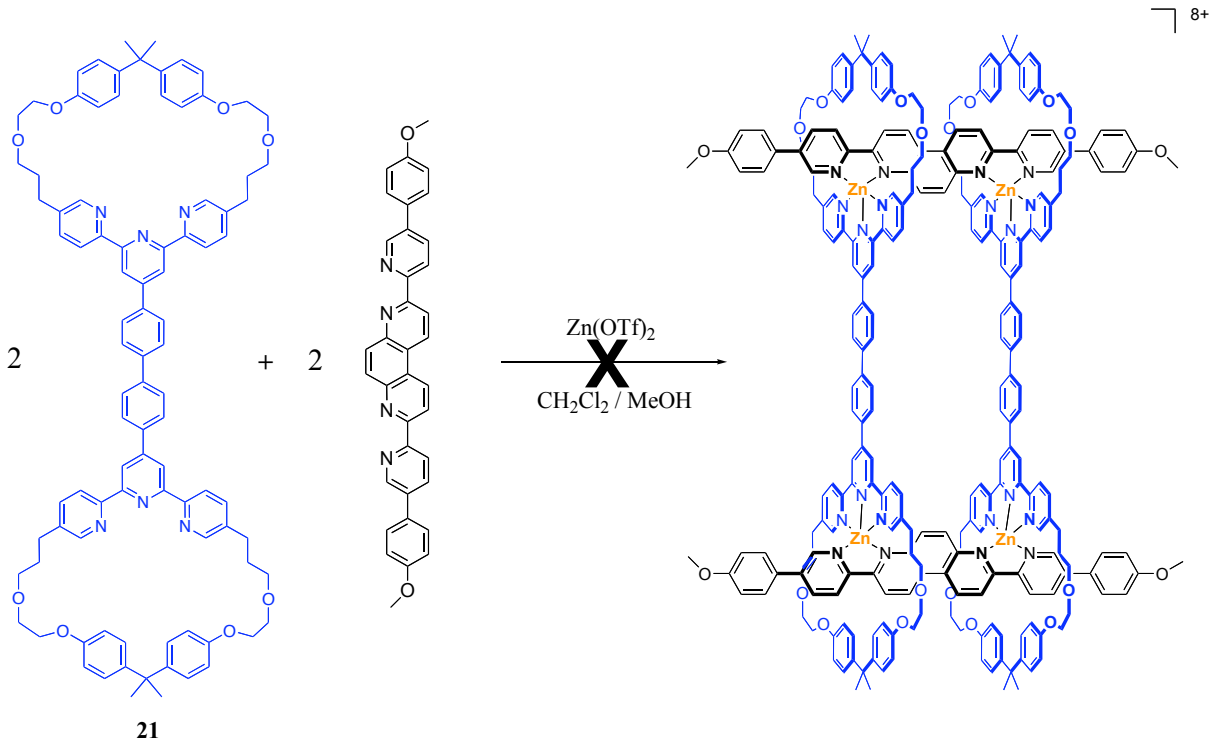

21

Figure 4.5: First attempt toward a cyclic pseudo[4]rotaxane using zinc(II) as a template

The purity of the zinc salt has been checked, therefore we think that the chlorine atoms can only come from the dichloromethane used as a solvent. Anyway, the presence of chlorine atoms coordinated to the zinc(II) explains why no threaded species could be observed. Chlorine atoms are strong counter-ions, and especially stronger than any bipy or terpy nucleus of the ligands. Once coordinated, the chlorine atoms won't move and the coordination dynamics necessary to form the desired product is stopped.

Due to time constraints, we could not investigate that reaction further on, but we are quite confident that when the solution was still clear, the desired product was there. Further studies should confirm this fact.

4.4 Conclusion

A new bis-macrocycle compound built around two terpyridine units attached back to back has been synthesized. The classical homocoupling strategy using a nickel catalyst gave poor yields, but compound **21** could be achieved very efficiently *via* a Suzuki coupling between two derivatives of macrocycle MT34 bearing an aryl bromide and a boronic ester function at the back respectively.

The first attempt to thread two bis-macrocycles on two bis-bipy rails in order to obtain a cyclic [4]rotaxane did not succeed by now, in spite of the instantaneous solubilization of the ligands upon addition of the metal ion. Still, we are quite confident that formation of the desired product will be demonstrated in further studies.

We point out that such kind of ditopic bis-macrocycle compound bearing two terdentate chelates should be very useful in the future. It would be interesting to synthesize homo- and/or heterodinuclear complexes with it, study its photochemical properties and compare it with the previous similar systems synthesized in the laboratory. It could also be used as an interesting building block toward complex two-dimensional molecular devices.

Chapter 5
General conclusion

The work described in this thesis belongs to the field of topological chemistry. The initial goal was to synthesize a rotaxane tetramer using molecular threads and rings woven around pentacoordinated metal centres.

The main part of the project was the design and the synthesis of a macrocyclic and highly rigid phen-terpy conjugate, whose chelate coordination axes are orthogonal to one another. Considering the long and difficult synthetic route leading to a macrocycle bearing a terpy functionalized in the back, we first reported in Chapter 2 the synthesis of an acyclic analogue, which was obtained in 8 steps from commercially available reagents, *via* several C-C Suzuki coupling reactions. Coordination of this ditopic ligand on zinc(II) metal centres yielded surprisingly a dimer species as the sole product formed. By using metal centers having more demanding stereoelectronic requirements such as copper(II), we obtained a mixture of the dimer and the trimer species, showing that in both cases, translational entropy is a prevailing factor leading to the smallest possible complex in spite of the enthalpic cost of the organic backbone distortion.

In Chapter 3, we reported the synthesis in 15 steps of the desired target molecule, the macrocyclic analogue of the previous phen-terpy conjugate, where the terpy nucleus is incorporated in a macrocycle bearing 34 atoms in its interior. Coordination of this macrocycle ditopic ligand with zinc(II) yielded a rotaxane dimer, and the use of copper(II) afforded a

mixture of rotaxane dimer and trimer. Hence, compared to the acyclic system, the presence of the ring did not change the nuclearity of the complexes formed and entropy still has a great influence on the coordination process.

In chapter 4, we described an alternative strategy affording another kind of rotaxane tetramer: a bis-[3]-rotaxane made of two bis-macrocyclic compounds threaded on two molecular rods. The synthesis in 13 steps of a new bis-macrocycle built around two terpy nuclei attached back-to-back is reported here, and two different synthetic routes were investigated: a classical homocoupling reaction, and a heterocoupling pathway *via* Suzuki coupling reaction. The latter was far more efficient, and the new terpy-based bis-macrocycle could be engaged in a coordination reaction on bis-bipy rods using zinc(II) as a template. Coordination studies are still in progress.

In this manuscript, we reported the synthesis of a whole new family of terpy-based ligands, incorporated or not in a macrocyclic structure, and connected in the back either to a phen nucleus or to another terpy moiety. Such kinds of ligands are very promising and could be used in the future as building blocks or precursors for molecular machines. The rotaxane dimer and trimer presented here would indeed be ideal candidates towards new expandable architectures reminiscent to the molecular muscle prototype. It would also be interesting to study the photochemical properties of homo- and heterodinuclear complexes of the terpy-based bis-macrocycle, and use this ‘handcuff-like” compound as building block towards new topologies and complex two-dimensional molecular devices.

Chapter 6
References

1. Gokel, G. W.; Editor, *Crown Ethers and Cryptands*. 1991.
2. Dietrich, B.; Lehn, J. M.; Sauvage, J. P., *Tetrahedron Letters* **1969**, (34), 2889.
3. Truter, M. R.; Pedersen, C. J., *Endeavour* **1971,** 30, (111), 142.
4. Moran, J. R.; Karbach, S.; Cram, D. J., *Journal of the American Chemical Society* **1982,** 104, (21), 5826.
5. Cram, D. J., *Science* **1983,** 219, (4589), 1177.
6. Canceill, J.; Lacombe, L.; Collet, A., *Journal of the American Chemical Society* **1985,** 107, (24), 6993.
7. Collet, A., *Tetrahedron* **1987,** 43, (24), 5725.
8. Kroto, H. W.; Heath, J. R.; O'Brien, S. C.; Curl, R. F.; Smalley, R. E., *Nature* **1985,** 318, (6042), 162.
9. Kroto, H., *Pure and Applied Chemistry* **1990,** 62, (3), 407.
10. Frisch, H. L.; Wasserman, E., *Journal of the American Chemical Society* **1961,** 83, 3789.
11. Wasserman, E., *Scientific American* **1962,** 207, (5), 94.
12. Schill, G., *Catenanes, rotaxanes and knots*. Academic Press: New York (NY), 1971.
13. Sokolov, V., *Russian Chemical Reviews* **1973,** 42, 452.
14. Walba, D. M., *Tetrahedron* **1985,** 41, (16), 3161.
15. Sauvage, J. P.; Dietrich-Buchecker, C., *Molecular catenanes, rotaxanes and knots*. Wiley-VCH: Weinheim, 1999.
16. Mitchell, D. K.; Chambron, J. C., *Journal of Chemical Education* **1995,** 72, (12), 1059.
17. Mislow, K., *Bulletin de la Société Chimique Belge* **1977,** 86, 595.
18. Harray, F., *Graph theory*. Addison-Wesley: Reading (MA), 1969.
19. Kuck, D.; Schuster, A., *Angewandte Chemie Int. Ed. Engl.* **1988,** 27, 1192.
20. Otsubo, T.; Ogura, F.; Misumi, S., *Tetrahedron Letters* **1983,** 24, 4851.
21. Walba, D. M.; Richards, R. M.; Haltiwanger, R. C. J., *Journal of the American Chemical Society* **1982,** 104, 3219.
22. Wasserman, E., *Journal of the American Chemical Society* **1960,** 82, 4433.
23. Harrison, I. T.; Harrison, S., *Journal of the American Chemical Society* **1967,** 89, 5723.
24. Agam, G.; Graiver, D.; Zilkha, A., *Journal of the American Chemical Society* **1976,** 98, 5206.
25. Schill, I. G.; Luettringhaus, A., *Angewandte Chemie* **1964,** 76, (13), 567.
26. Schill, G., *Chemische Berichte* **1967,** 100, (6), 2021.
27. Schill, G.; Zollenkopf, H., *Justus Liebigs Annalen der Chemie* **1969,** 721, 53.
28. Dietrich-Buchecker, C. O.; Sauvage, J. P.; Kintzinger, J. P., *Tetrahedron Letters* **1983,** 24, 5095.
29. Dietrich-Buchecker, C. O.; Sauvage, J. P., *Tetrahedron Letters* **1983,** 24, 5091.
30. Dietrich-Buchecker, C. O.; Kern, J. M.; Sauvage, J. P., *Journal of the American Chemical Society* **1984,** 106, 3043.

31. Ashton, P. R.; Goodnow, T. T.; Kaifer, A. E.; Reddington, M. V.; Slawin, A. M. Z.; Spencer, N.; Stoddart, J. F.; Vicent, C.; Williams, D. J., *Angewandte Chemie Int. Ed. Engl.* **1989,** 28, 1396.
32. Vögtle, F.; Meier, S.; Hoss, R., *Angewandte Chemie Int. Ed. Engl.* **1992,** 31, 1616.
33. Hunter, C. A., *Journal of the American Chemical Society* **1992,** 114, 5303.
34. Fujita, M.; Hagihara, H.; Ogura, K., *Nature* **1994,** 367, 720.
35. Ogino, H., *Journal of the American Chemical Society* **1981,** 103, 1303.
36. Ashton, P. R.; Fyfe, M. C. T.; Hickingbottom, S. K.; Menzer, S.; Stoddart, J. F.; White, A. J. P.; Williams, D. J., *Chemistry - A European Journal* **1998,** 4, (4), 577.
37. Gatti, F. G.; Leigh, D. A.; Nepogodiev, S. A.; Slawin, A. M. Z.; Teat, S. J.; Wong, J. K. Y., *Journal of the American Chemical Society* **2001,** 123, 5983.
38. Vögtle, F.; Duennwald, T.; Schmidt, T., *Accounts of Chemical Research* **1996,** 29, 451.
39. Anelli, P. L.; Ashton, P. R.; Ballardini, R.; Balzani, V.; Delgado, M.; Gandolfi, M.-T.; Goodnow, T. T.; Kaifer, A. E.; Philp, D.; Pietraszkiewicz, M.; Prodi, L.; Reddington, M. V.; Slawin, A. M. Z.; Spencer, N.; Stoddart, J. F.; Vicent, C.; Williams, D. J., *Journal of the American Chemical Society* **1992,** 114, 193.
40. Hamilton, D. G.; Feeder, N.; Prodi, L.; Teat, S. J.; Clegg, W.; Sanders, J. K. M., *Journal of the American Chemical Society* **1998,** 120, 1096.
41. Hiratani, K.; Suga, J.-I.; Nagawa, Y.; Houjou, H.; Tokuhisa, H.; Numata, M.; Watanabe, K., *Tetrahedron Letters* **2002,** 43, 5747.
42. Walba, D. M.; Armstrong, J. D.; Perry, A. E.; Richards, R. M.; Homan, T. C.; Haltiwanger, R. C. J., *Tetrahedron* **1986,** 42, 1883.
43. Dietrich-Buchecker, C. O.; Sauvage, J. P., *Angewandte Chemie Int. Ed.* **1989,** 28, 189.
44. Dietrich-Buchecker, C. O.; Sauvage, J. P.; De Cian, A.; Fischer, J., *Journal of the Chemical Society Chemical Communications* **1994**, 2231.
45. Dietrich-Buchecker, C. O.; Rapenne, G.; Sauvage, J. P., *Journal of the Chemical Society Chemical Communications* **1997**, 2053.
46. Nicolaou, K. C.; van Delft, F.; Ohshima, T.; Vourloumis, D.; Xu, J.; Hosokawa, S.; Pfefferkorn, J.; Kim, S.; Li, T., *Angewandte Chemie Int. Ed.* **1997,** 36, 2520.
47. Sasaki, M.; Matsumori, N.; Maruyama, T.; Nonomura, T.; Murata, M.; Tachibana, K.; Yasumoto, T., *Angewandte Chemie Int. Ed.* **1996,** 35, 1672.
48. Nicolaou, K. C.; Yang, Z.; Shi, G.-Q.; Gunzner, J. L.; Agrios, K. A.; Gartner, P., *Nature* **1998,** 392, (6673), 264.
49. Hudson, B.; Vinograd, J., *Nature* **1967,** 216, 647.
50. Clayton, D. A.; Vinograd, J., *Nature* **1967,** 216, 652.
51. Liu, L. F.; Depew, R. E.; Wang, J. C., *Journal of Molecular Biology* **1976,** 106, 439.
52. Wikoff, W. R.; Liljas, L.; Duda, R. L.; Tsuruta, H.; Hendrix, R. W.; Johnson, J. E., *Science* **2000,** 289, (5487), 2129.
53. Taylor, L. T.; Vergez, S. C.; Busch, D. H., *Journal of the American Chemical Society* **1966,** 88, (13), 3170.
54. Blinn, E. L.; Busch, D. H., *Inorganic Chemistry* **1968,** 7, (4), 820.
55. Fuhrhop, J. H.; Struckmeier, G.; Thewalt, U., *Journal of the American Chemical Society* **1976,** 98, 278.
56. Sheldrick, W. S.; Engel, J., *Journal of the Chemical Society Chemical Communications* **1980**, 5.
57. Bonfiglio, J. V.; Bonnet, R.; Buckley, D. G.; Hamzetash, D.; Hursthouse, M. B.; Malick, K. M. A.; McDonald, A. F.; Trotter, J., *Tetrahedron* **1983,** 39, 1865.
58. van Stein, G. C.; van der Poel, H.; van Koten, G., *Journal of the Chemical Society Chemical Communications* **1980**, 1016.

59. van Stein, G. C.; van Koten, G.; Passenier, H.; Steinebach, O.; Vrieze, K., *Inorganica Chimica Acta* **1984,** 89, 79.
60. van Stein, G. C.; van Koten, G.; Vrieze, K.; Brevard, C.; Spek, A. L., *Journal of the American Chemical Society* **1984,** 106, 4486.
61. Lehn, J. M.; Rigault, A.; Siegel, J.; Harrowfield, J.; Chevrier, B.; Moras, D., *Proceedings of the National Academy of Sciences of the United States of America* **1987,** 84, (9), 2565.
62. Lehn, J.-M.; Rigault, A., *Angewandte Chemie Int. Ed.* **1988,** 27, 1095.
63. Constable, E. C.; Drew, M. G. B.; Ward, M. D., *Journal of the Chemical Society Chemical Communications* **1987**, 1600.
64. Barley, M.; Constable, E. C.; Corr, S. A.; McQueen, R. C. S.; Nutkins, J. C.; Ward, M. D.; Drew, M. G. B., *Journal of the Chemical Society Dalton Transactions* **1988**, 2655.
65. Constable, E. C.; Ward, M. D., *Journal of the American Chemical Society* **1990,** 112, 1256.
66. Chichak, K. S.; Cantrill, S. J.; Pease, A. R.; Chiu, S.-H.; Cave, G. W. V.; Atwood, J. L.; Stoddart, J. F., *Science* **2004,** 304, (5675), 1308.
67. Swiegers, G. F.; Malefetse, T. J., *Chemical reviews* **2000,** 100, 3483.
68. Garrett, T. M.; Koert, U.; Lehn, J. M.; Rigault, A.; Meyer, D.; Fischer, J., *Journal of the Chemical Society Chemical Communications* **1990**, (7), 557.
69. Baxter, P. N. W.; Lehn, J.-M.; Fischer, J.; Youinou, M.-T., *Angewandte Chemie* **1994,** 106, (22), 2432.
70. Hanan, G. S.; Arana, C. R.; Lehn, J.-M.; Fenske, D., *Angewandte Chemie, Int. Ed. Engl.* **1995,** 34, (10), 1122.
71. Baxter, P. N.; Hanan, G. S.; Lehn, J.-M., *Chemical Communications* **1996**, (17), 2019.
72. Baxter, P. N.; Lehn, J.-M.; Kneisel, B. O.; Fenske, D., *Chemical Communications* **1997**, 2231.
73. Baxter, P. N.; Lehn, J.-M.; Kneisel, B. O.; Fenske, D., *Angewandte Chemie Int. Ed. Engl.* **1997,** 36, 1978.
74. Weissbuch, I.; Baxter, P. N.; Cohen, S.; Cohen, H.; Kjaer, K.; Howes, P. B.; Als-Nielsen, J.; Hanan, G. S.; Schubert, U. S.; Lehn, J.-M.; Leiserowitz, L.; Lahav, M., *Journal of the American Chemical Society* **1998,** 120, 4850.
75. Hanan, G. S.; Arana, C. R.; Lehn, J.-M.; Baum, G.; Fenske, D., *Chemistry - A European Journal* **1996,** 2, 1292.
76. Fujita, M.; Tominaga, M.; Hori, A.; Therrien, B., *Accounts of Chemical Research* **2005,** 38, (4), 371.
77. Fujita, M.; Yazaki, J.; Ogura, K., *Journal of the American Chemical Society* **1990,** 112, 5645.
78. Fujita, M.; Sasaki, O.; Mitsuhashi, T.; Fujita, T.; Yazaki, J.; Yamaguchi, K.; Ogura, K., *Journal of the Chemical Society Chemical Communications* **1996**, 1535.
79. Balzani, V.; Venturi, M.; Credi, A., *Molecular Devices and Machines*. Wiley-VCH: Weinheim, 2003.
80. *Accounts of Chemical Research* **2001,** 34, 341.
81. Schliwa, M., *Molecular Motors*. Wiley-VCH: Weinheim, 2002.
82. Soong, R. K.; Bachand, G. D.; Neves, H. P.; Olkhovets, A. G.; Montemagno, C. D., *Science* **2000,** 290, (5496), 1555.
83. Noji, H.; Yasuda, R.; Yoshida, M.; Kinosita Jr, K., *Nature* **1997,** 386, 299.
84. Bissel, R. A.; Cordova, E.; Kaifer, A. E.; Stoddart, J. F., *Nature* **1994,** 369, 133.
85. Badjic, J. D.; Balzani, V.; Credi, A.; Silvi, S.; Stoddart, J. F., *Science* **2004,** 303, 1845.
86. Ballardini, R.; Balzani, V.; Gandolfi, M. T.; Prodi, L.; Venturi, M.; Philp, D.; Ricketts, H. G.; Stoddart, J. F., *Angewandte Chemie Int. Ed.* **1993,** 32, 1301.

87. Livoreil, A.; Sauvage, J.-P.; Armaroli, N.; Balzani, V.; Flamigni, L.; Ventura, B., *Journal of the American Chemical Society* **1997,** 119, 12114.
88. Armaroli, N.; Balzani, V.; Collin, J.-P.; Gavina, P.; Sauvage, J.-P.; Ventura, B., *Journal of the American Chemical Society* **1999,** 121, 4397.
89. Murakami, H.; Kawabuchi, A.; Kotoo, K.; Kunitake, M.; Nakashima, N., *Journal of the American Chemical Society* **1997,** 119, 7605.
90. Balzani, V.; Credi, A.; Marchioni, F.; Stoddart, J. F., *Chemical Communications* **2001**, 1860.
91. Kelly, T. R.; de Silva, H.; Silva, R. A., *Nature* **1999,** 401, 150.
92. Koumura, N.; Zijistra, R. W. J.; van Delden, R. A.; Harada, N.; Feringa, B. L., *Nature* **1999,** 401, 152.
93. Leigh, D. A.; Wong Jenny, K. Y.; Dehez, F.; Zerbetto, F., *Nature* **2003,** 424, (6945), 174.
94. Katz, E.; Lioubashevsky, O.; Willner, I., *Journal of the American Chemical Society* **2004,** 126, 15520.
95. Shipway, A. N.; Willner, I., *Accounts of Chemical Research* **2001,** 34, 421.
96. Harada, A., *Accounts of Chemical Research* **2001,** 34, 456.
97. Zahn, S.; Canary, J. W., *Science* **2000,** 288, 1404.
98. Shinkai, S.; Nakaji, T.; Ogawa, T.; Shigematsu, K.; Manabe, O., *Journal of the American Chemical Society* **1981,** 103, 111.
99. Shinkai, S.; Ishihara, M.; Ueda, K.; Manabe, O., *Journal of Chemical Society Perkin Transactions 2* **1985**, 511.
100. Parthenopoulos, D. A.; Rentzepis, P. M., *Science* **1989,** 245, 843.
101. Willner, I.; Blonder, R.; Dagan, A., *Journal of the American Chemical Society* **1994,** 116, (7), 3121.
102. Irie, M.; Miyatake, O.; Uchida, K., *Journal of the American Chemical Society* **1992,** 114, (22), 8715.
103. Gilat, S. L.; Kawai, S. H.; Lehn, J. M., *Journal of the Chemical Society Chemical Communications* **1993**, (18), 1439.
104. Cardenas, D. J.; Livoreil, A.; Sauvage, J.-P., *Journal of the American Chemical Society* **1996,** 118, (47), 11980.
105. Livoreil, A.; Dietrich-Buchecker, C. O.; Sauvage, J.-P., *Journal of the American Chemical Society* **1994,** 116, (20), 9399.
106. Dietrich-Buchecker, C.; Sauvage, J.-P.; Kintzinger, J.-P., *Tetrahedron Letters* **1983,** 24, 5095.
107. Dietrich-Buchecker, C.; Sauvage, J. P., *Tetrahedron* **1990,** 46, (2), 503.
108. Korybut-Daszkiewicz, B.; Wieçkowska, A.; Bilewicz, R.; Domagata, S.; Wozniak, K., *Journal of the American Chemical Society* **2001,** 123, 9356.
109. Korybut-Daszkiewicz, B.; Wieçkowska, A.; Bilewicz, R.; Domagata, S.; Wozniak, K., *Angewandte Chemie Int. Ed.* **2004,** 43, 1668.
110. Poleschak, I.; Kern, J.-M.; Sauvage, J.-P., *Chemical Communications* **2004**, (4), 474.
111. Brouwer, A. M.; Frochot, C.; Gatti, F. G.; Leigh, D. A.; Mottier, L.; Paolucci, F.; Roffia, S.; Wurpel, G. W. H., *Science* **2001,** 291, (5511), 2124.
112. Ashton, P. R.; Ballardini, R.; Balzani, V.; Baxter, I.; Credi, A.; Fyfe, M. C. T.; Gandolfi, M. T.; Gomez-Lopez, M.; Martinez-Diaz, M. V.; Piersanti, A.; Spencer, N.; Stoddart, J. F.; Venturi, M.; White, A. J. P.; Williams, D. J., *Journal of the American Chemical Society* **1998,** 120, (46), 11932.
113. Balzani, V.; Credi, A.; Mattersteig, G.; Matthews, O. A.; Raymo, F. M.; Stoddart, J. F.; Venturi, M.; White, A. J. P.; Williams, D. J., *Journal of Organic Chemistry* **2000,** 65, (7), 1924.

114. Canevet, C.; Libman, J.; Shanzer, A., *Angewandte Chemie Int. Ed.* **1996,** 35, 2657.
115. Zeeikovich, L.; Libman, J.; Shanzer, A., *Nature* **1995,** 374, 790.
116. Amendola, V.; Fabbrizzi, L.; Mangano, C.; Pallavicini, P., *Accounts of Chemical Research* **2001,** 34, 488.
117. Mobian, P.; Kern, J.-M.; Sauvage, J.-P., *Angewandte Chemie Int. Ed.* **2004,** 43, (18), 2392.
118. Collin, J.-P.; Laemmel, A.-C.; Sauvage, J.-P., *New Journal of Chemistry* **2001,** 25, (1), 22.
119. Laemmel, A.-C., PhD thesis, Université Louis Pasteur, Strasbourg, 2000.
120. Adelt, M.; Devenney, M.; Meyer, T. J.; Thompson, D. W.; Treadway, J. A., *Inorganic Chemistry* **1998,** 37, (11), 2616.
121. van Houten, J.; Watts, J., *Inorganic Chemistry* **1978,** 17, 3381.
122. Suen, H. F.; Wilson, S. W.; Pomerantz, M.; Walsh, J. L., *Inorganic Chemistry* **1989,** 28, (4), 786.
123. Pinnick, D. V.; Durham, B., *Inorganic Chemistry* **1984,** 23, (24), 3841.
124. Durham, B.; Caspar, J. V.; Nagle, J. K.; Meyer, T. J., *Journal of the American Chemical Society* **1982,** 104, 4803.
125. Tachiyashiki, S.; Mizumachi, K., *Coordination Chemistry Reviews* **1994,** 132, 113.
126. Mobian, P.; Kern, J.-M.; Sauvage, J.-P., *Helvetica Chimica Acta* **2003,** 86, (12), 4195.
127. Ashton, P. R.; Ballardini, R.; Balzani, V.; Credi, A.; Dress, K. R.; Ishow, E.; Kleverlaan, C. J.; Kocian, O.; Preece, J. A.; Spencer, N.; Stoddart, J. F.; Venturi, M.; Wenger, S., *Chemistry - A European Journal* **2000,** 6, (19), 3558.
128. Credi, A.; Ferrer, B., *Pure and Applied Chemistry* **2005,** 77, (6), 1051.
129. de Silva, A. P.; Gunaratne, H. Q. N.; McCoy, C. P., *Nature* **1993,** 364, 42.
130. de Silva, A. P.; Gunaratne, H. Q. N.; Gunnlaugsson, T.; Huxley, A. J. M.; McCoy, C. P.; Rademacher, J. T.; Rice, T. E., *Chemical Reviews* **1997,** 97, (5), 1515.
131. Credi, A.; Balzani, V.; Langford, S. J.; Stoddart, J. F., *Journal of the American Chemical Society* **1997,** 119, (11), 2679.
132. Pina, F.; Roque, A.; Melo, M. J.; Maestri, M.; Belladelli, L.; Balzani, V., *Chemistry - A European Journal* **1998,** 4, (7), 1184.
133. de Silva, A. P.; Dixon, I. M.; Gunaratne, H. Q. N.; Gunnlaugsson, T.; Maxwell, P. R. S.; Rice, T. E., *Journal of the American Chemical Society* **1999,** 121, (6), 1393.
134. Ashton, P. R.; Balzani, V.; Kocian, O.; Prodi, L.; Spencer, N.; Stoddart, J. F., *Journal of the American Chemical Society* **1998,** 120, (43), 11190.
135. Fabbrizzi, L.; Foti, F.; Patroni, S.; Pallavicini, P.; Taglietti, A., *Angewandte Chemie Int. Ed.* **2004,** 43, 5073.
136. Amendola, V.; Fabbrizzi, L.; Mangano, C.; Miller, H.; Pallavicini, P.; Perotti, A.; Taglietti, A., *Angewandte Chemie Int. Ed.* **2002,** 41, 2553.
137. Karlin, K. D.; Hayes, J. C.; Juen, S.; Hutchinson, J. P.; Zubieta, J., *Inorganic Chemistry* **1982,** 21, 4108.
138. Amendola, V.; Brusoni, C.; Fabbrizzi, L.; Miller, H.; Pallavicini, P.; Perotti, A.; Taglietti, A., *Journal of Chemical Society Dalton Transactions* **2001**, 3528.
139. Coughlin, P. K.; Lippard, S. J.; Martin, A. E.; Bulkowski, J. E., *Journal of the American Chemical Society* **1980,** 102, 7616.
140. Jimenez, M. C.; Dietrich-Buchecker, C.; Sauvage, J.-P., *Angewandte Chemie Int. Ed.* **2000,** 39, (18), 3284.
141. Jimenez-Molero, M. C.; Dietrich-Buchecker, C.; Sauvage, J.-P., *Chemistry - A European Journal* **2002,** 8, (6), 1456.
142. Kraus, T.; Budesinksy, M.; Cvacka, J.; Sauvage, J.-P., *Angewandte Chemie Int. Ed.* **2006,** 45, (2), 258.

143. Collin, J.-P.; Dietrich-Buchecker, C.; Gavina, P.; Jimenez-Molero, M. C.; Sauvage, J.-P., *Accounts of Chemical Research* **2001,** 34, (6), 477.
144. Sauvage, J. P., *Molecular Machines and Motors*. Springer: Berlin, Heidelberg, 2001.
145. Sauvage, J. P., *Accounts of Chemical Research* **1990,** 23, (10), 319.
146. Leininger, S.; Olenyuk, B.; Stang, P. J., *Chemical Reviews* **2000,** 100, (3), 853.
147. Wurthner, F.; You, C.-C.; Saha-Moller Chantu, R., *Chemical Society Reviews* **2004,** 33, (3), 133.
148. Constable, E. C.; Dunphy, E. L.; Housecroft, C. E.; Kylberg, W.; Neuburger, M.; Schaffner, S.; Schofield, E. R.; Smith, C. B., *Chemistry - A European Journal* **2006,** 12, (17), 4600.
149. Gavina, P.; Tatay, S., *Tetrahedron Letters* **2006,** 47, (20), 3471.
150. Crabb, T. A.; Heywood, G. C., *Organic Magnetic Resonance* **1982,** 20, (4), 242.
151. Parks, J. E.; Wagner, B. E.; Holm, R. H., *Journal of Organometallic Chemistry* **1973,** 56, 53.
152. Korall, P.; Borje, A.; Norrby, P. O.; Akermark, B., *Acta Chemica Scandinavica* **1997,** 51, (6-7), 760.
153. Cave, G. W. V.; Raston, C. L., *Journal of the Chemical Society, Perkin Transactions 1* **2001**, (24), 3258.
154. Baret, P.; Einhorn, J.; Gellon, G.; Pierre, J. L., *Synthesis* **1998**, (4), 431.
155. Saitoh, Y.; Koizumi, T.-A.; Osakada, K.; Yamamoto, T., *Canadian Journal of Chemistry* **1997,** 75, (10), 1336.
156. Dietrich-Buchecker, C.; Jimenez, M. C.; Sauvage, J.-P., *Tetrahedron Letters* **1999,** 40, (17), 3395.
157. Miyaura, N.; Suzuki, A., *Chemical Reviews* **1995,** 95, (7), 2457.
158. Williams, J. A. G.; Aspley, C. J., *New Journal of Chemistry* **2001,** 25, (9), 1136.
159. Jimenez-Molero, M. C.; Dietrich-Buchecker, C.; Sauvage, J. P., *Chemistry - A European Journal* **2002,** 8, (6), 1456.
160. Hasenknopf, B. H.; Lehn, J.-M., *Helvetica Chimica Acta* **1996,** 79, 1643.
161. Newkome, G. R.; Kiefer, G. E.; Puckett, W. E.; Vreeland, T., *Journal of Organic Chemistry* **1983,** 48, 5112.
162. Beer, R. H.; Jimenez, J.; Drago, R. S., *Journal of Organic Chemistry* **1993,** 58, 1746.
163. Chandler, C. J.; Deady, L. W.; Reiss, J. A., *Journal of Heterocyclic Chemistry* **1981,** 18, 599.
164. Le Fave, G. M.; Scheurer, P. G., *Journal of the American Chemical Society* **1950,** 72, 2464.
165. Brown, M. S.; Rapoport, H., *Journal of Organic Chemistry* **1963,** 28, 3261.
166. Lehn, J.-M.; Ziessel, R., *Helvetica Chimica Acta* **1988,** 71, 1511.
167. Chambron, J.-C.; Sauvage, J.-P., *Tetrahedron* **1987,** 43, (5), 895.
168. Dietrich, B.; Hosseini, M. W.; Lehn, J. M.; Sessions, R. B., *Helvetica Chimica Acta* **1985,** 68, (2), 289.
169. McGeary, R. P.; Jablonkai, I.; Toth, I., *Tetrahedron* **2001,** 57, (41), 8733.
170. Livoreil, A.; Sauvage, J.-P.; Armaroli, N.; Balzani, V.; Flamigni, L.; Ventura, B., *Journal of the American Chemical Society* **1997,** 119, (50), 12114.
171. Nierengarten, J.-F, PhD thesis, Université Louis Pasteur, Strasbourg, 1994.
172. Wälchi, P. C.; Engster, R., *Helvetica Chimica Acta* **1978,** 61, 885.
173. Martin, A. E.; Bulkowski, J. E., *Journal of Organic Chemistry* **1982,** 47, 415.
174. Pomeranc, D.; Jouvenot, D.; Chambron, J.-C.; Collin, J.-P.; Heitz, V.; Sauvage, J.-P., *Chemistry - A European Journal* **2003,** 9, (17), 4247.
175. Collin, J.-P.; Frey, J.; Heitz, V.; Sakellariou, E.; Sauvage, J.-P.; Tock, C., *New Journal of Chemistry* **2006,** 30, 1386.

176. Arico, F.; Chang, T.; Cantrill, S. J.; Kahn, S. I.; Stoddart, J. F., *Chemistry - A European Journal* **2005,** 11, 4655.
177. Frey, J.; Kraus, T.; Heitz, V.; Sauvage, J.-P., *Chemical Communications* **2005,** 42, 5310.
178. Tiecco, M.; Testaferri, L.; Tingoli, M.; Chianelli, D.; Montanucci, M., *Synthesis* **1984**, 736.
179. Kende, A. S.; Liebeskind, L. S.; Braitsch, D. M., *Tetrahedron Letters* **1975**, 3375.
180. Zembayashi, M.; Tamao, K.; Yoshida, J.; Kumada, M., *Tetrahedron Letters* **1977**, 4089.
181. Indelli, M. T.; Scandola, F.; Collin, J.-P.; Sauvage, J.-P.; Sour, A., *Inorganic Chemistry* **1996,** 35, (2), 303.
182. Hammarstroem, L.; Barigelletti, F.; Flamigni, L.; Armaroli, N.; Sour, A.; Collin, J.-P.; Sauvage, J.-P., *Journal of the American Chemical Society* **1996,** 118, (47), 11972.
183. Barigelletti, F.; Flamigni, L.; Balzani, V.; Collin, J.-P.; Sauvage, J.-P.; Sour, A.; Constable, E. C.; Thompson, A. M. W. C., *Journal of the American Chemical Society* **1994,** 116, (17), 7692.
184. Gilman, H.; Cartledge, F. K., *Journal of Organometallic Chemistry* **1964,** 2, (6), 447.

Chapter 7
Experimental

General points

Instrumentation

Nuclear Magnetic Resonance (NMR) spectra for ^{1}H and ^{13}C were acquired on either a Bruker AVANCE 300 (300 MHz) or a Bruker AVANCE 400 (400 MHz) or a Bruker AVANCE 500 (500 MHz) spectrometer. The spectra were referenced to residual proton-solvent references (^{1}H: DMSO-d_6: 2.50 ppm, methanol-d_4: 3.31 ppm, CD_2Cl_2: 5.32 ppm, $CDCl_3$: 7.26 ppm; ^{13}C: methanol-d_4: 49.0 ppm, CD_2Cl_2: 53.7 ppm, $CDCl_3$: 77.1 ppm). In the assignments, the chemical shift (in ppm) is given first, followed, in brackets, by the multiplicity of the signal (s: singlet, d: doublet, t: triplet, dd: doublet doublet, tt: triplet triplet, dt: doublet triplet, m: multiplet, dm: doublet multiplet, br: broad signal), the number of protons implied, their assignments and the value of the coupling constants in Hertz if applicable. Protons are labelled in black and carbons in red.

Mass spectra were obtained by using a VG ZAB-HF (FAB) spectrometer, a VG-BIOQ triple quadrupole, positive mode or a Bruker MicroTOF spectrometer (ES-MS).

Cyclic voltammetry experiments were performed using an EG&G Princeton Applied Research 273A potentiostat, a Pt working electrode, a Pt counter electrode, a KCl-saturated calomel electrode (SCE) or a silver wire as a reference, and 0.1 M Bu_4NPF_6 as supporting electrolyte.

The EPR spectra have been recorded on X-band Bruker spectrometer (ESP-300-E) equipped with a rectangular TE 102 cavity. The static field was measured with an NMR Gaussmeter (Bruker ER035) while the microwave frequency was simultaneously recorded with a frequency counter (HP-5350 B). Solutions were degassed by bubbling Argon directly in the EPR tube prior to measurements. Temperature was measured with a thermocouple (AuFe/Chromel) introduced inside the tube, at 1.5 cm from the bottom. An ESR900 cryostat (Oxford Instruments) was used for the low-temperature measurements. Computer simulations of the EPR spectra were performed with the help of Simfonia (BRUKER) and WINEPR softwares.

UV-Visible absorption spectra were performed using a Kontron UVIKON 860 spectrophotometer. Wavelengths are given in nm and molar extinction coefficients (ε) are given in $L.mol^{-1}.cm^{-1}$.

Chromatographic supports

Thin-layer chromatography was performed using glass or plastic sheets coated with silica or neutral alumina. They were examined after dipping in an aqueous iron(II) solution (terpyridines), after oxidation with iodine (other organic compounds) or under the UV lamp. Column chromatography was carried out on silicagel (Kieselgel 60 (0.063-0.200 mm), Merck) or alumina (Aluminoxid 90 standardized (0.060-0.200mm), Merck).

Solvents and chemicals

Some solvents were dried in the laboratory by distillation under argon, over the appropriate drying agent: tetrahydrofuran, diethylether and dioxane over sodium/benzophenone, dichloromethane over CaH_2 and pyridine over KOH. All other anhydrous solvents used are commercially available ("analytical grade"): acetone, dimethylformamide (dried with molecular sieves), methanol, and absolute ethanol.

All commercial chemicals were of the best commercially available grade, and were used without further purification, except *n*-BuLi, titrated using the double titration method described by H. Gilman *et al.*[184]

Synthesis of compounds

2-acetyl-5-methylpyridine: 1

2-bromo-5-methylpyridine (10 g; 58 mmol) in anhydrous diethylether (150 mL) was cooled to -78°C under argon. n-butyllithium (38 mL; 64 mmol) was added dropwise to the solution mixture. After addition was complete, the reaction mixture was allowed to warm to -40°C for 30 min; a dark red solution resulted. N,N-dimethylacetamide (6 mL; 64 mmol) was added dropwise and cautiously at -78°C. The mixture was then allowed to warm to -40°C for 2h30, and hydrolysed with saturated aqueous NH_4Cl solution. The aqueous layer was separated, washed with diethylether, and the united ether extracts were washed with water, dried with anhydrous $MgSO_4$, and evaporated to give a brown oil (4.5 g). Chromatography (silica, CH_2Cl_2-MeOH 100% to 98%) gave 4.12 g (30 mmol; 52%) of a yellow oil.

^1H NMR ($CDCl_3$, 300 MHz): δ (ppm) = 2.40 (s, 3H, H_{CH3}); 2.69 (s, 3H, H_{CH3CO}); 7.61 (dd, 1H, H_4, J_{3-4} = 8.0 Hz, J_{4-6} = 0.6 Hz); 7.93 (d, 1H, H_3, J_{3-4} = 8.0 Hz); 8.47 (dd, 1H, H_6, J_{4-6} = 0.6 Hz)

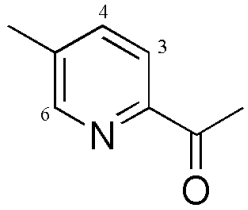

4-bromo-2'-azachalcone: 2

4-bromobenzaldehyde (6.25 g; 33.8 mmol) was dissolved in 80 mL methanol and 25 mL NaOH (1 M). 2-acetyl-5-methylpyridine **1** (4.56 g; 33.8 mmol) dissolved in methanol was added and a precipitate appeared after 5 min. The reaction mixture was stirred for 30 more minutes. The resulting precipitate was filtered off, dissolved in CH_2Cl_2 and washed once with water. The organic phase was dried over Na_2SO_4, filtered, and evaporated to dryness. The residue was recristallized from methanol to give **2** as a light yellow solid. Yield 8.76 g (29 mmol; 86%).

^1H NMR (300 MHz, $CDCl_3$): δ (ppm) = 2.44 (s, 3H, H_{CH3}); 7.56 (m, 4H, H_{arom}); 7.66-7.69 (dm, 1H, H_4, J_{3-4} = 8.2 Hz); 7.81-7.86 (d, 1H, H_a, J_{a-b} = 16.1 Hz); 8.08-8.11 (dm, 1H, H_3, J_{3-4} = 8.2 Hz); 8.26-8.31 (d, 1H, H_b, J_{a-b} = 16.1 Hz); 8.55 (m, 1H, H_6)

^{13}C NMR (300 MHz, $CDCl_3$): δ (ppm) = 196.1; 158.0; 155.6; 153.7; 149.3; 142.8; 137.4; 134.5; 132.0; 130.1; 129.9; 122.7; 121.6

EI-MS, m/z exp.: 301.0 (**2**, calc. for $C_{15}H_{12}BrNO$: 301.0)

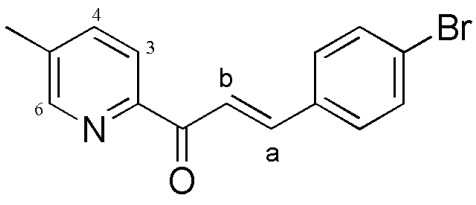

1-(5-methyl-2-pyridylacetyl)pyridinium iodide: 3

To a solution of iodine (10.50 g; 41.4 mmol) in freshly distilled pyridine (50 mL) was added 2-acetyl-5-methylpyridine **1** (5.08 g; 37.6 mmol). The mixture was refluxed under argon for 1h, and then stirred at room temperature overnight. The resulting green precipitate was filtered off, washed with pyridine and recrystallized from absolute ethanol. Yield 9.479 g (27.9 mmol; 74%)

^{1}H NMR (300 MHz, DMSO-d_6): δ (ppm) = 2.47 (s, 3H, H_{CH3}); 6.48 (s, 2H, H_{CH2}); 7.97 (m, 2H, H_3-H_4); 8.24-8.29 (dd, 2H, $H_{2'}$, $J_{2'-3'}$ = 7.8 Hz, $J_{2'-1'}$ = 6.7 Hz); 8,71 (m, 1H, H_6); 8.70-8.75 (tt, 1H, $H_{3'}$, $J_{3'-2'}$ = 7.8 Hz, $J_{3'-1'}$ = 1.4 Hz); 8.99-9.02 (dd, 2H, $H_{1'}$, $J_{1'-2'}$ = 5.5 Hz, $J_{1'-3'}$ = 1.2 Hz)

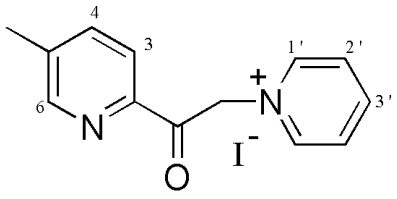

4'-(4-bromophenyl)-5,5"-dimethyl-2,2':6',2"-terpyridine: 4

4-bromo-2'-azachalcone **2** (6.04 g; 20 mmol), 1-(5-méthyl-2-pyridylacetyl)pyridinium iodide **3** (6.80 g; 20 mmol) and ammonium acetate (39.3 g; 35 mmol) were dissolved in 50 mL of glacial acetic acid and refluxed for 7h. The reaction mixture was kept at room temperature for 14h and was then made alkaline with NaOH (10 M). The reaction mixture was extracted with CH_2Cl_2. The combined organic phases were dried with anhydrous $MgSO_4$ and evaporated on aluminium oxide. Chromatography (400g aluminium oxide, pentane-CH_2Cl_2-EtOAc (8:2:1)) gave 4.985 g (12 mmol; 60%) of **4** as a light yellow solid.

^{1}H NMR (300 MHz, $CDCl_3$): δ (ppm) = 2.43 (s, 6H, H_{CH3}); 7.61-7.64 (dm, 2H, H_{m2}); 7.67-7.69 (dm, 2H, H_4-$H_{4"}$, J_{3-4} = 8.0 Hz); 7.76-7.79 (dm, 2H, H_{o2}); 8.53-8.56 (d, 2H, H_3-$H_{3"}$, J_{3-4} = 7.9 Hz); 8.54 (m, 2H, H_6-$H_{6"}$); 8.63 (s, 2H, $H_{3'}$-$H_{5'}$)

^{13}C NMR (500 MHz, $CDCl_3$, assigned using HMQC and HMBC 2D ^{1}H-^{13}C HETCORR experiments): δ (ppm) = 156.17 (*2'*); 153.65 (*2*); 149.56 (*6*); 148.93 (*4'*); 137.63 (*y*); 137.43 (*4*); 133.61 (*5*); 132.02 (*m2*); 128.93 (*o2*); 123.34 (*x*) ; 120.92 (*3*); 117.96 (*3'*); 18.43 (*CH_3*)

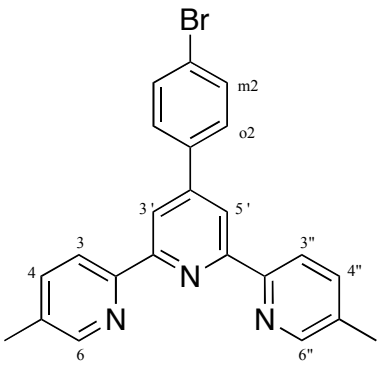

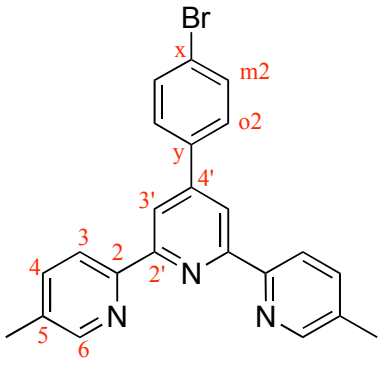

EI-MS, m/z exp.: 414.9 (**4**, calc. for [M]: 415.1)

Anal. Found (Calc.) for $C_{23}H_{18}BrN_3$*:* %C, 66.38 (66.36); %H, 4.52 (4.36); %N, 10.01 (10.09)

3,8-dibromo-1,10-phenanthroline: 5

A solution of 1,10-phenanthroline (2.5 g; 13.8 mmol), S_2Cl_2 (4.34 mL; 52.7 mmol), pyridine (4.21 mL; 52.4 mmol) and Br_2 (2.6 mL; 50.7 mmol) in 90 mL of 1-chlorobutane was stirred overnight at reflux (80°C). After cooling to room temperature, the solid formed was separated by filtration over a sintered glass (porosity 4). The solid was taken up in 50 mL of an aqueous NaOH solution and 50 mL of $CHCl_3$. The organic phase was separated, the aqueous layer was washed twice with $CHCl_3$. The collected organic phases were dried over $MgSO_4$ and the solvent evaporated under vacuum. The crude mixture was purified by column chromatography (SiO_2, CH_2Cl_2). The dibromo derivative **5** (CH_2Cl_2-MeOH (97:3)) was obtained as a white solid (1.4 g; 30%).

^{1}H NMR (300 MHz, $CDCl_3$): δ (ppm) = 7.76 (s, 2H, $H_{p5,p6}$); 8.42 (d, 2H, $H_{p4,p7}$, $J_{p2\text{-}p4}$ = 2.2 Hz); 9.19 (d, 2H, $H_{p2,p9}$, $J_{p2\text{-}p4}$ = 2.2 Hz)

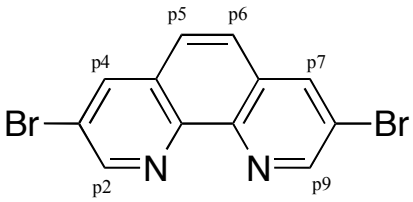

3-bromo-8-(4-methoxyphenyl)-1,10-phenanthroline : 6

To a degassed solution of 3,8-dibromo-1,10-phenanthroline (100 mg; 0.296 mmol) and $Pd(PPh_3)_4$ (18 mg; 0.015 mmol) in 5 mL of toluene were added, under argon, 1.5 mL of a degassed solution of 2M aqueous Na_2CO_3 and a solution of p-anisylboronic acid (45 mg; 0.296 mmol) in 2 mL of toluene with few drops of methanol. It is very important to respect

the following sequence in the additions: a) dibromophenanthroline in toluene, b) 3 vacuum-argon cycles, c) addition of the catalyst, d) 3 vacuum-argon cycles, e) addition of the degassed solution of Na_2CO_3, f) 3 vacuum-argon cycles, g) addition of the degassed solution of the boronic acid.
The reaction was monitored by TLC, and after 14 hours of reflux, the reaction mixture was allowed to cool to room temperature. The solvent was removed by rotary evaporation and chromatography (aluminium oxide, pentane-$CHCl_3$ (1:1)) gave 50 mg (0.137 mmol; 46%) of pure product as a slightly yellow solid.

^1H NMR (300 MHz, $CDCl_3$): δ (ppm) = 3.90 (s, 3H, OCH_3); 7.06-7.11 (dm, 2H, H_{o1}, $J_{o1\text{-}m1}$ = 8.8 Hz); 7.70-7.75 (dm, 2H, H_{m1}, $J_{o1\text{-}m1}$ = 8.9 Hz); 7.72-7.89 (dd, 2H, $H_{p5,p6}$, $J_{p5\text{-}p6}$ = 9.0 Hz); 8.33-8.34 (d, 1H, H_{p7}, $J_{p7\text{-}p9}$ = 2.4 Hz); 8.40-8.41 (d, 1H, H_{p4}, $J_{p4\text{-}p2}$ = 2.3 Hz); 9.18-9.19 (d, 1H, H_{p2}, $J_{p4\text{-}p2}$ = 2.4 Hz); 9.40-9.41 (d, 1H, H_{p9}, $J_{p7\text{-}p9}$ = 2.4 Hz)

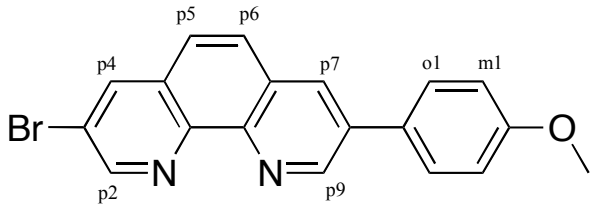

4'-(4-(Neopentyl glycolatoboron)phenyl)-5,5"-dimethyl-2,2':6',2"-terpyridine : 7

A round-bottom flask was charged with Pd(dppf)Cl_2 (6 mg; 0.007 mmol), KOAc (70.7 mg; 0.721 mmol), bis(neopentyl glycolato)diboron (B_2neo_2, 57 mg; 0.252 mmol) and 4'-(4-bromophenyl)-5,5"-dimethyl-2,2':6',2"-terpyridine (**4**, 100 mg; 0.240 mmol) and flushed with nitrogen. Freshly distilled dioxane (10 mL) was then added and the mixture was heated at 80°C for 18h. It was then diluted with toluene and the resulting solution washed with water. The toluene layer was dried over Na_2SO_4 and the solvent removed by rotary evaporation. The residue was dried overnight on a vacuum pump giving **7** as a brownish white solid (quantitative yield). It was used directly for the next step without further purification.

^1H NMR (300 MHz, $CDCl_3$): δ (ppm) = 1.05 (s, 6H, CH_{3neo}); 2.43 (s, 6H, H_{CH3}); 3.81 (s, 4H, CH_{2neo}); 7.65-7.69 (ddd, 2H, H_4-$H_{4"}$, J = 8.2 Hz, 2.2 Hz, 0.7 Hz); 7.88-7.94 (dm, 4H, H_{m2}-H_{o2}); 8.54-8.56 (d, 2H, H_3-$H_{3"}$, $J_{3\text{-}4}$ = 7.5 Hz); 8.54-8.56 (dt, 2H, H_6-$H_{6"}$, J = 2.2 Hz, 0.7 Hz); 8.69 (s, 2H, $H_{3'}$-$H_{5'}$)

^{13}C NMR (300 MHz, $CDCl_3$, assigned using HMQC and HMBC 2D ^1H-^{13}C HETCORR experiments): δ (ppm) = 155.97 (*2'*); 153.88 (*2*); 150.13 (*4'*); 149.55 (*6*); 140.55 (*y*); 137.36 (*4*); 134.38 (*m2*); 133.41 (*5*); 132.77 (*x*); 126.46 (*o2*); 120.90 (*3*); 118.29 (*3'*); 72.35 (CH_{2neo}); 31.92 (C_{neo}); 21.95 (CH_{3neo}); 18.44 (CH_3)

ES-MS, m/z exp.: 450.24 (**7**, calc. for [M]: 450.23)

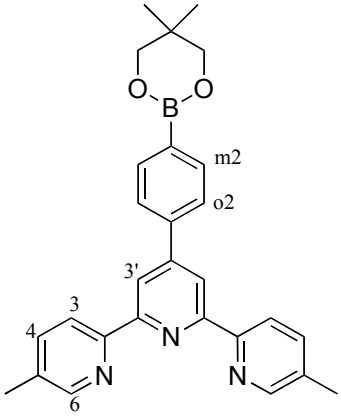

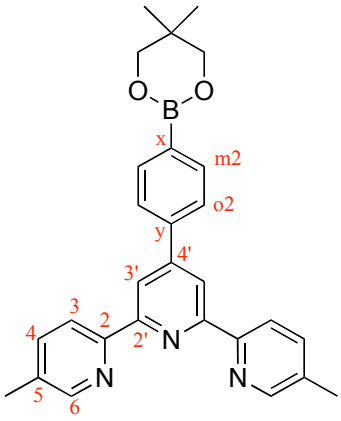

Acyclic phen-terpy conjugate: 8

To a degassed solution of 3-bromo-8-(4-methoxyphenyl)-1,10-phenanthroline (**6**, 49 mg; 0.134 mmol) and $Pd(PPh_3)_4$ (7.8 mg; 0.007 mmol) in 10 mL of toluene were added, under argon, 1 mL of a degassed solution of 2M aqueous Na_2CO_3 and a solution of 4'-(4-(Neopentyl glycolatoboron)phenyl)-5,5"-dimethyl-2,2':6',2"-terpyridine (**7**, 62 mg; 0.138 mmol) in 5 mL of toluene. It is very important to respect the following sequence in the additions: a) bromophenanthroline in toluene, b) 3 vacuum-argon cycles, c) addition of the catalyst, d) 3 vacuum-argon cycles, e) addition of the degassed solution of Na_2CO_3, f) 3 vacuum-argon cycles, g) addition of the degassed solution of the boronic ester.
The reaction was monitored by TLC, and after 30 hours of reflux, the reaction mixture was allowed to cool to room temperature. The solvent was removed by rotary evaporation and the crude mixture was taken in CH_2Cl_2 and washed with water. The combined organic layers were dried over Na_2SO_4 and the solvent evaporated. Chromatography (aluminium oxide, CH_2Cl_2 to CH_2Cl_2-MeOH (99:1)) gave 20 mg (0.032 mmol; 24%) of pure product **8** as a white solid.

^{1}H NMR (300 MHz, $CDCl_3$): δ (ppm) = 2.44 (s, 6H, H_{CH3}); 3.90 (s, 3H, OCH_3); 7.08-7.11 (dm, 2H, H_{o1}, $J_{o1\text{-}m1}$ = 8.8 Hz); 7.67-7.71 (dm, 2H, H_4-$H_{4"}$, J = 8.1 Hz, 2.0 Hz, 0.5 Hz); 7.72-7.75 (dm, 2H, H_{m1}, $J_{o1\text{-}m1}$ = 8.8 Hz); 7.88 (d, 2H, $H_{p5,p6}$, $J_{p5\text{-}p6}$ = 1.5 Hz); 7.91-8.11 (dd, 4H, H_{m2}-H_{o2}, J = 8.3 Hz); 8.34 (d, 1H, H_{p7}, $J_{p4\text{-}p7}$ = 2.3 Hz); 8.46 (d, 1H, H_{p4}, $J_{p4\text{-}p7}$ = 2.3 Hz); 8.57 (m, 2H, H_6-$H_{6"}$); 8.56-8.58 (d, 2H, H_3-$H_{3"}$, J = 7.4 Hz); 8.75 (s, 2H, $H_{3'}$-$H_{5'}$); 9.42 (d, 1H, H_{p9}, $J_{p9\text{-}p2}$ = 2.25 Hz); 9.50 (d, 1H, H_{p2}, $J_{p2\text{-}p9}$ = 2.25 Hz)

^{13}C NMR (300 MHz, $CDCl_3$, assigned using HMQC and HMBC 2D ^{1}H-^{13}C HETCORR experiments): δ (ppm) = 160.07 (*i*); 156.19 (*2'*); 153.80 (*2*); 149.62 (*6*); 149.43 (*4'*); 149.36 (*p9*); 149.30 (*p2*); 146.02 (*p12*); 145.40 (*p3*) 144.72 (*p11*); 138.68 (*y*); 137.44 (*4*); 135.46

(*p8*); 134.92 (*x*); 133.57 (*5*); 133.41 (*p4*); 132.59 (*p7*); 130.00 (*p*); 128.69 (*m1*); 128.67 (*p14*); 128.37 (*p13*); 128.21 (*o2*); 127.97 (*m2*); 127.24 (*p6*); 127.06 (*p5*); 120.96 (*3*); 118.16 (*3'*); 114.78 (*o1*); 55.47 (OCH_3); 18.48 (CH_3)

HR ES-MS, m/z exp.: 622.254 (**8**, calc. for [M+H]: 622.260)

DOSY NMR (500 MHz, CD_2Cl_2): D = 1000 $\mu m^2.s^{-1}$; r_h = 5.3 Å

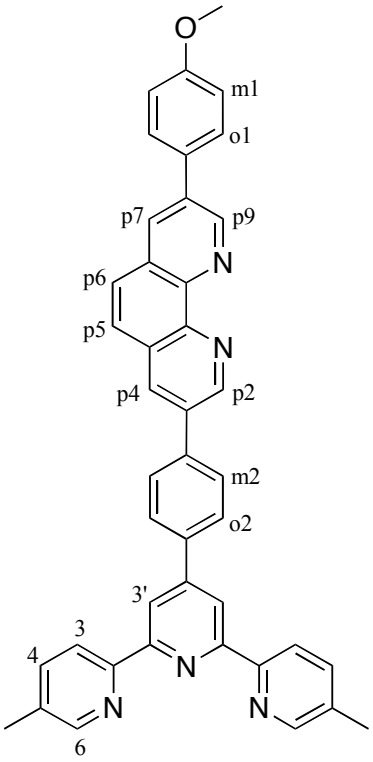

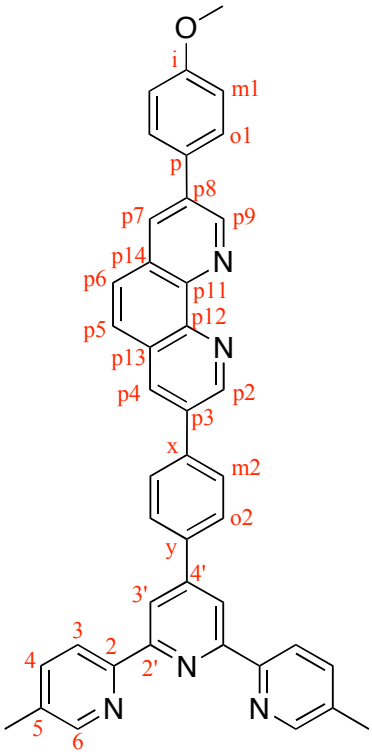

Dimer complex with Zinc (II): $[Zn_2.(\mathbf{8})_2].4OTf$

Phen-terpy conjugate **8** (10 mg; 0.016 mmol) was dissolved in 0.25 mL of CD_2Cl_2. A solution of $Zn(OTf)_2$ in CD_3OD (23.8 mg in 1 mL) was prepared, and 0.25 mL (0.016 mmol) were added to the ligand solution, which became clear and orange. The solution was transferred to an NMR tube and the reaction was monitored by ^1H NMR. After 6 hours at room temperature and 22 hours at 30°C, the NMR spectrum remained the same as after 1 hour of reaction. The solvent was then evaporated and the crude mixture taken in methanol, filtered, and the filtrate evaporated to dryness yielding $[Zn_2.(\mathbf{8})_2].4OTf$ as a yellow solid (10.5 mg; 78%).

^1H NMR (500 MHz, CD_3OD): δ (ppm) = 2.37 (s, 6H, H_{CH3}); 4.02 (s, 3H, OCH_3); 6.68 (s, 1H, H_{p2}); 7.35-7.37 (d, 2H, H_{o1}, J = 8.85 Hz); 7.64-7.66 (dm, 2H, H_{m2}, J = 8.0 Hz); 8.12 (m, 2H, H_4); 8.14-8.16 (dm, 2H, H_{o2}, J = 8.0 Hz); 8.20 (m, 4H, H_{p5}-H_{p6}-H_{m1}); 8.25 (m, 2H, H_6-$H_{6''}$);

8.44-8.46 (d, 1H, H_{p9}); 8.76-8.78 (d, 2H, H_3-$H_{3''}$, J = 8.1 Hz); 8.94 (m, 1H, H_{p4}); 9.04 (s, 2H, $H_{3'}$-$H_{5'}$); 9.39 (s, 1H, H_{p7})

HR ES-MS, m/z exp.: 342.592 (calc. for $[Zn_2(\mathbf{8})_2]^{4+}$: 342.590); 506.439 (calc. for $[Zn_2(\mathbf{8})_2$, $OTf]^{3+}$: 506.438); 834,681 (calc. for $[Zn_2(\mathbf{8})_2$, $2OTf]^{2+}$: 834.637)

DOSY NMR (500 MHz, CD_3OD): D = 470 $\mu m^2.s^{-1}$; r_h = 8.5 Å
ellipsoïd parameters : a = 14 Å; b = c = 6 Å

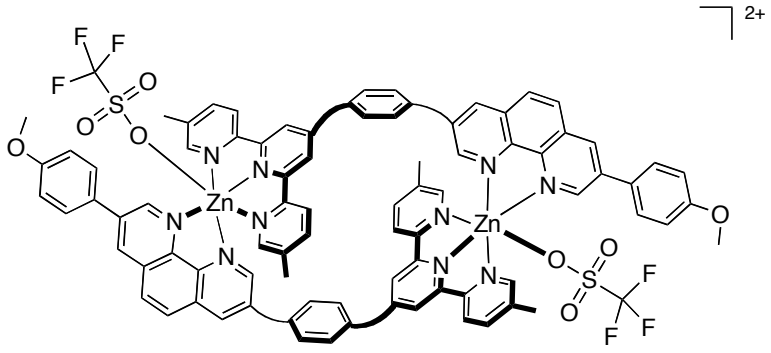

Dimer and trimer complexes with Copper(II): $[Cu_2(\mathbf{8})_2].4BF_4$ and $[Cu_3(\mathbf{8})_3].6BF_4$

Phen-terpy conjugate **8** (12.5 mg; 0.020 mmol) was dissolved in 2 mL of CH_2Cl_2. A solution of $Cu(BF_4)_2$ in CH_3CN (47.7 mg in 10 mL) was prepared, and 1 mL was added to the ligand solution, which turned instantaneously clear and olive green. The solution was let stir for 19 hours at room temperature, and by addition of diethyl ether a green solid precipitated out, which was then filtered, washed, dissolved again in an acetone/acetonitrile/methylene chloride mixture, and recovered as a solid by addition of diethyl ether in a good yield (13.8 mg; 89%).

HR ES-MS, m/z exp.: 342.6107 (calc. for $[Cu_2(\mathbf{8})_2]^{4+}$: 342.5909; calc. for $[Cu_3(\mathbf{8})_3]^{6+}$: 342.5912); 428.5336 (calc. for $[Cu_3(\mathbf{8})_3$, $BF_4]^{5+}$: 428.5102); 485.8158 (calc. for $[Cu_2(\mathbf{8})_2$, $BF_4]^{3+}$: 485.7893); 557.1697 (calc. for $[Cu_3(\mathbf{8})_3$, $2BF_4]^{4+}$: 557.1386); 772.2273 (calc. for $[Cu_2(\mathbf{8})_2$, $2BF_4]^{2+}$: 772.1861; calc. for $[Cu_3(\mathbf{8})_3$, $3BF_4]^{3+}$: 772.1864)

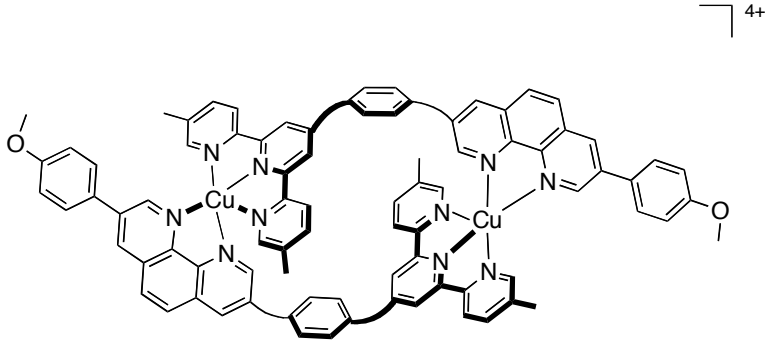

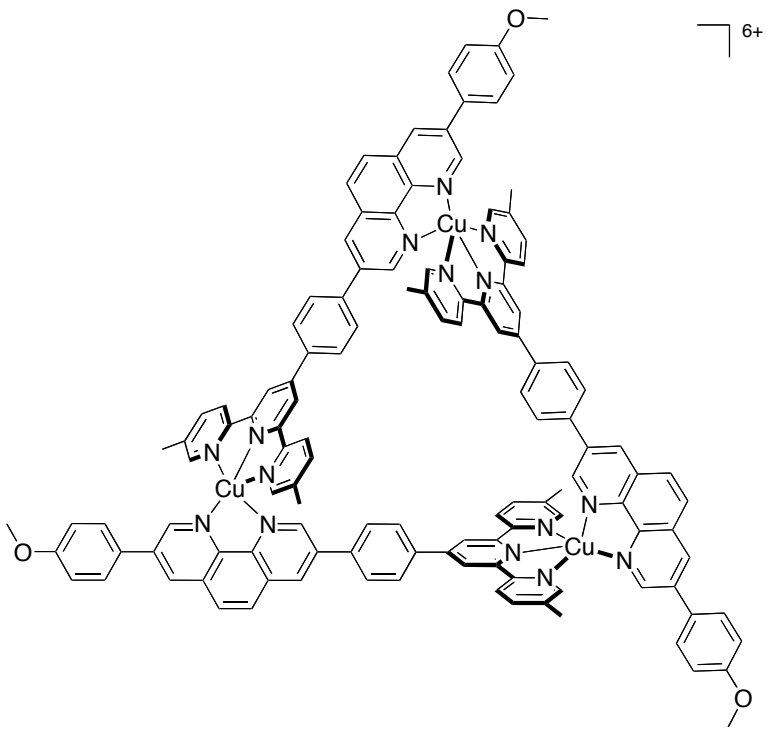

UV-Vis (CH_2Cl_2 + nBu_4NPF_6 0.1M) λ_{max} (ε): 292 (1.2 10^5); 359 (9.2 10^4); 573 (560)

2-[2-(2-chloroethoxy)ethoxy]tetrahydro-*2H*-pyran: 12

To 2-chloroethoxyethanol (11.0 g; 88.3 mmol) and CH_2Cl_2 (30 mL), a solution of freshly distilled 3,4-dihydro-2H-pyran (DHP, 8.770 g; 104.3 mmol) in CH_2Cl_2 (10 mL) was added within 15 min while stirring. After the addition was completed, 4 drops of HCl (37%) were added, and the solution was heated for 1h15min at 40°C. After cooling the light blue solution, K_2CO_3 (3g) was added, the solution filtered and the solvent evaporated. The residue was dried overnight on a vacuum pump giving **12** as a yellowish oil (18.3 g; 99%). It was used directly for the next step.

^{1}H NMR (300 MHz, $CDCl_3$): δ (ppm) = 1.49-1.85 (m, 6H, $H_{b,c,d}$); 3.46-3.90 (m, 10H, $H_{\alpha,\beta,\gamma,\delta,e}$); 4.63 (m, 1H, H_a)

^{13}C NMR (300 MHz, $CDCl_3$): δ (ppm) = 98.97 (-CH_a-); 71.32; 70.60; 66.65; 62.25; 42.71 (-CH_2-Cl); 30.54; 25.39; 19.46

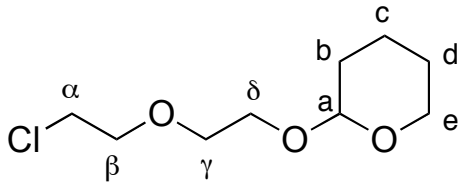

2-[2-(2-iodoethoxy)ethoxy]tetrahydro-*2H*-pyran: 13

2-[2-(2-chloroethoxy)ethoxy]tetrahydro-*2H*-pyran **12** (18.3 g; 88.3 mmol) was added without further purification to a solution of sodium iodide (16.4 g; 109.4 mmol) in dry acetone (110 mL), then the mixture was heated under reflux for 24h. The solution was cooled down, the NaCl precipitated salt was filtered off and the solvent was evaporated. The residue was taken up in CH_2Cl_2 (100 mL) and the precipitate was again filtered off. The filtrate was washed with 3*30 mL of water and then dried over Na_2SO_4 and concentrated to give the iodide **13** as an oil which was purified by column chromatography (silica, pentane-EtOAc 80% to 70%) (21.9 g; 83%).

^{1}H NMR (300 MHz, $CDCl_3$): δ (ppm) = 1.48-1.86 (m, 6H, $H_{b,c,d}$); 3.22-3.90 (m, 10H, $H_{\alpha,\beta,\gamma,\delta,e}$); 4.63 (m, 1H, H_a)

^{13}C NMR (300 MHz, $CDCl_3$): δ (ppm) = 98.94 (-CH_a-); 71.93; 70.18; 66.63; 62.25; 30.54; 25.40; 19.45; 2.99 (-CH_2-I)

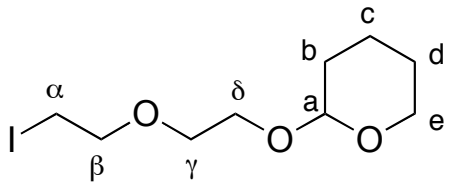

4'-(4-bromophenyl)-5,5"-di(ε-tetrahydropyranyl-(2-(2'-ethoxy)ethyl))-terpyridine: 14

A solution of n-BuLi (4.95 mL; 7.93 mmol) was added dropwise and under argon on a solution of freshly distilled diisopropylamine (1.2 mL; 8.58 mmol) in anhydrous THF (15 mL) at -78°C. The mixture is allowed to warm to 0°C for 15 min, and then cooled down to -78°C. A degassed solution of **4** (1.5 g; 3.60 mmol) in anhydrous THF (30 mL) was cooled to -78°C. While this temperature was maintained, the freshly prepared solution of LDA was added *via* the canula transfer technique. The solution turned dark green and was stirred at -78°C for 1h45min. The temperature was then allowed to rise to -10°C and brought down to -78°C again. A solution of 2-[2-(2-iodoethoxy)ethoxy]tetrahydro-*2H*-pyran **13** (6.5 g; 21.65 mmol) in anhydrous THF (10 mL) was cooled to -78°C and then added *via* the canula transfer technique. The solution was then stirred for 1h at -78°C, and then allowed to warm to room temperature overnight. The solution turned brownish orange and was hydrolysed with 15 mL of water. After evaporation of the THF, the residue was taken up in a CH_2Cl_2/H_2O mixture, the organic phase washed with water and dried over Na_2SO_4. After the solvent was evaporated, the resulting oil was chromatographied (Al_2O_3, pentane/ether (60:40) to pure ether and then ether/MeOH (99:1)) to give **14** in 22% yield (603.0 mg; 0.793 mmol).

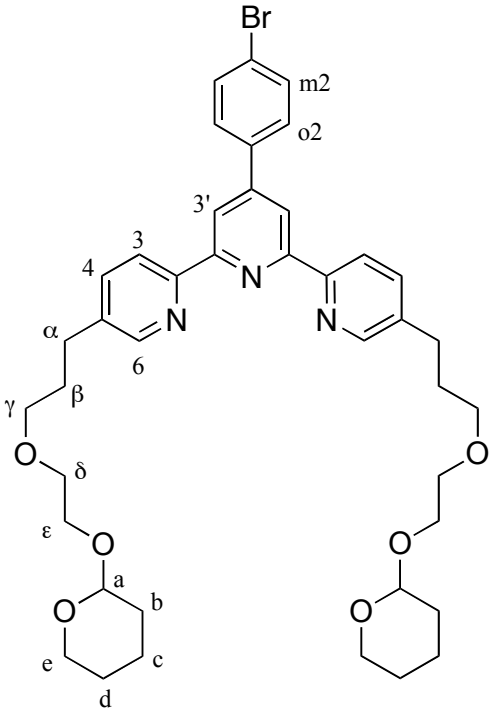

^{1}H NMR (300 MHz, $CDCl_3$): δ (ppm) = 1.60-1.90 (m, 12H, $H_{b,c,d}$); 1.98 (q, 4H, H_β); 2.81 (t, 4H, H_α); 3.53 (t, 4H, H_γ); 3.65 (m, 8H, $H_{\delta,\varepsilon}$); 3.86-3.94 (m, 4H, H_e); 4.67 (t, 2H, H_a); 7.62-7.65 (dm, 2H, H_{m2}); 7.70-7.73 (dm, 2H, H_4-$H_{4''}$, $J_{3\text{-}4}$ = 7.5 Hz); 7.76-7.79 (dm, 2H, H_{o2}); 8.56 (m, 2H, H_6-$H_{6''}$); 8.56-8.59 (d, 2H, H_3-$H_{3''}$, $J_{3\text{-}4}$ = 8.1 Hz); 8.64 (s, 2H, $H_{3'}$-$H_{5'}$)

4'-(4-bromophenyl)-5,5''-di(ε-hydroxy-(2-(2'-ethoxy)ethyl))-terpyridine: 15

Terpyridine **14** (177.4 mg; 0.233 mmol) dissolved in 40 mL of ethanol was brought to reflux under argon before 2 drops HCl 37% were added. The solution turned from light yellow to light orange and was refluxed overnight for 14h. Ethanol was then removed and the residue was taken up in CH_2Cl_2/H_2O. $NaHCO_3$ was carefully added and the aqueous layer was extracted with CH_2Cl_2. The organic layers were combined, dried over Na_2SO_4 and the solvent was removed to give **15** quantitatively which was used directly for the next step.

^{1}H NMR (300 MHz, $CDCl_3$): δ (ppm) = 1.99 (q, 4H, H_β); 2.81 (t, 4H, H_α); 3.52-3.58 (m, 8H, $H_{\delta,\gamma}$); 3.77 (t, 4H, H_ε); 7.62-7.65 (dm, 2H, H_{m2}); 7.69-7.72 (dm, 2H, H_4-$H_{4''}$, $J_{3\text{-}4}$ = 8.1 Hz); 7.76-7.79 (dm, 2H, H_{o2}); 8.56-8.58 (d, 2H, H_3-$H_{3''}$, $J_{3\text{-}4}$ = 8.1 Hz); 8.56 (m, 2H, H_6-$H_{6''}$); 8.64 (s, 2H, $H_{3'}$-$H_{5'}$)

^{13}C NMR (300 MHz, $CDCl_3$, assigned using HMQC and HMBC 2D ^{1}H-^{13}C HETCORR experiments): δ (ppm) = 156.10 (*2'*); 154.07 (*2*); 149.28 (*6*); 148.96 (*4'*); 137.50 (*y*); 137.50 (*5*); 136.87 (*4*); 132.07 (*m2*); 128.89 (*o2*); 123.39 (*x*); 121.08 (*3*); 118.07 (*3'*); 71.92 (*δ*); 69.97 (*γ*); 61.89 (*ε*); 30.90 (*β*); 29.38 (*α*)

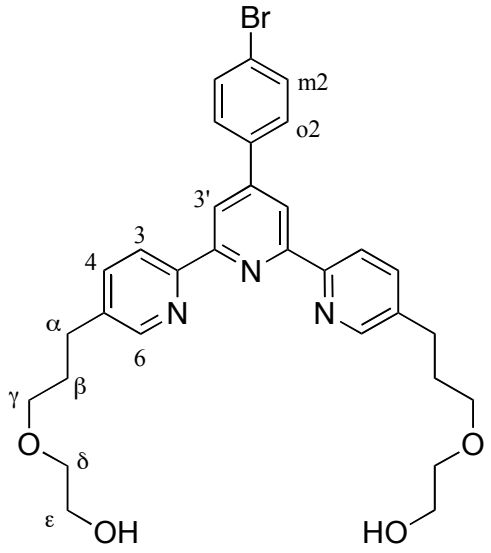

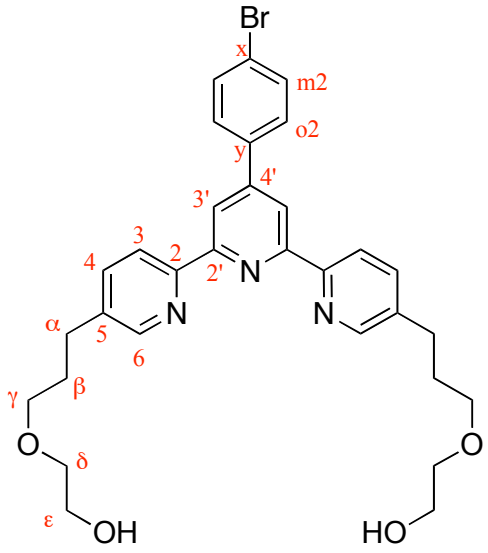

4'-(4-bromophenyl)-5,5"-di(ε-mesilyl-(2-(2'-ethoxy)ethyl))-terpyridine: 16

To a solution of terpyridine **15** (138.17 mg; 0.233 mmol) in anhydrous CH_2Cl_2 (30 mL) was added freshly distilled triethylamine (0.258 mL; 1.865 mmol). The mixture was cooled to 0°C in an ice-bath under argon, and an excess of mesyl chloride (0.15 mL; 1.925 mmol) was added. After 1h30min stirring at 0°C, the mixture was brought to room temperature, then washed once with water and dried over Na_2SO_4. Evaporation of the solvent gave **16** as a light yellow oil in a quantitative yield. It was used with no further purification for the next step.

^{1}H NMR (300 MHz, $CDCl_3$): δ (ppm) = 1.99 (q, 4H, H_β); 2.81 (t, 4H, H_α); 3.08 (s, 6H, $-SO_2-CH_3$) 3.54 (t, 4H, H_γ); 3.73 (m, 4H, H_δ); 4.39 (m, 4H, H_ε); 7.63-7.66 (dm, 2H, H_{m2}); 7.69-7.72 (dm, 2H, H_4-$H_{4''}$, $J_{3\text{-}4}$ = 8.1 Hz); 7.77-7.79 (dm, 2H, H_{o2}); 8.59-8.62 (d, 2H, H_3-$H_{3''}$, $J_{3\text{-}4}$ = 8.1 Hz); 8.59 (m, 2H, H_6-$H_{6''}$); 8.67 (s, 2H, $H_{3'}$-$H_{5'}$)

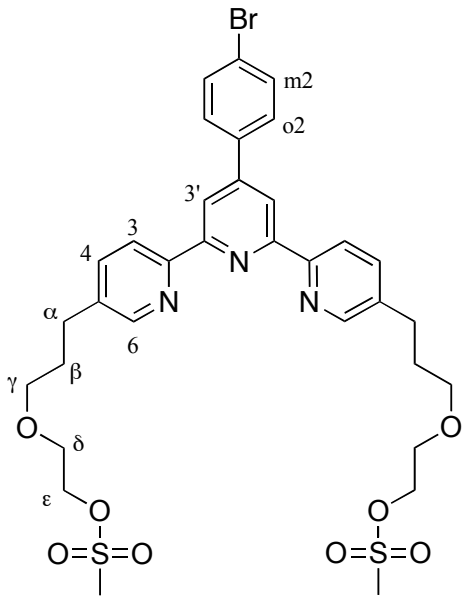

4'-(4-bromophenyl)-5,5"-di(ε-bromo-(2-(2'-ethoxy)ethyl))-terpyridine: 17

A solution of terpyridine **16** (174.6 mg; 0.233 mmol) in dry acetone (40 mL) was refluxed overnight (19h) in presence of lithium bromide (231 mg; 2.67 mmol) under argon. After the solvent was removed, the residue was taken up in CH_2Cl_2/H_2O. The aqueous layer was extracted by CH_2Cl_2 and the combined organic layers were dried over Na_2SO_4. The solvent was evaporated to give an orange oil which was purified by flash chromatography (standardised alumina, CH_2Cl_2). Terpyridine **17** (120 mg; 0.167 mmol) was obtained with a 71% overall yield from terpyridine **14**.

^1H NMR (300 MHz, $CDCl_3$): δ (ppm) = 1.98 (q, 4H, H_β); 2.82 (t, 4H, H_α); 3.47-3.55 (m, 8H, $H_{\delta,\gamma}$); 3.77 (t, 4H, H_ε); 7.61-7.64 (dm, 2H, H_{m2}); 7.69-7.72 (dm, 2H, H_4-$H_{4"}$, J_{3-4} = 8.1 Hz); 7.75-7.78 (dm, 2H, H_{o2}); 8.56-8.58 (d, 2H, H_3-$H_{3"}$, J_{3-4} = 8.0 Hz); 8.56 (m, 2H, H_6-$H_{6"}$); 8.64 (s, 2H, $H_{3'}$-$H_{5'}$)

^{13}C NMR (300 MHz, $CDCl_3$, assigned using HMQC and HMBC 2D ^1H-^{13}C HETCORR experiments): δ (ppm) = 156.12 (*2'*); 154.05 (*2*); 149.33 (*6*); 148.92 (*4'*); 137.51 (*y*); 137.47 (*5*); 136.93 (*4*); 132.06 (*m2*); 128.89 (*o2*); 123.38 (*x*); 121.05 (*3*); 118.04 (*3'*); 70.74 (*δ*); 69.65 (*γ*); 30.87 (*β*); 30.58 (*ε*); 29.22 (*α*)

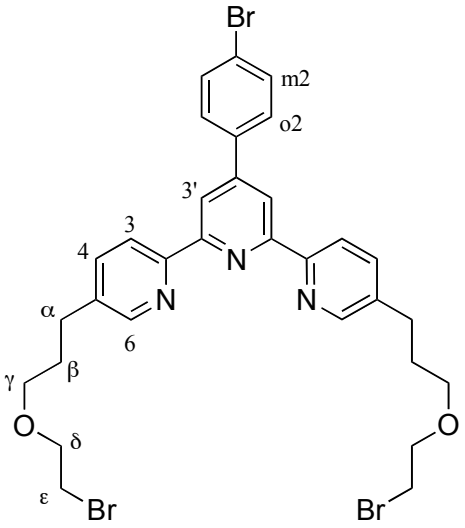

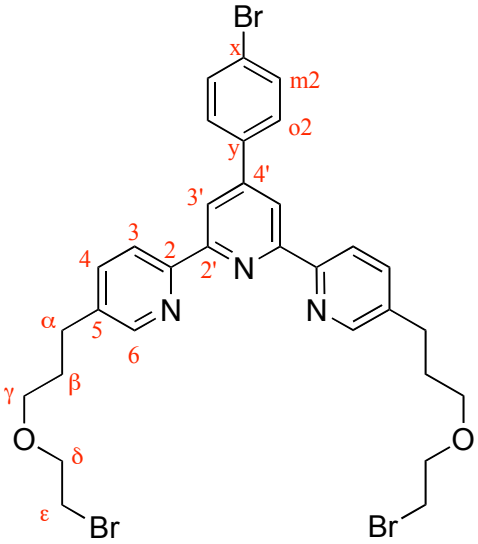

Macrocycle MT_{34}: 18

A mixture of terpyridine **17** (143 mg; 0.199 mmol) and commercial 4,4'-isopropylidenediphenol (45.4 mg; 0.199 mmol) in 50 mL of degassed DMF was introduced in a 100mL Hamilton gastight syringe fitted on a syringe pump and connected *via* a needle to a one liter round-bottom flask containing Cs_2CO_3 (227 mg; 0.696 mmol) in suspension in

200 mL of degassed DMF. The vessel was heated at 60°C under argon and the mixture was added dropwise during 89h. The solvent was removed and the residue taken up in CH_2Cl_2/H_2O. The aqueous layer was extracted with CH_2Cl_2 and the combined organic layers were dried over Na_2SO_4. After the solvent was removed, the resulting brown oil was purified by column chromatography (standardised alumina, pentane/CH_2Cl_2 60:40 to pure CH_2Cl_2) to give **18** as a white solid (88.4 mg; 57%).

^1H NMR (300 MHz, $CDCl_3$): δ (ppm) = 1.58 (s, 6H, CH_3); 1.98 (q, 4H, H_β); 2.85 (t, 4H, H_α); 3.48 (t, 4H, H_γ); 3.74 (m, 4H, H_δ); 4.08 (m, 4H, H_ε); 6.81-6.84 (dm, 4H, H_b); 7.09-7.12 (dm, 4H, H_a); 7.62-7.64 (dm, 2H, H_{m2}); 7.67-7.70 (dm, 2H, H_4-$H_{4''}$, J_{3-4} = 7.9 Hz); 7.75-7.78 (dm, 2H, H_{o2}); 8.51-8.53 (d, 2H, H_3-$H_{3''}$, J_{3-4} = 8.3 Hz); 8.54 (m, 2H, H_6-$H_{6''}$); 8.64 (s, 2H, $H_{3'}$-$H_{5'}$)

^{13}C NMR (300 MHz, $CDCl_3$, assigned using HMQC and HMBC 2D ^1H-^{13}C HETCORR experiments): δ (ppm) = 156.55 (*u*); 156.15 (*2'*); 153.86 (*2*); 149.31 (*6*); 148.92 (*4'*); 143.34 (*t*); 137.92 (*4*); 137.59 (*y*); 137.45 (*5*); 132.08 (*m2*); 128.91 (*o2*); 127.70 (*a*); 123.38 (*x*); 120.93 (*3*); 117.84 (*3'*); 114.06 (*b*); 69.30 (*δ*); 68.91 (*γ*); 67.41 (*ε*); 41.68 (*s*); 30.97 (*Me*); 30.34 (*β*); 28.76 (*α*)

FAB-MS, m/z exp.: 784.3 ([**18**+H]$^+$, calc. for [M+H]$^+$: 784.3)

Anal. Found (Calc.) for $C_{23}H_{18}BrN_3$ + 1.5 H_2O: %C, 68.09 (68.06); %H, 6.15 (6.08); %N, 5.15 (5.18)

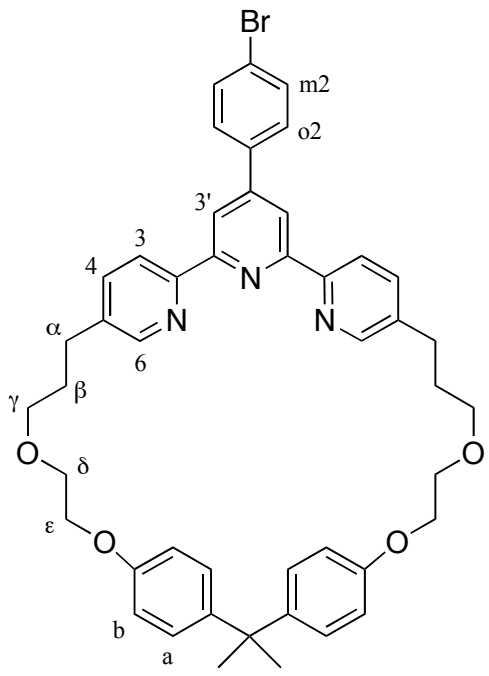

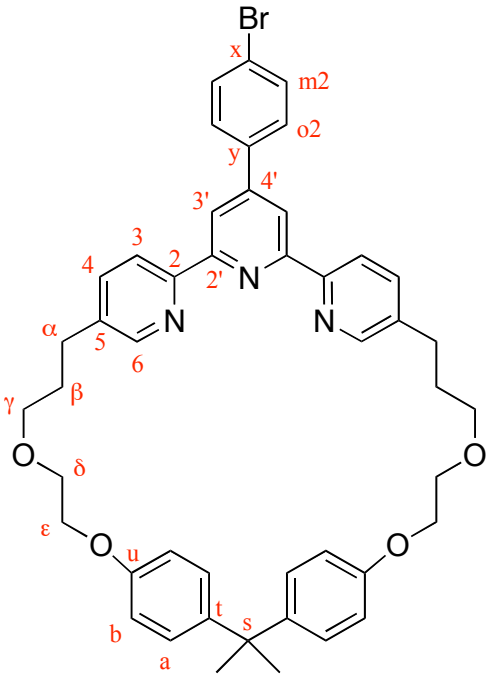

Boronic ester derivative of MT_{34}: 19

A round-bottom flask was charged with $Pd(dppf)Cl_2$ (1 mg; 0.001 mmol), KOAc (11.2 mg; 0.115 mmol), bis(neopentyl glycolato)diboron (B_2neo_2, 9.1 mg; 0.040 mmol) and MT_{34} (**18**, 30 mg; 0.038 mmol) and flushed with nitrogen. Freshly distilled dioxane (10 mL) was then added and the mixture was heated at 80°C for 19h. The resulting orange solution was then diluted with toluene and washed with water. The toluene layer was dried over Na_2SO_4 and the solvent removed by rotary evaporation. The residue was dried overnight on a vacuum pump giving **19** as a brownish white solid (quantitative yield). It was used directly for the next step without further purification.

^1H NMR (300 MHz, $CDCl_3$): δ (ppm) = 1.06 (s, 6H, CH_{3neo}); 1.58 (s, 6H, CH_3); 1.98 (q, 4H, H_β); 2.85 (t, 4H, H_α); 3.48 (t, 4H, H_γ); 3.74 (m, 4H, H_δ); 3.81 (s, 4H, CH_{2neo}); 4.08 (m, 4H, H_ε); 6.81-6.84 (dm, 4H, H_b); 7.09-7.13 (dm, 4H, H_a); 7.65-7.69 (dd, 2H, H_4-$H_{4''}$, J = 8.1 Hz, 2.3 Hz); 7.89-7.95 (dm, 4H, H_{m2}-H_{o2}); 8.52-8.55 (d, 2H, H_3-$H_{3''}$, J_{3-4} = 8.1 Hz); 8.55 (m, 2H, H_6-$H_{6''}$); 8.70 (s, 2H, $H_{3'}$-$H_{5'}$)

^{13}C NMR (300 MHz, $CDCl_3$, assigned using HMQC and HMBC 2D ^1H-^{13}C HETCORR experiments): δ (ppm) = 156.55 (*u*); 155.96 (*2'*); 154.14 (*2*); 150.18 (*4'*); 149.30 (*6*); 143.36 (*t*); 140.53 (*y*); 137.88 (*4*); 137.27 (*5*); 134.44 (*m2*); 130.09 (*x*); 127.71 (*a*); 126.46 (*o2*); 120.97 (*3*); 118.24 (*3'*); 114.08 (*b*); 72.39 (CH_{2neo}); 69.30 (*δ*); 68.92 (*γ*); 67.42 (*ε*); 41.68 (*s*); 31.95 (C_{neo}); 30.97 (CH_3); 30.34 (*β*); 28.75 (*α*); 21.97 (CH_{3neo})

HR ES-MS, m/z exp.: 818.4353 ([**19**+H]$^+$, calc. for [M+H]$^+$: 818.4344)

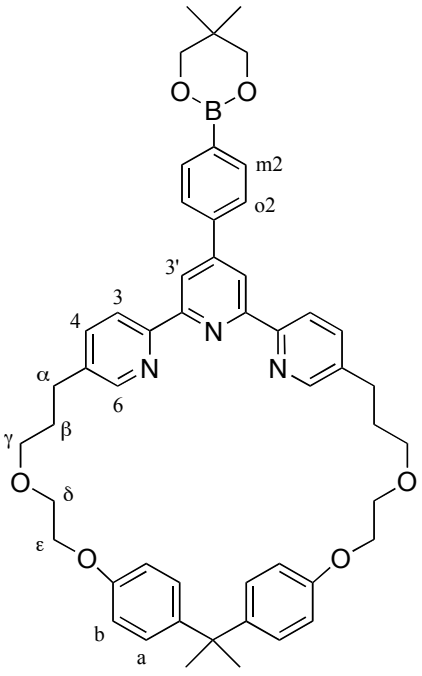

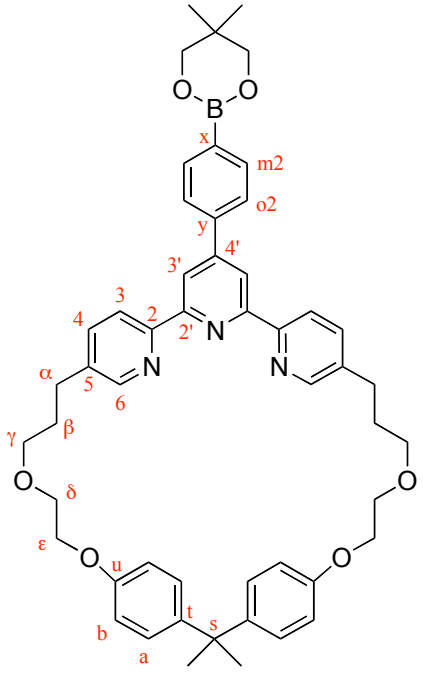

Cyclic phen-terpy conjugate: 20

To a degassed solution of 3-bromo-8-(4-methoxyphenyl)-1,10-phenanthroline (**6**, 14 mg; 0.038 mmol) and Na_2CO_3 (40.5 mg; 0.382 mmol) in 10 mL of toluene and water were added, under argon, a solution of **19** (>31 mg; 0.0382 mmol) in 5 mL of toluene. $Pd(PPh_3)_4$ (2.2 mg; 0.002 mmol) was then added as a solid to the solution under argon. It is very important to respect the following sequence in the additions: a) Na_2CO_3 and phenanthroline **6** in toluene and water, b) 3 vacuum-argon cycles, c) addition of the degassed solution of the boronic ester **19**, d) 3 vacuum-argon cycles, e) addition of the catalyst, f) 3 vacuum-argon cycles.
The reaction was monitored by TLC, and after 46 hours at 110°C, the reaction mixture was allowed to cool to room temperature. The solvent was removed by rotary evaporation and the crude mixture was taken in CH_2Cl_2 and washed with water. The combined organic layers were dried over Na_2SO_4 and the solvent evaporated. Chromatography (aluminium oxide, CH_2Cl_2/pentane (80:20) to CH_2Cl_2-MeOH (99:1)) gave 15 mg (0.015 mmol; 40% from **18**) of pure product **20** as a white solid.

^{1}H NMR (300 MHz, $CDCl_3$): δ (ppm) = 1.58 (s, 6H, CH_3); 1.98 (q, 4H, H_β); 2.88 (t, 4H, H_α); 3.48 (t, 4H, H_γ); 3.74 (m, 4H, H_δ); 3.91 (s, 3H, OCH_3); 4.08 (t, 4H, H_ε); 6.82-6.85 (dm, 4H, H_b, $J_{a\text{-}b}$ = 8.7 Hz); 7.09-7.12 (d, 2H, H_{o1}, $J_{o1\text{-}m1}$ = 8.7 Hz); 7.10-7.13 (dm, 4H, H_a, $J_{a\text{-}b}$ = 8.7 Hz); 7.74-7.77 (m, 4H, H_{m1}, H_4-$H_{4''}$, $J_{o1\text{-}m1}$ = 8.7 Hz); 7.91 (s, 2H, H_{p5}-H_{p6}); 7.95 (d, 2H, H_{m2}, J = 8.4 Hz); 8.15 (d, 2H, H_{o2}, J = 8.4 Hz); 8.37 (d, 1H, H_{p7}, $J_{p4\text{-}p7}$ = 2.1 Hz); 8.50 (d, 1H, H_{p4}, $J_{p4\text{-}p7}$ = 2.2 Hz); 8.57-8.60 (m, 4H, H_3-$H_{3''}$, H_6-$H_{6''}$); 8.86 (s, 2H, $H_{3'}$-$H_{5'}$); 9.44 (d, 1H, H_{p9}, $J_{p9\text{-}p2}$ = 2.1 Hz); 9.52 (d, 1H, H_{p2}, $J_{p2\text{-}p9}$ = 2.1 Hz)

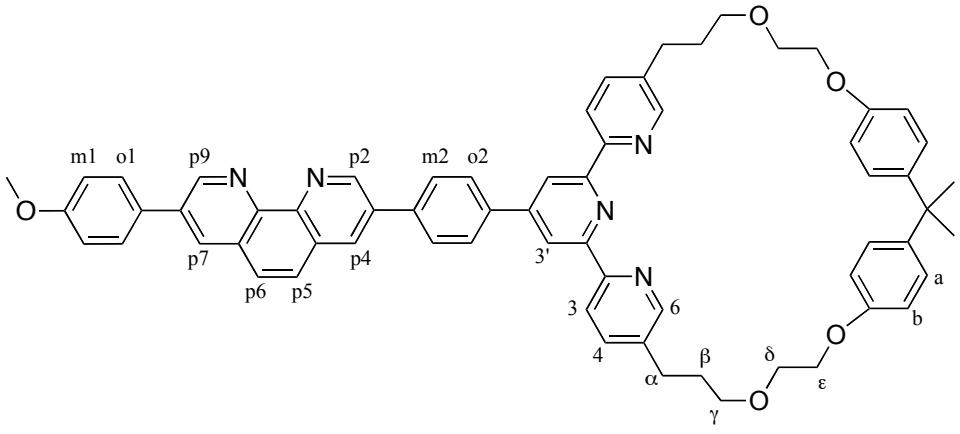

^{13}C NMR (300 MHz, $CDCl_3$, assigned using HMQC and HMBC 2D ^{1}H-^{13}C HETCORR experiments): δ (ppm) = 160.15 (*i*); 156.57 (*u*); 156.01 (*2'*); 153.58 (*2*); 149.27 (*6*); 149.04 (*4'*); 148.99 (*p9, p2*); 145.11 (*p12*); 144.77 (*p3*); 144.15 (*p11*); 143.21 (*t*); 138.48 (*y*); 137.74 (*4*); 135.37 (*p8*); 134.76 (*x*); 133.43 (*5*); 133.38 (*p4*); 132.51 (*p7*); 129.65 (*p*); 128.52 (*m1*);

128.04 (*o2*); 127.93 (*m2*); 127.54 (*a*); 127.28 (*p6*); 127.08 (*p5*); 120.67 (*3*); 117.79 (*3'*); 114.67 (*o1*); 113.90 (*b*); 69.11 (*δ*); 68.93 (*γ*); 67.55 (*ε*); 55.36 (OCH_3); 41.44 (*s*); 30.56 (CH_3); 30.18 (*β*); 28.81 (*α*)

Carbons p_{13} and p_{14} could not be assigned.

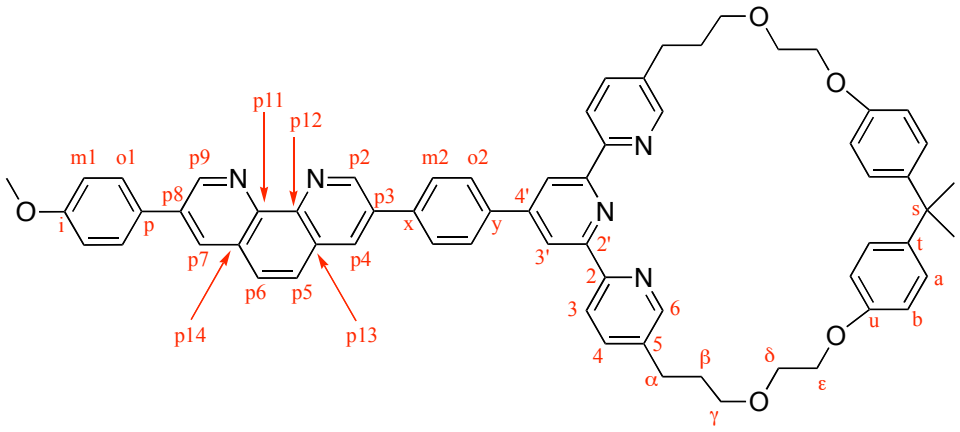

HR ES-MS, m/z exp.: 990.4553 (**20**, calc. for [M]: 990.4589)

DOSY NMR (500 MHz, CD_2Cl_2): D = 1000 $\mu m^2.s^{-1}$

Rotaxane dimer with Zinc(II): $[Zn_2.(\mathbf{20})_2].4OTf$

Phen-terpy conjugate **20** (5.5 mg; $5.5x10^{-3}$ mmol) was dissolved in 0.25 mL of CD_2Cl_2. A solution of $Zn(OTf)_2$ in CD_3OD (16.48 mg in 2 mL) was prepared, and 0.25 mL ($5.5x10^{-3}$ mmol) were added to the ligand solution, which became clear and orange. The solution was transferred to an NMR tube and the reaction was monitored by ^1H NMR. After 24 hours at room temperature, the NMR spectrum remained the same as after 1 hour of reaction. The solvent was then evaporated and the crude mixture taken in methanol, filtered, and the filtrate evaporated to dryness yielding $[Zn_2.(\mathbf{8})_2].4OTf$ as a yellow solid (5.1 mg; 76%).

HR ES-MS, m/z exp.: 527.7011 (calc. for $[Zn_2(\mathbf{20})_2]^{4+}$: 527.6900); 753.2495 (calc. for $[Zn_2(\mathbf{20})_2, OTf]^{3+}$: 753.2375); 1204.3467 (calc. for $[Zn_2(\mathbf{20})_2, 2OTf]^{2+}$: 1204.3325)

DOSY NMR (500 MHz, CD_2Cl_2): D = 510 $\mu m^2.s^{-1}$; r_h = 10.4 Å
ellipsoïd parameters : a = 15 Å; b = c = 8 Å

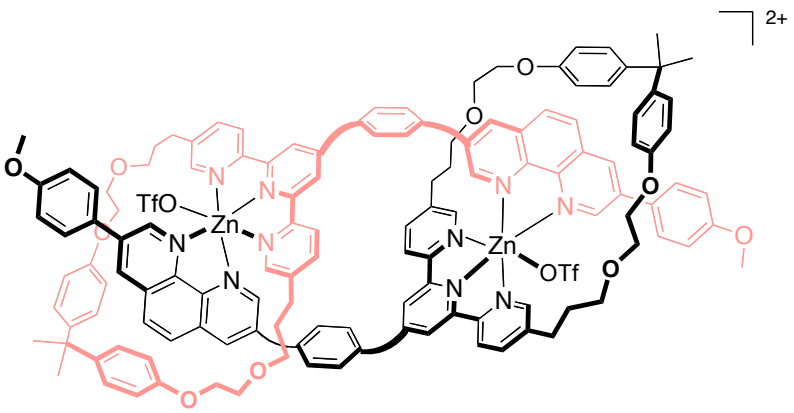

Rotaxane dimer and trimer with Copper(II): $[Cu_2(\mathbf{20})_2].4BF_4$ and $[Cu_3(\mathbf{20})_3].6BF_4$

Phen-terpy conjugate **20** (10.2 mg; 0.0103 mmol) was dissolved in 5 mL of CH_2Cl_2. A solution of $Cu(BF_4)_2$ in CH_3CN (24.4 mg in 10 mL) was prepared, and 1 mL was added to the ligand solution, which turned instantaneously clear and olive green. The solution was let stir for 15 hours at room temperature, and by addition of diethyl ether a green solid precipitated out, which was then filtered, washed, dissolved again in an acetone/acetonitrile/methylene chloride mixture, and recovered as a solid by addition of diethyl ether in a good yield (10.8 mg; 92%).

HR ES-MS, m/z exp.: 526.1925 (calc. for $[Cu_2(\mathbf{20})_2]^{4+}$: 526.1901; calc. for $[Cu_3(\mathbf{20})_3]^{6+}$: 526.1901); 649.4337 (calc. for $[Cu_3(\mathbf{20})_3, BF_4]^{5+}$: 649.4299); 731.2454 (calc. for $[Cu_2(\mathbf{20})_2, BF_4]^{3+}$: 731.2558)

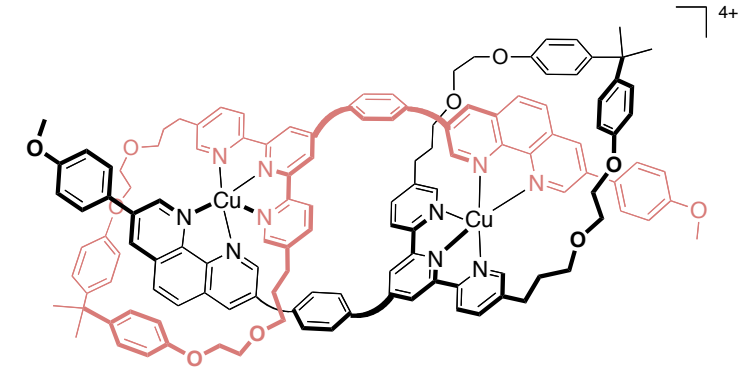

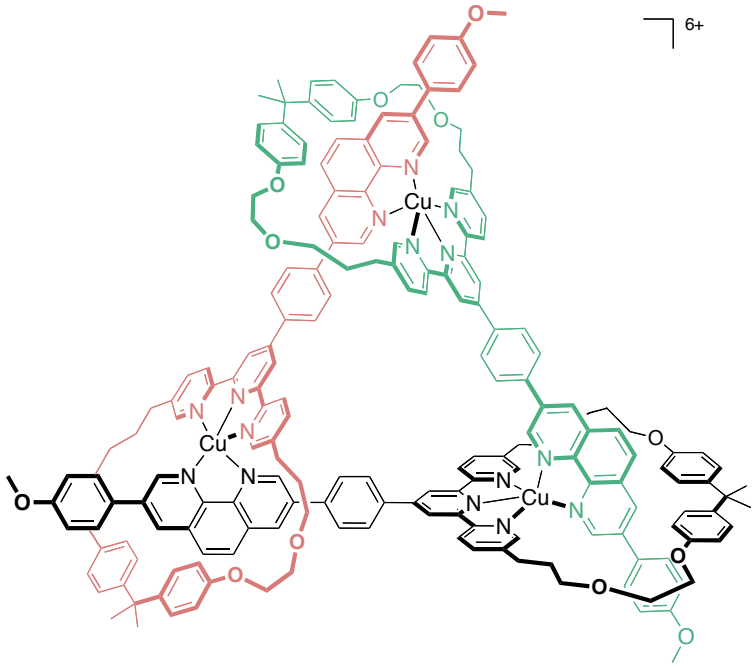

Terpy-based bis-macrocycle : 21

a) Strategy 1: Homocoupling

To a solution of $Ni(PPh_3)_2Cl_2$ (22.8 mg; 0.035 mmol) and PPh_3 (18.3 mg; 0.070 mmol) in DMF (5 mL) under argon, was added zinc powder (2.3 mg; 0.035 mmol) and the mixture was stirred for 20 minutes at room temperature, during which time it became deep red. MT_{34} (**18**, 27.4 mg; 0.035 mmol) in DMF (2 mL) was then added and the mixture was stirred at 50°C for 14 hours. After evaporation of the solvent, acetonitrile (10 mL), water (5 mL) and KCN (40 mg) were added. The mixture was heated at 50°C for 1.5 hour. The organic layer was decanted and column chromatography (aluminium oxide, $CHCl_3$/pentane (50:50) to pure $CHCl_3$) afforded **21** as a white solid (4 mg; 20%).

b) Strategy 2: Heterocoupling using Suzuki's strategy

To a degassed solution of MT_{34} (**18**, 17.5 mg; 0.021 mmol) and Na_2CO_3 (22.7 mg; 0.210 mmol) in 8 mL of toluene and 2 mL of water were added, under argon, a solution of **19** (16.8 mg; 0.021 mmol) in 2 mL of toluene and 1 mL of ethanol. $Pd(PPh_3)_4$ (1.2 mg; 0.001 mmol) was then added as a solid to the solution under argon. It is very important to respect the following sequence in the additions: a) Na_2CO_3 and bromo derivative **18** in toluene and water, b) 3 vacuum-argon cycles, c) addition of the degassed solution of the boronic ester **19**, d) 3 vacuum-argon cycles, e) addition of the catalyst, f) 3 vacuum-argon cycles.
The reaction was monitored by TLC, and after 5 hours at 110°C, reagent **18** was consumed and the reaction mixture was allowed to cool to room temperature. The solvent was removed by rotary evaporation and the crude mixture was taken in CH_2Cl_2 and washed with water. The combined organic layers were dried over Na_2SO_4 and the solvent evaporated. Chromatography (aluminium oxide, CH_2Cl_2/pentane (50:50) to CH_2Cl_2-MeOH (99:1)) gave 14.5 mg (0.010 mmol; 96%) of pure product **21** as a white solid.

^1H NMR (300 MHz, CD_2Cl_2): δ (ppm) = 1.54 (s, 12H, CH_3); 1.98 (q, 8H, H_β); 2.85 (t, 8H, H_α); 3.49 (t, 8H, H_γ); 3.72 (t, 8H, H_δ); 4.04 (t, 8H, H_ε); 6.77-6.80 (dm, 8H, H_b, $J_{a\text{-}b}$ = 8.8 Hz); 7.05-7.08 (dm, 8H, H_a, $J_{a\text{-}b}$ = 8.8 Hz); 7.69-7.73 (dd, 4H, H_4-$H_{4''}$, J = 8.2 Hz, 2.0 Hz); 7.88-7.91 (dm, 4H, H_{m2}, $J_{o2\text{-}m2}$ = 8.4 Hz); 8.04-8.07 (dm, 4H, H_{o2}, $J_{o2\text{-}m2}$ = 8.4 Hz); 8.56-8.58 (d, 4H, H_3-$H_{3''}$, $J_{3\text{-}4}$ = 7.5 Hz); 8.57 (d, 4H, H_6-$H_{6''}$); 8.79 (s, 4H, $H_{3'}$-$H_{5'}$)

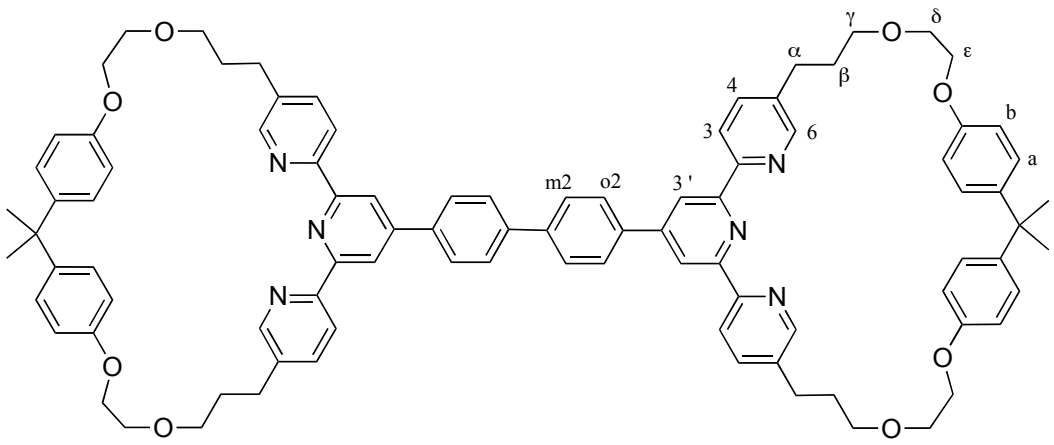

^{13}C NMR (300 MHz, $CDCl_3$, assigned using HMQC and HMBC 2D ^{1}H-^{13}C HETCORR experiments): δ (ppm) = 156.56 (*u*); 155.97 (*2'*); 154.10 (*2*); 150.22 (*4'*); 149.31 (*6*); 143.35 (*t*); 138.67 (*y*); 137.86 (*4*); 137.27 (*5*); 128.92 (*x*); 128.88 (*m2*); 127.71 (*a*); 127.36 (*o2*); 120.91 (*3*); 118.23 (*3'*); 114.08 (*b*); 69.30 (*δ*); 68.92 (*γ*); 67.42 (*ε*); 41.69 (*s*); 30.97 (CH_3); 30.35 (*β*); 28.76 (*α*)

HR ES-MS, m/z exp.: 1409.7092 (**21**, calc. for $[M + H]^+$: 1409.7082)

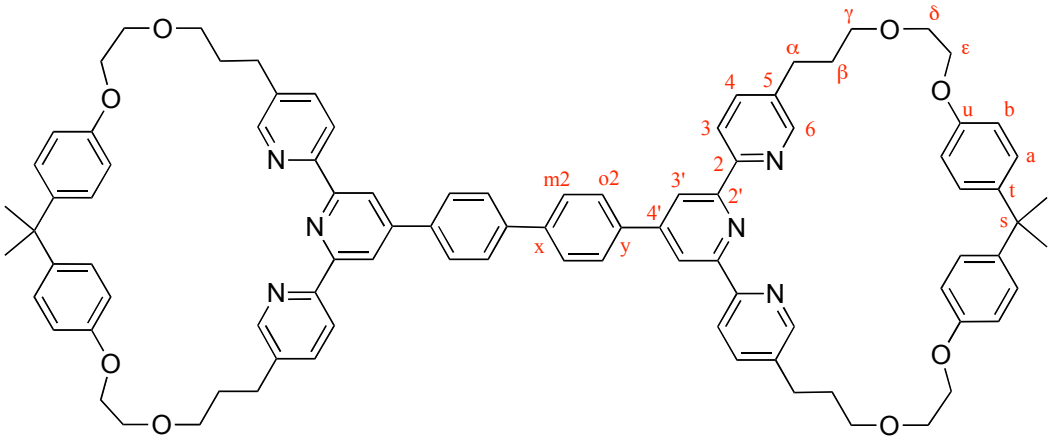

Résumé étendu en français

Depuis plusieurs années, divers groupes de recherche ont ouvert une nouvelle voie dans la chimie de synthèse de composés complexes : l'élaboration de molécules ayant une topologie non triviale, c'est-à-dire dont on ne peut représenter l'enchaînement des liaisons sur une feuille de papier sans faire apparaître au moins un croisement entre deux liaisons. C'est ainsi que les premiers caténanes, rotaxanes et nœuds moléculaires ont été fabriqués. Loin d'être de simples curiosités de laboratoire, ces molécules sont aussi présentes dans la nature. En effet, la publication récente d'une structure aux rayons X a montré que la membrane (ou capside) du virus HK97, appartenant à la famille des virus bactériophages, est constituée d'arrangements cycliques de protéines formant des anneaux entrelacés. Cette structure rappelle fortement celle des cottes de mailles du Moyen Age. La nature a donc réalisé une membrane fine et résistante, d'un point de vue chimique, mécanique et physique. Il est alors très tentant pour les chimistes d'essayer de créer des arrangements bidimensionnels contenant des anneaux et des fils moléculaires entrelacés, ayant une structure et une topologie proches de celles de la membrane du capside de HK97. Cela constitue un formidable défi synthétique auquel nous avons décidé de nous attaquer, grâce à la stratégie développée au laboratoire depuis une vingtaine d'années pour construire des caténanes et rotaxanes complexes.

Afin d'assembler les ligands, de pouvoir « tisser » au mieux les mailles du « réseau moléculaire » et que les anneaux et fils moléculaires s'entrelacent, la stratégie classique du laboratoire est d'utiliser des métaux de transition en tant qu'éléments assembleurs de ligands portant divers groupes chélatants. Une telle stratégie a été utilisée par bien d'autres groupes, et a donné naissance à d'abondantes et magnifiques structures telles que des grilles, des complexes hélicoïdaux ainsi que de nouvelles topologies telles que des nœuds ou des dimères de rotaxanes.

Ce dernier exemple, précurseur d'un prototype de muscle moléculaire, est très révélateur de l'importance du design du ligand pour construire des architectures complexes à topologie non triviale. Le ligand de base est en effet dans ce cas constitué d'un anneau contenant un groupement chélatant de type 1,10-phénanthroline (phen), connecté à un axe contenant un autre groupement phen. Or au moment de l'assemblage des ligands autour d'un métal

tétracoordiné tel que le cuivre(I), on s'aperçoit que rien n'empêche la déformation de la molécule au niveau de la jonction entre l'anneau et l'axe, ce qui conduit alors exclusivement à l'obtention d'un dimère de pseudo-rotaxane (Figure 1).

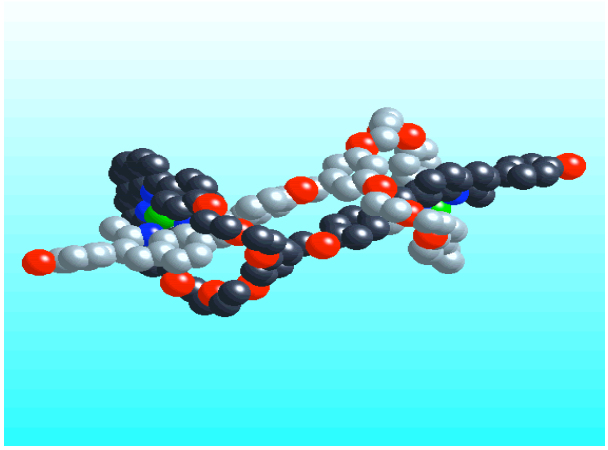

Figure 1

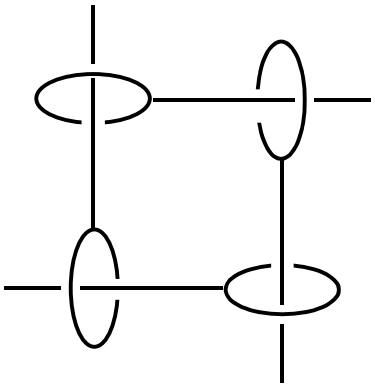

Figure 2

C'est dans la lignée de ces résultats que ce projet de thèse a été construit, l'idée consistant à empêcher la déformation du ligand au niveau de la jonction entre l'anneau et le fil afin de s'assurer de créer un ligand portant deux groupements chélatants dont les axes de coordination resteront perpendiculaires l'un par rapport à l'autre. Une telle molécule doit alors favoriser l'obtention de complexes multinucléaires possédant des géométries et nucléarités bien définies. La structure du tétramère est représentée sur la Figure 2. La synthèse de tels édifices étant longue et délicate, nous avons tout d'abord orienté nos efforts sur l'obtention d'un ligand dont les groupements chélatants auraient leurs axes de coordination effectivement orthogonaux l'un par rapport à l'autre, mais au sein d'un système acyclique. Des études de complexation ont pu être faites dès lors sur ce ligand acyclique. C'est seulement dans un deuxième temps que la synthèse du ligand final auquel on incorpore un macrocycle est envisagée, et que l'on a pu étudier la formation de multi-rotaxanes.

Il est à noter que deux projets complémentaires ont été lancés dans le même temps au laboratoire : tous les deux ont pour objectif de synthétiser des multi-rotaxanes à nucléarité la plus élevée possible, la différence résidant dans le choix des groupes chélatants utilisés. Un travail post doctoral a ainsi porté sur la synthèse et l'assemblage de tels ligands autour de métaux tétracoordinés tels que le cuivre(I), et incorporait donc le groupement phen dans la structure du ligand. Ceci a conduit à l'observation d'un équilibre entre le trimère et le

tétramère de rotaxane, cet équilibre pouvant être déplacé en jouant sur la concentration des espèces en solution.

Dans mon cas, nous avons fait le choix de nous intéresser à l'assemblage autour de métaux pentacoordinés tels que le zinc(II) et le cuivre(II). Les groupements chélatants choisis sont donc une phen sur l'axe et une terpy dans l'anneau. L'avantage de prendre une terpy dans ce cas est double : contrairement au cas avec la phen, la fonctionnalisation axiale en arrière de la terpy est « naturelle » *via* la position para du cycle central, et cela n'induit alors aucun problème de diastéréoisomérie, présents avec les cycles oxazoles ou imidazoles.

1 Synthèse du ligand acyclique portant des chélates aux axes de coordination orthogonaux ; Etude de sa chimie de coordination autour de métaux pentacoordinés

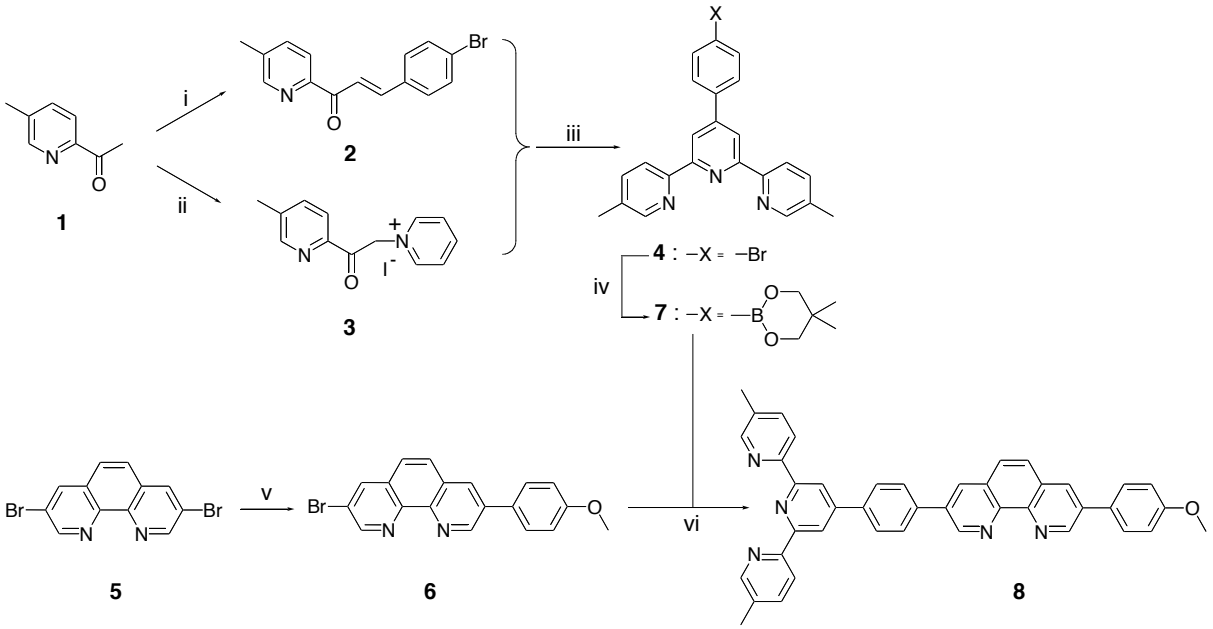

Figure 3

Comme nous l'avons vu dans l'exemple du précurseur du muscle moléculaire, le design du ligand doit être optimisé afin de mener au résultat désiré lors de l'étape de complexation au métal de transition. Afin de pallier l'inconvénient de la déformation du ligand qui conduit uniquement au dimère, nous avons décidé pour rigidifier la structure de placer le groupement chélatant à la jonction entre l'anneau et le fil. Dans un premier temps, nous avons donc

synthétisé la terpyridine **4**. La procédure employée passe par la synthèse de la 2-acétyl-5-méthylpyridine **1**, qui permet de former en parallèle l'iodure de pyridinium **3** et l'azachalcone **2** qui seront couplés dans une dernière étape par réaction de Kröhnke. Les rendements de toutes ces étapes ont été optimisés et la terpyridine **4** a pu être synthétisée à l'échelle de plusieurs grammes.

Nous avons ensuite choisi de coupler les deux chélates phen et terpy par la méthode de Suzuki. Pour cela, il nous a fallu synthétiser la phen dissymétrique **6**, comprenant d'un côté une fonction anisyl qui nous servira de sonde RMN par suivi du déplacement chimique du groupement méthoxyl, et de l'autre un bromo susceptible de se coupler avec l'ester boronique **7,** dérivé de la terpy **4**. Compte tenu du caractère statistique de la synthèse de la partie phen dissymétrique, cette dernière a été obtenue avec un bon rendement, et le couplage de Suzuki a permis d'obtenir sans ambiguïté le ligand **8** qui a été complètement caractérisé et qui contient 7 cycles aromatiques.

L'étude de la complexation de ce ligand a tout d'abord été faite avec un sel de triflate de zinc. En effet, le zinc(II) forme des complexes pentacoordinés stables, et il est suffisamment labile pour permettre la formation de composés de coordination sous contrôle thermodynamique. Il est à noter que l'on s'attend à ce que des géométries de type bipyramides trigonales non distordues, avec des chélates ayant leurs axes de coordination orthogonaux, favorisent la formation d'assemblages à 4 métaux. Au contraire, d'autres géométries pentacoordinées, telles qu'une pyramide à base carrée ou une bipyramide trigonale distordue, devraient fournir de plus petits assemblages, à 3 voire même 2 métaux. Il s'agit donc d'un combat entre entropie et enthalpie : les facteurs entropiques tendent en effet à favoriser les plus petits assemblages possibles tandis que l'enthalpie de déformation sera la plus petite pour de grands assemblages.

À notre surprise, il s'est avéré que la réaction entre le ligand **8** et le sel de zinc(II) a conduit avec un bon rendement à la formation du dimère comme seul produit de la réaction, sans aucune trace de trimère ou de tétramère (Figure 4). Le dimère a été complètement caractérisé par ES-MS, RMN ^{1}H et DOSY. Il semble donc que dans ce cas l'entropie l'ait complètement emporté, malgré le coût enthalpique de la déformation du squelette carboné et de la sphère de coordination du métal.

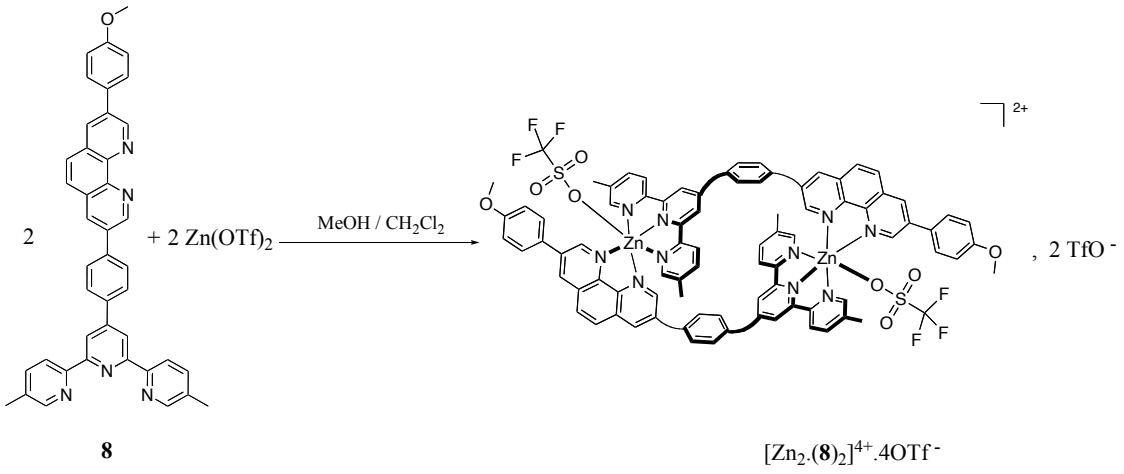

Figure 4

Nous avons donc décidé d'utiliser d'autres métaux de transition possédant des caractéristiques stéréoélectroniques plus exigeantes que le zinc(II), et qui devraient donc rendre la distorsion plus difficile et favoriser la formation de trimères ou tétramères. C'est pourquoi nous avons réalisé la complexation du ligand **8** avec du tétrafluoroborate de cuivre(II) qui a conduit à la formation d'un solide vert que nous avons analysé par ES-MS, électrochimie, spectroscopie UV-visible et RPE. Le spectre de masse montre sans ambiguïté la présence de deux espèces, possédant respectivement 2 et 3 atomes de cuivre(II). L'électrochimie et la RPE donnent des résultats qui corroborent la présence de deux espèces en solution et dans lesquelles le cuivre a un environnement pentacoordiné. Par cette expérience, on peut donc constater, une fois de plus, que le design du ligand a beau avoir été optimisé afin de favoriser les assemblages à haute nucléarité, ce dernier parvient à se déformer afin de conduire au dimère de cuivre(II). Mais les contraintes stéréoélectroniques imposées par l'atome de cuivre sont plus fortes que celles du zinc, et on peut donc observer cette fois la présence de l'espèce trimérique, absente dans le cas de l'assemblage au zinc(II).

2 Synthèse du ligand cyclique portant des chélates aux axes de coordination orthogonaux ; Etude de sa chimie de coordination autour de métaux pentacoordinés

Afin d'inclure la terpyridine dans un macrocycle et pouvoir envisager la formation de multi-rotaxanes, il faut fonctionnaliser les positions méthyles 5 et 5''. Pour cela plusieurs stratégies ont été employées : nous avons dans un premier temps tenté de réaliser une monobromation

benzylique sur chaque position, mais la séparation des différents produits bromés n'a pas été possible. Nous avons alors envisagé de faire une perhalogénation (X = Br, Cl) de ces positions, pouvant mener ultérieurement à l'obtention d'un dialcool primaire, mais aucun des essais réalisés dans diverses conditions n'a conduit à une halogénation totale des positions considérées.

Nous avons alors décidé d'employer une procédure plus ancienne consistant à faire réagir la terpyridine avec du LDA pour former un dianion pouvant ensuite réagir sur une chaîne diéthylèneglycol portant à une extrémité un atome de brome et à l'autre extrémité une protection OTHP. Une fois que le produit dialkylé est isolé, il suffit ensuite de déprotéger l'alcool, de le mésyler puis de le bromer pour obtenir le précurseur du macrocycle final. Ce dernier est synthétisé en fermant le cycle par un groupement bisphénol A dans des conditions classiques de haute dilution, et le macrocycle MT34 contenant 34 atomes en son intérieur est isolé à hauteur de 57% de rendement et complètement caractérisé.

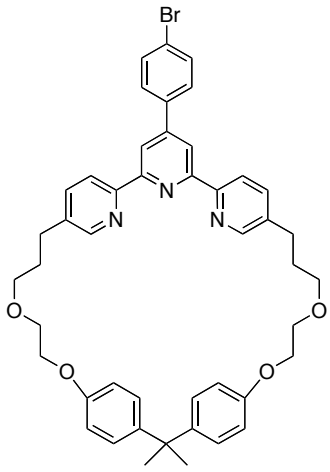

Macrocycle MT_{34}

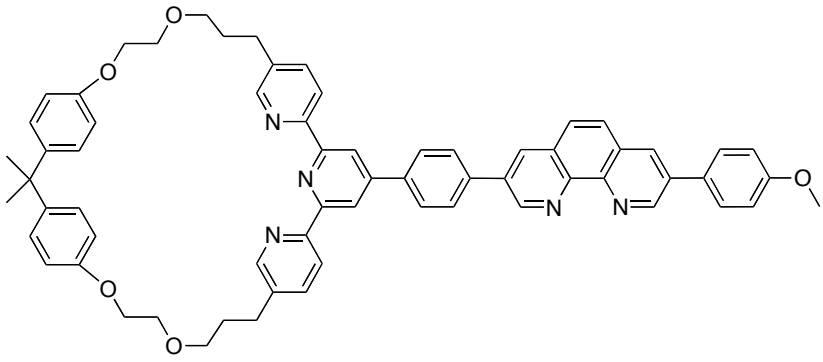

Ligand **20**

La stratégie employée pour obtenir le ligand final **20** portant les deux groupements chélatants phen et terpy est la même que dans le cas du système acyclique. Nous avons donc transformé le macrocycle MT34 en son dérivé ester boronique de manière quantitative, puis un couplage de Suzuki dans les conditions classiques avec la phen dissymétrique **6** fournit le ligand recherché **20** qui a été complètement caractérisé.

Comme pour le système acyclique, nous avons commencé par étudier la complexation du ligand avec un sel de triflate de zinc(II). Il était alors intéressant de savoir si la présence du macrocycle allait avoir une influence sur la nature de l'assemblage, et notamment si l'encombrement dû à la présence du macrocycle allait défavoriser la formation du dimère ou non.

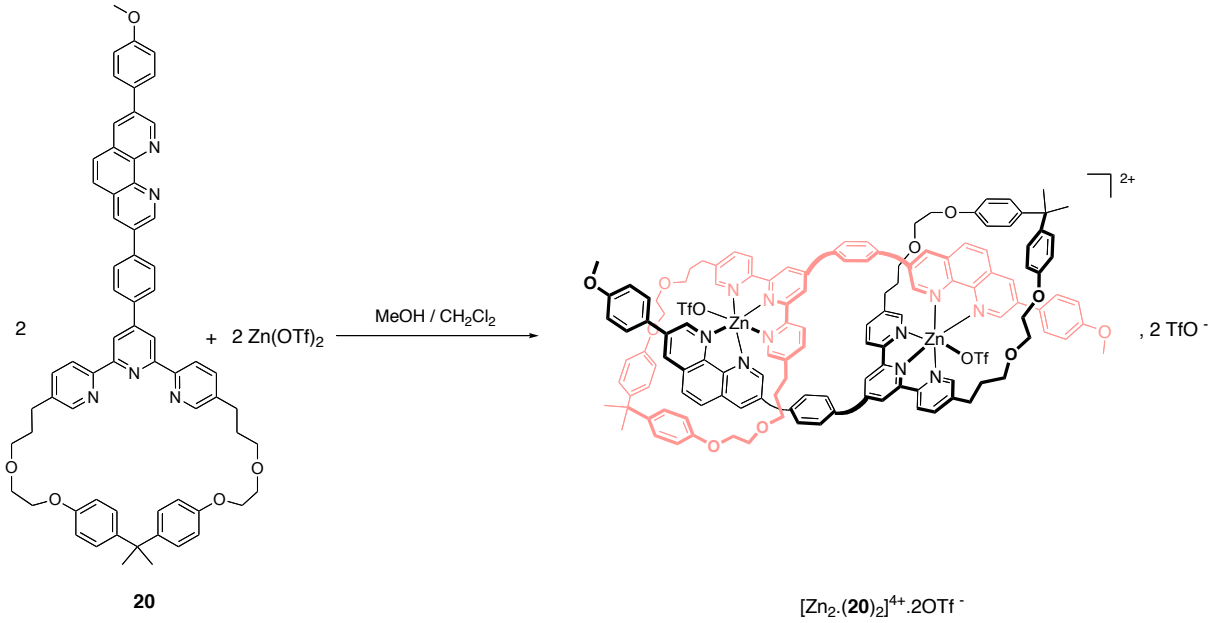

Figure 5

À notre surprise à nouveau, la réaction d'assemblage a conduit à la formation du dimère de pseudo-rotaxane comme seul produit de réaction, sans aucune trace d'espèces de plus haute nucléarité (Figure 5). L'étude DOSY du complexe a confirmé que le produit formé peut être modélisé par un ellipsoïde de dimensions 3 nm x 1.6 nm possédant le même coefficient de diffusion (D = 500 $\mu m^2/s$), ce qui est cohérent avec la structure attendue du dimère. Il semble donc encore une fois que l'entropie l'ait emporté sur le coût enthalpique de la déformation et que la plus petite espèce possible soit favorisée.

L'étude de la complexation de **20** autour de cuivre(II) a montré le même type de résultat que pour le système acyclique (Figure 6). En effet, les contraintes stéréoélectroniques imposées par le cuivre(II) permettent la formation du mélange de dimère et trimère de rotaxane, comme prouvé par ES-MS. Des études plus complètes par RPE et cyclovoltamétrie n'ont pas pu être réalisées par manque de temps et de quantité de matière.

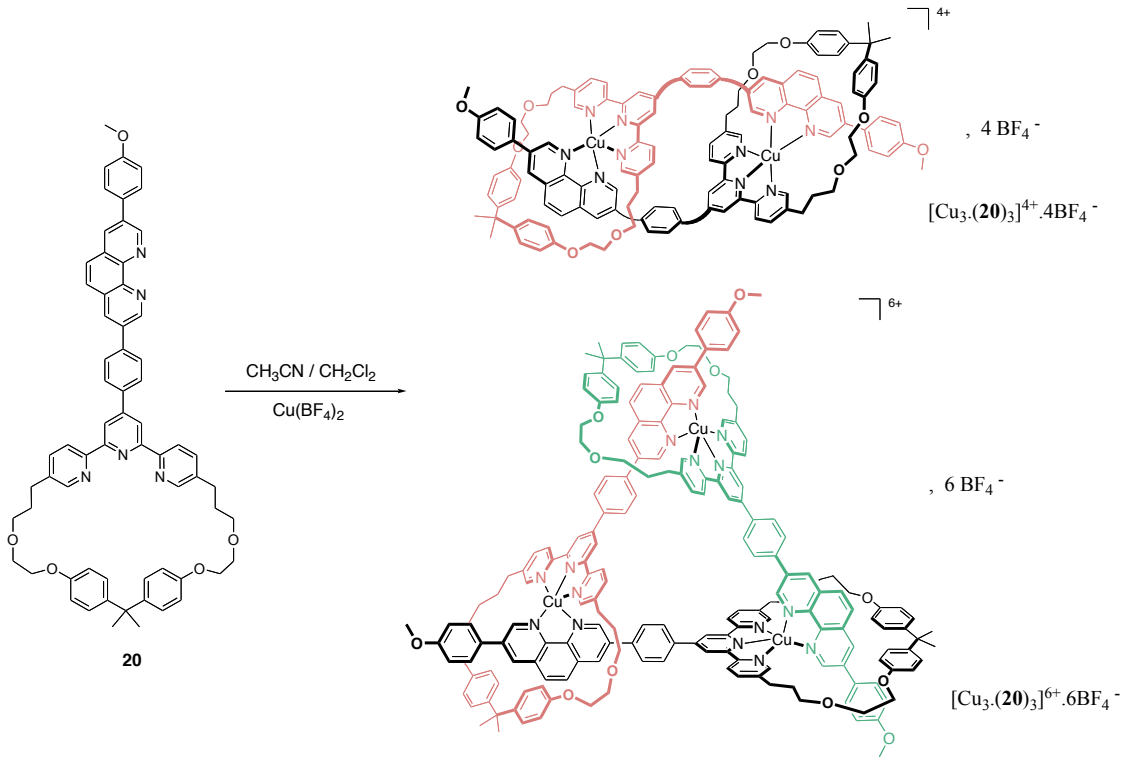

Figure 6

3 Synthèse d'un ligand bis-macrocyclique comportant deux noyaux terpy ; vers un autre type de tétramère de rotaxane

Un projet de recherche au laboratoire a pour objectif de synthétiser un modèle de presse moléculaire qui mimerait l'action des chaperons, molécules naturelles modifiant la conformation des protéines pour les rendre actives. Une telle presse serait constituée de l'enfilage de deux ligands bi-macrocycliques sur deux rails moléculaires contenant deux types de groupements chélatants. En changeant la nature du métal ou son degré d'oxydation, on passerait comme dans le cas du muscle moléculaire d'une station à l'autre du rail par glissement des bis-macrocycles (Figure 7).

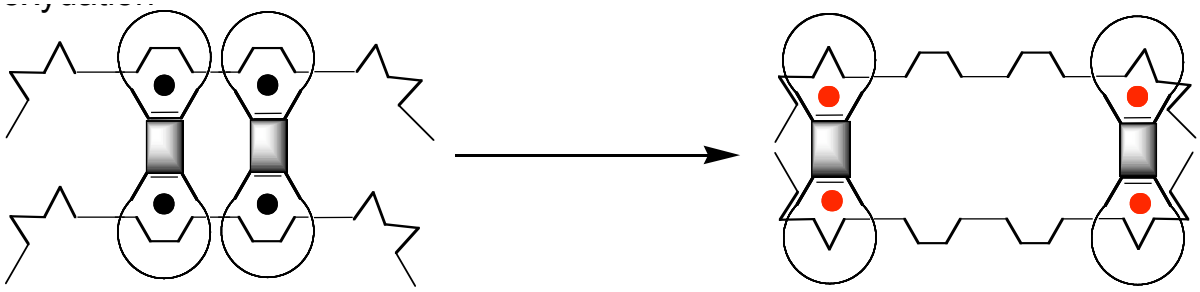

Figure 7

Le système est constitué de deux dianneaux comportant dans chaque macrocycle un noyau phen, enfilés sur un rail comportant pour l'instant une seule station de type bipyridine. L'assemblage est donc réalisé par la formation d'un complexe tétracoordiné de cuivre(I).

Or dans le cadre de mon projet de recherche, j'ai pu synthétiser le macrocycle MT34 qui porte en position arrière de la terpy une fonctionnalisation bromophényl. Cette molécule est donc un très bon candidat de précurseur pour la synthèse d'un dianneau comportant cette fois un noyau terpy dans chaque macrocycle. On peut donc envisager de réaliser avec un tel dianneau un assemblage sur le rail existant autour de métaux pentacoordinés, et ainsi former un pseudo[4]rotaxane cyclique.

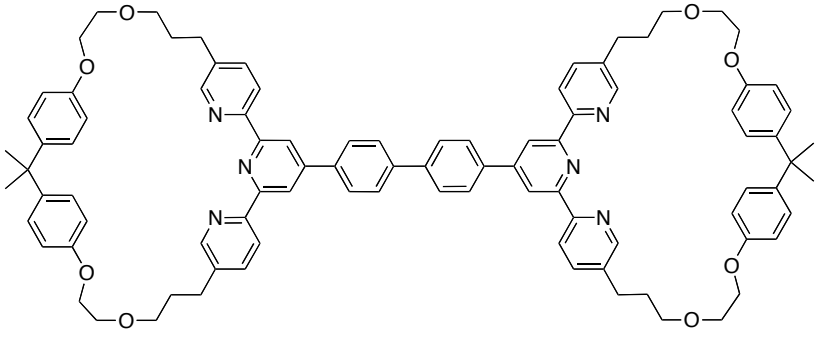

21

Figure 8

La synthèse du dianneau **21** a été réalisée de deux manières différentes. Nous avons dans un premier temps réalisé un homocouplage direct du macrocycle MT34 en présence d'un catalyseur de nickel, et nous avons obtenu le produit désiré, complètement caractérisé, avec un rendement assez moyen de 20%. Afin d'améliorer le rendement, nous avons envisagé une stratégie dissymétrique consistant à transformer l'un des macrocycles en son dérivé ester boronique, et à le coupler avec un équivalent de MT34 dans des conditions classiques de Suzuki. Par cette méthode, le produit a pu être synthétisé avec plus de 80% de rendement sur les deux étapes (Figure 8). Les premiers essais d'enfilage de deux molécules **21** autour de deux rails bis-bipy en utilisant le zinc(II) comme métal assembleur n'ont pour l'instant pas été concluants, mais les études sont toujours en cours (Figure 9).

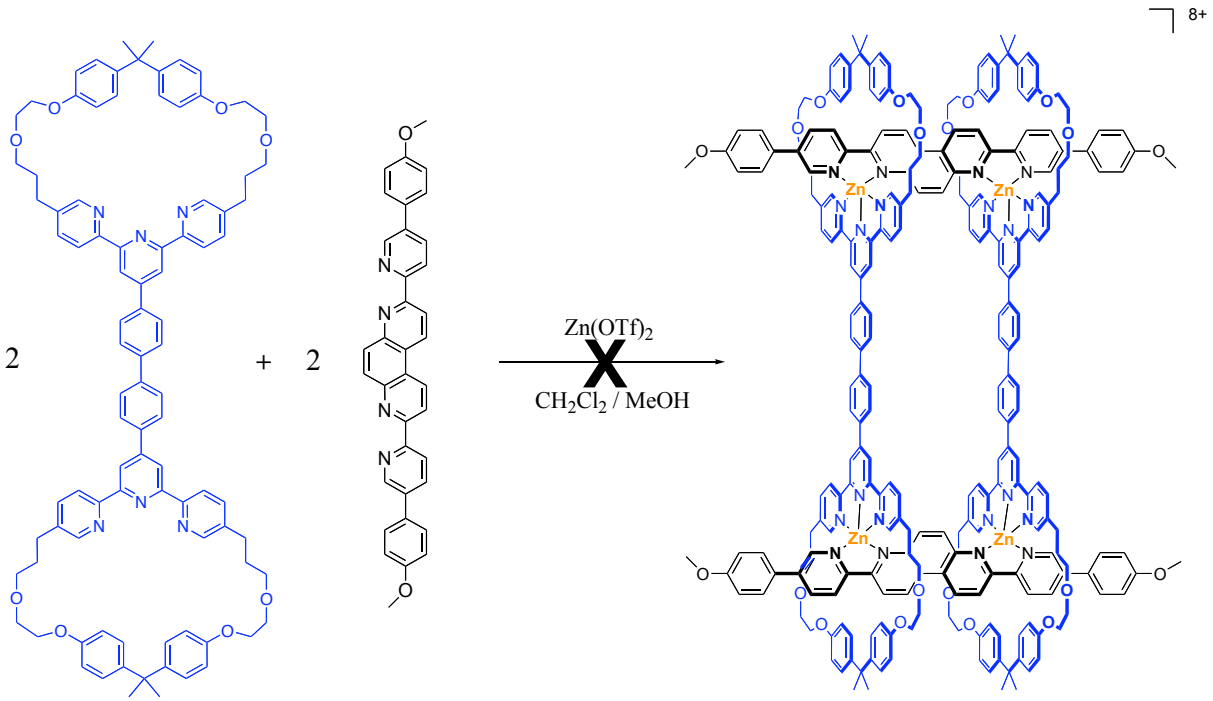

21

Figure 9

Publications

A phen-terpy conjugate whose coordination axes are orthogonal to one another and its zinc complex, B. Champin, V. Sartor and J.-P. Sauvage, *New J. Chem.*, 2006, **30**, 22-25

Rédaction d'un chapitre du livre *Intelligent Materials* (Royal Society of Chemistry), à paraître en 2006 : *Transition metal complex-based molecular machines*, B. Champin, U. Létinois-Halbes and J.-P. Sauvage (in press)

Tutorial Review à paraître dans le numéro spécial de *Chem. Soc. Rev.* consacré au 40ème anniversaire de la chimie supramoléculaire : *Transition metal complexes as molecular machine prototypes*, B. Champin, P. Mobian and J.-P. Sauvage, feb. 2007 (in press)

Communications

Présentation orale lors du Congrès organisé le 4 novembre 2005 à ISIS (Institut de Science et d'Ingénierie Supramoléculaire, Strasbourg) dans le cadre de la Work Week'05 du SMCT (SupraMolecular Chemistry and Technology), groupe de recherche du Pr. Dr. Ir. D. Reinhoudt (Eschede, The Netherlands)
Polydentate chelates with orthogonal coordination axes: towards a tetramer of rotaxane

Présentation orale lors du mini-symposium organisé le 16 avril 2005 au LCOM pour la venue des professeurs F. Stoddart (UCLA, USA) et M. Fujita (University of Tokyo, Japan)
Polydentate chelates with orthogonal coordination axes